

*Maximization of sulfur formation in the presence
of organic sulfur compounds in a dual bioreactor
gas desulfurization system*



Karine Kiragosyan

Maximization of sulfur formation in the presence
of organic sulfur compounds in a dual bioreactor gas
desulfurization system

Karine Kiragosyan

Thesis committee

Promotor

Prof. Dr A.J.H. Janssen
Special professor Biological Gas Treating Processes
Wageningen University & Research

Co-promotors

Dr P. Roman
Post-doc
Wetsus-European Centre of Excellence for Sustainable Water Technology, Leeuwarden
Dr ir. J.B.M. Klok
Scientific project manager
Wetsus-European Centre of Excellence for Sustainable Water Technology, Leeuwarden

Other members

Prof. Dr H. Smidt, Wageningen University & Research
Prof. Dr G. Muijzer, University of Amsterdam
Dr F. Geuzebroek, Shell Technology Centre, Amsterdam
Prof. Dr E. Volcke, Ghent University, Belgium
The thesis was conducted under the auspices of the Graduate School for Socio-Economic and Natural Sciences of the Environment (SENSE)

Maximization of sulfur formation in the presence
of organic sulfur compounds in a dual bioreactor gas
desulfurization system

Karine Kiragosyan

Thesis

submitted in fulfilment of the requirements for the degree of doctor
at Wageningen University
by the authority of the Rector Magnificus,
Prof. Dr A.P.J. Mol,
in the presence of the
Thesis Committee appointed by the Academic Board
to be defended in public
on Wednesday 8 April 2020
at 1.30 p.m. in the Aula

Karine Kiragosyan

Maximization of sulfur formation in the presence of organic sulfur compounds in a dual bioreactor gas desulfurization system,
180 pages,

PhD thesis, Wageningen University, The Netherlands (2020)
With references, with summary in English

ISBN 978-94-6395-258-3

DOI <https://doi.org/10.18174/510040>

Table of contents

CHAPTER 1	Introduction	11
1.1	Why do we need gas desulfurization?	12
1.2	Characteristics of hydrogen sulfide and thiols	12
1.3	Sulfur recovery technologies	13
1.4.	Biotechnological sulfide removal	16
1.4.1.	Thiopaq process concept	16
1.4.2.	Sulfur-oxidizing bacteria	17
1.4.3.	Thiol toxicity effect on biological sulfide oxidation	18
1.4.4.	Control of oxygen supply to achieve higher sulfur selectivity	19
1.5	Aims and thesis outline	20
	References	23
 CHAPTER 2	 Development and validation of a physiologically based kinetic model for starting up and operation of the biological gas desulfurization process under haloalkaline conditions	 29
2.1	Introduction	30
2.2	Materials and Methods	31
2.2.1	Experimental setup and design	31
2.2.2	Biomass sources	33
2.2.3	Medium composition	33
2.2.4	Respiration test	34
2.2.5	Application of a physiologically based kinetic model	35
2.2.6	Analytical techniques	36
2.2.7	DNA extraction and 16S rRNA sequencing	37
2.3	Results	38
2.3.1	Biodesulfurization process performance	38
2.3.2	Bacterial community analyses	41
2.4	Discussion	42
2.5	Conclusions	45
	Acknowledgments	45
	References	47
	Appendix A - <i>Nomenclature.</i>	52
	Appendix B - <i>Non-linear least squares estimation of the kinetic model describing biological sulfide oxidation.</i>	53
	Appendix C - <i>Non-linear least squares estimation of formation rates.</i>	54
	Appendix D – <i>Predicted sulfate and sulfur selectivities</i>	55

CHAPTER 3	Development of quantitative PCR for the detection of <i>Alkalilimnicola ehrlichii</i>, <i>Thioalkalivibrio sulfidophilus</i> and <i>Thioalkalibacter halophilus</i> in gas biodesulfurization processes	57
3.1.	Introduction	58
3.2.	Materials and methods	59
3.2.1.	Microbial sludge sampling and sample preparation	59
3.2.2.	DNA isolation and purification	59
3.2.3.	Clone Library Construction and Sequencing	59
3.2.4.	Target species-specific primer design	60
3.2.5.	In vitro primer evaluation on target species pure cultures	60
3.2.6.	qPCR assay optimization	61
3.2.7.	Validation of the developed qPCR assay	62
3.2.8.	Accession number	63
3.3.	Results	63
3.3.1.	Primers evaluation and qPCR assay optimization	63
3.3.2.	Validation of the developed qPCR assay	65
3.4.	Discussion	65
	Acknowledgments	67
	References	68
	Appendix A – <i>Melting curves</i> .	71

CHAPTER 4	Effect of dimethyl disulfide on the sulfur formation and microbial community composition during the biological H₂S removal from sour gas streams	75
4.1	Introduction	76
4.2	Materials and Methods	77
4.2.1	Experimental setup and experimental design	77
4.2.2	Medium composition	79
4.2.3.	Inoculum	79
4.2.4	Respiration tests	79
4.2.5	Analytical techniques	80
4.2.6	Analysis of DMDS using Gas Chromatography with Flame Photometric Detector (GC-FPD)	82
4.2.6.1	GC-FPD system and calibration and gas samples analysis	82
4.2.6.2	Liquid samples analysis	82
4.2.6.3	Liquid-liquid extraction and sample injection	83
4.2.7	DNA isolation and purification	84

4.2.8 16S amplicon sequencing and qPCR	84
4.3. Results and discussion	85
4.3.1 Effect of DMDS on biological sulfide oxidation and product formation	85
4.3.2 Effect of DMDS on the microbial community composition	90
4.4 Conclusion	94
Acknowledgments	94
References	95
Appendix A - <i>Optimization of the GC-FPD method</i>	101
Appendix B - <i>Factor for conversion of ppm mole H₂S to mM S</i>	103
Appendix C – <i>Respiration tests</i>	104
Appendix D – <i>The lab-scale gas biodesulfurization process performance at high biomass concentration and addition of DMDS.</i>	105
Appendix F – <i>Reaction between sulfide and dimethyl disulfide in the bioreactor medium</i>	105
Appendix G – <i>Finding IC₅₀ value for Thioalkalibacter halophilus strain ALCO-1</i>	107

CHAPTER 5	Effect of methanethiol on the growth dynamics of sulfur-oxidizing bacteria and sulfur formation in the dual bioreactor gas biodesulfurization line-up	109
5.1	Introduction	110
5.2	Materials and Methods	111
5.2.1	Reactor operation	111
5.2.2	Inoculum	112
5.2.3	Microbial sludge sampling, sample preparation, and DNA extraction	113
5.2.4	qPCR	113
5.2.5	Bacterial community analyses	114
5.2.6	Statistical analysis	114
5.2.7	Analytical techniques	115
5.3.	Results and Discussion	117
5.3.1	Effect of methanethiol on process performance	117
5.3.2	Effect of methanethiol on sulfur-oxidizing bacterial community dynamics	121
5.4	Conclusions	124
	Acknowledgments	125

References	126
Appendix A – <i>Closing sulfur balance</i>	130
Appendix B – <i>Respiration tests</i>	131
Appendix C – <i>GC-FPD analysis of liquid and gas samples from the biodesulfurization lab-scale setup</i>	132
Appendix D – <i>Non-metric multidimensional scaling of 16S amplicon sequences</i>	133
Appendix E – <i>Statistical analysis of the qPCR results</i>	134

CHAPTER 6	A feedforward control strategy for oxygen supply in a gas biodesulfurization process	137
6.1	Introduction	138
6.2	Materials and Methods	140
6.2.1	Reactor operation	140
6.2.2	ORP-based feedback control	142
6.2.3	Alternative feedforward control	143
6.2.4	Medium composition	144
6.2.5	Inoculum	144
6.2.6	Analytical techniques	144
6.3	Results and Discussion	146
6.3.1	Importance of oxygen concentration	146
6.3.2	Process performance	148
6.4	Conclusions	151
	Acknowledgments	151
	References	152
Appendix A	<i>A dependency of ORP on sulfide concentration and oxygen concentration</i>	155
Appendix B	<i>Gas biodesulfurization process performance with use of ORP-based feedback control for oxygen supply</i>	156
Appendix C	<i>Concentrations of inorganic and organic sulphur compounds in the liquid and gas samples from the lab-scale gas biodesulfurization setup operation with ethanethiol addition.</i>	157

CHAPTER 7	Summary and general discussion	159
	7.1. Introduction	160
	7.2. Achieving optimal process performance	161
	7.3. Identified knowledge gaps	164
	7.3.1 Ecophysiology of the species within SOB community	165
	7.3.2 Development of molecular tools to monitor expression of FCC and SQR enzymes	166
	7.3.3 Robustness of the feedforward control at thigh thiol loadings	167
	References	168
 Epilogue		 171
	Author's publications and patents	172
	Acknowledgments	173
	About the author	176

CHAPTER 1



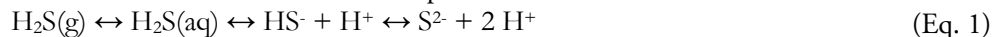
Introduction

1.1 Why do we need gas desulfurization?

Hydrogen sulfide (H_2S) and thiols are toxic and malodorous compounds, which have a low odor threshold and highly corrosive nature. These sulfur compounds are formed in the pulp industry, wastewater facilities, sewer systems, landfill sites, and are highly abundant in natural gas and crude oil [1,2]. The release of formed H_2S and thiols from the industrial sites into the environment has been regulated since 1970 by the Environmental Protection Agency (EPA) as it constitutes to severe health problems and causes the formation of sulfur dioxide (SO_2). SO_2 is a well-known gas that contributes to environmental pollution and affects health and Earth's biodiversity [3,4]. Therefore, all industries should comply with the set emission regulations by removing all sulfur components from the gas streams [5]. Through the years, regulations on sulfur emissions became even more stringent with the decreasing permitted emission limits. For instance, the most recent legislation caps the global sulfur content of shipping fuels at 0.5 % with a maximum for ships in EU ports at 0.1 % of sulfur. This regulation will be in force in 2020 [6] and will put pressure on the petrochemical industry to improve the desulfurization of crude oil and natural gas in order to comply with emission regulations.

1.2 Characteristics of hydrogen sulfide and thiols

Under ambient conditions, H_2S and methanethiol (MT) are gasses. H_2S is a colorless and flammable gas that has a distinctive smell of rotten eggs, and exposure to and above 500 ppm can be lethal [7] noting information gaps that may require further investigation. Several recommendations are listed for possible consideration for either toxicological research or additional short- and long-term tests. Two bibliographies have been provided to assist in locating references considered in this report: (1. H_2S is soluble in water; its solubility depends on conditions such as temperature, salinity, pH, partial gas pressure, and solvent content. Even when dissolved, H_2S remains volatile and equilibrates between the gas and aqueous phase. In the aqueous phase, H_2S equilibrates further with its anion forms HS^- and S^{2-} (Eq. 1) as it is a weak acid [8]. The pK_a values are 6.90 for HS^- and 12.92 for S^{2-} in pure water at 25 °C.



H_2S can react with oxidants, e.g., oxygen and nitrate, to form polysulfanes, sulfite, thiosulfate, and sulfate. In addition, it reacts with metals such as iron with which it can form insoluble iron-sulfide complexes.

Thiols are analogs of alcohol, in which the oxygen molecule is substituted by a sulfur atom creating a sulfhydryl group (R-SH), in which R can be an alkylic or aromatic group. Methanethiol (CH_3SH) is the most common thiol. All thiols are notorious for

their obnoxious smell, low odor threshold, and toxicity (Table 1), which can cause severe issues in the food industry [9]. For example, in the wine industry, certain thiols are considered desired provided they remain below their sensory threshold value as they contribute to pleasant grapefruit, passion fruit, and blackcurrant aromas [10].

The behavior and properties of thiols are determined by the properties of their hydrocarbons and weak acid gas components. For example, the longer the hydrocarbon chain is, the greater the hydrophobicity of a thiol. All thiols are weaker acids in comparison to H₂S, with a pK_a of 10.6 vs. 7.0 at 25 °C [11]. Similar to HS⁻, thiolates (the RS⁻ groups in thiols) are strong nucleophiles and poor bases [12]. Therefore, thiols easily undergo oxidation and form disulfides (Eq. 2):



H₂S and thiols can also react and form hydrodisulfide (Eq. 3), as well as it can reduce oxidized thiol/disulfide via nucleophilic displacement mechanism (Eq. 4) [13]:



Table 1 Properties of some thiols and associated diorgano polysulfanes.

Compound	Chemical formula	Odor threshold, ^a ppb	Smell
Methanethiol	HS—CH ₃	0.3 – 8.5	Rotten egg, fish, cabbage, garlic
Ethanethiol	H ₃ C—CH ₂ —SH	1.1	Onion, rubber, putrefaction
Dimethyl sulfide	H ₃ C—S—CH ₃	0.6 – 40	Cabbage, asparagus, corn, molasses
Dimethyl disulfide	H ₃ C—S—S—CH ₃	0.1 – 3.6	cooked cabbage, asparagus, onions
Dimethyl trisulfide	H ₃ C—S—S—S—CH ₃	0.1	Cabbage, onions, cooked vegetables
Diethyl sulfide	H ₃ C—CH ₂ —S—CH ₂ —CH ₃	0.93 – 18	Garlic
Diethyl disulfide	H ₃ C—CH ₂ —S—S—CH ₂ —CH ₃	4.3 – 40	Garlic, onion, burnt rubber

^a[14], ^b[15]

1.3 Sulfur recovery technologies

Nowadays, various desulfurization technologies are available to remove H₂S from gas streams and convert them into elemental sulfur (Fig. 1). Most of these sulfur recovery processes can be roughly divided into three niches: small-size (<0.05 tons per day (TPD) of H₂S), medium-size (0.5 to 20 TPD), and large-size (>20 TPD). These categories are based on the applicability of different desulfurization techniques.

For low H_2S loads (< 0.05 TPD), liquid and solid scavengers are applied. Various solvents are used to absorb sulfide, such as polyamines (triazines), nitrite, and caustic. Caustic scavengers are often applied to absorb sulfide from acid gas streams resulting in the formation of spent caustic waste streams. The advantage of the use of a scavenger is that the capital expenditure (CAPEX) is relatively low. However, as the liquid in scavengers is not reusable, they are not suitable for large sulfur loads given the high operating expense (OPEX) (i.e., \$5200 per ton processed H_2S) [16].

For H_2S loadings of up to 20 TPD, regenerable processes are the most cost-effective, such as Thiopaq (H_2S loading of to 70 TPD) and liquid redox processes (see Section 1.4 for biodesulfurization). Liquid redox processes with an OPEX between \$1000 - \$2000 per ton of processed H_2S [16], use an alkaline solution with high valent metal ions, such as iron (LoCat and Sulferox). Iron ions convert dissolved sulfide into elemental sulfur and are then regenerated by oxidation with air. As the formed elemental sulfur is hydrophobic, process malfunctions can occur, such as caused by plug formation in tubing and foaming [17]. An alternative for liquid redox processes is CrystaSulf technology. It is a catalytic oxidation process that uses a non-aqueous hydrocarbon solvent that contains SO_2 [18]. The process solution comes into contact with H_2S , and elemental sulfur and water are formed. Afterward, the formed sulfur is dissolved in the solvent, followed by precipitation in a crystallizer. This step was designed to overcome issues of plugging and foaming. However, it increases solvent use, resulting in higher costs for larger-scale operations or high sulfide loads [19].

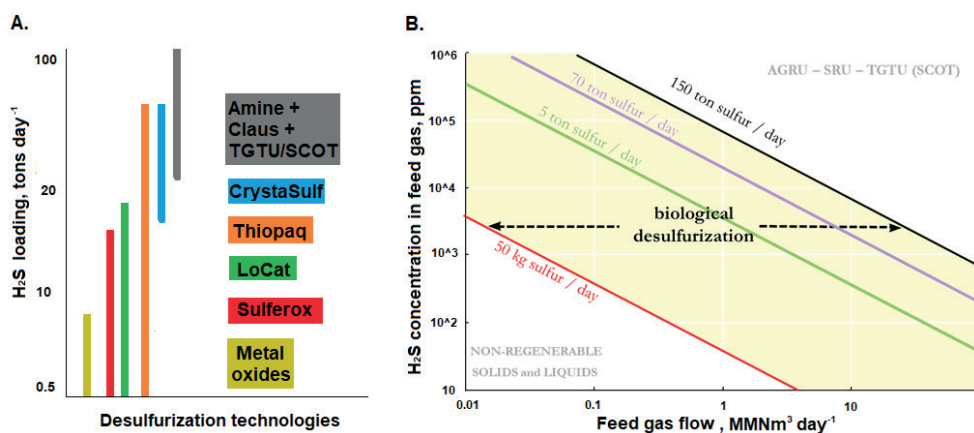
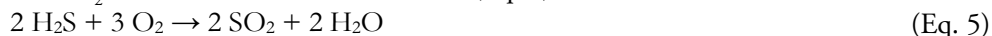


Fig. 1. Schematic overview of (A) available desulfurization technologies that produce elemental sulfur from different sulfide loadings (adapted from [20]) and (B) operational window of Thiopaq O&G based on feed gas flow and H_2S concentrations in the feed gas. AGRU = acid gas removal unit, SRU – sulfur recovery unit (Claus), TGTU = tail gas treatment unit, SCOT = Shell Claus Off-gas Treating process (personal communication Paqell BV, 2019).

For H_2S loading rates above 20 TPD, the AGRU-SRU-TGTU process is vastly applied (Fig. 1B). The process starts in the acid gas removal unit (AGRU), using amine-based solvents to absorb H_2S from the sour gas. An acid gas mixture is stripped in the regenerator; it contains H_2S , CO_2 , thiols, and some hydrocarbons [21]. In the next step, the acid gas is routed to the Claus unit for sulfur recovery (SRU). The Claus process is a two or three-stage process, with a thermal stage in which one-third of the H_2S gas is burned to SO_2 (Eq. 5), followed by one or two thermal-catalytic stages in which H_2S and SO_2 react and form elemental sulfur (Eq. 6).



The Claus process is a highly cost-efficient process for large scale H_2S conversion and is vastly applied in the industry, with an OPEX of \$3 to \$4 per ton of processed H_2S [22]. Downsides of this process are a) relative complex process schemes to optimize heat integration resulting in high CAPEX and b) that the H_2S removal and process recovery efficiency is limited to about 95 to 97 % due to the equilibrium of the catalyzed reactions (Eq. 6) [23]. Meeting the stringent regulations for SO_2 emissions generally requires a sulfur recovery of more than 99 %. Hence, off-gas that leaves the Claus process needs to be treated as well. In general, the Shell Claus off-gas treating (SCOT[®]) unit is installed after the Claus process to achieve 99.9 % efficiency. This SCOT process converts all sulfur compounds to H_2S which is subsequently rerouted to the thermal stage of the Claus process. The gaseous effluent stream of the SCOT[®] process still contains <200 ppmv H_2S , which is incinerated to avoid release of H_2S into the environment. CAPEX of SCOT unit is almost similar to Claus process, what makes removal of the last 3-5 % of H_2S same expensive as the first 95 %.

Several chemical processes were developed for the combined removal of H_2S gas and volatile organic sulfur compounds (VOSCs). One of the most commonly used technologies applied for the removal of VOSCs, and particularly thiols, is the Merox[™] process [24]. This process is based on the catalytic oxidation of thiols to disulfides, which are separated from the solvent and reused in other application areas [25]. For instance, dimethyl disulfide is used as a soil fumigant [26,27].

The available technologies for the removal of H_2S and thiols are efficient and find their niches on the market. Nevertheless, these technologies are neither flexible nor cost-effective for small to medium sulfur load. Thiopaq O&G, on the other hand, is a flexible biotechnological process with minimized operational costs and chemical consumption. In the world that is packed with human waste and battles global warming, sustainable technologies are a must, to decrease the human footprint on nature.

1.4. Biotechnological sulfide removal

1.4.1. Thiopaq process concept

The traditional Thiopaq gas biodesulfurization process consists of a gas absorber, a bioreactor, and a sulfur recovery section (Fig. 2). Supplied H_2S and CO_2 are absorbed by the haloalkaline solvent in an absorber, and the resulting sulfide solution is fed to an aerobic bioreactor, in which haloalkaline sulfur-oxidizing bacteria (SOB) biologically oxidize the sulfide to sulfur and sulfate:

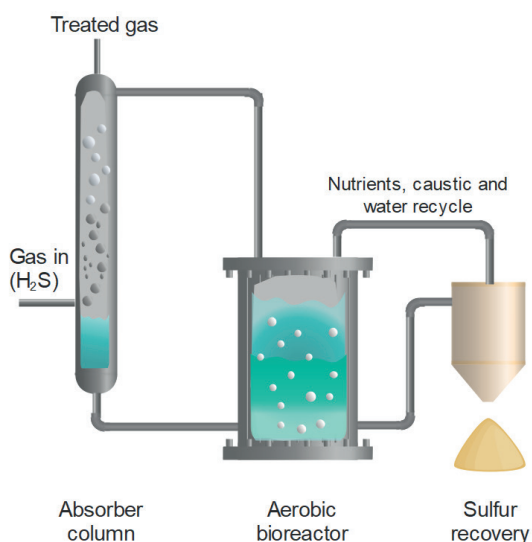


Fig. 2. Schematic representation of the classical (i.e., 1-stage) Thiopaq process technology.

Sulfur is the preferred end-product as the formed hydroxyl ions (Eq. 7) neutralize the process solution, which allows its reuse in the gas absorber. This results in a decrease in chemical consumption and OPEX, and therefore higher sustainability [29]. The formation rate of sulfur and sulfate is related to the amount of oxygen/air that is supplied to the system per sulfide ($\text{O}_2/\text{H}_2\text{S}$ ratio), which determines the oxidation-reduction potential (ORP) of the process solution [30]. The formed bio-sulfur is separated from the solvent by the decanter centrifuge in the final stage of the process (Fig. 2). The recovered bio-sulfur is hydrophilic and can be used as a fertilizer, for chemical processing, metal manufacturing, and rubber vulcanization [31–33]. Thus, through decades of scientific research by our research group, key process parameters have been identified and optimized in order to achieve higher sulfur selectivity. The largest limitations for

achieving sulfur selectivity above 85 - 90 mol% are a) the SOB biomass inoculum b) their inability to withstand the toxicity of thiols and c) oversupply of oxygen, due to the bias of the ORP sensor towards thiols and diorgano polysulfanes [34–38].

1.4.2. Sulfur-oxidizing bacteria

Haloalkaline SOB are microorganisms that are naturally occurring in highly saline and alkaline environments such as soda lakes [39,40]. These SOB can grow chemolithoautotrophically using inorganic sulfur compounds as electron donors and CO_2 as a carbon source (Fig. 3) [41]. Because of their metabolism, these SOB are employed in biotechnological processes to remove H_2S from industrial gas streams [42,43]. Recently, haloalkaliphilic SOB have also found an application for sulfide removal and hydrogen production in bioelectrochemical systems [44].

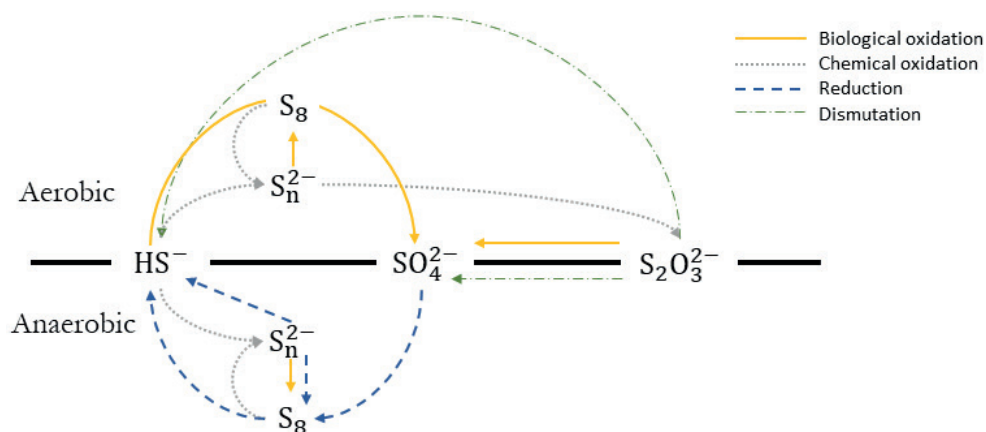


Fig. 3. Schematic representation of the biogeochemical sulfur cycle in the gas biodesulfurization process (adapted from [45]).

In the Thiopaq process solution, the SOB community composition is complex and species-rich, consisting of microorganisms involved in both anaerobic and aerobic processes [29]. Such microbial communities are known for their metabolic flexibility and resilience. Therefore, SOB community compositions have been studied under different conditions in full- and lab-scale installations to unveil their structure and sulfur metabolism with the aim of enabling higher sulfur selectivity. The dominant SOB species found in systems treating H_2S gas are *Thioalkalivibrio sulfidiphilus* [29,46–48]. These species belong to the genus of haloalkaliphilic and chemolithoautotrophic *Thioalkalivibrio* (0.2 – 4 M Na^+ at pH 10), of which the members use reduced sulfur compounds, such as sulfide, polysulfide, thiosulfate and elemental sulfur, as an energy source [49]. A peculiar feature of *Tv. sulfidiphilus* is its complete sulfide specialization

with no thiosulfate oxidizing activity [50]. The SOB community in full- and lab-scale installations treating various gas compositions can undergo changes in microbial composition and abundance based on process conditions and SOB species metabolism. This means that changes in the composition are usually accompanied by changes in sulfur and sulfate selectivity. The significant changes in SOB communities were found to occur when methanethiol (MT) was added to the feed gas. It was found that *Thioalkalibacter halophilus* species proliferate under conditions of elevated MT concentrations, whereas there is a drastic abundance decrease of usually dominating *Tv. sulfidiphilus* [48]. As soon as the abundance of *Thb. halophilus* increases, the sulfur selectivity starts to increase as well. These community changes show that different process conditions also require different SOB inocula to enable high sulfur selectivities. However, no clear causal correlation is known yet between SOB community composition/inoculum and sulfur selectivity.

1.4.3. Thiol toxicity effect on biological sulfide oxidation

Thiols are highly toxic compounds not only for humans but also for microorganisms. Research groups at Technical University Delft, Radboud University, in cooperation with Warwick University studied cycling of organic sulfur compounds in microbial ecosystems. For example, bacteria was isolated from microbial mats [51,52] or freshwater sediments [53–55] and characterized on the oxidation capacity of organic sulfur compounds (i.e., thiols, DMS and DMDS), and cycling of these sulfur compounds in different ecosystems. The first insights into the effect of volatile organic sulfur compounds on the gas biodesulfurization process was assessed by Van den Bosch et al. who investigated the effect of MT and dimethyl polysulfanes on biological sulfide oxidation at relatively low MT loading rates, without addressing SOB community dynamics [34,35]. The investigation of the effect of MT on the gas biodesulfurization process (performance) was continued by Roman et al., who studied the effect of thiols in the traditional Thiopaq setup and found that sulfur selectivity is negatively affected by thiols and their concentrations [36,38]. Roman et al. (2016c) assessed the toxicity of thiols and corresponding diorgano polysulfanes to understand how inhibition of biological sulfide oxidation occurs and at which level; they found that thiols inhibit sulfur formation (Fig. 4 R1), whereas the formed diorgano polysulfanes (DOPS) selectively inhibit sulfate formation (Fig. 4 R2). Giving this, it may be possible to engineer the gas biodesulfurization process to avoid SOB poisoning and achieve higher sulfur selectivity. Furthermore, sulfate selectivity may be minimized by selective inhibition with DOPS.

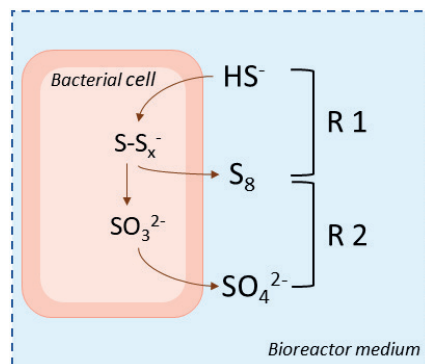


Fig. 4. Schematic representation of biological sulfide oxidation by SOB. R1 – reaction 1, R2 – reaction 2 (adapted from [37]).

The inhibition of sulfide oxidation occurs in the SOB cell at the beginning of the electron transport chain, when thiol binds to the sulfide oxidizing enzyme flavocytochrome *c* oxidase (FCC), leading to SOB deactivation and prevalence of chemical sulfide oxidation. However, not all SOB are inhibited. Some SOB use a different enzyme for sulfide oxidation, i.e., sulfide-quinone oxidoreductase (SQR). Thus, these SOB species will dominate the SOB community [36]. To answer why certain SOB species proliferate in the presence of thiols and others decline with certainty, more detailed information on the gene level is required.

1.4.4. Control of oxygen supply to achieve higher sulfur selectivity

The selectivity for sulfur formation is not only determined by biological factors, but also by the availability of oxygen in the bioreactor. Oxidation of sulfide to sulfur is highly sensitive to oxygen concentration [30,42]. Therefore, to enable higher sulfur selectivity and eliminate overoxidation of sulfide to sulfate, the oxygen supply should be accurately controlled.

In biodesulfurization, the process solution's ORP is mainly determined by the sulfide concentration [30]. Hence, pairing an ORP sensor with a proportional integral derivative (PID) controller allows controlling the oxygen supply to the aerobic bioreactor (Fig. 5). The advantage of this control strategy is its simplicity. However, volatile organic sulfur compounds such as thiols and diorgano polysulfanes affect the ORP of the solution by reducing it more [48]. Hence, the ORP of the process solvent is no longer determined by only the sulfide concentration, which makes the use of ORP-based system control for oxygen supply challenging.

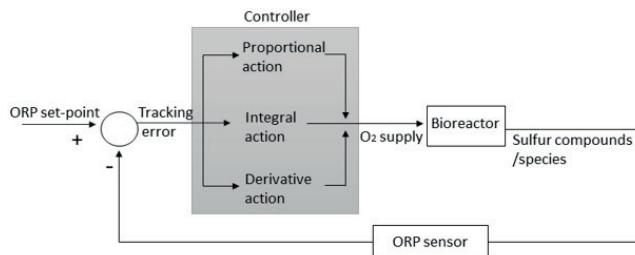


Fig. 5. Schematic representation of the ORP-based PID feedback control for oxygen supply in the gas biodesulfurization process.

1.5 Aims and thesis outline

This thesis aims to study H_2S removal from sour gas streams in the presence of thiols in the new gas biodesulfurization line-up called Thiopaq Ultra. The traditional gas biodesulfurization line-up was modified to overcome the above-mentioned limitations and facilitate higher sulfur selectivities (Fig. 6). In this setup, an anaerobic bioreactor is added between the absorber and the aerobic bioreactor. This makes it possible to increase the SOB retention time in the sulfide-rich process solution that comes from the absorber. This increased retention time (0 vs. 15 min, in a lab-scale system) allows the reduction of sulfate and thiosulfate selectivity, consequently increasing sulfur selectivity [56]. De Rink et al. also found that the microbial community changed after 73 days of continuous process operation; the regularly dominating *Thioalkalivibrio sulfidiphilus* was replaced by *Alkalilimnicola ehrlichii*. These results provided the first insights into the capacity and efficiency of the Thiopaq Ultra lineup, whereas the process efficiency in the presence of thiols was still unknown. Therefore, to widen the operational window of Thiopaq Ultra and to enable biodesulfurization of feed gases containing thiols, the effect of thiols on sulfur selectivity had to be investigated. For my Ph.D. research, I studied the underlying biochemical processes and factors that govern SOB community dynamics in the Thiopaq Ultra line-up in the presence of thiols. The main question was whether it is possible to achieve higher sulfur selectivities (>95 mol%) at elevated thiol concentrations?

To achieve this goal, several research tasks were defined:

- Investigation of the process operation dependency on the origin of the SOB biomass and sulfur selectivity in order to develop a methodology for SOB biomass selection to start-up full-scale installations;
- Method development for an absolute SOB key-species quantification;
- Evaluation of the dual biodesulfurization line-up in the presence and absence of thiols, understanding underlying biochemical reactions of H_2S oxidation and SOB community dynamics;

- Investigation of the selective inhibition of sulfate formation by the addition of dimethyl disulfide;
- Development of an alternative oxygen supply control strategy to enable stable process operation with high sulfur selectivity (>95 mol%) in the presence of thiols.

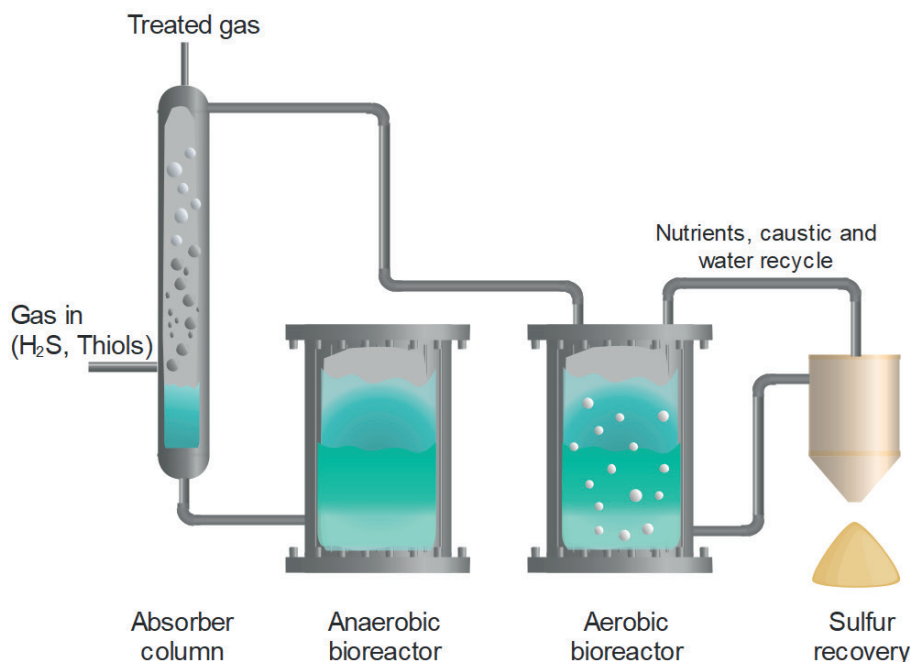


Fig. 6. Schematic representation of the Thiopaq Ultra process.

Chapter 2 describes the effects of SOB microbial composition and kinetics of biological sulfide oxidation on the efficiency of the traditional gas biodesulfurization process. To unveil the dependencies between SOB composition, SOB kinetics, and process operation, a physiologically based kinetic model was developed and applied to the four studied SOB inocula. The model was calibrated by measuring biological sulfide oxidation rates for different inocula obtained from four full-scale biodesulfurization installations fed with gases from various industries. The model relies on a ratio of two key enzymes involved in the sulfide oxidation process, i.e., flavocytochrome c oxidase and sulfide-quinone oxidoreductase (FCC and SQR). However, most of the SOB contain both enzyme systems. Therefore, we introduced a new model parameter α , which describes the ratio between the expression levels of FCC and SQR.

When working with a biotechnological process, it is crucial to understand why the microbial community changes over time, and how it influences process performance. Moreover, will we be able to find key SOB species that enable safe and stable process

operation in the presence of thiols? To be able to relate SOB community dynamics and process operation conditions, my colleagues and I developed a quantitative PCR assay (qPCR) with designed target-specific primers (**Chapter 3**). The developed assay allowed me to monitor absolute species abundance of the three most dominant haloalkaliphilic SOB species found in full- and lab-scale biodesulfurization installations so far: *Alkalilimnicola ehrlichii*, *Thioalkalivibrio sulfidophilus*, and *Thioalkalibacter halophilus*.

Chapter 4 is a follow-up to the study by Roman et al. [37], who looked into inhibition modes of commonly present thiols and diorgano polysulfanes. Thiols were found to inhibit biological sulfide oxidation from sulfide to sulfur, whereas diorgano polysulfanes were selectively inhibiting sulfate formation. To explore this finding further, I studied the effects of dimethyl disulfide (DMDS) on sulfate selectivity in the dual-bioreactor lab-scale gas biodesulfurization setup in order to maximize sulfur formation. In addition, I monitored the SOB community composition dynamics. Moreover, this chapter presents a new analytical method developed in-house for the detection and measurement of organic sulfur compounds in liquid and gas phases.

Chapter 5 describes the continuation of the work with volatile organic sulfur compounds, a study of the effects of MT addition on the process performance and dynamics of the SOB microbial community. We were interested to find out whether sulfur selectivity can be increased in the presence of thiols in a dual-bioreactor setup in comparison with a traditional single-bioreactor. Our results show that with the use of a dual-bioreactor setup, the sulfur formation can be increased by 10 mol%. Moreover, the sulfur formation can be enhanced by the preselection of SOB. For instance, a higher abundance of *Thiolakalibacter halophilus* and *Alkalilimnicola ehrlichii* at the start-up of the process will enable more stable process operation and higher sulfur formation in the presence of thiols. However, the results also show a re-occurring issue with the process control strategy, as in the presence of volatile organic sulfur compounds ORP-based feedback control strategy is compromised.

Chapter 6 details how we developed and tested an alternative feedforward process control strategy based on the O_2/H_2S supply ratio.

Finally, **Chapter 7** provides a general discussion of the topics covered in this thesis and an outlook for future research.

References

- [1] N.P. Cheremisinoff, P.E. Rosenfeld, *Handbook of Pollution Prevention and Cleaner Production*, Elsevier, 2010. doi:10.1016/C2009-0-20361-8.
- [2] M.A. Fahim, T.A. Alsahhaf, A. Elkilani, Acid Gas Processing and Mercaptans Removal, in: *Fundam. Pet. Refin.*, 2010: pp. 377–402. doi:10.1016/b978-0-444-52785-1.00015-2.
- [3] A. Singh, M. Agrawal, Acid rain and its ecological consequences, *J. Environ. Biol.* 29 (2008) 15–24.
- [4] J.O. Reuss, D.W. Johnson, *Acid deposition and the acidification of soil and waters*, Ecological, Springer International Publishing, 1986.
- [5] S. Adhikari, N. Abdoulmoumine, H. Nam, O. Oyediji, Biomass gasification producer gas cleanup, in: *Bioenergy Syst. Futur. Prospect. Biofuels Biohydrogen*, Elsevier Ltd., 2017: pp. 541–557. doi:10.1016/B978-0-08-101031-0.00016-8.
- [6] International Chamber of Shipping, Compliance with the 2020 ‘Global Sulphur Cap’, (2019) 40.
- [7] R.O. Beauchamp, J.S. Bus, J.A. Popp, C.J. Boreiko, D.A. Andjelkovich, P. Leber, A critical review of the literature on hydrogen sulfide toxicity, *Crit. Rev. Toxicol.* 13 (1984) 25–97. doi:10.3109/10408448409029321.
- [8] K.Y. Chen, J.C. Morris, Kinetics of oxidation of aqueous sulfide by oxygen, *Environ. Sci. Technol.* 6 (1972) 529–537. doi:10.1021/es60065a008.
- [9] C. Yeretizian, I. Blank, Y. Wyser, *Protecting the Flavors-Freshness as a Key to Quality*, Elsevier Inc., 2017. doi:10.1016/B978-0-12-803520-7.00014-1.
- [10] G.Y. Kreitman, R.J. Elias, D.W. Jeffery, G.L. Sacks, Loss and formation of malodorous volatile sulfhydryl compounds during wine storage, *Crit. Rev. Food Sci. Nutr.* (2019). doi:10.1080/10408398.2018.1427043.
- [11] C. Tsonopoulos, D.M. Coulson, B.I. Lawrence, Ionization Constants of Water Pollutants, *J. Chem. Eng. Data.* 21 (1976) 190–193. doi:10.1021/je60069a008.
- [12] D. Klein, *Organic Chemistry*, 2nd ed., Wiley, 2014. doi:10.1001/jama.1945.02860350099036.
- [13] Q. Li, J.R. Lancaster, Chemical foundations of hydrogen sulfide biology, *Nitric Oxide - Biol. Chem.* 35 (2013) 21–34. doi:10.1016/j.niox.2013.07.001.
- [14] D. Fracassetti, I. Vigentini, Occurrence and analysis of sulfur compounds in wine, in: *Grapes Wines - Adv. Prod. Process. Anal. Valorization*, InTech, 2018: pp. 225–251. doi:10.5772/57353.
- [15] B.P. Lomans, C. Van der Drift, A. Pol, H.J.M. Op den Camp, Microbial cycling of volatile organic sulfur compounds, *Cell. Mol. Life Sci.* 59 (2002) 575–588.
- [16] B. Echt, D. Leppin, D. Mamrosh, D. Miradian, D. Seeger, B. Warren, Fundamentals of Low-Tonnage Sulfur Removal and Recovery, in: *Laurance Reid Gas Cond. Conf.*, 2017.

- [17] D. Deberry, Chemical evolution of liquid redox processes, *Environ. Prog.* 16 (1997) 193–199. doi:10.1002/ep.3300160316.
- [18] D.A. Dalrymple, T.W. Trofe, J.M. Evans, Liquid redox sulfur recovery options, costs, and environmental considerations, *Environ. Prog.* 8 (1989) 217–222. doi:10.1002/ep.3300080412.
- [19] D. Dalrymple, Hybrid Sulfur Recovery Process for Natural Gas Upgrading, 2002.
- [20] P. Hauwert, Sweetening and Sulfur recovery of sour associate gas and lean acid gas in the Middle East, in: Abu Dhabi Int. Pet. Exhib. Conf., 2014: p. 22.
- [21] U. Shoukat, D. Pinto, H. Knuutila, Study of Various Aqueous and Non-Aqueous Amine Blends for Hydrogen Sulfide Removal from Natural Gas, *Processes*. 7 (2019) 160. doi:10.3390/pr7030160.
- [22] Y. Al Wahedi, A.I. Torres, S. Al Hashimi, N.I. Dowling, P. Daoutidis, M. Tsapatsis, Economic assessment of Temperature Swing Adsorption systems as Claus Tail Gas Clean Up Units, *Chem. Eng. Sci.* 126 (2015) 186–195. doi:10.1016/j.ces.2014.12.015.
- [23] U.S. Environmental Protection Agency, Sulfur Recovery, *Compil. Air Pollut. Emiss. Factors AP-42*. 93 (1995) 2–6. http://www.epa.gov/ttn/chief/ap42/ch08/final/c08s13_2015.pdf.
- [24] S. Zendehboudi, A. Bahadori, Shale gas processing, in: *Shale Oil Gas Handb.*, 2017: pp. 153–192. doi:10.1016/B978-0-12-802100-2.00005-8.
- [25] J.C. Bricker, L. Laricchia, Advances in Merox™ process and catalysis for thiol oxidation, *Top. Catal.* 55 (2012) 1315–1323. doi:10.1007/s11244-012-9913-0.
- [26] US-Environmental Protection Agency, Pesticide Fact Sheet - Dimethyl Disulfide, (2010) 1–25. https://www3.epa.gov/pesticides/chem_search/reg_actions/pending/fs_PC-029088_09-Jul-10.pdf.
- [27] A.H. Putnam, Frequently Asked Questions about Dimethyl Disulfide, (2014) 7–10.
- [28] Gaylord Chemical Company, Catalyst Sulfiding Overview, *Bull.* 205. (2015) 1–8.
- [29] A.J.H. Janssen, P.N.L. Lens, A.J.M. Stams, C.M. Plugge, D.Y. Sorokin, G. Muyzer, H. Dijkman, E. Van Zessen, P. Luimes, C.J.N. Buisman, Application of bacteria involved in the biological sulfur cycle for paper mill effluent purification, *Sci. Total Environ.* 407 (2009) 1333–1343. doi:10.1016/j.scitotenv.2008.09.054.
- [30] A.J.H. Janssen, S. Meijer, J. Bontsema, G. Lettinga, Application of the Redox Potential for Controlling a Sulfideoxidizing Bioreactor, *Biotechnol. Bioeng.* 60 (1998) 147–155. doi:10.1002/(SICI)1097-0290(19981020)60:2<147::AID-BIT2>3.0.CO;2-N.
- [31] A.J.H. Janssen, A. De Keizer, G. Lettinga, Colloidal properties of a microbiologically produced sulphur suspension in comparison to a LaMer sulphur sol, *Colloids Surfaces B Biointerfaces*. 3 (1994) 111–117.
- [32] Ceradis Agro Formulation, CeraSulfur® SC The Natural Way to Higher Yield, (2017).
- [33] A.Y. Coran, Vulcanization, in: *Sci. Technol. Rubber*, 2013: pp. 337–381. doi:10.1016/B978-0-12-394584-6.00007-8.

- [34] P.L.F. Van Den Bosch, M. De Graaff, M. Fortuny-Picornell, R.C. Van Leerdam, A.J.H. Janssen, Inhibition of microbiological sulfide oxidation by methanethiol and dimethyl polysulfides at natron-alkaline conditions, *Appl. Microbiol. Biotechnol.* 83 (2009) 579–587. doi:10.1007/s00253-009-1951-6.
- [35] P.L.F. Van Den Bosch, M. Fortuny-Picornell, A.J.H. Janssen, Effects of Methanethiol on the Biological Oxidation of Sulfide at Natron-Alkaline Conditions, *Environ. Sci. Technol.* 43 (2009) 453–459. doi:10.1021/es801894p.
- [36] P. Roman, R. Veltman, M.F.M. Bijmans, K.J. Keesman, A.J.H. Janssen, Effect of Methanethiol Concentration on Sulfur Production in Biological Desulfurization Systems under Haloalkaline Conditions, *Environ. Sci. Technol.* 49 (2015) 9212–9221. doi:10.1021/acs.est.5b01758.
- [37] P. Roman, J. Lipińska, M.F.M. Bijmans, D.Y. Sorokin, K.J. Keesman, A.J.H. Janssen, Inhibition of a biological sulfide oxidation under haloalkaline conditions by thiols and diorgano polysulfanes, *Water Res.* 101 (2016) 448–456. doi:10.1016/j.watres.2016.06.003.
- [38] P. Roman, M.F.M. Bijmans, A.J.H. Janssen, Influence of methanethiol on biological sulphide oxidation in gas treatment system, *Environ. Technol.* 3330 (2016) 1–11. doi:10.1080/09593330.2015.1128001.
- [39] D.Y. Sorokin, J.G. Kuenen, Haloalkaliphilic sulfur-oxidizing bacteria in soda lakes, *FEMS Microbiol. Rev.* 29 (2005) 685–702. doi:10.1016/j.femsre.2004.10.005.
- [40] D.Y. Sorokin, H. Banciu, L.A. Robertson, J.G. Kuenen, M.S. Muntyan, G. Muyzer, Halophilic and haloalkaliphilic sulfur-oxidizing bacteria, in: E. Rosenberg, E.F. DeLong, E. Stackebrandt, S. Lory, F. Thompson (Eds.), *Prokaryotes Prokaryotic Physiol. Biochem.*, Springer-Verlag, Berlin-Heidelberg, 2013: pp. 530–555. doi:10.1007/978-3-642-30141-4.
- [41] W. Ghosh, B. Dam, Biochemistry and molecular biology of lithotrophic sulfur oxidation by taxonomically and ecologically diverse bacteria and archaea, *FEMS Microbiol. Rev.* 33 (2009) 999–1043. doi:10.1111/j.1574-6976.2009.00187.x.
- [42] P.L.F. Van Den Bosch, O.C. Van Beusekom, C.J.N. Buisman, A.J.H. Janssen, Sulfide oxidation at halo-alkaline conditions in a fed-batch bioreactor, *Biotechnol. Bioeng.* 97 (2007) 1053–1063. doi:10.1002/bit.21326.
- [43] D.Y. Sorokin, J.G. Kuenen, G. Muyzer, The microbial sulfur cycle at extremely haloalkaline conditions of soda lakes, *Front. Microbiol.* 2 (2011). doi:10.3389/fmicb.2011.00044.
- [44] G. Ni, P. Harnawan, L. Seidel, A. Ter Heijne, T. Sleutels, C.J.N. Buisman, M. Dopson, Haloalkaliphilic microorganisms assist sulfide removal in a microbial electrolysis cell, *J. Hazard. Mater.* 363 (2019) 197–204. doi:10.1016/j.jhazmat.2018.09.049.
- [45] T. Berben, Comparative analysis of sulfur oxidation pathways in haloalkaliphilic thiocyanate-utilizing species of the genus, Universitit van Amsterdam, 2019.
- [46] D.Y. Sorokin, M.S. Muntyan, A.N. Panteleeva, G. Muyzer, *Thioalkalivibrio sulfidiphilus* sp. nov., a haloalkaliphilic, sulfur-oxidizing gammaproteobacterium from alkaline habitats, *Int. J. Syst. Evol. Microbiol.* 62 (2012) 1884–1889. doi:10.1099/ij.s.0.034504-0.

- [47] D.Y. Sorokin, P.L.F. Van Den Bosch, B. Abbas, A.J.H. Janssen, G. Muyzer, Microbiological analysis of the population of extremely haloalkaliphilic sulfur-oxidizing bacteria dominating in lab-scale sulfide-removing bioreactors, *Appl. Microbiol. Biotechnol.* 80 (2008) 965–975. doi:10.1007/s00253-008-1598-8.
- [48] P. Roman, J.B.M. Klok, J.A.B. Sousa, E. Broman, M. Dopson, E. Van Zessen, M.F.M. Bijmans, D.Y. Sorokin, A.J.H. Janssen, Selection and Application of Sulfide Oxidizing Microorganisms Able to Withstand Thiols in Gas Biodesulfurization Systems, *Environ. Sci. Technol.* (2016) acs.est.6b04222. doi:10.1021/acs.est.6b04222.
- [49] A.-C. Ahn, L. Overmars, D.Y. Sorokin, J.P. Meier-Kolthoff, G. Muyzer, M. Richter, T. Woyke, Genomic diversity within the haloalkaliphilic genus *Thioalkalivibrio*, *PLoS One*. 12 (2017) e0173517. doi:10.1371/journal.pone.0173517.
- [50] G. Muyzer, D.Y. Sorokin, K. Mavromatis, A. Lapidus, A. Clum, N. Ivanova, A. Pati, P. D’Haeseleer, T. Woyke, N.C. Kyrpides, Complete genome sequence of “*Thioalkalivibrio sulfidophilus*” HL-EbGr7, *Stand. Genomic Sci.* 4 (2011) 23–35. doi:10.4056/sigs.1483693.
- [51] J.M.M. De Zwart, J.G. Kuenen, C1-cycle of sulfur compounds, *Biodegradation*. 3 (1992) 37–59. doi:10.1007/BF00189634.
- [52] J.M.M. De Zwart, P.N. Nelisse, J.G. Kuenen, Isolation and characterization of *Methylophaga sulfidovorans* sp. nov.: An obligately methylotrophic, aerobic, dimethylsulfide oxidizing bacterium from a microbial mat, *FEMS Microbiol. Ecol.* 20 (1996) 261–270. doi:10.1016/0168-6496(96)00038-4.
- [53] B.P. Lomans, A. Pol, H.J.M. Op den Camp, Microbial cycling of volatile organic sulfur compounds in anoxic environments, *Water Sci. Technol.* 45 (2002) 55–60. doi:10.1007/s00018-002-8450-6.
- [54] B.P. Lomans, P. Leijdekkers, J.J. Wesselink, P. Bakkes, A. Pol, C. Van Der Drift, H.J.M. Op Den Camp, Obligate Sulfide-Dependent Degradation of Methoxylated Aromatic Compounds and Formation of Methanethiol and Dimethyl Sulfide by a Freshwater Sediment Isolate, *Parasporobacterium paucivorans* gen. nov., sp. nov., *Appl. Environ. Microbiol.* 67 (2001) 4017–4023. doi:10.1128/AEM.67.9.4017-4023.2001.
- [55] B.P. Lomans, R. Maas, R. Luderer, H.J.M.O. den Camp, A. Pol, C. van der Drift, G.D. Vogels, Isolation and characterization of *Methanomethylovorans hollandica* gen. nov., sp. nov., isolated from freshwater sediment, a methylotrophic methanogen able to grow on dimethyl sulfide and methanethiol, *Appl. Environ. Microbiol.* 65 (1999) 3641–3650.
- [56] R. De Rink, J.B.M. Klok, D.Y. Sorokin, G.J. Van Heeringen, A. Ter Heijne, R. Zeijlmaker, Y.M. Mos, V. De Wilde, K.J. Keesman, C.J.N. Buisman, Increasing the selectivity for sulfur formation in biological gas desulfurization, *Environ. Sci. Technol.* 53 (2019) 4519–4527. doi:10.1021/acs.est.8b06749.

CHAPTER 2



Development and validation of a physiologically based kinetic model for starting up and operation of the biological gas desulfurization process under haloalkaline conditions

Abstract

Hydrogen sulfide is a toxic and corrosive gas that must be removed from gaseous hydrocarbon streams prior to combustion. This paper describes a gas biodesulfurization process where sulfur-oxidizing bacteria (SOB) facilitate sulfide conversion to both sulfur and sulfate. In order to optimize the formation of sulfur, it is crucial to understand the relations between the SOB microbial composition, kinetics of biological and abiotic sulfide oxidation and the effects on the biodesulfurization process efficiency. Hence, a physiologically based kinetic model was developed for four different inocula. The resulting model can be used as a tool to evaluate biodesulfurization process performance. The model relies on a ratio of two key enzymes involved in the sulfide oxidation process, i.e., flavocytochrome c and sulfide-quinone oxidoreductase (FCC and SQR). The model was calibrated by measuring biological sulfide oxidation rates for different inocula obtained from four full-scale biodesulfurization installations fed with gases from various industries. Experimentally obtained biological sulfide oxidation rates showed dissimilarities between the tested biomasses which could be explained by assuming distinctions in the key-enzyme ratios. Hence, we introduce a new model parameter α to whereby α describes the ratio between the relative expression levels of FCC and SQR enzymes. Our experiments show that sulfur production is the highest at low α values.

This chapter has been published as: Kiragosyan K., Klok J.B.M., Keesman K.J., Roman P., Janssen A.J.H. (2019) Development and validation of a physiologically based kinetic model for starting up and operation of the biological gas desulfurization process under haloalkaline conditions. *Water Res X* 4:100035. doi: 10.1016/j.wroa.2019.100035

2.1 Introduction

During the anaerobic treatment of wastewater, biogas is produced from organic matter [1,2]. When sulfate is present in the wastewater, this will be converted to sulfide, and a fraction hereof will transfer to the biogas. H_2S concentrations in the biogas generally range between 100 and 40 000 ppm(v) [2]. To be able to use this biogas, strict specifications have to be applied with respect to hydrogen sulfide (H_2S) levels. In natural gas, the H_2S concentration has to be below 3 ppm(v). The release of H_2S to the environment is regulated due to its toxic and corrosive properties [3,4]. Thus, removal of H_2S is required.

Nowadays, a variety of desulfurization processes are available to remove H_2S from sour gas streams. Among these technologies, the biological conversion of H_2S is the most environmentally friendly because no toxic chemicals are required, and the process is operated at ambient conditions, i.e. no high pressures or temperatures. A biotechnological process for the removal of H_2S was developed in the 1990s, which has been applied in different industrial sectors worldwide [2,5]. The process is based on the absorption of H_2S from sour gas streams in an haloalkaline solvent with a salinity between 0.5 – 2 M Na^+ and a pH between 8 – 10 [6,7].

The dissolved bisulfide (HS^-) is subsequently directed to a bioreactor where haloalkaline sulfur-oxidizing bacteria (SOB) consume reduced sulfur ions and produce elemental sulfur (S_8) as the end-product (Eq. 1) [8].



In addition, a small part of the sulfide is oxidized to sulfate according to:



Next to biological sulfide oxidation, chemical oxidation can take place:



The formation of sulfur is preferred as hydroxide ions are re-generated, which are required to absorb hydrogen sulfide from the gas stream [2]. In addition, the formed sulfur particles can be used as a fertilizer and for sulfuric acid production [9]. On the other hand, (thio)sulfate production leads to acidification of the reactor suspension, which requires the addition of sodium hydroxide to maintain the pH for the bacterial optimum conditions and adsorption of sulfide. Hence, in order to optimize the formation of sulfur, the oxygen supply should be carefully controlled [10].

Haloalkaline SOB are naturally occurring microorganisms that can be found in alkaline and highly saline environments, such as soda lakes [11,12]. Most known haloalkaline SOB are members of the *Gammaproteobacteria* class, belonging to the genera *Ectothiorodospira*, *Thioalkalivibrio*, *Thioalkalimicrobium*, and *Thioalkalispira* [13]. Bacteria from *Ectothiorodospira* genus are phototrophic sulfur purple bacteria, whereas the other three genera are obligate chemolithoautotrophs using various reduced

inorganic sulfur compounds as an electron donor (Ghosh and Dam 2009). SOB can use two groups of enzymes for sulfide oxidation: the periplasmic FAD-containing flavocytochrome *c* (FCC) and the membrane-bound sulfide-quinone oxidoreductase (SQR) donating electrons to the UQ pool [15]. When (bi)sulfide oxidation is mediated by FCC, (bi)sulfide is oxidized to sulfane (S^0), using oxidized cytochrome *c* (cyt^+) as an electron acceptor [15,16]:



Subsequently, the reduced cytochrome *c* (cyt) is oxidized through the reduction of oxygen to water and governed by cytochrome *c* oxidase [17]:



However, the role of FCC as the major responsible enzyme for sulfide oxidation has been questioned as many SOB species lack this protein [18]. The SQR pathway is energetically more favorable and less sensitive to inhibition by toxic compounds, for example, methanethiol [19]. The SQR mediated sulfide oxidation end-product is a soluble polysulfide [20]. The SQR route prevails when sulfide oxidation takes place at oxygen-limiting conditions [21]. In addition, it is postulated that SOB may contain both enzymes and the environmental conditions regulate which enzyme activity prevails [22]. To be able to grow, the haloalkaliphilic chemolithoautotrophic SOB must have specially adapted bioenergetics [23].

In full-scale gas biodesulfurization installations differences between microbial community compositions were observed [24]. Expression of sulfide-oxidizing routes, which define reaction kinetics, and observed bacterial growth rates influence the process efficiency. The aim of this study is to understand the relation between the bacterial community composition, biological sulfide oxidation kinetics and the biodesulfurization process efficiency to optimize sulfur formation.

2.2 Materials and Methods

2.2.1 Experimental setup and design

The laboratory setup consisted of a falling film gas absorber integrated with a gas-lift reactor (Fig. 1) [25]. Gases were supplied to the gas absorber using mass flow controllers (type EL-FLOW, model F-201DV-AGD-33-K/E, Bronkhorst, the Netherlands). For each gas, a mass flow controller was selected based on the dosing rate, for hydrogen sulfide $0\text{--}17\text{ mL min}^{-1}$ was used, for nitrogen $0\text{--}350\text{ mL min}^{-1}$, for oxygen $0\text{--}30\text{ mL min}^{-1}$ and carbon dioxide $0\text{--}40\text{ mL min}^{-1}$. Hydrogen sulfide and nitrogen gas were continuously supplied, whereas the oxygen and carbon dioxide dosing rates were pulse-wise controlled with a multiparameter transmitter (Liquiline CM442-1102/0 Endress+Hauser, Germany) based on the signals from a redox sensor, equipped

with an internal Ag/AgCl reference electrode (Orbisint 12D-7PA41; Endress+Hauser, Germany) and a pH sensor (Orbisint 11D-7AA41; Endress+Hauser, Germany).

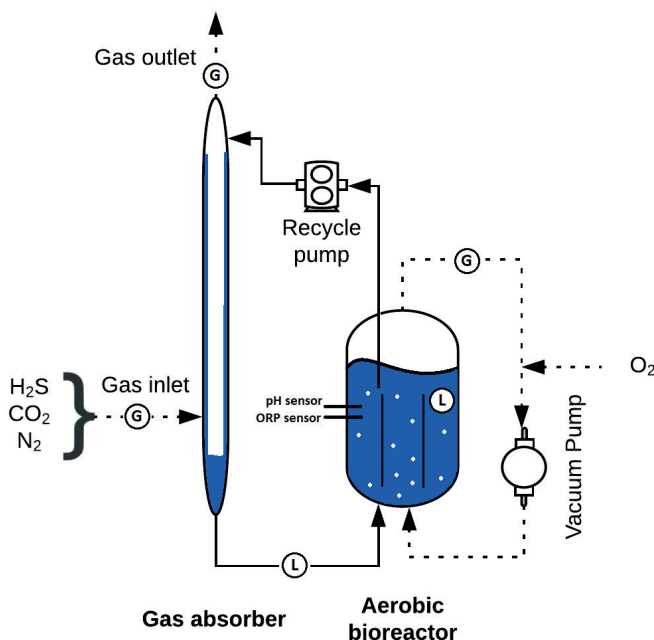


Fig. 1. Schematic representation of the experimental setup, operated in the fed-batch mode, used for the experiments (adapted from [26]).

A digital gear pump was used to assure liquid recirculation between the bioreactor and the gas absorber (EW-75211-30, Cole-Palmer, USA) at a constant flow of 0.166 L min^{-1} . A gas compressor (N-820 FT.18, KNF Laboport, USA) was used to continuously recycle gas (20 L min^{-1}) over the bioreactor. The gas absorber and the bioreactor temperature were regulated at 35°C by a thermostat bath (DC10, Thermo Haake, Germany). The system was sampled in gas and liquid phases. Liquid samples were taken from two sampling points located at the bottom section of the absorber and in the bioreactor (Fig. 1). Gas phase samples were taken from three locations: gas inlet, bioreactor headspace, and absorber outlet.

We conducted four similar experimental runs under stable operating conditions (Table 1) with different inocula (section 2.2). Each experimental run lasted for about six days during which a stable reactor performance was achieved. Sampling was done in technical triplicates at regular time intervals. In our experiments, pH and temperature were kept constant. Oxidation-reduction potential (ORP) setpoint value was chosen at -390 mV to suppress sulfate formation [24].

Table 1 Overview of the process conditions.

Total liquid volume, L	2.5
pH	8.50 ± 0.05
Salinity, Na ⁺ M	1
Temperature, °C	35.0 ± 0.1
H ₂ S loading, mM S day ⁻¹	58.2
ORP setpoint, mV	-390

2.2.2 Biomass sources

Biomass samples for inoculation were collected from four different full-scale systems for gas biodesulfurization, which have been in operation for more than ten years. Each biomass was studied separately (one-by-one) under similar experimental conditions. The lab-scale setup was inoculated with cells obtained by centrifugation (15 min at 16 000 × *g*) of a 2.5 L culture collected from full-scale installation. These full-scale systems were selected based on the feed gas composition it treats and on the industry of application.

Table 2 provides a brief overview of the selected installations. Two full-scale systems, which treat sour gas from the anaerobic digestion of the wastewater from the paper pulp industry were sampled. In this paper, the various biomasses will be denoted by the location of the sampling installation.

Table 2 A brief description of the origin and averaged operational parameters of the chosen installations.

Location	Industry	Sour gas composition	Sour gas load, m ³ h ⁻¹	ORP set-point, mV	Na ⁺ , M	K ⁺ , mM
Eerbeek (NL) ¹	Paper mill	biogas, 0.7 % H ₂ S	418	-335	0.8	0.7
Zuelpich (DE) ²	Paper mill	biogas, 0.5 % H ₂ S	700	-370	0.9	1.5
Amersfoort (NL)	Landfill waste	landfill gas, 0.3 % H ₂ S	NA	NA	1.3	1.6
Southern Illinois (USA) ³	Oil and gas	associated gas, 1-5 % H ₂ S, 50-200 ppm VOSC	800-1100	NA	0.9	3.7

¹ - [27], ² - [2], ³ - [24].

2.2.3 Medium composition

The haloalkaline medium for inoculum was buffered with 0.045 M Na₂CO₃ and 0.91 M NaHCO₃. The medium contained 1.0 g K₂HPO₄, 0.20 g MgCl₂ × 6H₂O and 0.60g urea, each per 1 L of ultrapure water (Millipore, the Netherlands) and trace elements solution as described in Pfenning and Lippert [27]. The pH of the medium was 8.50 ± 0.05 at 35 °C. For the respiration test, the medium contained carbonate/bicarbonate buffer only. Trace elements were excluded because they enhance the chemical oxidation of sulfide [28].

2.2.4 Respiration test

Respiration tests, also known as biological activity monitoring (BOM) tests, were performed to measure biological sulfide oxidation reaction rates in an air saturated medium. A similar setup was used by Roman et al. [29], consisting of a glass mini-reactor (45 mL), a magnetic stirrer, and a Teflon piston to avoid any oxygen ingress (Fig. 2). Sulfide was added to the reactor, from a freshly prepared stock solution ($\text{Na}_2\text{S} \times 9\text{H}_2\text{O}$, Sigma Aldrich, the Netherlands), with a glass syringe passing through the piston. The concentration of the prepared stock solution was verified with a sulfide Methylene blue cuvette test (LCK653). If the stock was used for several days, the concentration of the stock was verified every time before use. The sulfide oxidation rate was calculated from measuring the oxygen removal rate with a dissolved-oxygen (DO) sensor (Oxymax COS22D, Endress+ Hauser, Germany). The DO concentration was recorded using a multiparameter transmitter (Liquiline CM442-1102/0, Endress+Hauser, the Netherlands). All experiments were performed at 35 °C (DC10, Thermo Haake, Germany) which is in agreement with the conditions in the lab-scale fed-batch setup. As temperature and medium composition were similar to previous studies, a proper comparison of our results can be performed [21,29–31].

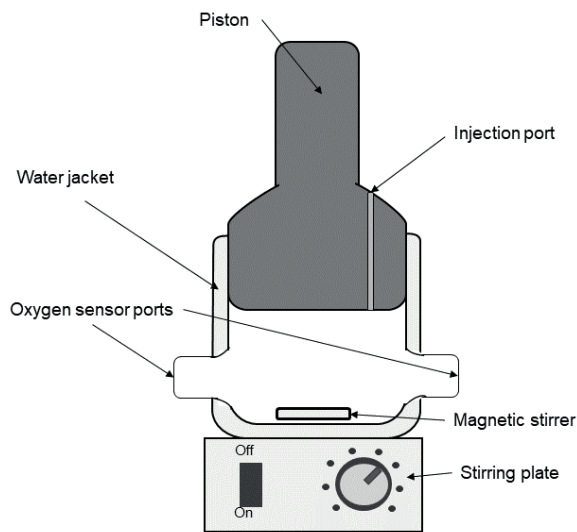


Fig. 2. Schematic representation of the thermostated batch reactor used for the respiration tests.

At the end of each fed-batch bioreactor run the tested biomass was collected to measure specific biomass activities. Biomass was centrifuged and separated from sulfur particles, salts by washing with a 1 M carbonate/bicarbonate buffer. Hereafter biomass was ready to be used for the respiration tests at constant concentration 2 mg N L^{-1} . Firstly, biomass

was aerated as described elsewhere [30]. Experiments started by injection of sulfide and the initial slope of the recorded oxygen consumption profile was used to calculate the oxygen consumption rate. Biological reaction rates were determined by subtracting the chemical oxidation rates from the measured overall oxygen consumption rates. Chemical rates were measured in the absence of biomass. In addition, we calculated the endogenous oxygen consumption rate based on the respiration measurements without sulfide addition [30].

2.2.5 Application of a physiologically based kinetic model

The proposed model describes both oxidation rates of sulfide through FCC and SQR enzymes, i.e. primary dehydrogenases involved in biological sulfide oxidation, and the effect on end-product formation, i.e. sulfur and sulfate [21]. The calculated maximum sulfide oxidation rate (μ) of the involved enzymes was determined by the results from respiration tests.

The electrons released from HS⁻ are transferred to the oxidized form of intermediate acceptors, i.e. either cytochrome *c* or ubiquinones. The reduced co-factors are subsequently oxidized through other enzymes, such as cytochrome *c*-oxidase (CCO) and quinol oxidases (SQRo_x) [21]. Irrespective of the type of sulfide dehydrogenase employed, part of the electrons is transferred to oxidized nicotinamide adenine dinucleotide (NAD⁺). The kinetic model contains expressions for the rates of four respiratory enzymes (μ_{FCC} , μ_{SQR} , μ_{CCO} , μ_{SQRo} in mmol S mg N⁻¹ h⁻¹) and the associated affinity constants (K_{FCC} , K_{SQR} , K_{CCO} , K_{SQRo} in mM). In addition, CCO is inhibited by sulfide and therefore an inhibition constant is included (K_i in mM). Lastly, the reduction degree (F) of cytochrome *c* and quinone (Q) pool is included in the rates equations, which change instantaneously according to sulfide and oxygen levels (i.e. quasi-steady state) [21]. The rates for the oxidation of dissolved (bi)sulfide and reduction of dissolved oxygen are described by:

$$q_{FCC} = \mu_{FCC} \cdot (1 - F) \cdot \frac{[HS^-]}{K_{FCC} + [HS^-]} \quad (\text{Eq. 6})$$

$$q_{CCO} = \mu_{CCO} \cdot F \cdot \frac{[O_2]}{K_{CCO} + [O_2]} \cdot \frac{K_i}{K_i + [HS^-]} \quad (\text{Eq. 7})$$

$$q_{SQR} = \mu_{SQR} \cdot (1 - Q) \cdot \frac{[HS^-]}{K_{SQR} + [HS^-]} \quad (\text{Eq. 8})$$

$$q_{SQRo} = \mu_{SQRo} \cdot Q \cdot \frac{[O_2]}{K_{SQRo} + [O_2]} \quad (\text{Eq. 9})$$

with q in mmol S mgN⁻¹ h⁻¹, [HS⁻] in mM and [O₂] in mM.

Expression levels for both FCC and SQR were estimated from respiration tests for all tested biomasses described in Table 2. The maximum rates for sulfide oxidation through

FCC, i.e. μ_{FCC} and μ_{CCO} , and SQR, i.e. μ_{SQR} and μ_{SQRox} , were estimated using a non-linear least-squares estimation routine. As FCC and SQR expression levels do not describe the reduction of oxygen, it was assumed that increased expression levels of the sulfide-oxidizing enzyme systems would lead to a homologous increase of expression levels of the oxidase enzymes associated with the oxidizing sulfide enzymes, i.e. CCO is associated with FCC and SQRox is associated with SQR. The affinity constants for sulfide and oxygen remained equal to the parameters estimated by [21] (Table 3). More details concerning the parameter estimation and associated standard deviations can be found in Appendix B.

The reduction degree of CCO dictates the formation rate of sulfate in the kinetic model. The stronger the oxidation degree of the cytochrome pool (i.e. smaller F), the higher the potential for the formation of sulfate [21,32]. We hypothesize that the ratio of expression of oxidation routes of sulfide through either FCC (requiring cytochrome c as a cofactor) and SQR (require quinones as a cofactor) is an indicator for the sulfate forming (and thus sulfur forming) potential of SOB under oxygen-limiting conditions. Hence, we postulate that the ratio of μ_{FCC} and μ_{SQR} is a predictor of sulfur forming potential. Therefore, we introduce the parameter α , defined as $\alpha = \frac{\mu_{\text{FCC}}}{\mu_{\text{SOR}}}$. Based on the dependencies between sulfate formation, the overall biological activity under oxygen-limiting conditions and the oxidation state of the cytochrome system, we hypothesize that the smaller the value of α , the higher the potential for sulfur formation as the end-product.

Table 3 Parameters for the physiologically based kinetic model (adapted from [21]).

Affinity constants	
K_{FCC} , mM	0.05
K_{SQR} , mM	1.80
K_{CCO} , μM	2.30
K_{SQRox} , μM	0.23
Inhibition constants	
K_i , mM	0.62

2.2.6 Analytical techniques

Two types of samples were prepared, i.e. filtrated and precipitated with zinc acetate for anions measurements and non-filtrate for biomass quantification and TOC analysis. All liquid samples were stored at 4 °C before being analyzed (about three days).

Biomass quantification was based on the amount of organic nitrogen that was oxidized to nitrate by peroxodisulphate (LCK238 and LCK338, Hach Lange, the

Netherlands). The cell pellet was washed twice at $20,238 \times g$ for 5 min with the nitrogen-free medium to remove any nitrogen present in the medium.

Sulfate and thiosulfate were measured by ion chromatography (Metrohm Compact IC 761, Switzerland) with an anion column (Metrohm Metrosep A Supp 5, 150/4.0 mm, Switzerland) equipped with a pre-column (Metrohm Metrosep A Supp 4/5 Guard, Switzerland). Immediately after sampling all solids were removed by filtration over a $0.45 \mu\text{m}$ membrane syringe filter (HPF Millex, Merck, the Netherlands) and mixed with 0.2 M zinc acetate in a 1:1 ratio to prevent any chemical sulfide oxidation. Produced and accumulated sulfur concentration was calculated from the molar sulfur mass balance, which is based on the supplied sulfide load and measured sulfate and thiosulfate concentrations at each sampling time point by following this equation:

$$d[S^0] = d(\text{H}_2\text{S supplied} / V_{\text{liquid}}) - d[\text{SO}_4^{2-}] - 2 * d[\text{S}_2\text{O}_3^{2-}] - \text{S}_x^{2-} \quad (\text{Eq. 10})$$

Initial sulfur concentration is assumed to be “0”. Concentrations of dissolved sulfide and polysulfides were not taken into account, as their combined contribution to the total concentration of sulfur species is negligible [33,34].

Sulfide and bisulfide were measured as total sulfide ($\text{S}_{\text{tot}}^{2-}$) using the methylene blue method with a cuvette test (LCK653, Hach Lange, USA). Total sulfide quantification was carried out immediately after sampling and samples were diluted in oxygen-free Milli-Q water (sparged with N_2 stream for 30 min) to exclude chemical sulfide oxidation [35].

In addition to sulfur-containing anions, sodium and potassium concentration were measured with ion chromatography as described earlier [29]. Using a Metrohm Metrosep C4-150/4.0 mm column with three mM HNO_3 as the eluent at 0.9 mL min^{-1} .

To close the electron balance as described by [24] carbonate and bicarbonate ions concentration were established using the Henderson-Hasselbalch equation [36]. For that, liquid samples were analyzed on total inorganic carbon using high-temperature catalytic oxidation at 680°C with TOC-VCPH/CPN analyzer (Shimadzu, The Netherlands).

The gas phase (H_2S , N_2 , CO_2 , and O_2) was analyzed with a gas chromatograph (Varian CP4900 Micro GC, Agilent, the Netherlands) equipped with two separate column modules, namely a 10-m-long Mol Sieve 5A PLOT (MS5) and a 10-m-long PoraPlot U (PPU).

2.2.7 DNA extraction and 16S rRNA sequencing

Biomass samples were collected for microbial community analysis at the beginning and the end of each experimental run. The samples were washed twice with a buffer solution of pH 8.5 and 0.5 M Na^+ to prevent the occurrence of an osmotic shock. Afterward, the genomic DNA was extracted from the washed biomass using the DNeasy PowerLyzer

PowerSoil Kit (Qiagen) following the manufacturer's instructions. All the above procedures were performed in technical duplicates for each sample, and average values with standard deviations are presented. Library construction and Next-generation sequencing were carried out at the European genome and diagnostics center Eurofins GATC Biotech GmbH (Constance, Germany). The workflow started from 16S rRNA gene amplification in the V3-V5 variable region using 357F (5'- CCTACGGGAGGCAGCAG - 3') and 926R (5'- CCGTCAATTCMTTTRAGT - 3') primer set, afterward merging read pairs by overlapping was performed using FLASH [37] with maximum mismatch density of 0.25. The next step was to cluster sequences based on the similarity with chimera removal with UCHIME [38] using a full length, good quality, and non-chimeric 16S rRNA reference database. Cleaned and clustered sequences were BLASTn [39] analyzed using non-redundant 16S rRNA reference sequences with an E-value cutoff of 10^{-6} . Only good quality and unique 16S rRNA sequences were taxonomically assigned to the operational taxonomic unit (OTU) to the clusters. The taxonomic classification was based on the NCBI database (www.ncbi.nlm.nih.gov/taxonomy). The EMBL-EBI accession number for presented 16S rRNA sequencing set is PRJEB27163.

2.3 Results

2.3.1 Biodesulfurization process performance

An overview of the results is shown in Table 4. The calculated selectivities for sulfur, sulfate, and thiosulfate are presented as an average value. The term “selectivity” describes the mol fractions of products formed from a reactant or substrate. Detailed information on the obtained experimental data and determination of product selectivities can be found in Appendix C. The lowest selectivity for thiosulfate formation (0.8 ± 0.2 mol%) was obtained for experiments with Landfill biomass and the highest with Paper mill - 1 biomass (17.6 ± 0.3 mol%). Sulfate selectivity was the lowest for Paper mill - 1 system operation (1.1 ± 0.1 mol%), and the highest for Paper mill - 2 and Landfill operation with (7.2 ± 0.4 mol%) and (7.0 ± 0.9 mol%) respectively. The highest sulfur selectivity was achieved with biomass from installations treating Landfill and Oilfield gasses, 92.2 ± 0.9 mol% and 91.0 ± 0.2 mol% respectively.

The O_2/H_2S supply ratio is a critical parameter to control product formation [7]. This parameter can be calculated from the supplied gas flows, as no accumulation of O_2 nor H_2S was observed, indicating that all supplied compounds are indeed were consumed. The O_2/H_2S supply ratio is compared with the value obtained from the formed products based on the reaction's stoichiometry. The electron balance was validated by comparing the O_2/H_2S ratios versus the formed products and that no significant differences were found (Table 4).

Table 4 Product selectivity for four different inoculates measured in the lab-scale biodesulfurization set-up for about six days.

Parameter	Inoculate	Paper mill - 1	Paper mill - 2	Oilfield	Landfill
Selectivity for SO_4^{2-} formation, mol%		1.1 ± 0.1	7.2 ± 0.4	3.1 ± 0.1	7.0 ± 0.9
Selectivity for $\text{S}_2\text{O}_3^{2-}$ formation, mol%		17.6 ± 0.3	6.2 ± 0.2	5.9 ± 0.2	0.8 ± 0.2
Selectivity for S_8 formation, mol%		81.3 ± 0.3	86.7 ± 0.5	91.0 ± 0.2	92.2 ± 0.9
$\text{O}_2/\text{H}_2\text{S}$ supplied ratio, mol mol ⁻¹		0.60 ± 0.01	0.59 ± 0.03	0.65 ± 0.07	0.63 ± 0.04
$\text{O}_2/\text{H}_2\text{S}$ based on formed products, mol mol ⁻¹		0.60 ± 0.04	0.60 ± 0.01	0.54 ± 0.15	0.57 ± 0.01
Biomass concentration at the beginning, mg N L ⁻¹		47 ± 2	33 ± 2	32 ± 3	4 ± 1
Biomass concentration at the end, mg N L ⁻¹		49 ± 1	76 ± 17	54 ± 8	40 ± 7
Observed biomass growth, mg N L ⁻¹ h ⁻¹		0.02 ± 0.01	0.34 ± 0.03	0.25 ± 0.07	0.52 ± 0.03
R_{\max} , mM O_2 (mg N) ⁻¹ h ⁻¹		0.64 ± 0.03	0.53 ± 0.05	0.79 ± 0.03	0.30 ± 0.02
Specific loading rate at the end, mM H_2S (mg N) ⁻¹ h ⁻¹		1.2	0.8	1.1	1.5

Hence, we conclude that the mass balance for sulfur compounds is closed albeit that at very low concentrations compounds could be formed that were not analyzed by us. We studied the rates of underlying biological and chemical reactions by performing respiration tests to better understand the formation of various end-products. Therefore, biological kinetic rates were measured using respiration tests. Our results show that the highest maximum biological oxidation rate (R_{\max}) was achieved with Oilfield biomass 0.79 ± 0.03 mM O_2 (mg N)⁻¹ h⁻¹, and the lowest R_{\max} value was achieved with Landfill biomass 0.30 ± 0.02 mM O_2 (mg N)⁻¹ h⁻¹. Nevertheless, both biomasses showed about 90 mol% of sulfur formation in the lab-scale experiments. In addition, the specific substrate loading rate of bacteria is in the same order of magnitude. Hence, the achieved end-product selectivities cannot be solely explained by R_{\max} . Next to maximum rates, the observed reaction kinetics are controlled by substrate affinities [40]. In respiration tests, oxygen levels are typically elevated (100 % of DO), i.e. $[\text{O}_2] > K_{\text{CCO}}$, whereas in gas biodesulfurization process DO levels are below the detection limit, i.e. $[\text{O}_2] < K_{\text{CCO}}$. Hence, we have applied a physiologically based kinetic model to describe sulfide oxidation under oxygen-limiting conditions. Moreover, to correlate biological kinetics obtained from respiration tests to values measured in the biodesulfurization process, parameter α was introduced. This parameter is defined as $\alpha = \frac{\mu_{\text{FCC}}}{\mu_{\text{SQR}}}$, and indicates the relative expression levels of sulfate formation routes. High relative expression levels of the μ_{FCC} and CCO resulted in higher production of sulfate, which in turn is responsible for cytochrome c pool re-generation. Whereas high levels of the μ_{SQR} yield in the high formation of sulfur [21].

The parameters in the physiologically-based model proposed by Klok et al. [21] were recalibrated for four inocula originated from full-scale installations based on the

obtained respiration data (Table 5, Fig. 3). Results show that Paper mill - 1 biomass has a high potential for sulfate formation (α at 1.23 ± 0.17). Hence, using Paper mill - 1 biomass under oxygen-limiting conditions (ORP -390 mV) results in low biomass activity and consequently in high chemical oxidation rates (17.6 ± 0.3 mol%). The other three biomasses showed significantly lower α values, indicating a higher potential for sulfur formation under oxygen-limiting conditions. In addition, the calibrated model was used to predict sulfur selectivities for four tested biomasses at various oxygen concentrations (Appendix D).

Table 5 Parameters calculated by the physiological kinetic model.

Parameter	Inoculate	Paper mill - 1	Paper mill - 2	Oilfield	Landfill
μ_{FCC} , mmol S (mg N) ⁻¹ h ⁻¹		1.37 ± 0.14	1.14 ± 0.03	1.43 ± 0.09	0.50 ± 0.05
μ_{SQR} , mmol S (mg N) ⁻¹ h ⁻¹		1.11 ± 0.08	1.40 ± 0.13	2.00 ± 0.13	1.04 ± 0.12
μ_{CCO} , mmol S (mg N) ⁻¹ h ⁻¹		6.53 ± 0.68	5.44 ± 0.15	6.82 ± 0.41	2.41 ± 0.23
μ_{SQRox} , mmol S (mg N) ⁻¹ h ⁻¹		1.92 ± 0.14	2.43 ± 0.23	3.46 ± 0.23	1.80 ± 0.21
α , -		1.23 ± 0.17	0.81 ± 0.10	0.71 ± 0.07	0.48 ± 0.12

μ is the maximum sulfide oxidation rate for the enzymes FCC, SQR, CCO, and SQROx respectively α the ratio between rates of μ_{FCC} and μ_{SQR} .

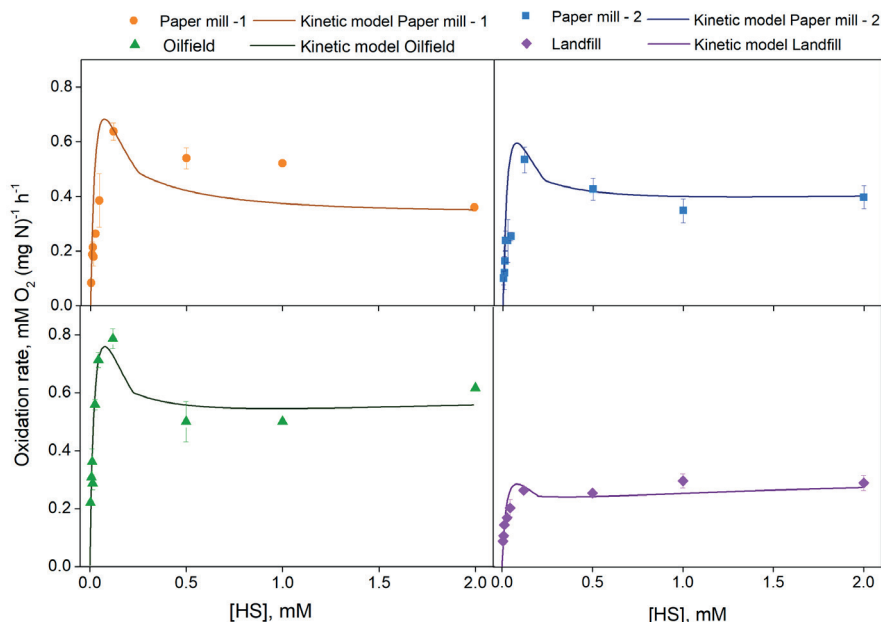


Fig. 3. Biological oxidation rates at different concentrations of HS⁻ in oxygen saturated buffer at pH 8.5, 1 M Na⁺ and 35 °C. Measured data points are average values of the experimentally measured duplicates. The solid lines indicate the estimated physiologically-based kinetic model.

2.3.2 Bacterial community analyses

Total DNA was extracted and analyzed using next-generation sequencing of the 16S rRNA gene, at the beginning and at the end of the experimental runs to enable monitoring of the microbial community change. The most dominant species of the microbial communities in the Paper mill - 1, Paper mill - 2 and Landfill inocula were *Thiobacillus thiooxidans* with an estimated abundance of 92.6 %, 96.5 %, and 82.7 %, respectively (Fig. 4). In contrast, in the Oilfield inoculum, a heterotrophic gammaproteobacterium *Halomonas shengliensis* was the most abundant species with 43.1 % in comparison to 39.3 % of *T. thiooxidans* (Fig. 4). *Halomonas* species become abundant when organic hydrocarbons are present in the feed streams [41]. Oilfield biomass is fed by a gas stream originating from crude oil extraction, which can explain the presence of *Halomonas* species. In Landfill biomass, the second dominant species was an anoxygenic purple nonsulfur producing alphaproteobacterium *Roseibaca ekhonensis* with 15.5 % abundance, whereas its population decreased by a factor of two at the end of the process operation. The least abundant in Paper mill - 1 biomass inoculum were lithoautotrophic SOB *Thiomicrospira thyasirae* and heterotrophic *Halomonas meridiana* with only 3 % and 2.3 % respectively. In Paper mill - 2 prominent biomass species were *Halomonas campaniensis* 1.3 %, and two haloalkaliphilic anaerobes (0.7 % each) – sulfur-reducing *Desulfurispirillum alkaliphilum* and fermentative clostridium *Anoxynatronum sibiricum*. *Desulfurispirillum* has been described previously as a dominant sulfur-reducing bacterium in the Eerbeek plant (Paper mill - 1) [42], while a close relative of *Anoxynatronum sibiricum* has been enriched and isolated in pure culture from Eerbeek plant in 2009 using thiosulfate as electron acceptor (Sorokin, unpublished results). This indicates that a full sulfur cycle might be functional in micro-aerophilic biodesulfurization bioreactors maintaining highly negative redox potential.

Minor changes in the microbial composition were noticed in the samples collected at the end of the experiments with Paper mill - 1, Paper mill - 2 and Landfill biomass. In Landfill biomass, *R. ekhonensis* abundance decreased to 7.8 %, but the other two species *Thiomicrospira thyasirae* and *Thioalkalimicrobium sibiricum* became detectable with 1.3 % and 1.2 %. Microbial compositions in Paper mill - 1 and Paper mill - 2 biomass at the end of the experiments were similar to the inoculum. In contrast, the Oilfield biomass underwent a profound shift in the microbial community during the performed experiments: the population of *Halomonas shengliensis* decreased from 43.1 to 3.8 % and was overtaken by lithoautotrophic *Thiobacillus thiooxidans* (66 %). Also, two other haloalkaliphilic SOB species proliferated - *Thioalkalimicrobium sibiricum* and *Roseibaca ekhonensis* with 16.6 % and 6.0 %, respectively. Changes in the microbial composition of the Oilfield biomass are probably caused by a change in the feed gas composition that was lacking an organic carbon source.

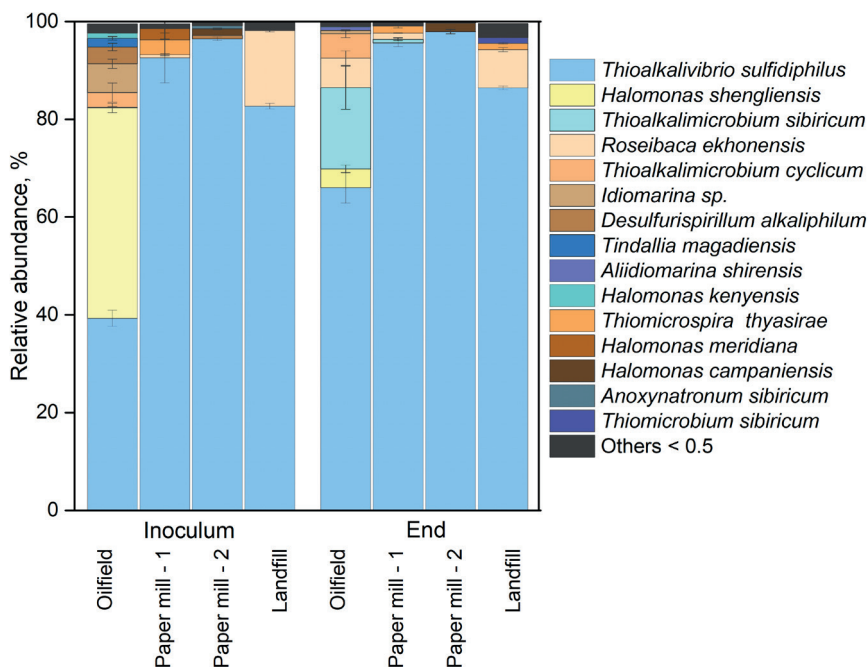


Fig. 4. Microbial composition profile of OUTs showing the relative abundance of the species in the inoculum and at the end of each experiment. Oilfield, Paper mill - 1, Paper mill - 2, and Landfill denote biomass origin. Only bacteria with a relative abundance higher than 0.5 % are listed (remaining species are clustered into “Others”).

2.4 Discussion

From our experiments, it can be seen that the sulfur selectivity was above 90 mol% for biomasses that originates from Oilfield and Landfill full-scale installations whilst the consortia that come from Paper mill - 1 shows lower sulfur selectivity and a significantly higher thiosulfate formation. In gas biodesulfurization systems thiosulfate is usually formed chemically when the enzymatic oxidation capacity is limited. Thus, it can be used as an indication of limited biological oxidative capacity [43]. Chemically formed thiosulfate can be further oxidized to sulfate by SOB [44]. However, in our lab-scale gas biodesulfurization set-up thiosulfate only accumulated in the process liquid when the abiotic formation rates of thiosulfate were higher than the biological oxidation rates.

To understand the observed differences in formed end-products by different biomasses, we investigated the underlying biological reaction mechanism and kinetics, such as maximum biological respiration rates. Our results of the kinetic experiments are in good agreement with reported literature. Our measurements of R_{max} (0.64 mM O₂ (mg N)⁻¹ h⁻¹) corresponds to data reported by [30,35,45], who tested Paper mill - 1 biomass in their studies and observed R_{max} in the order of 0.3 – 0.6 mM O₂ (mg N)⁻¹

h^{-1} . Differences between these reported values can be explained by fluctuations in the operating conditions over time. For example, at Paper mill - 1 we learned that the solutions' pH buffer capacity, sulfide concentration in the gas feed, and ORP setpoint fluctuated significantly in the period before the inoculum was collected (personal communication with the plant manager). It is known that variations in ORP setpoint value in time will vary the oxygen supply rates and thus the $\text{O}_2/\text{H}_2\text{S}$ ratio. This, in turn, will affect the selectivities for the various end-products [7]. For example, in the work of Roman et al. (2015) Paper mill - 1 inoculum was also used. In their studies, thiosulfate selectivity was reported two times lower than found in this study. A possible explanation is the observed operational fluctuations (since 2016) at the Paper mill - 1 full-scale installation that affected the potential of the biomass for sulfate and sulfur formation at different ORP setpoints.

It can be expected that changes in the biological activity are explained by the differences in microbial physiology. In this study, parameter α is introduced to link physiology of biological sulfide oxidation and formation of end-products in the biodesulfurization process. In Fig. 5, the relation between the formed products and α is presented for systems operated at oxygen-limiting conditions (ORP = -390 mV). It can be seen that the highest selectivity for sulfur formation (92.2 mol%) was found for the lowest α values, i.e. 0.35 – 0.7, whilst the highest selectivity for sulfate formation (7.2 mol%) was found for the highest α value (above 0.8). The highest α was found for Paper mill - 1 biomass (1.23 ± 0.17), which correlates to a high potential for sulfate formation. However, under oxygen-limiting conditions Paper mill - 1 biomass has low biomass activity. Thus, the formation of thiosulfate is high (17.6 mol%), and sulfate is almost not formed due to oxygen limitation. From these, it follows that α can be an effective parameter to screen biomasses, which are able to generate elemental sulfur under oxygen-limiting conditions.

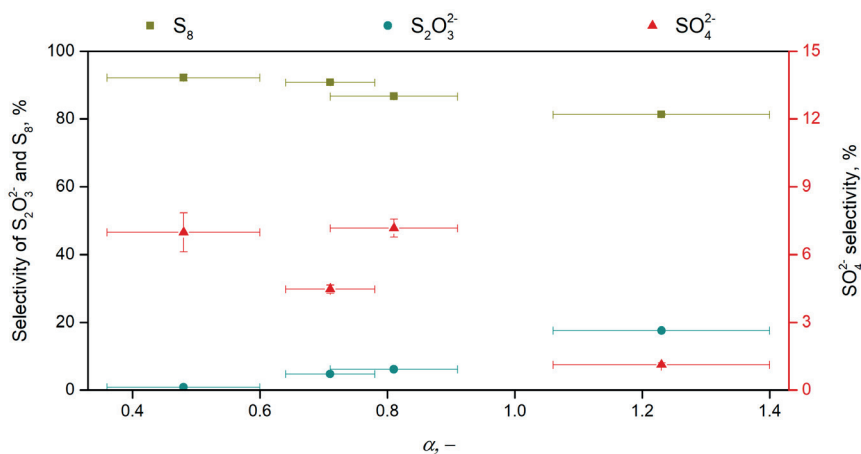


Fig. 5. Relationships between sulfur products selectivity and enzymatic ratio α .

Higher biomass growth rates were found at increasing selectivities for sulfate formation because more energy is liberated from sulfide oxidation compared to the sulfur formation [21,46,47]. However, growth rates are also dependent on the microbial community composition, as different species have different growth rates and oxidation capacities. For example, the highest measured biomass growth ($0.52 \pm 0.03 \text{ mg N L}^{-1} \text{ h}^{-1}$) was observed for Landfill biomass, but the highest measured selectivity for sulfate production ($7.2 \pm 0.4 \%$) was observed for Paper mill - 2 biomass (Table 4). As well as, growth rates of Oilfield and Paper mill - 2 are similar, but selectivity for sulfate is two-fold different. This deviation is possibly caused by the abundance of *Thioalkalimicrobium sibiricum* in Oilfield biomass. *Thioalkalimicrobium* species are known for their high capacity for sulfide oxidation and fast but inefficiently opportunistic growth during short periods of substrate excess [11]. In contrast, highly abundant *Thioalkalivibrio* species in Paper mill - 1 are slow growing with high growth yield and survive longer during substrate limitation [42]. Hence, in the absence of sulfate formation, the relatively low energy yield from sulfide oxidation was used for cell maintenance rather than Paper mill - 1 biomass growth.

To deepen our understanding of the process performance, a relation between microbial composition and process conditions need to be established. Microbial community composition was determined with 16S rRNA amplicon sequencing and showed that *Thioalkalivibrio sulfidiphilus* was the dominant SOB species in samples from Paper mill - 1, Paper mill - 2, and Landfill. Also, Sorokin et al. found that *Thioalkalivibrio sulfidiphilus* was dominant in Paper mill - 1 [48]. The gas composition fed to the Paper mill - 1 and Paper mill - 2 full-scale plants are almost the same, but operating conditions differ (Table 2). Microbial composition of the Landfill biomass was different from that to Paper mill - 1 and Paper mill - 2. It is known that feed gas composition at landfill installations contains hydrocarbons impurities [49]. Hence, it possibly triggered a shift in the microbial composition of the Landfill biomass. A second dominant species in the inoculum is *Roseibaca ekhonensis* described as marine aerobic, heterotrophic and alkalitolerant alphaproteobacterium [50], which also might have taken advantage of the presence of organic compounds in the Landfill plant. As supplied gas composition in the lab-scale setup differs from the full-scale installation, we observe a microbial composition shift with the reduction of heterotrophs in favor of chemolithoautotrophic SOB.

In comparison to the three tested biomasses, the Oilfield original community changed the most (Fig. 4). Inoculum from the full-scale Oilfield plant contained about 43.1 % of *Halomonas shengliensis* – alkalitolerant heterotroph capable of utilizing hydrocarbons that are present in the feed gas [51]. Its relative abundance drastically decreased as feed gas composition at lab-scale biodesulfurization system contained sulfide only. Second dominant species was *Tv. sulfidiphilus* with an abundance of 39.3

%. It is known that *Tv. sulfidophilus* is the most dominant SOB in gas biodesulfurization bioreactors when the only sulfide is supplied [25,44]. Thus, at the end of the process operation abundance of *Tv. sulfidophilus* increased (65 %). In addition, a fast-growing haloalkaliphilic SOB *Thioalkalimicrobium sibiricum* also proliferated as it grows in the presence of thiosulfate and sulfide [52].

2.5 Conclusions

In this work, we show that α can be used as a screening parameter that is applied for the biomass selection in order to predict process performance. Thus, to achieve desired products formation Factor α represents the ratio between the rates of two enzymatic routes for sulfide oxidation. We found that this parameter is a good indicator for the assessment of the end-product formation under oxygen-limiting conditions. In practice, this means that the biomass composition is linked to the process performance and sudden changes in process conditions (e.g., mixing) will not instantaneously change the S_8 forming potential of the biomass. In addition, α will be more determined by the process conditions rather than the bacterial community composition, as process conditions will eventually structure the community composition. Moreover, using process parameters, such as oxygen and sulfide concentration, together with biomass concentration and its activity, its possible to predict the relative formation of biological end-products: sulfate and sulfur. Despite showed variations in four tested biomasses at the inoculum stage, it is expected that under the similar experimental conditions all microbial communities will converge to a similar end composition. We further calibrated an existing kinetic model based on the measured sulfide oxidation rates in batch experiments. The kinetic model relies on a ratio of two key enzymes involved in sulfide oxidation, i.e. flavocytochrome c and sulfide-quinone oxidoreductase (FCC and SQR). The updated kinetic model can be used as a tool to evaluate process performance, estimate relative formation of biological end-products, and as an indicator, to select inocula for full-scale installations.

Acknowledgments

This work has been performed within the cooperation framework of Wetsus, European Centre of Excellence for Sustainable Water Technology (wetsus.nl) and Wageningen University and Research (wur.nl). Wetsus is co-funded by the Netherlands' Ministry of Economic Affairs and Ministry of Infrastructure and Environment, the European Union's Regional Development Fund, the Province of Fryslan and the Northern

Netherlands Provinces. Wetsus is also a coordinator of the WaterSEED project that received funding from European Union's Horizon 2020 research and innovation program under Marie Skłodowska-Curie grant agreement No. 665874. We acknowledge Dr Dimitry Sorokin for valuable input regarding the sulfur-oxidizing bacteria metabolism. We also would like to thank all full-scale facilities for kind supply of the inoculum for this study.

References

- [1] G. Lettinga, Anaerobic digestion and wastewater treatment systems, *Antonie Van Leeuwenhoek*. 67 (1995) 3–28. doi:10.1007/BF00872193.
- [2] W. Driessen, E. Van Zessen, M. Visser, Full-scale experience with biological biogas desulfurization, in: 16th Eur. Biosolids Org. Resour. Conf., 2011.
- [3] World health organization, Concise International Chemical Assessment Document 53 – Hydrogen Sulphide: Human Health Aspects, 2003.
- [4] J.K.B. Schnele, R.F. Dunn, M.E. Ternes, Control of SO_x, in: J.K.B. Schnele, R.F. Dunn, M.E. Ternes (Eds.), *Air Pollut. Control Technol. Handb.*, Second, CRC Press, Boca Raton, 2016: pp. 285–304.
- [5] C.J.N. Buisman, B. Wit, G. Lettinga, Biotechnological sulphide removal in three polyurethane carrier reactors: stirred reactor, biorotor reactor and upflow reactor, *Water Res.* 24 (1990) 245–251. doi:10.1016/0043-1354(90)90110-R.
- [6] A.J.H. Janssen, P.N.L. Lens, A.J.M. Stams, C.M. Plugge, D.Y. Sorokin, G. Muyzer, H. Dijkman, E. Van Zessen, P. Luimes, C.J.N. Buisman, Application of bacteria involved in the biological sulfur cycle for paper mill effluent purification, *Sci. Total Environ.* 407 (2009) 1333–1343. doi:10.1016/j.scitotenv.2008.09.054.
- [7] P.L.F. Van Den Bosch, O.C.C. Van Beusekom, C.J.N. Buisman, A.J.H. Janssen, Sulfide Oxidation at Halo-Alkaline Conditions in a Fed-Batch Bioreactor, *Biotechnol. Bioeng.* 97 (2007) 1053–1063. doi:10.1002/bit.
- [8] C.J.N. Buisman, R. Post, P. Ijspeert, G. Geraats, G. Lettinga, Biotechnological process for sulphide removal with sulphur reclamation, *Acta Biotechnol.* 9 (1989) 255–267. doi:10.1002/abio.370090313.
- [9] A.J.H. Janssen, A. De Keizer, G. Lettinga, Colloidal properties of a microbiologically produced sulphur suspension in comparison to a LaMer sulphur sol, *Colloids Surfaces B Biointerfaces*. 3 (1994) 111–117.
- [10] A.J.H. Janssen, R. Sleyster, C. Van der Kaa, A. Jochemsen, J. Bontsema, G. Lettinga, Biological sulphide oxidation in a fed-batch reactor, *Biotechnol. Bioeng.* 47 (1995) 327–333. doi:10.1002/bit.260470307.
- [11] D.Y. Sorokin, J.G. Kuenen, Haloalkaliphilic sulfur-oxidizing bacteria in soda lakes, *FEMS Microbiol. Rev.* 29 (2005) 685–702. doi:10.1016/j.femsre.2004.10.005.
- [12] D.Y. Sorokin, T.P. Tourova, G. Muyzer, Isolation and characterization of two novel alkalitolerant sulfidogens from a Thiopaq bioreactor, *Desulfonatronum alkalitolerans* sp. nov., and *Sulfurospirillum alkalitolerans* sp. nov, *Extremophiles*. 17 (2013) 535–543. doi:10.1007/s00792-013-0538-4.

- [13] M. Foti, D.Y. Sorokin, B. Lomans, M. Mussman, E.E. Zacharova, N. V Pimenov, J.G. Kuenen, G. Muyzer, Diversity, Activity, and Abundance of Sulfate-Reducing Bacteria in Saline and Hypersaline Soda Lakes, *Appl. Environ. Microbiol.* 73 (2007) 2093–2100. doi:10.1128/AEM.02622-06.
- [14] W. Ghosh, B. Dam, Biochemistry and molecular biology of lithotrophic sulfur oxidation by taxonomically and ecologically diverse bacteria and archaea, *FEMS Microbiol. Rev.* 33 (2009) 999–1043. doi:10.1111/j.1574-6976.2009.00187.x.
- [15] C. Griesbeck, G. Hauska, M. Schütz, Biological sulfide oxidation: sulfide-quinone reductase (SQR), the primary reaction, in: S.G. Pandalai (Ed.), *Recent Res. Dev. Microbiol.*, Research Signpost, Trivandrum, India, 2000: pp. 179–203.
- [16] C. Dahl, Inorganic Sulfur compounds as electron donors in purple sulfur bacteria, in: R. Hell, C. Dahl, D. Knaff, T. Leustek (Eds.), *Sulfur Metab. Phototrophic Org.*, Springer, Dordrecht, 2006: pp. 289–317.
- [17] P. Mitchell, J. Moyle, Chemiosmotic hypothesis of oxidative phosphorylation, *Nature.* 213 (1967) 137–139. doi:10.1038/213137a0.
- [18] U. Kappler, Bacterial Sulfite-Oxidizing Enzymes – Enzymes for Chemolithotrophs Only?, in: C. Dahl, C.G. Friedrich (Eds.), *Microb. Sulfur Metab.*, Springer-Verlag, 2007: pp. 151–169. doi:10.1007/978-3-540-72682-1_13.
- [19] D.C. Brune, Sulfur oxidation by phototrophic bacteria, *Biochem. Biophys. Acta.* 975 (1989) 189–221.
- [20] C. Griesbeck, M. Schütz, T. Schödl, S. Bathe, L. Nausch, N. Mederer, M. Vielreicher, G. Hauska, Mechanism of sulfide-quinone reductase investigated using site-directed mutagenesis and sulfur analysis, *Biochemistry.* 41 (2002) 11552–11565. doi:10.1021/bi026032b.
- [21] J.B.M. Klok, M. de Graaff, P.L.F. van den Bosch, N.C. Boelee, K.J. Keesman, A.J.H. Janssen, A physiologically based kinetic model for bacterial sulfide oxidation, *Water Res.* 47 (2013) 483–492. doi:10.1016/j.watres.2012.09.021.
- [22] D.P. Kelly, J.K. Shergill, W. Lu, A.P. Wood, Oxidative metabolism of inorganic sulfur compounds by bacteria, *Antonie Van Leeuwenhoek.* (1997) 95–107.
- [23] G. Muyzer, D.Y. Sorokin, K. Mavromatis, A. Lapidus, A. Clum, N. Ivanova, A. Pati, P. D’Haeseleer, T. Woyke, N.C. Kyrpides, Complete genome sequence of “*Thioalkalivibrio sulfidophilus*” HL-EbGr7, *Stand. Genomic Sci.* 4 (2011) 23–35. doi:10.4056/sigs.1483693.
- [24] P. Roman, J.B.M. Klok, J.A.B. Sousa, E. Broman, M. Dopson, E. Van Zessen, M.F.M. Bijmans, D.Y. Sorokin, A.J.H. Janssen, Selection and Application of Sulfide Oxidizing Microorganisms Able to Withstand Thiols in Gas Biodesulfurization Systems, *Environ. Sci. Technol.* (2016) acs.est.6b04222. doi:10.1021/acs.est.6b04222.
- [25] P. Roman, M.F.M. Bijmans, A.J.H. Janssen, Influence of methanethiol on biological sulphide oxidation in gas treatment system, *Environ. Technol.* 3330 (2016) 1–11. doi:10.1080/09593330.2015.1128001.

- [26] P. Roman, M.F.M. Bijmans, A.J.H. Janssen, Quantification of individual polysulfides in lab-scale and full-scale desulfurisation bioreactors, *Environ. Chem.* 11 (2014) 702–708. doi:10.1071/EN14128.
- [27] N. Pfennig, K.D. Lippert, Über das Vitamin B₁₂-Bedürfnis phototropher Schwefelbakterien, *Arch. Mikrobiol.* 55 (1966) 245–256. doi:10.1007/BF00410246.
- [28] G.W. Luther, A.J. Findlay, D.J. MacDonald, S.M. Owings, T.E. Hanson, R.A. Beinart, P.R. Girguis, Thermodynamics and kinetics of sulfide oxidation by oxygen: A look at inorganically controlled reactions and biologically mediated processes in the environment, *Front. Microbiol.* 2 (2011) 1–9. doi:10.3389/fmicb.2011.00062.
- [29] P. Roman, R. Veltman, M.F.M. Bijmans, K.J. Keesman, A.J.H. Janssen, Effect of Methanethiol Concentration on Sulfur Production in Biological Desulfurization Systems under Haloalkaline Conditions, *Environ. Sci. Technol.* 49 (2015) 9212–9221. doi:10.1021/acs.est.5b01758.
- [30] P.L.F. Van Den Bosch, M. De Graaff, M. Fortuny-Picornell, R.C. Van Leerdam, A.J.H. Janssen, Inhibition of microbiological sulfide oxidation by methanethiol and dimethyl polysulfides at natron-alkaline conditions, *Appl. Microbiol. Biotechnol.* 83 (2009) 579–587. doi:10.1007/s00253-009-1951-6.
- [31] M. De Graaff, J.B.M. Klok, M.F.M. Bijmans, G. Muyzer, A.J.H. Janssen, Application of a 2-step process for the biological treatment of sulfidic spent caustics, *Water Res.* 46 (2012) 723–730. doi:10.1016/j.watres.2011.11.044.
- [32] J.M. Visser, L.A. Robertson, H.W. Van Verseveld, J.G. Kuenen, Sulfur production by obligately chemolithoautotrophic *Thiobacillus* species, *Appl. Environ. Microbiol.* 63 (1997) 2300–2305.
- [33] P.L.F. Van Den Bosch, M. Fortuny-Picornell, A.J.H. Janssen, Effects of Methanethiol on the Biological Oxidation of Sulfide at Natron-Alkaline Conditions, *Environ. Sci. Technol.* 43 (2009) 453–459. doi:10.1021/es801894p.
- [34] W.E. Kleinjan, A. De Keizer, A.J.H. Janssen, Kinetics of the chemical oxidation of polysulfide anions in aqueous solution, *Water Res.* 39 (2005) 4093–4100. doi:10.1016/j.watres.2005.08.006.
- [35] P. Roman, J. Lipińska, M.F.M. Bijmans, D.Y. Sorokin, K.J. Keesman, A.J.H. Janssen, Inhibition of a biological sulfide oxidation under haloalkaline conditions by thiols and diorgano polysulfanes, *Water Res.* 101 (2016) 448–456. doi:10.1016/j.watres.2016.06.003.
- [36] H.N. Po, N.M. Senozan, The Henderson-Hasselbalch Equation: Its History and Limitations, *J. Chem. Educ.* 78 (2001) 1499–1503. doi:10.1021/ed080p146.
- [37] T. Magoč, S.L. Salzberg, FLASH: Fast length adjustment of short reads to improve genome assemblies, *Bioinformatics.* 27 (2011) 2957–2963. doi:10.1093/bioinformatics/btr507.
- [38] R.C. Edgar, B.J. Haas, J.C. Clemente, C. Quince, R. Knight, UCHIME improves sensitivity and speed of chimera detection, *Bioinformatics.* 27 (2011) 2194–2200. doi:10.1093/bioinformatics/btr381.

- [39] S.F. Altschul, W. Gish, W. Miller, E.W. Myers, D.J. Lipman, Basic local alignment search tool., *J. Mol. Biol.* 215 (1990) 403–10. doi:10.1016/S0022-2836(05)80360-2.
- [40] A.G. Marangoni, *Enzyme Kinetics: A Modern Approach*, John Wiley & Sons, Inc., Hoboken, NJ, USA, 2003. doi:10.1002/0471267295.
- [41] B.M. Peyton, M.R. Mormille, V. Alva, C. Oie, F. Roberto, W.A. Apel, A. Oren, Biotransformation of toxic organic and inorganic contaminants by halophilic bacteria, in: A. Ventosa (Ed.), *Halophilic Microorg.*, Springer Berlin Heidelberg, Berlin, Heidelberg, 2004: pp. 315–331. doi:10.1007/978-3-662-07656-9.
- [42] D.Y. Sorokin, M. Foti, B.J. Tindall, G. Muyzer, *Desulfurispirillum alkaliphilum* gen. nov. sp. nov., a novel obligately anaerobic sulfur- and dissimilatory nitrate-reducing bacterium from a full-scale sulfide-removing bioreactor, *Extremophiles*. 11 (2007) 363–370. doi:10.1007/s00792-006-0048-8.
- [43] B.B. Jørgensen, F. Bak, Pathways and microbiology of thiosulphate transformations and sulfate reduction in a marine sediment (Kattegat, Denmark)., *Appl. Environ. Microbiol.* 57 (1991) 847–856.
- [44] D.Y. Sorokin, P.L.F. Van Den Bosch, B. Abbas, A.J.H. Janssen, G. Muyzer, Microbiological analysis of the population of extremely haloalkaliphilic sulfur-oxidizing bacteria dominating in lab-scale sulfide-removing bioreactors, *Appl. Microbiol. Biotechnol.* 80 (2008) 965–975. doi:10.1007/s00253-008-1598-8.
- [45] J.B.M. Klok, P.L.F. Van Den Bosch, C.J.N. Buisman, A.J.M. Stams, K.J. Keesman, A.J.H. Janssen, Pathways of sulfide oxidation by haloalkaliphilic bacteria in limited-oxygen gas lift bioreactors, *Environ. Sci. Technol.* 46 (2012) 7581–7586. doi:10.1021/es301480z.
- [46] C.J.N. Buisman, P.I. Jspeert, A. Hof, A.J.H. Janssen, R. Ten Hagen, G. Lettinga, Kinetic parameters of a mixed culture oxidizing sulfide and sulfur with oxygen, *Biotechnol. Bioeng.* 38 (1991) 813–820. doi:10.1002/bit.260380803.
- [47] A.J.H. Janssen, S. Meijer, J. Bontsema, G. Lettinga, Application of the Redox Potential for Controlling a Sulfideoxidizing Bioreactor, *Biotechnol. Bioeng.* 60 (1998) 147–155. doi:10.1002/(SICI)1097-0290(19981020)60:2<147::AID-BIT2>3.0.CO;2-N.
- [48] D.Y. Sorokin, M.S. Muntyan, A.N. Panteleeva, G. Muyzer, *Thioalkalivibrio sulfidiphilus* sp. nov., a haloalkaliphilic, sulfur-oxidizing gammaproteobacterium from alkaline habitats, *Int. J. Syst. Evol. Microbiol.* 62 (2012) 1884–1889. doi:10.1099/ijs.0.034504-0.
- [49] R. Bove, P. Lunghi, Experimental comparison of MCFC performance using three different biogas types and methane, 145 (2005) 588–593. doi:10.1016/j.jpowsour.2005.01.069.
- [50] M. Labrenz, P.A. Lawson, B.J. Tindall, P. Hirsch, *Roseibaca ekhonensis* gen. nov., sp. nov., an alkalitolerant and aerobic bacteriochlorophyll a-producing alphaproteobacterium from hypersaline Ekho Lake, *Int. J. Syst. Evol. Microbiol.* 59 (2009) 1935–1940. doi:10.1099/ijs.0.016717-0.

- [51] Y.N. Wang, H. Cai, C.Q. Chi, A.H. Lu, X.G. Lin, Z.F. Jiang, X.L. Wu, *Halomonas shengliensis* sp. nov., a moderately halophilic, denitrifying, crude-oil-utilizing bacterium, *Int. J. Syst. Evol. Microbiol.* 57 (2007) 1222–1226. doi:10.1099/ijso.0.64973-0.
- [52] D.Y. Sorokin, A.M. Lysenko, L.L. Mityushina, T.P. Tourova, B.E. Jones, F.A. Rainey, L.A. Robertson, G.J. Kuenen, *Thioalkalimicrobium aerophilum* gen. nov., sp. nov. and *Thioalkalimicrobium sibericum* sp. nov., and *Thioalkalivibrio versutus* gen. nov., sp. nov., *Thioalkalivibrio nitratis* sp. nov. and *Thioalkalivibrio denitrificans* sp. nov., novel obligately a, *Int. J. Syst. Evol. Microbiol.* 51 (2001) 565–580.

Appendix A - Nomenclature.

Symbol	Parameter
HS^-	Bisulfide anions
H_2S	Sulfide
SO_4^{2-}	Sulfate anions
$\text{S}_2\text{O}_3^{2-}$	Thiosulfate anions
S_8	Biological sulfur
O_2	Oxygen
R_{\max}	Maximum reaction rate
SOB	Sulfur-oxidizing bacteria
FCC	Flavocytochrome c
SQR	Sulfide-quinone reductase
μ_{FCC}	Maximum enzyme rate of flavocytochrome c
μ_{SQR}	Maximum enzyme rate of sulfide-quinone reductase
μ_{CCO}	Maximum enzyme rate of cytochrome c oxidase
μ_{SQRox}	Maximum enzyme rate of sulfide: quinone reductive oxidase
α	Ratio between maximum enzyme rates of flavocytochrome c and sulfide-quinone reductase
K_{FCC}	Affinity constant for flavocytochrome c
K_{SQR}	Affinity constant for sulfide-quinone reductase
K_{CCO}	Affinity constant for cytochrome c oxidase
K_{SQRox}	Affinity constant for sulfide-quinone reductive oxidase
K_i	Affinity constant for inhibition

Appendix B - Non-linear least squares estimation of the kinetic model describing biological sulfide oxidation.

The unknown parameters in the kinetic model for sulfide oxidation under halo-alkaline conditions, represented by the parameter vector θ , are estimated using the experimental data of the respiration test also known as biological oxygen monitoring tests. Via a least square routine, the estimated single-output gives:

$$\hat{\theta}_N = \arg \min_{\theta \in D} \sum_{k=1}^N \varepsilon([HS^-]_k | \theta)^2 \quad \text{Eq. (B.1)}$$

Where $\varepsilon(\cdot | \theta) = y(k) - \hat{y}(\cdot | \theta)$ is the output error at time index k with sulfide concentration $[HS^-]$, $y(k)$ the measured sulfate / thiosulfate concentrations at k , $\hat{y}(\cdot | \theta)$ the predicted model output at k given estimate of θ ($\hat{\theta}$), D is the prior parameter domain. The error variance σ_ε^2 , a measure for the model fit, is given by

$$\sigma_\varepsilon^2 = \frac{1}{N-p} \sum_{k=1}^N \varepsilon([HS^-]_k | \theta)^2 \quad \text{Eq. (B.2)}$$

With p the number of parameters. The vector with standard deviations for each parameter is found, after taking the square root of the diagonal of the covariance matrix of the estimates (COV), which is defined by

$$COV \hat{\theta}_N = \sigma_\varepsilon^2 (X^T X)^{-1} \quad \text{Eq. (B.3)}$$

Where X is the $(N \times p)$ sensitivity matrix with elements $\frac{\partial \varepsilon([HS^-]_k | \theta)}{\partial \theta_j}$ with $k = 1, \dots, N$ and $j = 1, \dots, p$. While the standard deviation for the μ_{FCC} and μ_{SQR} follow from the estimation routine, the standard deviation for the parameter $\alpha = \frac{\mu_{FCC}}{\mu_{SQR}}$ is given by

$$\sigma_\alpha^2 = \left(\frac{\partial \alpha}{\partial \mu_{SQR}} \right)^2 \cdot \sigma_{\mu_{SQR}}^2 + \left(\frac{\partial \alpha}{\partial \mu_{FCC}} \right)^2 \cdot \sigma_{\mu_{FCC}}^2 \quad \text{Eq. (B.4)}$$

Which results in

$$\sigma_\alpha^2 = \left(\frac{\mu_{FCC}}{\mu_{SQR}} \right)^2 \cdot \sigma_{\mu_{SQR}}^2 + \left(\frac{1}{\mu_{SQR}} \right)^2 \cdot \sigma_{\mu_{FCC}}^2 \quad \text{Eq. (B.5)}$$

Appendix C - Non-linear least squares estimation of formation rates.

The formation rate of both SO_4^{2-} and $\text{S}_2\text{O}_3^{2-}$ in the fed-batch experiments were estimated via a linear regression model given by:

$$\widehat{y}(\theta) = \theta(1) \cdot x1 + \theta(2) \cdot x2 \quad \text{Eq. (C.1)}$$

Where $\widehat{y}(\theta)$ is the vector containing the predicted model outputs of either sulfate or thiosulfate, $\theta(1)$ the formation rate of sulfate / thiosulfate, $\theta(2)$ the estimated initial concentration of sulfate / thiosulfate, $x1$ a vector of length N containing sampling times and $x2$ a vector of ones with length N .

The unknown parameters vector $[\theta(1) \ \theta(2)]^T$ was estimated using a non-linear estimation routine, which for the single-output case gives

$$\hat{\theta}_N = \arg \min_{\theta \in D} \sum_{k=1}^N \varepsilon(k|\theta)^2 \quad \text{Eq. (C.2)}$$

Where $\varepsilon(\cdot|\theta) = y(k) - \hat{y}(\cdot|\theta)$ is the output error at time index k with operation time $x1$, $y(k)$ the measured sulfate / thiosulfate concentrations at k , $\hat{y}(\cdot|\theta)$ the predicted model output at k given an estimate of θ ($\hat{\theta}$), D is the prior parameter domain. The error variance σ_ε^2 , a measure for the model fit, is given by

$$\sigma_\varepsilon^2 = \frac{1}{N-p} \sum_{k=1}^N \varepsilon(x1_k|\theta)^2 \quad \text{Eq. (C.3)}$$

With p the number of parameters. The vector with standard deviations for each parameter are found, after taking the square root of the diagonal of the covariance matrix of the estimates (COV), which is defined by

$$COV\hat{\theta}_N = \sigma_\varepsilon^2 (X^T X)^{-1} \quad \text{Eq. (C.4)}$$

Where X is the $(N \times p)$ sensitivity matrix with elements $\frac{\partial \varepsilon(x1_k|\theta)}{\partial \theta_j}$ and with $k = 1, \dots, N$ and $j = 1, \dots, p$, in case of A.1 $X = [x1 \ x2]$. While the standard deviation for both sulfate (σ_{sulfate}) and thiosulfate ($\sigma_{\text{thiosulfate}}$) follows from the estimation routine, the selectivity for sulfur formation follows from the mass balance according to:

$$dS^0 = (dH_2S_{\text{supplied}}/V_{\text{liq}}) - dSO_4^{2-} - dS_2O_3^{2-}$$

As a result, the standard deviation for sulfur formation (σ_{sulfur}) can be determined from the variance:

$$\sigma_{\text{sulfur}}^2 = \sigma_{\text{sulfate}}^2 + \sigma_{\text{thiosulfate}}^2 \quad \text{Eq. (C.5)}$$

The experiment using the Oilfield seed sludge as well as Paper mill - 1, consisted out of two runs with a small interruption due to the system maintenance and medium refreshment. The selectivity for sulfate and thiosulfate was estimated as an average of both experiments. Hence, the standard deviation for both sulfate as thiosulfate can be calculated from the variance

$$\sigma^2 = \frac{\sigma_{\text{run1}}^2 + \sigma_{\text{run2}}^2}{2} \quad \text{Eq. (C.6)}$$

The standard deviation of sulfur follows subsequently from Eq. (C.5). In the following subsections, for each experiment a regression model is identified. The corresponding estimates with standard deviations can be found in Table 4.

Appendix D – Predicted sulfate and sulfur selectivities

To be able to predict the formation of biological products of sulfide oxidation (sulfate and sulfur) it is essential to know α value that was calculated based on the performed respiration tests. In addition, it is required to know the concentration of biomass, sulfide loading, and ORP setpoint, as oxygen concentration will be determined by ORP value. More details can be found in [21].

In this supplementary material, we present three figures. On these figures, we predict sulfate and sulfur selectivity at different oxygen concentrations for four analyzed biomasses. For the prediction we consider α values calculated for each biomass, biomass concentration (see Table 4), sulfide loading rate ($58.2 \text{ mM S day}^{-1}$) and ORP setpoint (-390 mV).

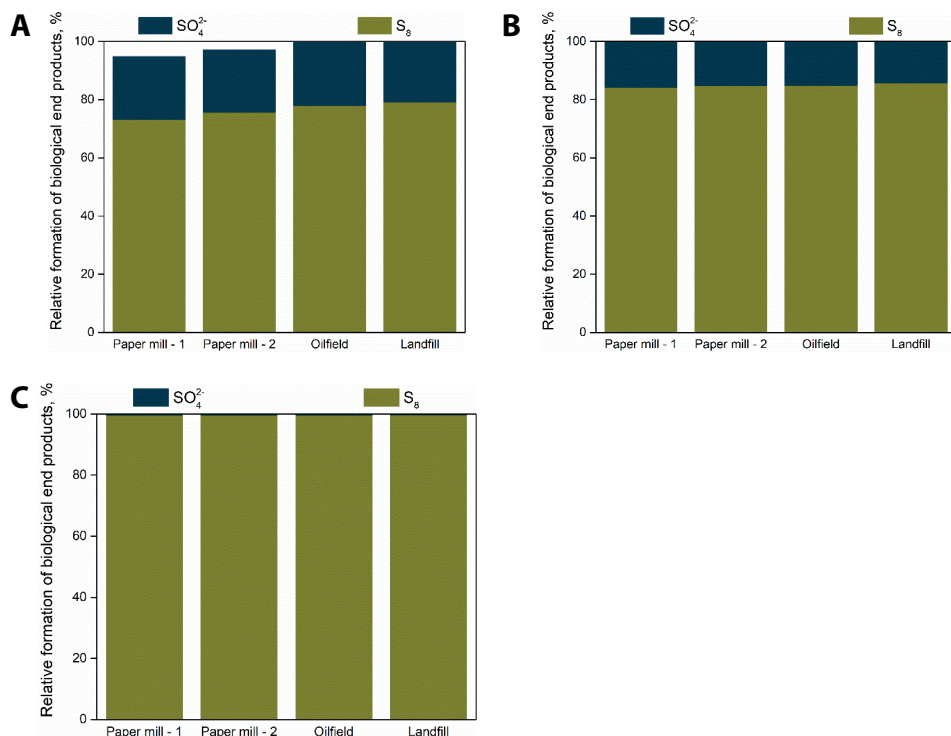


Fig. D1. Predicted sulfate and sulfur selectivities at (A) high oxygen concentration (200 nM), (B) at elevated oxygen concentration (100 nM), and (C) at limiting oxygen concentration (10 nM).

CHAPTER 3

3

Development of quantitative PCR for the detection of *Alkalilimnicola ehrlichii*, *Thioalkalivibrio sulfidophilus* and *Thioalkalibacter halophilus* in gas biodesulfurization processes

Abstract

Chemolithoautotrophic sulfur-oxidizing bacteria (SOB) are crucial key players in biotechnological processes to remove hydrogen sulfide from sour gas streams. Several different haloalkaliphilic SOB have been detected and isolated from lab- and full-scale facilities, which all performed differently considering end product yields (sulfur and sulfate) and conversion rates. Understanding and regulating bacterial community dynamics in biodesulfurization processes will enable optimization of the process operation. We developed quantitative PCR (qPCR) assays to quantify haloalkaliphilic sulfur-oxidizing gammaproteobacterial species *Alkalilimnicola ehrlichii*, *Thioalkalivibrio sulfidophilus*, and *Thioalkalibacter halophilus* that dominate bacterial communities of biodesulfurization lab- and full-scale installations at haloalkaline conditions. The specificity and PCR efficiency of novel primer sets were evaluated using pure cultures of these target species. We further validated the qPCR assays by quantification of target organisms in five globally distributed full-scale biodesulfurization installations. The qPCR assays perform a sensitive and accurate quantification of *Alkalilimnicola ehrlichii*, *Thioalkalivibrio sulfidophilus* and *Thioalkalibacter halophilus*, thus providing rapid and valuable insights into process performance and SOB growth dynamics in gas biodesulfurization systems.

This chapter has been published as: Kiragosyan K., van Veelen P., Gupta S., Tomaszewska-Porada A., Roman P., Timmers P.H.A., Development of quantitative PCR for the detection of *Alkalilimnicola ehrlichii*, *Thioalkalivibrio sulfidophilus* and *Thioalkalibacter halophilus* in gas biodesulfurization processes, AMB Express. 9 (2019) 99. doi:10.1186/s13568-019-0826-1.

3.1. Introduction

Sulfur-oxidizing bacteria (SOB) are microorganisms that naturally occur in highly saline and alkaline environments such as soda lakes [1,2]. SOB are known to be present in complex and species-rich consortia of microorganisms involved in both anaerobic and aerobic processes [3] and can grow chemolithoautotrophically using inorganic sulfur compounds as electron donor and CO_2 as carbon source [4]. These chemolithoautotrophic SOB are specifically enriched in biotechnological processes to remove hydrogen sulfide (H_2S) from industrial gas streams by producing sulfur [5,6]. Biodesulfurization processes of the Thiopaq® family are operated under haloalkaline conditions, i.e. high pH (≥ 8.5) and high soda concentrations (1 M Na^+) [5].

Since 2009, the number of gas biodesulfurization installations increased globally [7]. All full-scale installations operate at different process conditions i.e. pH, salinity, oxidation-reduction potential (ORP) and treat feed gas of a various compositions (i.e. presence of different organic carbon compounds or contaminants such as thiols and BTEX) [8]. To investigate which factors ensure stable process operation, a number of lab- and full-scale gas biodesulfurization installations have been monitored on the microbial community composition and process conditions. In sulfide-fed lab-scale installations, *Thioalkalivibrio sulfidiphilus* was the dominant SOB [8,9]. In other lab-scale installations with sulfide feed gas supplemented with thiols, *Alkalilimnicola* sp. and *Thioalkalibacter* sp. were found to dominate [10]. The addition of these toxic thiols not only affected SOB community composition, but alterations of the biodesulfurization process conditions can also cause a community change. For example, changes in the bioreactor design or addition of an extra bioreactor can also result in SOB community composition shift [11].

In most cases, these SOB community dynamics were monitored using 16S rRNA gene amplicon sequencing. This method provides only estimates of relative taxon abundances and it is time consuming and costly. Monitoring SOB dynamics with quantitative PCR (qPCR), would provide absolute numbers of key SOB species in biodesulfurization processes, and is relatively fast, less costly and results can be analyzed and interpreted with ease. The ability to monitor SOB species dynamics rapidly and inexpensively will help to monitor the key population dynamics and to optimize biodesulfurization process efficiency. qPCR is widely used for microbial quantification in many types of environmental studies [12], but so far no SOB-specific primers are currently available to monitor dynamics of relevant SOB species. The qPCR specificity for different SOB species depends on several parameters: the primer sequences for the target, time and temperature of primer annealing, annealing, amplicon product size, concentration of Mg^{2+} , dNTPs, fidelity of enzymes, and the purity of the DNA sample [13].

In this work we designed target-specific primers and developed specific qPCR assays to monitor absolute abundances of the three most dominant haloalkaliphilic SOB species found in operational biodesulfurization Thiopaq® installations until now: *Alkalilimnicola ehrlichii*, *Thioalkalivibrio sulfidophilus* and *Thioalkalibacter halophilus*. The resulting quantitative measures provide insights in species growth dynamics and interactions. Hence, developed quantitative PCR assays can be used to establish relationships between the operational conditions and the biological community in biodesulfurization processes in order to establish stable SOB communities that ensure predictable and stable process conditions.

3.2. Materials and methods

3.2.1. Microbial sludge sampling and sample preparation

Biomass from a lab-scale, fed-batch biodesulfurization system, which was fed with H₂S and methanethiol gas, was obtained after 76 days of continuous operation. H₂S gas was continuously supplied at a loading rate of 58.15 mM S day⁻¹, whereas methanethiol loading rate was stepwise (add steps from 0 to 2 mM) increased for biomass acclimatization during the 76 days to a maximum concentration of 2 mM S day⁻¹. On the last day of operation, microbial sludge was sampled and centrifuged for 15 min at 16,000 *g* to obtain the cell pellet. The cell pellet was washed twice with 0.5 M Na⁺ buffer solution (pH 8.5) to prevent cell lysis and was subsequently stored at -80 °C until DNA extraction.

3.2.2. DNA isolation and purification

Genomic DNA was extracted using the DNeasy PowerLyzer PowerSoil Kit (Qiagen, Venlo, the Netherlands) following the manufacturer's instructions. After DNA extraction, DNA was purified with the DNA Clean & Concentrator kit (Zymo Research, Irvine, CA, USA). Extracted DNA was quantified using the QuantiFluor dsDNA system on a Quantus™ fluorometer (Promega, Leiden, the Netherlands). DNA quality was evaluated using gel electrophoresis.

3.2.3. Clone Library Construction and Sequencing

To design primers targeting the most dominant SOB species present in the established mixed SOB population, full-length 16S rRNA gene sequences recovered from the community DNA. The full 16S rRNA gene was amplified from the extracted and purified DNA using universal bacterial primers 27F (5'-GTTTGATCCTGGCTCAG-3') [14] and 1492R (5'-CGGCTACCTTGTACGAC-3') [15]. The PCR program started with initial denaturation (95 °C for 2 min) followed by 30 cycles of denaturation for 30

sec at 95 °C, annealing for 40 sec at 52 °C, elongation for 1.30 min at 72 °C, and with a final 7 min elongation at 72 °C. The PCR products were again purified with the DNA Clean & Concentrator kit and ligated into the pGEM-T Easy Vector System, according to the manufacturer's instructions (Promega, City, the Netherlands). The ligation mixture was used to transform *Escherichia coli* JM109 competent cells (Promega, City, the Netherlands). Colonies were picked and DNA was extracted and sent for Sanger sequencing to BaseClear B.V. (Leiden, the Netherlands). Obtained forward and reverse sequences were assembled into contigs, and ends were quality trimmed with the DNA Baser software (v4, Heracle Biosoft, www.DnaBaser.com, Romania). Subsequently, sequences were cleaned by cutting off primer sequences and were screened for vector contamination using VecScreen (NCBI, MD, USA).

3.2.4. Target species-specific primer design

The full length 16S rRNA gene sequences were aligned and taxonomically classified using the SINA alignment tool (v1.2.11) according to the global SILVA alignment [16] nucleic acid based detection and quantification of microbial diversity. The ARB software suite with its corresponding rRNA datasets has been accepted by researchers worldwide as a standard tool for large scale rRNA analysis. However, the rapid increase of publicly available rRNA sequence data has recently hampered the maintenance of comprehensive and curated rRNA knowledge databases. A new system, SILVA (from Latin *silva*, forest). Sequence identity was also investigated with the online nucleotide BLAST tool [17]. Aligned sequences of the species of interest (*Thioalkalivibrio sulfidiphilus*, *Alkalilimnicola ehrlichii* and *Thioalkalibacter halophilus*) were merged with the SILVA 16S rRNA gene database version SSU rl 28 [18] using the ARB software package (arb-6.0.6) [19]. Primer sets were designed based on the highest specificity (100 % with 0 mismatches) for *Alkalilimnicola ehrlichii* and *Thioalkalibacter halophilus* species. For *Thioalkalivibrio* spp., primers were designed to target the *Thioalkalivibrio denitrificans* cluster (highlighted in Fig. 1). The designed primers were then validated *in silico* using the TestProbe and TestPrime services of Silva [20], Primer-BLAST [21] and *in silico* PCR (http://insilico.ehu.es/user_seqs/). After validation, designed primer sequences were ordered from Biolegio (Nijmegen, the Netherlands).

3.2.5. In vitro primer evaluation on target species pure cultures

To be able to test the specificity of the designed primers and to optimize the qPCR protocol, every designed primer set was tested using pure cultures. Two strains used in this study were obtained from the German Collection of Microorganisms and Cell Cultures (DSMZ): *Alkalilimnicola ehrlichii* strain MLHE-1 (DSM-17681) and *Thioalkalibacter halophilus* strain ALCO 1 (DSM-19224). *Thioalkalivibrio sulfidiphilus*

strain HL-EbGr7 was provided from the personal collection of Prof. Dr Gerard Muyzer (Amsterdam University, the Netherlands).

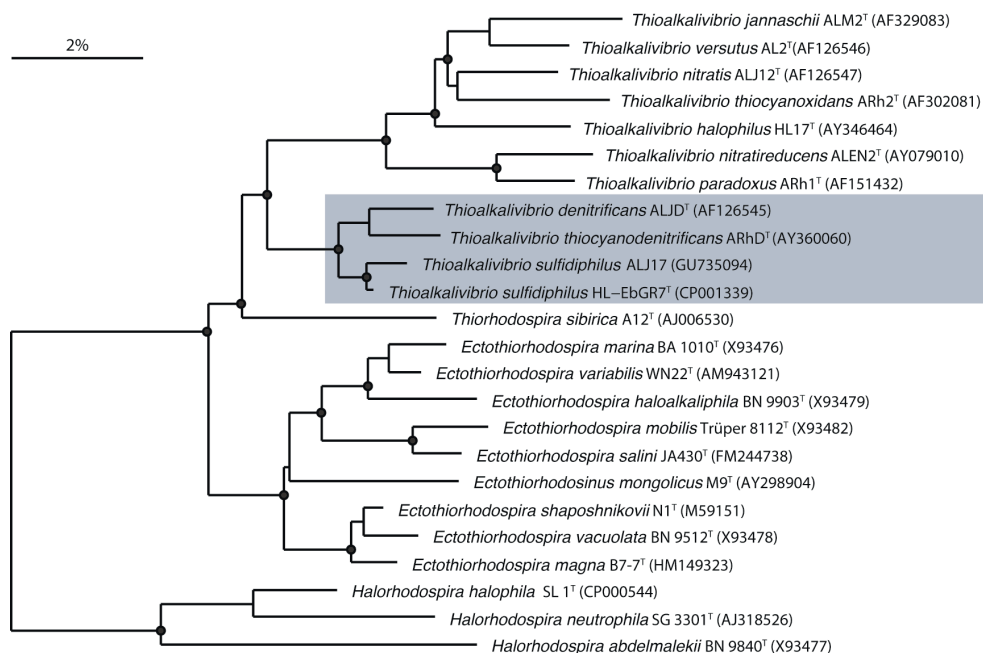


Fig. 1. Phylogenetic position of *Thioalkalivibrio sulfidiphilus* in the cluster for which primers for *Thioalkalivibrio* spp. were designed (adapted from [22]). Bar indicates 2 % sequence divergence.

3.2.6. qPCR assay optimization

For the optimization of qPCR assays the workflow was as follows:

1. Firstly, the annealing temperature was optimized based on the theoretical melting temperature (T_m) via gradient PCR (± 10 °C). In this step, pure cultures were used as positive controls for the selected primer sets. After each temperature gradient run, gel electrophoresis (GE) was performed to confirm the size of the PCR product(s) based on expected insert lengths of the developed primer sets.
2. For each primer set, primer specificity for a target species was assessed by simultaneous testing against the non-target cultured pure strains (*Thioalkalivibrio sulfidiphilus* strain HL-EbGr7, *Thioalkalivibrio denitrificans* strain ALJD (DSM-13742), *Alkalilimnicola ehrlichii* strain MLHE-1 and *Thioalkalibacter halophilus* strain ALCO 1) and cultured clones found in our cloned biomass (*Thioalkalimicrobium* spp, *Halomonas* sp. HB. Br (GU228481)) at the selected optimal annealing temperature for each primer set. When bright bands of the positive target strain were visible on GE and no bands of non-target strain negative controls appeared,

- fine-tuning of the optimal annealing temperature was continued with a narrower temperature gradient ranging between ± 3 °C.
3. To further assess primer specificity, melting curve analysis was performed (50 – 95 °C, with 0.5 °C increments) using quantitative PCR (Bio Rad CFX96 Touch™, City, the Netherlands) with SYBR® Green fluorescent dye (Bio Rad, the Netherlands). The qPCR reaction volume was 20 µl with 0.33 pmol µl⁻¹ of forward and reverse primers. Melt curves revealed target-specific product formation at the determined optimal annealing temperatures for all three primer sets (Appendix A, Fig. A1, A2 and A3). The optimal annealing temperatures for cultured positive control strains were then applied in the qPCR analysis of bioreactor experimental samples. For primer set *Thioalkalivibrio* spp. Thio-6F and Thio-8R, the optimal T_m was 55 °C, for Alkali-4AF and Alkali-6BR T_m was 53 °C, and for Tab-137-G_F and Tab-210R best T_m was at 66 °C.
 4. To verify that our developed primer sets specifically amplified the target species in our experimental samples, melting curves of experimental samples were analyzed for qPCR amplicon specificity, and then a random subset of ($n = 4$ to 6 per primer set) qPCR products were sent for Sanger sequencing to BaseClear B.V. (Leiden, The Netherlands). Sequences were assembled using the DNA Baser software (v4, Heracle Biosoft, www.DnaBaser.com, Romania) and identified with BLAST [17]. When qPCR amplicons from the experimental samples were positively identified as the target species, we continued with the preparation of standard curves using the DNA of the pure cultures.
 5. As a positive control, cultured pure strains were used in target species-specific qPCR assays to establish a standard curve in order to quantify each of their copy numbers in the experimental samples. The concentrations of the positive control DNA were measured using QuantiFluor dsDNA systems and a Quantus™ fluorometer (Promega, the Netherlands). Positive controls were then serially diluted in 10-fold dilutions ranging between 10^6 to 10^1 copies · µl⁻¹ of the 16S rRNA gene. These serial dilutions were used to generate standard curves which allowed minimal reaction efficiencies of 90-100 % and $0.997 < R_2 < 0.999$.

3.2.7. Validation of the developed qPCR assay

To validate the developed qPCR methods, we used biomass from different five full-scale gas biodesulfurization installations (Table 1). Additional research focusing on the microbial community compositions of these full-scale installations was based on 16S rRNA gene amplicon sequencing [8]. The applicability of the qPCR assay was validated by comparing qPCR-based relative target abundances with relative abundances obtained from the 16S rRNA gene amplicon sequence data. To calculate relative target

abundances, total bacterial 16S rRNA gene copy abundance was quantified using the universal bacterial primer set 338F/518R [15,23] and an in-house protocol [24].

Table 1 A brief description of the full-scale biodesulfurization installations, and averaged operational parameters.

Location	Industry	Sour gas composition	Sample ID
Eerbeek (NL)	Paper mill	biogas, 0.7 % H ₂ S	Paper mill – 1
Zülrich (DE)	Paper mill	biogas, 0.5 % H ₂ S	Paper mill – 2
Amersfoort (NL)	Landfill waste	landfill gas, 0.3 % H ₂ S	Landfill
Southern Illinois (USA)	Oil and gas	associated gas, 1-5 % H ₂ S, 50-200 ppm VOSC*	Oilfield – 1
Sulawesi (ID)	Oil and gas	acid gas 80 – 90 %, 10 – 20 % H ₂ S, X ppm thiols	Oilfield – 2

*VOSC – volatile organic sulfur compounds, e.g., thiols and diorganopolysulfides.

3.2.8. Accession number

The EMBL-EBI accession numbers of the full-length 16S rRNA clonal gene sequences of *Alkalilimnicola ehrlichii*, *Thioalkalivibrio sulfidiphilus* and *Thioalkalibacter halophilus* are LR214448 - LR214450 in the project number PRJEB30777. 16S rRNA gene amplicon sequences from the full-scale installations are deposited under EMBL-EBI project accession number PRJEB27163 and PRJEB32000.

3.3. Results

3.3.1. Primers evaluation and qPCR assay optimization

For each of the three targets, we designed three primer sets for which we subsequently optimized the qPCR protocols. The properties of the primers that were tested *in silico* and *in vitro* are summarized in Table 2.

Table 2 Description of designed species-specific primers description.

Primer ID	Primer sequence	E. coli position	Theoretical T _m , °C	Length, bp	GC content, %
Thio-6F	AGG GCT AGA GTT TGG TAG	647	52	18	50
Thio-8R	AGA GGC ATA ATC CTC CCA	834	54	18	50
Alkali-4AF	GTT AAT AGC CGT GGG TCT	462	54	18	50
Alkali-6BR	TAC CAG ACT CTA GCC CGA	646	56	18	56
Tab-137-G_F	CTT AGG TGG GGG ATA ACA CG	137	57	20	55
Tab-210R	ATC CTT TGG CGC GAG GTC CG	210	65	20	65

F- forward; R- reverse; Thio - *Thioalkalivibrio* spp.; Alkali - *Alkalilimnicola ehrlichii*; Tab - *Thioalkalibacter halophilus*.

In silico amplification demonstrated that primer set Thio-6F/Thio8-R quantified *Tv. sulfidiphilus* and closely related *Tv. denitrificans*. Empirical qPCR experiments and

subsequent melt-curve analysis on DNA extracted from pure cultures of *Tv. sulfidophilus* and *Tv. denitrificans* correspondingly showed amplification of both species at the same annealing temperature (Appendix A, Fig. A1). qPCR assays for *Alk. ehrlichii* and *Th. halophilus* showed species-specificity *in silico* and *in vitro* (Fig. A2 and A3). Yet, our temperature gradient experiment conducted for the *Alk. ehrlichii*-targeting primer set Alkali-4AF/Alkali-6BR suggested amplification of non-target DNA at temperatures exceeding 55 °C. Melt curve analysis of this temperature gradient demonstrated that non-target amplification reduced with decreasing temperatures. A subsequent temperature gradient including lower temperatures revealed that at 53 °C, the desired specificity for *Alkalilimnicola ehrlichii* was reached. Optimal reaction parameters for the developed qPCR assays were initial denaturation for 5 min at 95 °C followed by 30 amplification cycles of denaturation for 10 sec at 95 °C, annealing for 30 sec at 53 °C for *Alkalilimnicola ehrlichii*, 55 °C for *Thioalkalivibrio sulfidophilus* and 66 °C for *Thioalkalibacter halophilus*.

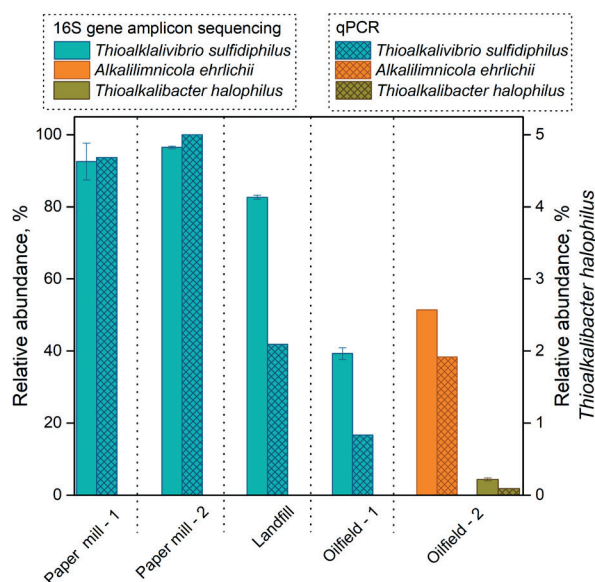


Fig. 2. Comparison of relative taxon abundances using 16S rRNA gene amplicon sequencing (NGS) and species-specific qPCR from five full-scale gas biodesulfurization installations. The results represent the average value per full-scale biodesulfurization installation for each of the target species that was positively detected. Error bars represent the standard deviation of technical duplicates. Amplicon sequence data are modified from [8].

3.3.2. Validation of the developed qPCR assay

To validate the applicability of the developed qPCR assays, we quantified absolute abundances of the target species and total bacteria in five full-scale gas biodesulfurization installations geographically distributed across Europe, Asia, and North America (Table 1). Our results demonstrated that the qPCR-based relative species abundances (i.e. ratio species-specific to total bacterial 16S rRNA amplicon count) are analogous to the relative abundances obtained by 16S rRNA gene amplicon sequencing (i.e. ratio taxon-specific to total read count) of the microbial community structure in the full-scale biodesulfurization installations (Fig. 2). In both Paper mill installations, the relative abundance of *Thioalkalivibrio* spp. quantified by qPCR and amplicon sequence data are of the same magnitude. However, in three other full-scale installations quantified abundances by qPCR assays differed from amplicon sequencing data. Relative abundances of *Thioalkalivibrio* spp. detected by qPCR in Oilfield and Landfill plants were two times less than the relative abundance of *Tv. sulfidophilus* in amplicon sequencing data (Fig. 2). The same two-fold difference was found for less abundant *Th. halophilus* in Oilfield - 2 installation (0.22 % vs. 0.09 %) (Fig. 2). Collectively, these results indicate that the developed qPCR assays can be applied for detection and quantification of *Alkalilimnicola ehrlichii*, *Thioalkalivibrio sulfidophilus* and *Thioalkalibacter halophilus* in various gas biodesulfurization installations.

3.4. Discussion

Developed qPCR assays for fast and accurate quantification of *Alkalilimnicola ehrlichii*, *Thioalkalivibrio sulfidophilus* and *Thioalkalibacter halophilus* were optimized to achieve maximal specificity and sensitivity to detect potentially low abundance of target species. For *Alk. ehrlichii* and *Th. halophilus*, the designed primers achieved 100% specificity by allowing 0 mismatches in the primer binding region. For *Thioalkalivibrio* spp., primers were designed for a subcluster of this genus (Fig. 1). *Thioalkalivibrio sulfidophilus* HL-EbGR7 is genetically related to another *Tv. sulfidophilus* ALJ17 and to *Tv. denitrificans* [22,25]. Hence, we can conclude that the designed primer set quantified *Tv. sulfidophilus* in the samples as it is the only *Thioalkalivibrio* species detected and dominantly present at low salt conditions in the gas biodesulfurization lab- and full-scale installations. The targeted sub-cluster contains other two closely related species, which are *Tv. denitrificans* and *Tv. thiocyanodenitrificans* [22]. The designed primer set Thio6F/Thio8R is specific for *Tv. sulfidophilus* and *Tv. denitrificans*, whereas *Tv. thiocyanodenitrificans* was not tested (Appendix A, Fig. A1). However, *Tv. denitrificans* and *Tv. thiocyanodenitrificans* have never been detected as thiodenitrifying conditions are not provided in the full-scale biodesulfurization process. It is therefore confirmed that the primer set Thio6F/

Thio8R only quantified *Thioalkalivibrio sulfidophilus* in the experimental samples from biodesulfurization full- and lab-scale installations.

Optimization of the quantitative real-time PCR protocols enhanced the specificity of the designed primer sets in experimental samples. Conventionally, regular PCR temperature gradients are advisable to be performed with subsequent visualization of product bands using gel electrophoresis. However, the detection by agarose gel electrophoresis is limited for low (expected) product concentrations [26,27]. For the Alkali-4AF/Alkali-6BR primer set targeting *Alkalilimnicola ehrlichii*, we reached specificity at a lower than expected annealing temperature. Similarly, Sipos et al. [28] found that three universal bacterial primers showed better performance at lower temperatures based on temperature gradients with varying annealing temperatures (47 to 61 °C). Furthermore, Ishii and Fukui [29] also found that at low temperatures, mismatch biases of primers were reduced. Apparently, decreasing annealing temperatures can yield improved target specificity of qPCR assays, which proved a beneficial property for the *Alkalilimnicola ehrlichii* assay. In addition, the reverse primer with relatively high GC content Alkali-6BR (56 %, Table 2), was more specific for detection of *Alkalilimnicola ehrlichii* at lower temperatures.

Sequencing based methods give the possibility to resolve the community composition of complex experimental samples, where further qPCR assay can be complementary applied to answer more profound questions on population dynamics of a specific target organism. In our work, we showed that with use of both techniques similar results can be achieved, which confirms the accuracy of the developed qPCR assays. Relative abundance estimates for dominant species between qPCR and 16S amplicon sequence data were comparable in both Paper mill installations, while in other full-scale installations there was a two-fold difference. Observed difference might be caused by the use of different universal primer sets for 16S rRNA gene quantification in qPCR and NGS, because no primer set is truly universal [30]. Primers have different affinity for different taxonomic groups what prevents detection of certain operational taxonomic units (OTUs) in NGS [31]. This results in biased relative abundances especially within complex samples [32]. In addition, variation between qPCR and NGS counts can be explained by a PCR bias (in NGS) introduced by less dominant species [33]. Hence, we suggest that it is reasonable to expect that the final number of reads for the target species is higher using universal primers after a defined number of exponential amplification cycles. Detection limits of rare taxa are strongly dependent on the sequencing depths of sample (i.e. number of sequence reads per sample). In 16S rRNA gene amplicon sequencing methods, competition for primers occurs between rare and abundant taxa, where most likely abundant taxa outcompete amplification of rare taxa [34]. With qPCR however, species-specific absolute quantification of rare and abundant taxa can be done.

The development of three novel qPCR assays allows for accurate, sensitive, fast and cost-efficient quantification of *Alkalilimnicola ehrlichii*, *Thioalkalivibrio* spp. and *Thioalkalibacter halophilus* in complex samples, such as lab- and full-scale gas biodesulfurization installations. The presented qPCR assays will have ample applicability for monitoring dynamics of key SOB species in the gas biodesulfurization process, especially in the presence of common process perturbations such as thiols. Moreover, established dynamics will allow us to expand our understanding of the gas biodesulfurization process and thus, will enable us to improve process performance.

Acknowledgments

This work has been performed within the cooperation framework of Wetsus, European Centre of Excellence for Sustainable Water Technology (wetusus.nl) and Wageningen University and Research (wur.nl). Wetsus is co-funded by the Netherlands' Ministry of Economic Affairs and Ministry of Infrastructure and Environment, the European Union's Regional Development Fund, the Province of Fryslan and the Northern Netherlands Provinces. Wetsus is also a coordinator of the WaterSEED project that received funding from European Union's Horizon 2020 research and innovation programme under Marie Skłodowska-Curie grant agreement No. 665874. The research of Peer H.A. Timmers was supported by the Soehngen Institute of Anaerobic Microbiology (SIAM) Gravitation grant (024.002.002) of the Netherlands Ministry of Education, Culture and Science and the Netherlands Organisation for Scientific Research (NWO). We would like to thank Franka Tulner (Wetsus and Van Hall Larenstein University of Applied Science, the Netherlands) for the help with *Thioalkalibacter halophilus* method optimization. We acknowledge Rebeca Pallarés Vega (Delft University of Technology and Wetsus, the Netherlands) and Gonçalo Macedo (Utrecht University and Wetsus, the Netherlands) for the support and guidance during qPCR methods development and data processing. We also would like to thank Prof. Dr. Gerard Muyzer (University of Amsterdam, the Netherlands) for providing *Thioalkalivibrio sulfidiphilus* pure strain and Dr. Caroline Plugge for fruitful discussions regarding optimization procedure.

References

- [1] D.Y. Sorokin, J.G. Kuenen, Haloalkaliphilic sulfur-oxidizing bacteria in soda lakes, *FEMS Microbiol. Rev.* 29 (2005) 685–702. doi:10.1016/j.femsre.2004.10.005.
- [2] D.Y. Sorokin, H. Banciu, L.A. Robertson, J.G. Kuenen, M.S. Muntyan, G. Muyzer, Halophilic and haloalkaliphilic sulfur-oxidizing bacteria, in: E. Rosenberg, E.F. DeLong, E. Stackebrandt, S. Lory, F. Thompson (Eds.), *Prokaryotes Prokaryotic Physiol. Biochem.*, Springer-Verlag, Berlin-Heidelberg, 2013: pp. 530–555. doi:10.1007/978-3-642-30141-4.
- [3] A.J.H. Janssen, P.N.L. Lens, A.J.M. Stams, C.M. Plugge, D.Y. Sorokin, G. Muyzer, H. Dijkman, E. Van Zessen, P. Luimes, C.J.N. Buisman, Application of bacteria involved in the biological sulfur cycle for paper mill effluent purification, *Sci. Total Environ.* 407 (2009) 1333–1343. doi:10.1016/j.scitotenv.2008.09.054.
- [4] W. Ghosh, B. Dam, Biochemistry and molecular biology of lithotrophic sulfur oxidation by taxonomically and ecologically diverse bacteria and archaea, *FEMS Microbiol. Rev.* 33 (2009) 999–1043. doi:10.1111/j.1574-6976.2009.00187.x.
- [5] P.L.F. Van Den Bosch, O.C. Van Beusekom, C.J.N. Buisman, A.J.H. Janssen, Sulfide oxidation at halo-alkaline conditions in a fed-batch bioreactor, *Biotechnol. Bioeng.* 97 (2007) 1053–1063. doi:10.1002/bit.21326.
- [6] D.Y. Sorokin, J.G. Kuenen, G. Muyzer, The microbial sulfur cycle at extremely haloalkaline conditions of soda lakes, *Front. Microbiol.* 2 (2011). doi:10.3389/fmicb.2011.00044.
- [7] W. Driessen, E. Van Zessen, M. Visser, Full-scale experience with biological biogas desulfurization, in: 16th Eur. Biosolids Org. Resour. Conf., 2011.
- [8] K. Kiragosyan, J.B.M. Klok, K.J. Keesman, P. Roman, A.J.H. Janssen, Development and validation of a physiologically based kinetic model for starting up and operation of the biological gas desulfurization process under haloalkaline conditions, *Water Res.* X. 4 (2019) 100035. doi:10.1016/j.wroa.2019.100035.
- [9] D.Y. Sorokin, P.L.F. Van Den Bosch, B. Abbas, A.J.H. Janssen, G. Muyzer, Microbiological analysis of the population of extremely haloalkaliphilic sulfur-oxidizing bacteria dominating in lab-scale sulfide-removing bioreactors, *Appl. Microbiol. Biotechnol.* 80 (2008) 965–975. doi:10.1007/s00253-008-1598-8.
- [10] P. Roman, J.B.M. Klok, J.A.B. Sousa, E. Broman, M. Dopson, E. Van Zessen, M.F.M. Bijmans, D.Y. Sorokin, A.J.H. Janssen, Selection and Application of Sulfide Oxidizing Microorganisms Able to Withstand Thiols in Gas Biodesulfurization Systems, *Environ. Sci. Technol.* (2016) acs.est.6b04222. doi:10.1021/acs.est.6b04222.
- [11] R. De Rink, J.B.M. Klok, D.Y. Sorokin, G.J. Van Heeringen, A. Ter Heijne, R. Zeijlmaker, Y.M. Mos, V. De Wilde, K.J. Keesman, C.J.N. Buisman, Increasing the selectivity for sulfur formation in biological gas desulfurization, *Environ. Sci. Technol.* 53 (2019) 4519–4527. doi:10.1021/acs.est.8b06749.

- [12] M. Filion, ed., *Quantitative Real-time PCR in Applied Microbiology*, Caiser Academic Press, Norfolk, UK, 2012.
- [13] J. Robertson, J. Walsh-Weller, An introduction to PCR primer design and optimization of amplification reactions, *Forensic DNA Profiling Protoc.* 98 (1998) 6–8. doi:10.1385/0-89603-443-7:121.
- [14] A. Felske, R. Weller, Cloning 16S rRNA genes and utilization to type bacterial communities, in: G.A. Kowalchuk, F.J. De Bruijn, I.M. Head, A.D.L. Akkermans, J.D. Van Elsas (Eds.), *Mol. Microb. Ecol. Man.*, Second, Kluwer Academic Publishers, Dordrecht, 2004: pp. 510–523. doi:10.1007/978-94-011-0351-0.
- [15] D.J. Lane, 16S/23S rRNA sequencing, in: E. Stackebrandt, M. Goodfellow (Eds.), *Nucleic Acid Tech. Bact. Syst.*, John Wiley & Sons, Inc., New York, 1991: pp. 115–175.
- [16] E. Pruesse, C. Quast, K. Knittel, B.M. Fuchs, W. Ludwig, J. Peplies, F.O. Glöckner, SILVA: A comprehensive online resource for quality checked and aligned ribosomal RNA sequence data compatible with ARB, *Nucleic Acids Res.* 35 (2007) 7188–7196. doi:10.1093/nar/gkm864.
- [17] T. Madden, The BLAST Sequence Analysis Tool, *NCBI Handbook*[Internet]. (2002) 1–15.
- [18] C. Quast, E. Pruesse, P. Yilmaz, J. Gerken, T. Schweer, P. Yarza, J. Peplies, F.O. Glöckner, The SILVA ribosomal RNA gene database project: Improved data processing and web-based tools, *Nucleic Acids Res.* 41 (2013) 590–596. doi:10.1093/nar/gks1219.
- [19] W. Ludwig, O. Strunk, R. Westram, L. Richter, H. Meier, A. Yadhukumar, A. Buchner, T. Lai, S. Steppi, G. Jacob, W. Förster, I. Brettske, S. Gerber, A.W. Ginhart, O. Gross, S. Grumann, S. Hermann, R. Jost, A. König, T. Liss, R. Lüßbmann, M. May, B. Nonhoff, B. Reichel, R. Strehlow, A. Stamatakis, N. Stuckmann, A. Vilbig, M. Lenke, T. Ludwig, A. Bode, K.H. Schleifer, ARB: A software environment for sequence data, *Nucleic Acids Res.* 32 (2004) 1363–1371. doi:10.1093/nar/gkh293.
- [20] A. Klindworth, E. Pruesse, T. Schweer, J. Peplies, C. Quast, M. Horn, F.O. Glöckner, Evaluation of general 16S ribosomal RNA gene PCR primers for classical and next-generation sequencing-based diversity studies, *Nucleic Acids Res.* 41 (2013) 1–11. doi:10.1093/nar/gks808.
- [21] J. Ye, G. Coulouris, I. Zaretskaya, I. Cutcutache, S. Rozen, T.L. Madden, Primer-BLAST: A tool to design target-specific primers for polymerase chain reaction, *BMC Bioinformatics.* 13 (2012) 11. doi:10.1186/1471-2105-13-134.
- [22] D.Y. Sorokin, M.S. Muntyan, A.N. Panteleeva, G. Muyzer, *Thioalkalivibrio sulfidiphilus* sp. nov., a haloalkaliphilic, sulfur-oxidizing gammaproteobacterium from alkaline habitats, *Int. J. Syst. Evol. Microbiol.* 62 (2012) 1884–1889. doi:10.1099/ijs.0.034504-0.
- [23] G. Muyzer, E.C.D.E. Waal, A.G. Uitierlinden, Profiling of Complex Microbial Populations by Denaturing Gradient Gel Electrophoresis Analysis of Polymerase Chain Reaction-Amplified Genes Coding for 16S rRNA, *Appl. Environ. Microbiol.* 59 (1993) 695–700.

- [24] R. Pallares-Vega, H. Blaak, R. van der Plaats, A.M. de Roda Husman, L.H. Leal, M.C.M. van Loosdrecht, D.G. Weissbrodt, H. Schmitt, Determinants of presence and removal of antibiotic resistance genes during WWTP treatment: A cross-sectional study, *Water Res.* (2019). doi:10.1016/j.watres.2019.05.100.
- [25] A.-C. Ahn, L. Overmars, D.Y. Sorokin, J.P. Meier-Kolthoff, G. Muyzer, M. Richter, T. Woyke, Genomic diversity within the haloalkaliphilic genus *Thioalkalivibrio*, *PLoS One.* 12 (2017) e0173517. doi:10.1371/journal.pone.0173517.
- [26] C.J. Smith, A.M. Osborn, Advantages and limitations of quantitative PCR (Q-PCR)-based approaches in microbial ecology, *FEMS Microbiol. Ecol.* 67 (2009) 6–20. doi:10.1111/j.1574-6941.2008.00629.x.
- [27] L. Garibyan, N. Avashia, Research Techniques Made Simple: Polymerase Chain Reaction (PCR), *J. Invest. Dermatol.* 133 (2013) 20382. doi:10.1038/jid.2013.1.Research.
- [28] R. Sipos, A.J. Székely, M. Palatinszky, S. Révész, K. Márialigeti, M. Nikolausz, Effect of primer mismatch, annealing temperature and PCR cycle number on 16S rRNA gene-targeting bacterial community analysis, *FEMS Microbiol. Ecol.* 60 (2007) 341–350. doi:10.1111/j.1574-6941.2007.00283.x.
- [29] K. Ishii, M. Fukui, Optimization of Annealing Temperature To Reduce Bias Caused by a Primer Mismatch in Multitemplate PCR, *Appl. Environ. Microbiol.* 67 (2001) 3753–3755. doi:10.1128/AEM.67.8.3753–3755.2001.
- [30] M. Leray, J.Y. Yang, C.P. Meyer, S.C. Mills, N. Agudelo, V. Ranwez, J.T. Boehm, R.J. Machida, A new versatile primer set targeting a short fragment of the mitochondrial COI region for metabarcoding metazoan diversity: Application for characterizing coral reef fish gut contents, *Front. Zool.* 10 (2013) 1–14. doi:10.1186/1742-9994-10-34.
- [31] M. Leray, N. Knowlton, Random sampling causes the low reproducibility of rare eukaryotic OTUs in Illumina COI metabarcoding, *PeerJ.* 5 (2017) e3006. doi:10.7717/peerj.3006.
- [32] J. Piñol, G. Mir, P. Gomez-Polo, N. Agustí, Universal and blocking primer mismatches limit the use of high-throughput DNA sequencing for the quantitative metabarcoding of arthropods, *Mol. Ecol. Resour.* 15 (2015) 819–830. doi:10.1111/1755-0998.12355.
- [33] J.R. Stokell, R.Z. Gharaibeh, T.J. Hamp, M.J. Zapata, A.A. Fodor, T.R. Steck, Analysis of changes in diversity and abundance of the microbial community in a cystic fibrosis patient over a multiyear period, *J. Clin. Microbiol.* 53 (2015) 237–247. doi:10.1128/JCM.02555-14.
- [34] B.M. Forde, P.W. O'Toole, Next-generation sequencing technologies and their impact on microbial genomics, *Brief. Funct. Genomics.* 12 (2013) 440–453. doi:10.1093/bfpg/els062.

Appendix A – Melting curves.

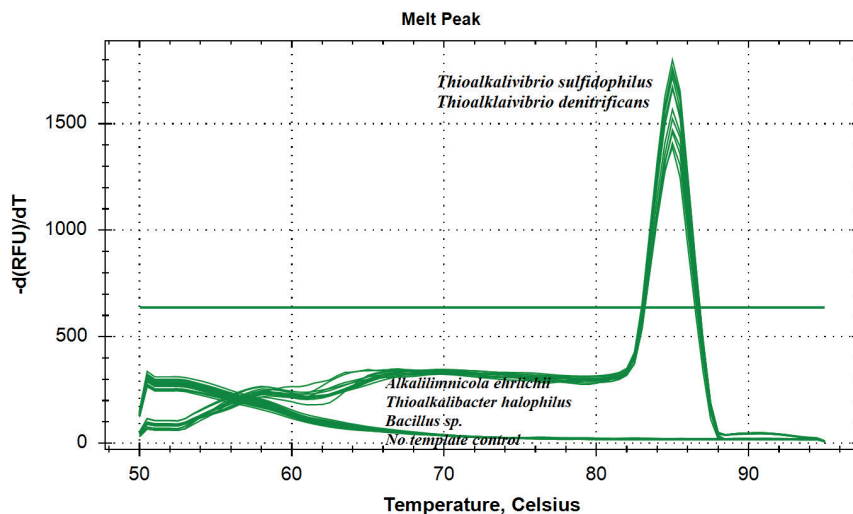


Fig. A1. Melting curve analysis of qPCR products of 16S rRNA gene of *Thioalkalivibrio* genus with use of SYBR Green.

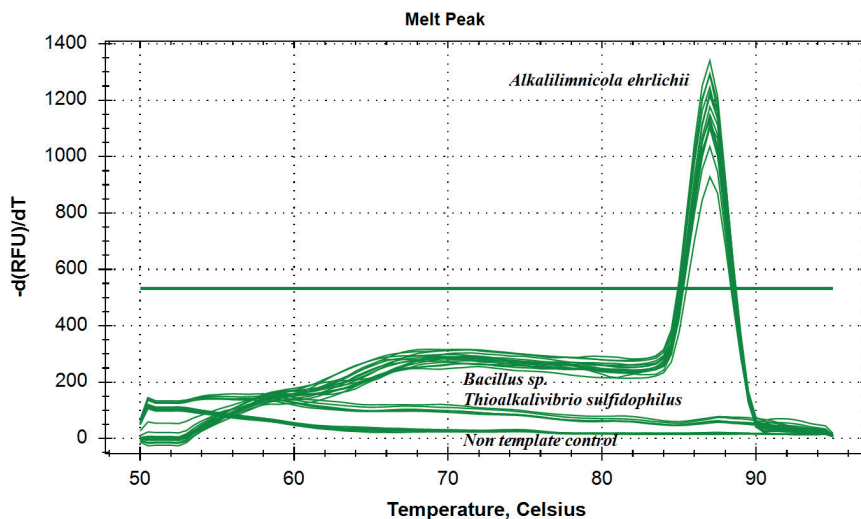


Fig. A2. Melting curve analysis of qPCR products of 16S rRNA gene of *Alkalilimnicola ehrlichii* with use of SYBR Green.

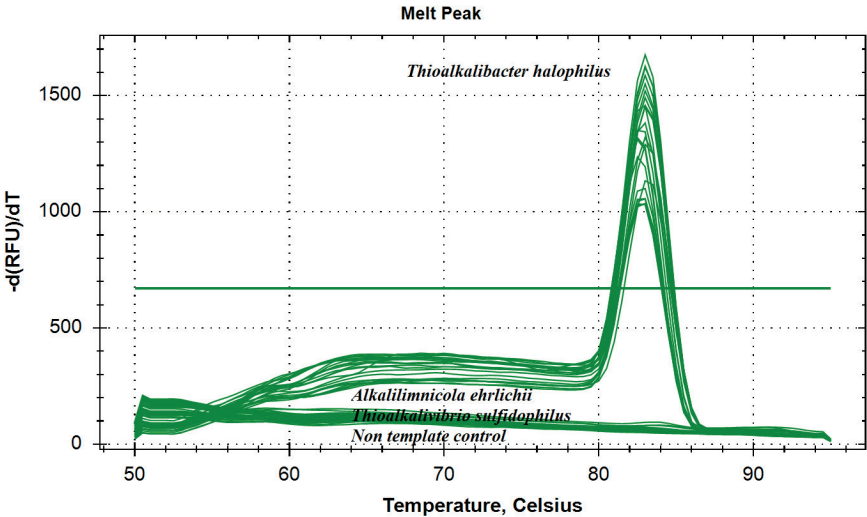


Fig. A3. Melting curve analysis of qPCR products of 16S rRNA gene of *Thioalkalibacter halophilus* with use of SYBR Green.

CHAPTER 4



Effect of dimethyl disulfide on the sulfur formation and microbial community composition during the biological H₂S removal from sour gas streams

Abstract

Removal of organic and inorganic sulfur compounds from sour gases is required because of their toxicity and atmospheric pollution. The most common are hydrogen sulfide (H₂S) and methanethiol (MT). Under oxygen-limiting conditions about 92 mol% of sulfide is oxidized to sulfur by haloalkaliphilic sulfur-oxidizing bacteria (SOB), whilst the remainder is oxidized either biologically to sulfate or chemically to thiosulfate. MT is spontaneously oxidized to dimethyl disulfide (DMDS), which was found to inhibit the oxidation of sulfide to sulfate. Hence, we assessed the effect of DMDS on product formation in a lab-scale biodesulfurization setup. DMDS was quantified using a newly, in-house developed analytical method. Subsequently, a chemical reaction mechanism was proposed for the formation of methanethiol and dimethyl trisulfide from the reaction between sulfide and DMDS. Addition of DMDS resulted in significant inhibition of sulfate formation, leading to 96 mol% of sulfur formation. In addition, a reduction in the dominating haloalkaliphilic SOB species, *Thioalkalivibrio sulfidophilus*, was observed in favor of *Thioalkaibacter halophilus* as a more DMDS-tolerant with the 50% inhibition coefficient at 2.37 mM DMDS.

This chapter has been published as: Kiragosyan, K., Picard, M., Sorokin, D.Y., Dijkstra, J., Klok, J.B.M., Roman, P., Janssen, A.J.H., 2020. Effect of dimethyl disulfide on the sulfur formation and microbial community composition during the biological H₂S removal from sour gas streams. J. Hazard. Mater. 386. <https://doi.org/10.1016/j.jhazmat.2019.121916>

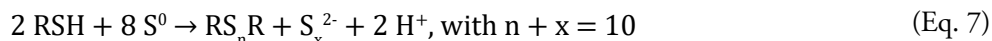
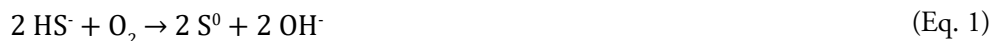
4.1 Introduction

Natural gas and other sour gas streams often contain (organo)sulfur compounds, such as hydrogen sulfide (H_2S) and thiols [1]. Sulfide and volatile organosulfur compounds (VOSCs) are highly toxic, corrosive, and malodorous compounds, which have adverse effects on animal and human health as well as the environment [2]. Hence, the removal of these pollutants is needed before the gas streams can be utilized further. This triggered a number of technological developments for efficient H_2S and VOSC removal [3]. Nowadays, a variety of desulfurization technologies is commercially available for the removal and conversion of sulfurous compounds among which the biological gas desulfurization technology described in this paper that has been developed by our group in collaboration with industry [4].

The technology studied relies on naturally occurring haloalkaliphilic sulfur-oxidizing bacteria (SOB). The process was first developed for the removal of H_2S from biogas generated by anaerobic digestion processes in wastewater treatment plants and landfills [5]. Subsequently, the process was further upgraded to treat high-pressure natural gas streams and refinery gas streams, often containing a number of other toxic compounds such as BTEX hydrocarbons, hydrogen cyanide, ammonia [6]. This process, also known as Thiopaq O&G, consists of an alkaline absorber column to remove H_2S from the gas, a microaerophilic bioreactor for dissolved sulfide oxidation to insoluble sulfur, and a gravity settler for the removal of the formed biosulfur particles [7]. Recently, the line-up was improved by the addition of an anaerobic bioreactor for achieving higher sulfide-to-sulfur bioconversion efficiencies [8].

In the biodesulfurization process, H_2S and thiols are counter-currently absorbed from gas streams into an alkaline aqueous solution (~1 M sodium bicarbonate) at a pH between 8 - 9 [9,10]. The loaded liquid containing bisulfide (HS^-) and thiols (RS^-) is subsequently directed to an anaerobic bioreactor to allow the microbial enzyme systems to reach a fully reduced redox state and to dissolve any small sulfur particles into polysulfides [11]. From our previous studies, it follows that the addition of an anaerobic reactor increases the overall sulfide conversion efficiency to elemental sulfur [10]. The dominating biological reactions are the conversions of HS^- into respectively elemental sulfur (S^0) and sulfate (SO_4^{2-}) under oxygen-limiting conditions (Eq. 1 and 2) [12]. Simultaneously, a number of chemical oxidation reactions occur mainly resulting in the formation of thiosulfate ($\text{S}_2\text{O}_3^{2-}$) either directly from the oxidation of sulfide or indirectly via autooxidation of polysulfide anions (S_x^{2-}) (Eq. 3 and 4) [10]. S_x^{2-} anions are chemically stable at high pH values in the absence of O_2 , but in the presence of O_2 they are rapidly oxidized chemically to thiosulfate or by SOB to sulfur and sulfate (Eq. 5) [11]. It was also found that formation rates of sulfate and sulfur depend on the SOB community composition and their activity status and the prevailing process conditions in the bioreactors [13]. When thiols are present, a

rapid reaction with O_2 will take place leading to the formation of diorgano polysulfanes (DOPS) (Eq. 6) [14]. In addition, diorgano polysulfanes ($n > 3$) will be formed from the reaction between thiols and biosulfur (Eq. 7). Subsequently, DOPS and diorgano polysulfanes will react to meta-stable intermediates that will quickly decompose to stable di- and trisulfides (Eq. 8) [10,15].



Several studies showed that the toxic effect of thiols, and especially methanethiol, on SOB result in a decrease of the sulfur formation rates [10,16]. Roman et al. unveiled the toxic effects of various thiols and DOPS on the activity of haloalkaliphilic SOB [17]. From this study, it follows that formation of sulfate as end-product of biological oxidation of sulfide is mostly affected by DOPS (dimethyl disulfide, diethyl disulfide, and dipropyl disulfide), while formation of sulfur as end-product is mainly affected by thiols [17]. In this paper, we studied the most commonly present DOPS, i.e. dimethyl disulfide (DMDS), in full-scale biodesulfurization reactors [13]. Therefore, this study aims to evaluate the effect of DMDS on both the reactor performance and SOB community composition with the objective to minimize sulfate formation and possibly maximize sulfur formation.

4.2 Materials and Methods

4.2.1 Experimental setup and experimental design

The laboratory setup consisted of a counter-current falling film gas absorber and two bioreactors in series; the first one is an anaerobic reactor for reducing the bacterial cytochromes followed by an aerobic reactor for sulfide oxidation (Fig. 1). The composition of the feed-gas was controlled using mass flow controllers (type EL-FLOW, model F-201DV-AGD-33-K/E, Bronkhorst, the Netherlands). For each type of gas, a dedicated mass flow controller was selected based on the gas supply rates. For hydrogen sulfide a range of 0-17 mL min⁻¹ was used; for nitrogen gas, the selected range was 0-350 mL min⁻¹; for O_2 0-30 mL min⁻¹ and carbon dioxide 0-40 mL min⁻¹. Hydrogen

sulfide and nitrogen gas were continuously supplied, whereas O_2 and carbon dioxide dosing rates were pulse-wise controlled with a multiparameter transmitter (Liquiline CM442-1102/0, Endress+Hauser, Germany). Supply of O_2 to the aerobic bioreactor was regulated based on a feedback controller (PID) receiving input signals from a redox sensor equipped with an internal $Ag/AgCl$ reference electrode (Orbisint 12D-7PA41; Endress+Hauser, Germany). CO_2 was supplied through the gas inlet, but the dosing rate was regulated based on signals from a pH sensor located in aerobic bioreactor (Orbisint 11D-7AA41; Endress+Hauser, Germany). Dimethyl disulfide (Sigma-Aldrich, the Netherlands) was supplied to the anaerobic bioreactor with a diaphragm metering pump (Simdos 10, KNF Lab, the Netherlands). The concentration of the DMDS was stepwise increased, starting from 0.15 up to 0.6 mM day⁻¹ (Table 1). The oxidation-reduction potential (ORP) setpoint was chosen at -390 mV to suppress sulfate formation [13].

A digital gear pump was used to assure liquid recirculation between the aerobic bioreactor and the gas absorber (EW-75211-30, Cole-Palmer, USA) at a constant flow of 10 L h⁻¹. A gas compressor (N 820 FT.18, KNF Laboport, USA) was used to continuously recycle gas (20 L min⁻¹ at atmospheric pressure) over the aerobic bioreactor. The anaerobic bioreactor was equipped with a stirrer to assure mixing. The gas absorber and the bioreactors temperatures were controlled at 35 °C by a thermostat bath (DC10, Thermo Haake, Germany). Both gas and liquid samples were taken from the experimental system. Liquid samples were taken in triplicate from two sampling points located at the bottom section of the absorber and in the bioreactor (Fig. 1). Single gas phase samples were taken from three locations: gas inlet, bioreactor headspace, and absorber outlet.

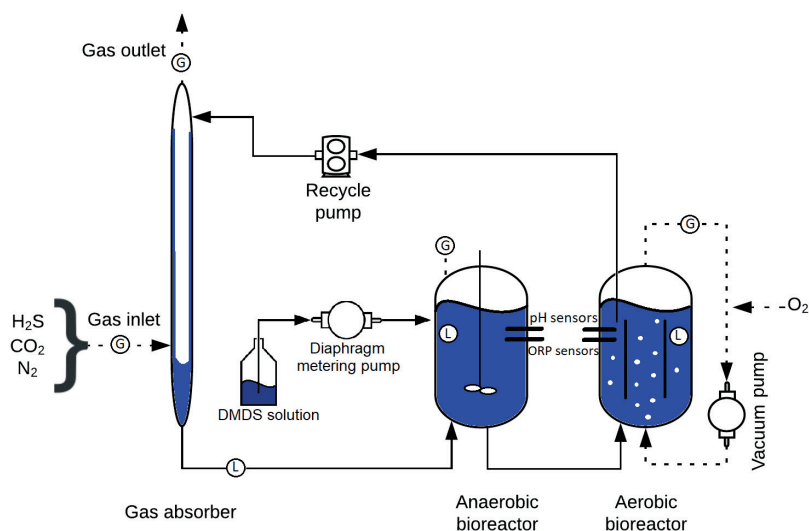


Fig. 1. Schematic representation of the experimental setup used for the experiments. G – gas sampling point, L – liquid sampling point, DMDS – dimethyl disulfide. Blue area indicates liquid.

Table 1 An overview of the process conditions in the experimental setup.

Parameter	Value
H ₂ S loading rate, mM S day ⁻¹	58.15
DMDS, mM S day ⁻¹	0.15 – 0.6
Salinity, M Na ⁺	1.0
Carbonate alkalinity, M	1.0
pH setpoint	8.5 ± 0.05
Temperature, °C	35 ± 1
ORP setpoint, mV	390

4.2.2 Medium composition

The haloalkaline medium was buffered with 0.045 M Na₂CO₃ and 0.91 M NaHCO₃. The fresh medium contained 1.0 g K₂HPO₄, 0.20 g MgCl₂ x 6H₂O and 0.60g urea, per 1 L of ultrapure water (Millipore, ISO 3696) and a trace element solution as described in Pfenning and Lippert [18]. The pH of the medium was controlled at 8.5 ± 0.05 at 35 °C.

4.2.3. Inoculum

The bioreactor inoculum consisted of a mix of different biomass sources, originating from four different biodesulfurization installations: Oilfield - 1, Oilfield - 2, Landfill and Pilot plant [19,20]. By preparing a mix of inoculum we enabled a higher microbial diversity and increased the chances for the best suitable organisms to become the dominating species. The inocula were mixed in the following volumetric ratio: 2:1:1:2. After mixing, the cells were concentrated by centrifugation (15 min at 16,000g). Hereafter the collected pellets containing the bacteria (and also a small fraction of sulfur) were used to inoculate 5 L experimental system. The description of the biomasses reflects the various industries where the installations are located. Oilfield - 1 full-scale installation treats associated gas from an oil production site containing low concentrations of thiols 50-200 ppm and 1-5 % of H₂S, whereas Oilfield - 2 treats acid gas from an amine installation, containing 10 - 20 % of H₂S and 20-500 ppm(v) thiols [20]. The landfill installation treats landfill gas containing 0.3 % of H₂S whilst the pilot plant treats pure (100%) H₂S gas [8].

4.2.4 Respiration tests

Respiration tests, also known as biological oxygen monitoring or activity tests, were performed to assess reaction rates of biological sulfide oxidation in an air-saturated carbonate/bicarbonate buffer. The setup and detailed test performance are described in [19]. In the current study, we measured the effect of DMDS on both sulfide and thiosulfate oxidation in thermostated batch reactors. The experiments were first carried out at a sulfide concentration of 0.12 mM because in our previous studies the maximum

reaction rate was reached at this concentration [15,19]. Then the experiments were repeated at thiosulfate of 0.12 mM and finally in the presence of both sulfide and thiosulfate at a total concentration of 0.12 mM. Although this concentration was below the normally measured values in the bioreactor, the experiments allowed us to estimate whether any thiosulfate oxidation would take place as the affinity constant for thiosulfate oxidation, K_s , is significantly lower, i.e. $6 \pm 3 \mu\text{M}$ [21] Russia. All stock solutions were freshly prepared and before usage the sulfide concentration was confirmed using the methylene blue test (LCK653, Hach Lange, Tiel, the Netherlands). Respiration tests were immediately performed after completion of the lab-scale bioreactor experiments using SOB cell pellets.

In addition, biological sulfide oxidation kinetics (in the presence and absence of DMDS) were studied with a pure culture of *Thioalkalibacter halophilus*, as this species proliferated in the presence of DMDS in our lab-scale bioreactor experiments. Based on the obtained data, we calculated IC_{50} values for DMDS. The obligate chemolithoautotrophic haloalkaliphilic SOB *Thioalkalibacter halophilus* ALCO 1 strain was obtained from the German Collection of Microorganisms and Cell Cultures (DSMZ).

4.2.5 Analytical techniques

Biomass quantification was based on the amount of organic nitrogen that was oxidized to nitrate by ammonium persulphate (LCK238 and LCK338, Hach Lange, Tiel, the Netherlands). Sample (1 mL) for biomass quantification contained both elemental sulfur particles and biomass. After centrifugation at $20\,238 \times g$, we washed and resuspended the pellet with 0.5 M sodium carbonate solution to separate sulfur and any dissolved N-containing salts from the sample. In the washing procedure, we mainly picked up biomass pellets and minor amounts of sulfur particles with a pipette and transferred them to another Eppendorf tube where the sample was resuspended and then allowed to settle by centrifugation. As biomass has a lower density than sulfur, it settles on top of the heavier sulfur particles and forms a separate pellet. After three cycles, sulfur particles were almost absent from the biomass sample. By using the before mentioned protocol, no sulfur was observed. Furthermore, we also would like to state that proteins attached to the sulfur are also considered biomass, even though they are extracellular. Moreover, data from our experiments on biomass concentration are compatible with results from our colleagues [13,22]. Sulfate and thiosulfate were measured by ion chromatography (Compact IC 761, Metrohm Nederland, Barendrecht, the Netherlands) with an anion column (Metrohm Metrosep A Supp 5, 150/4.0 mm, Metrohm Nederland, Barendrecht, the Netherlands) equipped with a pre-column (Metrohm Metrosep A Supp 4/5 Guard, Metrohm Nederland, Barendrecht, the Netherlands) to eliminate any particles. Immediately after sampling

all solids were removed by filtration over a 0.45 μm membrane syringe filter (HPF Millex, Merck, Amsterdam, the Netherlands) and mixed with 0.2 M zinc acetate in a 1:1 ratio to prevent chemical sulfide oxidation. The biological sulfur concentration was calculated from the sulfur mass balance based on the cumulative amount of supplied sulfide and the actual sulfate and thiosulfate concentrations, according to:

$$[\text{S}^0]_t = (\Delta t (\text{H}_2\text{S supplied}) / V_{\text{liquid}}) - [\text{SO}_4^{2-}]_t - 2*[\text{S}_2\text{O}_3^{2-}]_t - x*[\text{S}_x^{2-}]_t$$

The initial sulfur concentration is assumed to be zero. This is a general method to establish the concentration of accumulated sulfur per time interval (Δt) [8,9,15,23]. Concentrations of dissolved sulfide, polysulfides, and possible volatile organosulfur compounds were not taken into account, as their combined contribution to the total concentration of sulfur species is negligible [9]. We also assume pseudo 'steady-state' conditions of the system, which was confirmed by consecutive liquid and gas samples [13,19,24].

Sulfide and bisulfide were measured as total sulfide ($\text{S}^{2-}_{\text{tot}}$) using the methylene blue method with a commercially available method (LCK653, Hach Lange, Tiel, the Netherlands). Total sulfide quantification was carried out immediately after sampling and samples were diluted in oxygen-free Milli-Q water (sparged with N_2 gas for 30 min) to exclude any chemical sulfide oxidation [17].

In addition to sulfur-containing anions, sodium and potassium concentrations were measured with ion chromatography as described earlier [19]. A Metrohm Metrosep C4-, 150/4.0 mm column, was used with 3 mM HNO_3 as the eluent at 0.9 mL min^{-1} .

To close the electron balance as described by [13], carbonate and bicarbonate ion concentrations were established using the Henderson-Hasselbalch equation [25]. For that, liquid samples were analyzed for total inorganic carbon using high-temperature (680 $^{\circ}\text{C}$) catalytic oxidation with a TOC-L CPH analyzer (Shimadzu Benelux, 's-Hertogenbosch, the Netherlands).

In total, two types of liquid samples were prepared: (1) filtrated and precipitated with zinc acetate for anions measurements and (2) non-filtrate for biomass quantification and TOC analysis. All liquid samples were stored at 4 $^{\circ}\text{C}$ before being analyzed (about three days).

The various gas phases, i.e. absorber inlet and outlet and bioreactor gas recycle, were analyzed for H_2S , N_2 , CO_2 , and O_2 with a gas chromatograph (CP4900 Micro GC, Varian, Middelburg, the Netherlands) equipped with two separate column modules, namely a 10-m-long Mol Sieve 5A PLOT (MS5) and a 10-m-long PoraPlot U (PPU).

4.2.6 Analysis of DMDS using Gas Chromatography with Flame Photometric Detector (GC-FPD)

4.2.6.1 GC-FPD system and calibration and gas samples analysis

The Thermo Scientific Trace GC Ultra GC-FPD system consisted of a gas sampling valve (GSV) mounted in a valve oven, a split/splitless injector with a purge-and-trap adaptor as an interface for the GSV, a programmed temperature oven and an FPD detector (all supplied by Interscience, Breda, the Netherlands). An Agilent Technologies HP-5MS analytical column (Agilent Technologies, Amstelveen, the Netherlands) was used to separate the mixture of sulfur compounds with a constant helium flow of 1.3 mL min⁻¹.

The GC-FPD system was calibrated using a two-channel gas mixing device, the Alytech GasMix Aiolos II (Da Vinci Laboratory Solutions, Rotterdam, the Netherlands). Hydrogen sulfide was connected to channel 1 (volumetric flow range 1 - 50 NmL min⁻¹), and nitrogen was connected to channel 2 (volumetric flow range 30 - 2000 NmL min⁻¹). Calibration standards of 30, 50, 100, 150, 200, 300, 400 and 600 ppm mol H₂S were prepared and injected in triplicate to create the quadratic calibration curve, which is characteristic for FPD detectors. Limits of detection (LOD) and quantification (LOQ) were determined as described by [25], using a target RSD of 20% for LOQ; LOD and LOQ were found to be 2.25 and 7.50 ppm mol of H₂S, respectively. It should be noted that an FPD detector has equimolar sensitivity for sulfur atoms, which allowed us to use H₂S as a calibration standard for DMDS and, if needed, all other sulfur species. All stainless-steel gas lines going in and coming out of the GasMix as well as all gas lines in the GC-FPD system were Sulfinert treated by Restek (Bellefonte, USA) to prevent sulfide adsorption to the bare steel.

For identification of other VOSCs, the GC method parameters, as well as the analytical column, were transferred to an Agilent Technologies GC-MS system, consisting of a 6890N GC and a 5975 inert XL mass spectrometer (Agilent Technologies, Amstelveen, the Netherlands). The mass spectrometer allowed identification of all peaks based on their mass spectrum, which was compared with a mass spectrum library (NIST MS Search version 2.0d, 2005).

4.2.6.2 Liquid samples analysis

All reagents were of analytical grade unless stated otherwise. Thioanisole (TAS), methanethiol, and DMDS were supplied by Sigma Aldrich (Zwijndrecht, the Netherlands), while n-hexane was purchased from VWR International (Amsterdam, the Netherlands). Hydrogen sulfide gas (2500 ppm mol; balanced by nitrogen), nitrogen 5.0 and helium 5.0 were obtained from Linde Gas Benelux (Schiedam, the Netherlands). Colloidal particles of biologically produced sulfur were obtained and

purified as described elsewhere [10]. Matrix composition of all samples described in this section is the same as the reactor medium (section 4.2) unless stated otherwise.

4.2.6.3 Liquid-liquid extraction and sample injection

An in-house developed liquid-liquid extraction of sulfuric compounds was used because other analytical techniques such as GC analyses will suffer from the high content of sulfur particles and salts present in the bioreactor samples. The extraction was performed as follows: 500 μL of the liquid sample was added to 500 μL of thioanisole (388 mg L^{-1}) in hexane, which is equivalent to 0.1 g S L^{-1} , in a closed silanized glass vial using a glass syringe (Hamilton model 750, VWR International, Amsterdam, the Netherlands). Then, the vial was placed in a shaker for 30 minutes at 600 rpm. After removing the sample from the shaker, it was left to stand for at least 5 minutes to allow for phase separation to complete. During the process of method optimization, the efficiency of the extraction was found dependent on the extraction time (Appendix A).

Subsequently, 0.80 μL of the top hexane layer was injected into the GC-FPD system with a 10 μL Hamilton 1800 series gastight glass microsyringe (VWR International, Amsterdam, the Netherlands) for sulfur species quantification. During method optimization, an optimum injection volume was found to achieve a complete recovery (100 %) and a small relative standard deviation (1 %) (Appendix A). The 'sandwich' injection technique was employed: (a) first 1 μL of air was drawn into the syringe, followed by (b) 2 μL of extraction solvent from the sample vial. The next step was (c) to closely monitor the meniscus of the hexane inside the barrel of the syringe while the syringe needle still resided in the sample vial until meniscus was stagnant - indicating the gaseous headspace above the hexane in the barrel had been saturated with hexane vapors. Afterward, (d) the plunger was returned to the 1 μL mark, thereby expelling all liquid hexane from the syringe barrel, next (e) 0.8 μL of hexane was drawn into the syringe. Finally (f), the needle of the syringe was raised above the liquid level inside the sampling vial, and 1 μL of air was drawn into the syringe, resulting in a small hexane column sandwiched between two columns of gas. The syringe was then removed from the sample vial and transferred to the GC inlet, where it was quickly injected into the hot inlet. Because the sandwich technique was used, there was no direct contact of hexane with the hot inlet when penetrating the inlet septum with the needle, thus minimizing injection volume losses. Injection volume losses were further compensated by using thioanisole (TAS) as injection volume correction standard: the response factor (RF) of the pure extraction solvent containing 388 mg L^{-1} TAS was determined from the average of 10 replicate injections. Subsequently, this average RF was used to correct the results for all compounds of every injection of extraction liquid. To close the mass balance in a gas-liquid system, we converted the detected gas

concentrations (ppm mole H_2S) into mM S and vice versa by multiplying the ppm mole with the conversion factor as described in Appendix B.

4.2.7 DNA isolation and purification

Samples for genomic DNA extraction were taken at two-time points: inoculum and end of the process operation with DMDS. Taken 100 ml of the process medium from the bioreactor was centrifuged to obtain bacterial cells and washed with 0.5 M Na^+ solution to prevent osmotic shock. Washed and concentrated cell pallet was divided into three equal aliquots to obtain representative data. These triplicates are highly dependent as they originate from the same system. Thus, they are technical and not biological replicates.

Genomic DNA was extracted using the DNeasy PowerLyzer PowerSoil Kit (Qiagen) following the manufacturer's instructions. Extracted DNA was quantified using QuantiFluor dsDNA systems and a QuantusTM fluorometer (Promega, The Netherlands). DNA integrity was evaluated with gel electrophoresis.

4.2.8 16S amplicon sequencing and qPCR

16S rRNA gene amplicon sequence libraries were sequenced on an Illumina MiSeq using the V3 chemistry to generate 300 bp paired-end reads with 515f (5'-GTGCCAGCMGCCGCGGTAA-3') [27] and 926r (5'-CCGYCAATTYMTTTRAGTTT-3') [28] primer-set at MrDNA Molecular Research LP, Shallowater, TX, USA [29]. Sample identifier barcode sequences were extracted from forward and reverse reads in QIIME [30]. We then used the bioinformatics toolkit implemented in QIIME2 (version 2018.2 and 2018.11) to perform quality control and filtering of sequence data [31]. Briefly, samples were first demultiplexed, and primer sequences were then trimmed from sequence reads using *cutadapt* [32]. Subsequently, a feature table and a list of representative sequences for each unique amplicon sequence variant (ASV) were constructed after quality control of paired-end reads (i.e., denoising, error-correction, and chimera removal) using *DADA2* version 2018.2.0 [33]. Quality control warranted a minimum quality Phred score of 30 by removal of the first ten bases of all reads and trimming of forward and reverse reads at 210 and 240 bases, respectively. Representative sequences for each ASV were de novo aligned using MAFFT [34]. The alignment was subsequently filtered to construct a phylogenetic tree using *Fasttree2* [35]. Taxonomy assignment was performed on representative sequences using the scikit-learn naive Bayesian classifier [36] trained on full 16S rRNA sequences from the SILVA database version 132 [37]. The pre-trained classifier is publicly available from qiime2.org/2018.11/data-resources. Data analysis was performed using *phyloseq* version 1.22.3 [38] in R statistical software version 3.5.0 [39]. QIIME and R scripts are available as

supplementary information. The EMBL-EBI accession number for presented 16S rRNA sequencing set is PRJEB31230.

For absolute quantification of three species of interest, qPCR was used with designed species-specific primers. Detailed method description can be found in [20].

4.3. Results and discussion

4.3.1 Effect of DMDS on biological sulfide oxidation and product formation

In order to develop a performance baseline, the first experimental run only contained H_2S in the feed gas. Hereafter the effect of DMDS was studied under similar conditions. The H_2S experimental run lasted for 15 days, and the calculated average selectivities for sulfur, sulfate and thiosulfate formation were 91.5 ± 1.2 mol%, 6.7 ± 1.1 mol% and 1.8 ± 0.3 mol%, respectively (Fig. 2A). Then, DMDS was supplied for six days at a rate of $0.2 - 0.6$ mM S day^{-1} . From day 1-4, the formation of thiosulfate was 8 ± 1 mol% while no sulfate (i.e. 0 mol%) was formed (Fig. 2B). This shows an immediate inhibition of sulfate formation by DMDS. On day five and six, the DMDS supply rate was at its maximum value of 0.6 mM S day^{-1} , the thiosulfate formation was 9 ± 0.5 mol%, and sulfate formation was about 1.0 mol%. The root-cause for sulfate formation can be found in the ORP probe. Previous studies show that for sour gas streams that only contain H_2S , the measured ORP is governed by the dissolved sulfide concentration [40]. However, in the presence of DOPS, the measured ORP is affected by the DOPS [13]. Hence, we have tested the effect of dipropyl disulfide on the measured ORP, and our results show a decrease of 20 mV. Consequently, the supply of O_2 to the system increased in order to reach the ORP setpoint value, which resulted in increasing $\text{O}_2/\text{H}_2\text{S}$ supply ratios from 0.60 mol mol $^{-1}$ on day 1 to 0.85 mol mol $^{-1}$ on day six. Because significantly more oxygen is available, a part of the sulfide will be oxidized to sulfate as observed in many other studies [7,10,41]. From previous studies we know that a reduction of the ORP setpoint value to -450 mV does not lead to the desired $\text{O}_2/\text{H}_2\text{S}$ supply ratio because the probe becomes somewhat insensitive, which is similar to controlling pH at very low or very high values. Clearly, in future studies an alternative oxygen supply strategy should be developed to ensure the formation of elemental sulfur in the presence of organic sulfur compounds.

After six days of operation with DMDS in the feed stream, an average of 90.0 ± 0.5 mol% of sulfur formation was achieved with 9.0 ± 0.5 mol% of thiosulfate and 1.0 ± 0.2 mol% of sulfate. Hence, the addition of DMDS decreased sulfate formation, which was accompanied by increased rates of thiosulfate formation, resulting in a net-zero increase in sulfur formation. Increased thiosulfate formation was also observed in previous studies with organic sulfur compounds, which were found to severely inhibit

SOB and ultimately lead to a complete drop-in biological sulfide-oxidizing activity [10,15,17]. Generally, thiosulfate accumulation is commonly found in both full-scale and lab-scale biodesulfurization installations due to the chemical oxidation of (poly) sulfides [24], according to (Eq. 9-10) [42,43]:

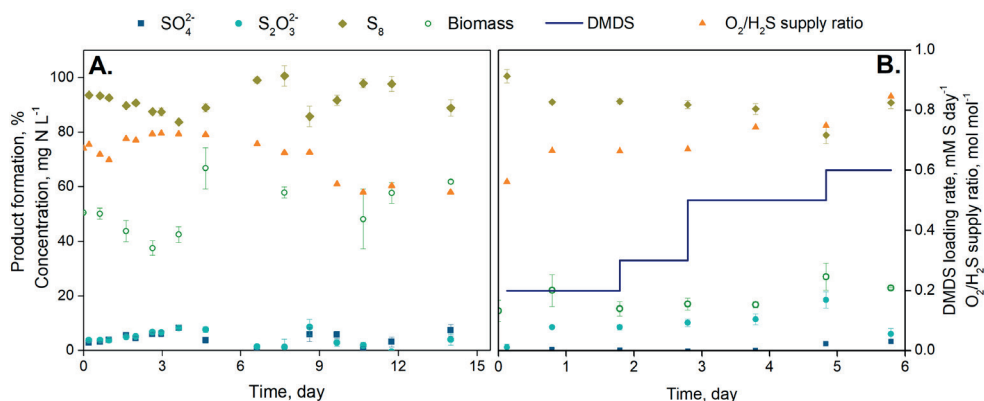


Fig. 2. Performance of the laboratory bioreactor during (A) experiment 1 - the addition of H_2S and (B) experiment 2 - the addition of H_2S + DMDS addition. The system was operated at ORP setpoint of -390 mV, pH setpoint of 8.5, T setpoint of 35 °C and the H_2S loading rate was 58.15 mM S day⁻¹.

Two reasons can be found to explain the production and accumulation of thiosulfate: Firstly, inhibition of biological thiosulfate oxidation to sulfate, according to Eq. 5 [44]. Secondly, inhibition of biological sulfide oxidation leading to enhanced abiotic oxidation rates of (poly)sulfides to thiosulfate [10]. To study the prevailing mechanism, we performed respiration tests with sulfide and thiosulfate as the sole substrates and SOB cells grown in the presence and absence of DMDS. Results from respiration tests show that the maximum specific biological sulfide oxidation capacity of biomass grown in the experiment with DMDS addition was almost a factor of three lower than for biomass grown in the experiment with H_2S only, i.e. 0.32 ± 0.02 mM O_2 (mg N h)⁻¹ and 0.86 ± 0.04 mM O_2 (mg N h)⁻¹ at 0.12 mM of sulfide (Appendix C, Fig. C1). Due to this decreased capacity for sulfide oxidation rate, more thiosulfate formation occurred in the presence of DMDS. This means that full scale systems treating sour gas streams containing both H_2S and DMDS have to be larger to accommodate for the reduced oxidation capacity, or alternatively, should be operated at higher biomass concentrations. In addition, to the observed differences in biological sulfide oxidation rates, specific loading rates also varied. In the experiment with DMDS addition the observed specific loading rates for sulfide oxidation are almost a factor three higher than

during H_2S addition only, $2.54 \text{ mM H}_2\text{S (mg N)}^{-1} \text{ h}^{-1}$ vs. $0.94 \text{ mM H}_2\text{S (mg N)}^{-1} \text{ h}^{-1}$. The difference in specific loading rates is a result of different biomass concentrations that can be noted in the Fig 2A and B. In addition, performed respiration tests indicate a slight decrease in the oxidation rates of both sulfide and thiosulfate in the presence of DMDS, i.e., a decrease of 19 % and 23 %, respectively (Fig. 3). In addition, we studied the simultaneous oxidation of sulfide and thiosulfate to identify sequence of reactions. From the recorded O_2 consumption profiles it appears that the initial maximum rates found for the simultaneous oxidation of thiosulfate and sulfide were in a similar order of magnitude as for HS^- oxidation only (Appendix C, Fig. C2). Thus, sulfide oxidation is the preferred oxidation reaction by SOB [45]. This is in accordance with Ang et al. [46], which reported that thiosulfate oxidation not occurred in a number of SOB as long as dissolved sulfide is present in solution. When analyzing the overall measurements of the simultaneous oxidation of sulfide:thiosulfate, it can be found that when all sulfide was consumed, similar oxidation rates were found for biological thiosulfate oxidation. The ability of bacteria to utilize two substrates is known as diauxy [47]. The order of substrate consumption depends on several factors such as amount of energy gained, toxicity of the compound [48], and by the ORP potential in case of sulfide/thiosulfate pair. Furthermore, lab- and full-scale biodesulfurization process operation is performed at a relatively low ORP value (i.e. -390 mV) at which SOB are induced for sulfide oxidation. Hence, in case of a combined sulfide/thiosulfate substrate, sulfide would be preferentially oxidized, and only in its absence, thiosulfate proceeds. This corresponds with our findings, i.e. the oxidation rates for sulfide are three times higher than those of thiosulfate as follows from the O_2 consumption profiles in Appendix C.

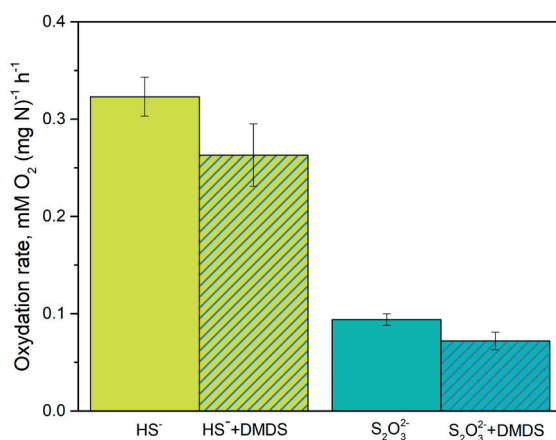


Fig. 3. Average reaction rates for sulfide (0.12 mM) and thiosulfate (0.12 mM) oxidation by the developed SOB biomass in the presence and absence of 0.30 mM of DMDS. The biomass was adapted to DMDS. The respiration tests vessel was operated at $T = 35^\circ \text{C}$ and with carbonate/bicarbonate buffered medium. The pH was 8.5. Error bars indicate the standard deviation between measured triplicates.

We found that both the aforementioned reasons can contribute to thiosulfate accumulation. However, based on the established order of sulfide and thiosulfate oxidation and reaction rates, we conclude that the primary reason for thiosulfate accumulation is chemical (poly)sulfide oxidation. In order to increase the biological conversion rates at the expense of the chemical oxidation rate of (poly)sulfide we increased the biomass concentration (from $23 \pm 1 \text{ mg N L}^{-1}$ to $51 \pm 3 \text{ mg N L}^{-1}$) and started another experiment with H_2S and DMDS as feed compounds. At increasing biomass concentrations, no thiosulfate formation (i.e. 0 mol%) was found, while the selectivity for sulfur formation was increased to $96 \pm 1 \text{ mol\%}$ at $0.6 \text{ mM S day}^{-1}$ supplied DMDS (Appendix D, Fig. D1). Moreover, we found that only $4 \pm 1 \text{ mol\%}$ of sulfate was formed.

The composition of the liquid in both bioreactors was analyzed for the presence of diorganopolysulfides using our newly developed GC-FPD method. No significant differences were found between the anaerobic and aerobic bioreactor, assuming that no conversion of DMDS taking place. Next, to DMDS, dimethyl trisulfide and MT were detected in the process solution (Fig. 4A and B). In Figure 4, only the results of the anaerobic bioreactor are presented, since concentrations of DMDS, DMTS, and MT were identical in both reactors. The DMDS concentration in the liquid of anaerobic bioreactor was on average $0.65 \pm 0.03 \text{ mM S}$ and, in the headspace, $0.41 \pm 0.01 \text{ mM S}$, regardless of an increase in the DMDS supply. This not a full absorption of DMDS can be explained by the saturation of the alkaline process medium.

In Figures 4A and B, it can be seen that during startup of the experiments, DMDS and DMTS were present in the process solution. The measured concentrations at the onset of the experimental run were two times higher than expected from the influent concentrations. To explain this phenomenon, we first reconfirmed the concentration in the DMDS stock solution to assure that no experimental errors were made. We also checked if the stock solution would contain any DMTS. As this was not the case, a likely explanation for the higher DMDS concentration is the presence of minor amounts of DMDS and DMTS attached on sulfur particles surface, which remained from previous experiments as diorganopolysulfanes have a high affinity for sulfur. For instance, Roman et al. tested the ability of dimethyl polysulfides (dimethyl di-, tri- and tetrasulfide) to adsorb onto the surface of biosulfur particles [10]. They found desorption of DOPS from sulfur particles into the vial headspace. From the result of gaseous DMDS, DMTS and MT (Fig. 4A), it follows that our experimental system was in equilibrium as the DMDS, DMTS and MT concentrations in the headspace of aerobic bioreactor and absorber outlet were identical.

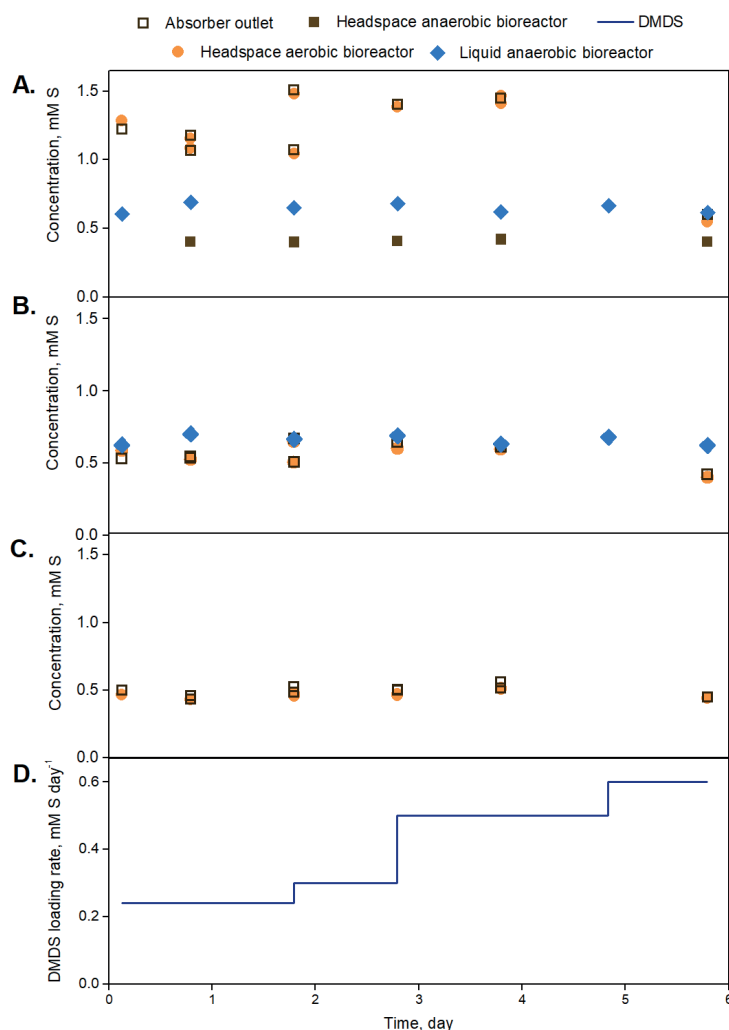
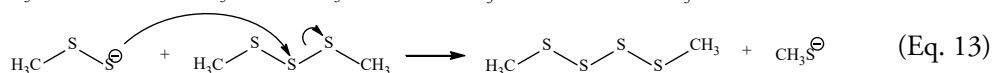
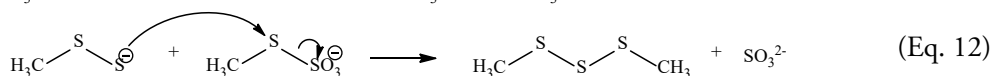
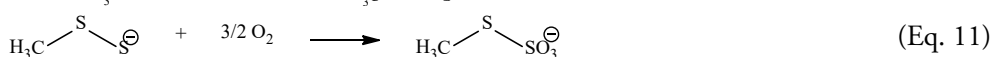
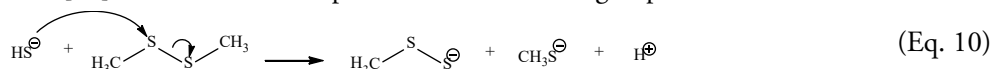


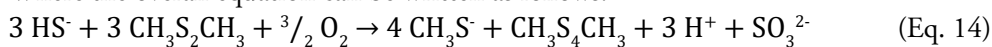
Fig. 4. Concentrations of **A.** dimethyl disulfide (DMDS), **B.** dimethyl trisulfide (DMTS) **C.** methanethiol (MT) in liquid and gas samples and **D.** loading rate of DMDS. Concentration is expressed per the molecule of sulfur (mM S) to enable comparison.

The DMDS and DMTS concentrations were almost similar, i.e., about 0.5 mM (Fig. 4A and B). Typically, both compounds are formed during the chemical oxidation of methanethiol (MT) (Eq. 6 - 8). Because no MT was added to the lab-scale biodesulfurization system, and biological degradation of DMDS was not feasible as electron donor was lacking for the reaction (Fig. 4C). Hence, a different reaction occurred, leading to DMTS formation. In the lab-scale biodesulfurization setup, significant levels

of sulfide and DMDS were present in the anaerobic bioreactor. It is known that sulfide is a strong nucleophile that can open sulfur-sulfur bonds, e.g., in S_8 rings [49]. In addition, sulfide can react with diorgano polysulfanes to form persulfides (Eq. 10). We found that in the presence of trace amounts of O_2 and at alkaline conditions, this reaction will lead to the formation of multiple products. For example, MT, dimethyl trisulfide, dimethyl tetrasulfide, and sulfite anions were formed when DMDS was exposed to sulfide (Appendix F). Therefore, it is proposed that this reaction can proceed with Bunte salts [50] as an intermediate product in the following steps:



Where the overall equation can be written as follows:



However, formed sulfite (SO_3^{2-}) will fast react with oxygen and form sulfate (Eq. 15), and will react with formed biosulfur particles to thiosulfate (Eq. 16):



The obtained results did not confirm the formation of dimethyl tetrasulfide, probably due to a low concentration. However, we found that methanethiol, dimethyl trisulfide, and dimethyl tetrasulfide formed from sulfide and DMDS in the batch test (Appendix F). For the Eq. 14, the free energy change at standard conditions (ΔG_R°) is $-341 \text{ kJ reaction}^{-1}$, indicating a spontaneous forward reaction. ΔG_R° value decreases linearly [51] with an increasing number of sulfur atoms in diorgano polysulfanes reaching $-738 \text{ kJ reaction}^{-1}$ for the reaction between sulfide and dimethyl octasulfide. This could indicate that sulfide will react with longer diorgano polysulfanes more readily.

As a result of the reaction between sulfide and DMDS, less volatile and more hydrophobic diorgano polysulfanes are formed that can be better removed from the bioreactor suspension by adsorption onto the surfaces of biosulfur particles [13].

4.3.2 Effect of DMDS on the microbial community composition

To elucidate any long-term effects of DMDS addition on the composition of the SOB community in the biodesulfurization setup, we collected biomass samples before and after DMDS addition ($0.6 \text{ mM S day}^{-1}$). We performed 16S rRNA gene amplicon sequencing to establish the microbial composition and additionally performed qPCR to establish

absolute counts of the three haloalkaliphilic SOB key-players. From the results of amplicon sequencing, it appears that the presence of DMDS provided a competitive advantage to the *Thioalkalibacter* genus. The only described species in this genus is a moderately halophilic and facultatively alkaliphilic obligate chemolithoautotrophic *Thioalkalibacter halophilus* [21]. This SOB species has a relatively low growth yield but relatively high growth rate (μ_{\max} 0.09-0.1 h⁻¹) over a broad range of pH and salinity [21]. Figure 5 shows that the gammaproteobacterial genera *Thioalkalivibrio*, *Thioalkalimicrobium*, *Alkalilimnicola*, and *Halomonas*, were abundant in the inoculum, but their numbers decreased after the DMDS addition. The genera *Thioalkalivibrio* and *Thioalkalimicrobium* (currently reclassified as *Thiomicrospira*) are obligate chemolithoautotrophic haloalkaliphilic SOB dominating in soda lakes and desulfurization bioreactors operating at haloalkaline conditions [52,53], which have different growth strategies. *Thioalkalimicrobium* species are characterized by low growth yield but high growth rates and extremely high sulfide and thiosulfate oxidizing activity, whereas *Thioalkalivibrio* species are relatively slowly growing organisms with at least two times higher specific growth yield on sulfide or thiosulfate [52,54]. Based on its highly specialized sulfide oxidation activity, *Thioalkalivibrio sulfidiphilus* is the dominant member of *Thioalkalivibrio* genus that was consistently found to dominate in the biogas desulfurization installations operating at low red-ox potential and haloalkaline conditions [55,56]. In previous studies, it was also found that *Tv. sulfidiphilus* was abundant in sulfide removing bioreactors in lab- and full-scale gas biodesulfurization systems in the absence of any organic sulfur compounds [8,10,19,20,57]. Other two genera, *Halomonas*, and *Alkalilimnicola*, that were identified in the inoculum and end samples, are commonly found in the haloalkaline environments containing both organic and reduced sulfur compounds [58]. *Alkalilimnicola* species, particularly *Alkalilimnicola ehrlichii*, are haloalkaliphilic facultative chemolithoautotrophic SOB, some of which can utilize sulfide, CO and formate as the electron donors and O₂ or nitrate as e-acceptor [59]. *Alk. ehrlichii* was previously found in gas biodesulfurization systems [8,13]. *Halomonas* species are aerobic or facultative anaerobic chemoorganotrophic halo- and haloalkaliphilic gammaproteobacteria that utilize a wide range of organic substrates, whilst inorganic sulfur compounds, particularly thiosulfate, are incompletely oxidized to tetrathionate [60,61].

The most important finding from the community profiling is that proliferation of *Thb. halophilus* occurred already after a short-term (i.e. 6 days) exposure to DMDS. This suggests the importance of *Thb. halophilus* in the gas biodesulfurization process in the presence of VOSCs. This conclusion was confirmed in a different study in which a qPCR protocol with target-specific primers was used [20]. In addition, we have analyzed the absolute abundance of *Tv. sulfidiphilus* and *Alk. ehrlichii* in the samples, as they are known to be key players in the biodesulfurization process as well [10,13,57].

The most important finding from the community profiling is that proliferation of *Thb. halophilus* occurred already after a short-term (i.e. 6 days) exposure to DMDS. This

suggests the importance of *Thb. halophilus* in the gas biodesulfurization process in the presence of VOSCs. This conclusion was confirmed in a different study in which a qPCR protocol with target-specific primers was used [20]. In addition, we have analyzed the absolute abundance of *Tv. sulfidophilus* and *Alk. ehrlichii* in the samples, as they are known to be key players in the biodesulfurization process as well [10,13,57].

Results of the qPCR showed a significant increase of one log-scale of 16S rRNA gene copies (ng DNA)⁻¹ of *Thb. halophilus* after exposure to DMDS (Fig. 5A). This indicates a preferential development of this SOB species in the presence of DMDS. Moreover, the results allow us to explain the findings in previous studies, where the increased relative abundance of *Thb. halophilus* was associated with thiol addition [13]. As a result, we have established the effect of DMDS on the microbial community. Thus, it can be concluded, that in the previous study formed DMDS from the oxidation of MT gave advantage to *Thb. halophilus*. Results for *Tv. sulfidophilus* and *Alk. ehrlichii* showed a slight reduction in the 16S rRNA gene copies (Fig. 5A), which corresponds with an observed decrease in relative abundance. Several studies have been performed on DMDS elimination in a biotrickling filter, including microbial community analyses. For example, Arellano-Garcia et al. found *Thioalkalivibrio sulfidophilus* as a dominant species (44.2 %) in the alkaline biotrickling filter that was used to simultaneously treat DMDS and H₂S [62]. Other studies did not observe proliferation or a high abundance of either *Thioalkalivibrio sulfidophilus* nor presence of *Thb. halophilus* and *Alk. ehrlichii* [63,64].

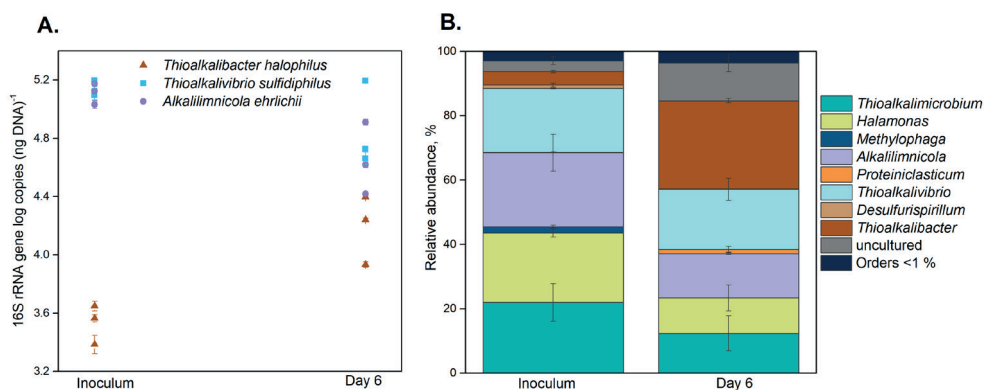


Fig. 5. A. Quantified 16S rRNA gene copies of *Thioalkalivibrio sulfidophilus*, *Thioalkalibacter halophilus* and *Alkalilimnicola ehrlichii* before and after the addition of 0.60 mM S day⁻¹ DMDS to the lab-scale gas biodesulfurization system. Presented data points are average values of measured triplicates, whereas each data point is a technical replicate at each time point. Error bars indicate the standard deviation between duplicates. **B.** The relative abundance of the microbial composition at the inoculum stage and after addition of 0.60 mM S day⁻¹ of DMDS (End) based on partial 16S rRNA gene amplicon could. The lab-scale gas biodesulfurization bioreactor system was operated at a low oxidation-reduction potential of -390 mV (against an Ag/AgCl reference), pH 8.5, and H₂S loading rate was 58.12 mM S day⁻¹. Only bacteria with a relative abundance higher than 0.5 % are listed (remaining species are clustered into “Others”). Results represent the average value between three pseudo-replicates, and the error bar represents the standard deviation.

To confirm the capacity of the pure culture of *Thb. halophilus* for sulfide oxidation in the presence of DMDS, we performed a respiration test at different DMDS concentrations. The obtained data were used to calculate an IC_{50} value, indicating the DMDS concentration at which 50 % inhibition occurs at a given sulfide concentration [17]. Results showed that *Thb. halophilus* maximum sulfide oxidation rate was reached at 0.12 mM sulfide, and the IC_{50} value was reached at 2.37 ± 0.1 mM of DMDS (Appendix G, Fig. G1). In comparison, the obtained IC_{50} value for *Tv. sulfidiphilus* (1.4 ± 0.1 mM) [17]. This finding prove the ability of *Thb. halophilus* to withstand high DMDS concentrations, which is relevant for industrial applications.

To understand the underlying cause for the inhibitory effects of DMDS on biological sulfide oxidation, we looked into the respiratory oxidases involved in the electron transport chain of the SOB species present in our lab-scale reactor system. For instance, *Thioalkalivibrio* species are known to only contain cytochrome *c* oxidases of the heme-copper superfamily, mostly of the *cbb₃* type [65–67]B-, and C-type oxidases. The C-type oxidases (*cbb3* cytochromes. Also enzymology studies of *Alkalilimnicola* spp. showed the presence of cytochrome *c* oxidase, which may be of the *cbb₃* type as well [68]. The same conclusion can be drawn from the analysis of publically available genome of *Alkalilimnocola ehrlichii*. In contrast, the genome of *Thioalkalibacter halophilus* strain ALCO1 encodes a quinol oxidase of the *bd* type (CydBAD) in addition to the cytochrome *c* oxidase *cbb₃* (CooNOQPHG) (our unpublished data). It is known that organic sulfur compounds inhibit cytochrome *c* oxidases [13], while the quinol oxidases, particularly of the *bd* type, are less prone to the commonly known cytochrome *c* oxidase inhibitors, such as cyanide and CO [69]. For instance, *Thioalkalibacter halophilus* ALCO1 has been enriched over the commonly dominating *Thioalkalivibrio* in high salt alkaline medium from soda lakes in the presence of 50 % CO in the gas phase [21]Russia. This could explain why *Thb. halophilus* is more resistant to the presence of DMDS.

Finally, we performed a serum bottle experiment to assess the ability of *Thb. halophilus* to biodegrade DMDS under both anaerobic and aerobic conditions. We measured methanethiol production from the reduction of DMDS. This is a known reaction studied by [70–72]. It is an oxygen-independent and reversible reaction where a molecule of DMDS is split by DMDS reductase to produces 2 mol of MT [73]. The results of the tests were negative, which clearly indicated the inability of *Thb. halophilus* and developed biomass to directly degrade DMDS, while still being active in sulfide oxidation in its presence.

Overall, the qPCR, amplicon sequencing, and respiration tests conclude that *Thb. halophilus* preferentially developed in the lab-scale gas biodesulfurization system in the presence of DMDS and most probably due to the presence of an alternative (quinol) oxidase of the *bd* type.

4.4 Conclusion

A critical success factor for the further development of the ascribed process for sour gas desulfurization is the quantification of DMDS, together with the formed degradation products, like methanethiol, dimethyl tri- and tetrasulfide. Hence, a new GC-FPD method was developed to gain more insights into the biochemistry of the prevailing gas biodesulfurization process. Moreover, the newly developed method can also be used in oil and gas operating sites to identify the presence of liquid DOPS in, e.g. produced water and gas condensates. Our studies show that DOPS will inhibit the sulfate formation rates and increase sulfur selectivity to 96 mol% at high biomass concentration ($51 \pm 3 \text{ mg N L}^{-1}$). Hence, organic sulfur compounds could be supplied to an oxidizing sulfide bioreactor to increase the yield of sulfur formation. A disadvantage is that DMDS decreases the rate of biological sulfide oxidation, what subsequently triggers an increase in thiosulfate formation. This means that full scale systems that treat sour gas streams containing both H_2S and DMDS will have to be larger to accommodate for the reduced oxidation capacity, or alternatively, should be operated at higher biomass concentrations. Addition of DMDS not only affected the product formation but also triggered changes in the microbial community. *Thioalkalibacter halophilus* proliferated as we found that it was highly resistant to elevated DMDS concentrations ($2.37 \pm 0.10 \text{ mM}$). In addition, a reduction of the dominating species *Tv. sulfidiphilus* and *Alkalilimnicola ehrlichii* was observed. In conclusion, we recommend that at the start-up of full-scale gas biodesulfurization installations the inoculum is abundant in *Thioalkalibacter halophilus*, to achieve a stable process operation and minimize the chemical consumption and formation of a diluted bleed stream.

Acknowledgments

This work has been performed within the cooperation framework of Wetsus, European Centre of Excellence for Sustainable Water Technology (wetsus.nl) and Wageningen University and Research (wur.nl). Wetsus is co-funded by the Netherlands' Ministry of Economic Affairs and Ministry of Infrastructure and Environment, the European Union's Regional Development Fund, the Province of Fryslan and the Northern Netherlands Provinces. Wetsus is also a coordinator of the WaterSEED project that received funding from European Union's Horizon 2020 research and innovation program under Marie Skłodowska-Curie grant agreement No. 665874. This research was co-financed by Paqell B.V. We want to thank all full-scale facilities for kind supply of the inoculum for this study. We would like to acknowledge Pieter van Veelen for the help with 16S amplicon sequence processing.

References

- [1] E. Smet, P. Lens, H. Van Langenhove, Treatment of waste gases contaminated with odorous sulfur compounds, *Crit. Rev. Environ. Sci. Technol.* 28 (1998) 89–117. doi:10.1080/10643389891254179.
- [2] D.P. Kelly, Global consequences of the microbial production and consumption of inorganic and organic sulfur compounds, in: K.N. Timmis, T.J. McGenity, J.R. van der Meer, V. de Lorenzo (Eds.), *Handb. Hydrocarb. Lipid Microbiol.*, Springer Berlin Heidelberg, 2010: pp. 3088–3098. doi:10.1007/978-3-540-77587-4.
- [3] A. De Angelis, Natural gas removal of hydrogen sulphide and mercaptans, *Appl. Catal. B Environ.* 113–114 (2012) 37–42. doi:10.1016/j.apcatb.2011.11.026.
- [4] A.J.H. Janssen, R.C. Van Leerdam, P.L.F. Van den Bosch, E. Van Zessen, G. Van Heeringen, C.J.N. Buisman, Development of a family of large-scale biotechnological processes to desulphurise industrial gasses, 2nd Int. Congr. Biotech. Air Pollut. Control. (2007) 167–183.
- [5] W. Driessen, E. Van Zessen, M. Visser, Full-scale experience with biological biogas desulfurization, in: 16th Eur. Biosolids Org. Resour. Conf., 2011.
- [6] A.J.H. Janssen, P.L.F. Van den Bosch, R.C. Van Leerdam, M. De Graaff, Bioprocesses for the Removal of Volatile Sulfur Compounds from Gas Streams, in: C. Kennes, M.C. Veiga (Eds.), *Air Pollut. Prev. Control Bioreact. Bioenergy*, John Wiley & Sons, Ltd., 2013: p. 570.
- [7] P.L.F. Van Den Bosch, O.C.C. Van Beusekom, C.J.N. Buisman, A.J.H. Janssen, Sulfide Oxidation at Halo-Alkaline Conditions in a Fed-Batch Bioreactor, *Biotechnol. Bioeng.* 97 (2007) 1053–1063. doi:10.1002/bit.
- [8] R. De Rink, J.B.M. Klok, D.Y. Sorokin, G.J. Van Heeringen, A. Ter Heijne, R. Zeijlmaker, Y.M. Mos, V. De Wilde, K.J. Keesman, C.J.N. Buisman, Increasing the selectivity for sulfur formation in biological gas desulfurization, *Environ. Sci. Technol.* 53 (2019) 4519–4527. doi:10.1021/acs.est.8b06749.
- [9] P.L.F. Van Den Bosch, M. Fortuny-Picornell, A.J.H. Janssen, Effects of Methanethiol on the Biological Oxidation of Sulfide at Natron-Alkaline Conditions, *Environ. Sci. Technol.* 43 (2009) 453–459. doi:10.1021/es801894p.
- [10] P. Roman, M.F.M. Bijmans, A.J.H. Janssen, Influence of methanethiol on biological sulphide oxidation in gas treatment system, *Environ. Technol.* 3330 (2016) 1–11. doi:10.1080/09593330.2015.1128001.
- [11] W.E. Kleinjan, A. De Keizer, A.J.H. Janssen, Kinetics of the chemical oxidation of polysulfide anions in aqueous solution, *Water Res.* 39 (2005) 4093–4100. doi:10.1016/j.watres.2005.08.006.
- [12] P. Roman, M.F.M. Bijmans, A.J.H. Janssen, Quantification of individual polysulfides in lab-scale and full-scale desulfurisation bioreactors, *Environ. Chem.* 11 (2014) 702–708. doi:10.1071/EN14128.

- [13] P. Roman, J.B.M. Klok, J.A.B. Sousa, E. Broman, M. Dopson, E. Van Zessen, M.F.M. Bijmans, D.Y. Sorokin, A.J.H. Janssen, Selection and Application of Sulfide Oxidizing Microorganisms Able to Withstand Thiols in Gas Biodesulfurization Systems, *Environ. Sci. Technol.* (2016) acs.est.6b04222. doi:10.1021/acs.est.6b04222.
- [14] R.C. Van Leerdam, P.L.F. Van Den Bosch, P.N.L. Lens, A.J.H. Janssen, Reactions between methanethiol and biologically produced sulfur particles, *Environ. Sci. Technol.* 45 (2011) 1320–1326. doi:10.1021/es102987p.
- [15] P. Roman, R. Veltman, M.F.M. Bijmans, K.J. Keesman, A.J.H. Janssen, Effect of Methanethiol Concentration on Sulfur Production in Biological Desulfurization Systems under Haloalkaline Conditions, *Environ. Sci. Technol.* 49 (2015) 9212–9221. doi:10.1021/acs.est.5b01758.
- [16] P.L.F. Van Den Bosch, M. De Graaff, M. Fortuny-Picornell, R.C. Van Leerdam, A.J.H. Janssen, Inhibition of microbiological sulfide oxidation by methanethiol and dimethyl polysulfides at natron-alkaline conditions, *Appl. Microbiol. Biotechnol.* 83 (2009) 579–587. doi:10.1007/s00253-009-1951-6.
- [17] P. Roman, J. Lipińska, M.F.M. Bijmans, D.Y. Sorokin, K.J. Keesman, A.J.H. Janssen, Inhibition of a biological sulfide oxidation under haloalkaline conditions by thiols and diorgano polysulfanes, *Water Res.* 101 (2016) 448–456. doi:10.1016/j.watres.2016.06.003.
- [18] N. Pfennig, K.D. Lippert, Über das Vitamin B₁₂-Bedürfnis phototropher Schwefelbakterien, *Arch. Mikrobiol.* 55 (1966) 245–256. doi:10.1007/BF00410246.
- [19] K. Kiragosyan, J.B.M. Klok, K.J. Keesman, P. Roman, A.J.H. Janssen, Development and validation of a physiologically based kinetic model for starting up and operation of the biological gas desulfurization process under haloalkaline conditions, *Water Res.* X. 4 (2019) 100035. doi:10.1016/j.wroa.2019.100035.
- [20] K. Kiragosyan, P. van Veelen, S. Gupta, A. Tomaszewska-Porada, P. Roman, P.H.A. Timmers, Development of quantitative PCR for the detection of *Alkalilimnicola ehrlichii*, *Thioalkalivibrio sulfidiphilus* and *Thioalkalibacter halophilus* in gas biodesulfurization processes, *AMB Express.* 9 (2019) 99. doi:10.1186/s13568-019-0826-1.
- [21] H.L. Banciu, D.Y. Sorokin, T.P. Tourova, E.A. Galinski, M.S. Muntyan, J.G. Kuenen, G. Muyzer, Influence of salts and pH on growth and activity of a novel facultatively alkaliphilic, extremely salt-tolerant, obligately chemolithoautotrophic sulfur-oxidizing Gammaproteobacterium *Thioalkalibacter halophilus* gen. nov., sp. nov. from South-Western Siber, *Extremophiles.* 12 (2008) 391–404. doi:10.1007/s00792-008-0142-1.
- [22] R. De Rink, J.B.M. Klok, G.J. Van Heeringen, K.J. Keesman, Biologically enhanced hydrogen sulfide absorption from sour gas under haloalkaline conditions, *J. Hazard. Mater.* 383 (2020) 121104. doi:10.1016/j.jhazmat.2019.121104.
- [23] J.B.M. Klok, P.L.F. Van Den Bosch, C.J.N. Buisman, A.J.M. Stams, K.J. Keesman, A.J.H. Janssen, Pathways of sulfide oxidation by haloalkaliphilic bacteria in limited-oxygen gas lift bioreactors, *Environ. Sci. Technol.* 46 (2012) 7581–7586. doi:10.1021/es301480z.

- [24] P.L.F. Van Den Bosch, D.Y. Sorokin, C.J.N. Buisman, A.J.H. Janssen, The effect of pH on thiosulfate formation in a biotechnological process for the removal of hydrogen sulfide from gas streams, *Environ. Sci. Technol.* 42 (2008) 2637–2642. doi:10.1021/es7024438.
- [25] H.N. Po, N.M. Senozan, The Henderson-Hasselbalch Equation: Its History and Limitations, *J. Chem. Educ.* 78 (2001) 1499–1503. doi:10.1021/ed080p146.
- [26] J. Vial, K. Le Mapihan, A. Jardy, What is the best means of estimating the detection and quantification limits of a chromatographic method?, *Chromatographia.* 57 (2003) 303–306. doi:10.1007/BF02492120.
- [27] J.G. Caporaso, C.L. Lauber, W.A. Walters, D. Berg-Lyons, J. Huntley, N. Fierer, S.M. Owens, J. Betley, L. Fraser, M. Bauer, N. Gormley, J.A. Gilbert, G. Smith, R. Knight, Ultra-high-throughput microbial community analysis on the Illumina HiSeq and MiSeq platforms, *ISME J.* 6 (2012) 1621–1624. doi:10.1038/ismej.2012.8.
- [28] C. Quince, A. Lanzen, R.J. Davenport, P.J. Turnbaugh, Removing Noise From Pyrosequenced Amplicons, *BMC Bioinformatics.* 12 (2011). doi:10.1186/1471-2105-12-38.
- [29] R.J. Chiodini, S.E. Dowd, W.M. Chamberlin, S. Galandiuk, B. Davis, A. Glassing, Microbial population differentials between mucosal and submucosal intestinal tissues in advanced Crohn's disease of the ileum, *PLoS One.* 10 (2015) 1–19. doi:10.1371/journal.pone.0134382.
- [30] J.G. Caporaso, J. Kuczynski, J. Stombaugh, K. Bittinger, F.D. Bushman, E.K. Costello, N. Fierer, A.G. Peña, K. Goodrich, J.I. Gordon, G.A. Huttley, S.T. Kelley, D. Knights, E. Jeremy, R.E. Ley, C.A. Lozupone, D. McDonald, B.D. Muegge, J. Reeder, J.R. Sevinsky, P.J. Turnbaugh, W.A. Walters, QIIME allows analysis of high-throughput community sequencing data, *Nat. Methods.* 7 (2011) 335–336. doi:10.1038/nmeth.f.303.QIIME.
- [31] E. Bolyen, J.R. Rideout, M.R. Dillon, N.A. Bokulich, C. Abnet, G.A. Al Ghalith, H. Alexander, E.J. Alm, M. Arumugam, Y. Bai, J.E. Bisanz, K. Bittinger, A. Brejnrod, J. Colin, C.T. Brown, B.J. Callahan, A. Mauricio, C. Rodríguez, J. Chase, E. Cope, R. Da Silva, P.C. Dorrestein, G.M. Douglas, C. Duvallet, C.F. Edwardson, M. Ernst, B.D. Kaehler, K. Bin Kang, C.R. Keefe, P. Keim, S.T. Kelley, J.L. Metcalf, S.C. Morgan, J.T. Morton, A.T. Naimey, QIIME 2 : Reproducible , interactive , scalable , and extensible microbiome data science, *PeerJ Prepr.* (2018). doi:10.7287/peerj.preprints.27295v1.
- [32] M. Martin, Cutadapt removes adapter sequences form high-throughput sequencing reads, *EMBnet J.* 17 (n.d.) 10–12.
- [33] B.J. Callahan, P.J. McMurdie, M.J. Rosen, A.W. Han, A.J. A, DADA2: High resolution sample inference from Illumina amplicon data, *Nat. Methods.* 13 (2016) 581–583. doi:10.1038/nmeth.3869.DADA2.
- [34] K. Katoh, D.M. Standley, MAFFT Multiple Sequence Alignment Software Version 7 : Improvements in Performance and Usability Article Fast Track, 30 (2013) 772–780. doi:10.1093/molbev/mst010.

- [35] M.N. Price, P.S. Dehal, A.P. Arkin, FastTree 2 – Approximately Maximum-Likelihood Trees for Large Alignments, 5 (2010). doi:10.1371/journal.pone.0009490.
- [36] F. Pedregosa, R. Weiss, M. Brucher, Scikit-learn : Machine Learning in Python, 12 (2011) 2825–2830.
- [37] C. Quast, E. Pruesse, P. Yilmaz, J. Gerken, T. Schweer, P. Yarza, J. Peplies, F.O. Glöckner, The SILVA ribosomal RNA gene database project: Improved data processing and web-based tools, Nucleic Acids Res. 41 (2013) 590–596. doi:10.1093/nar/gks1219.
- [38] P.J. Mcmurdie, S. Holmes, phyloseq : An R Package for Reproducible Interactive Analysis and Graphics of Microbiome Census Data, 8 (2013). doi:10.1371/journal.pone.0061217.
- [39] R Core Team, R: A language and environment for statistical computing., R Found. Stat. Comput. Vienna, Austria. (2018).
- [40] A.J.H. Janssen, S. Meijer, J. Bontsema, G. Lettinga, Application of the Redox Potential for Controlling a Sulfideoxidizing Bioreactor, Biotechnol. Bioeng. 60 (1998) 147–155. doi:10.1002/(SICI)1097-0290(19981020)60:2<147::AID-BIT2>3.0.CO;2-N.
- [41] A.J.H. Janssen, S.C. Ma, P. Lens, G. Lettinga, Performance of a sulfide-oxidizing expanded-bed reactor supplied with dissolved oxygen, Biotechnol. Bioeng. 53 (1997) 32–40. doi:10.1002/(SICI)1097-0290(19970105)53:1<32::AID-BIT6>3.0.CO;2-#.
- [42] R. Steudel, G. Holdt, R. Nagorka, On the Autoxidation of Aqueous Sodium Polysulfide [1], Zeitschrift Für Naturforsch. B. 41 (1986) 1519–1522. doi:10.1515/znB-1986-1208.
- [43] R. Steudel, Mechanism for the Formation of Elemental Sulfur from Aqueous Sulfide in Chemical and Microbiological Desulfurization Processes, Ind. Eng. Chem. Res. 35 (1996) 1417–1423. doi:10.1021/ie950558t.
- [44] D.C. Schreiber, S.G. Pavlostathis, Biological oxidation of thiosulfate in mixed heterotrophic/autotrophic cultures, Water Res. 32 (1998) 1363–1372. doi:10.1016/S0043-1354(97)00368-0.
- [45] G.C. Steffers, Oxidation of sulphide to elemental sulphur by aerobic *Thiobacilli*, TU Delft, 1993.
- [46] W.K. Ang, M. Mahbob, R. Dhouib, U. Kappler, Sulfur compound oxidation and carbon co-assimilation in the haloalkaliphilic sulfur oxidizers *Thioalkalivibrio versutus* and *Thioalkalimicrobium aerophilum*, Res. Microbiol. 168 (2017) 255–265. doi:10.1016/j.resmic.2016.12.004.
- [47] J.C. Gottschal, A. Pol, G.J. Kuenen, Metabolic flexibility of *Thiobacillus* A2 during substrate transitions in the chemostat, Arch. Microbiol. (1981) 23–28.
- [48] A.G. Marangoni, Enzyme Kinetics: A Modern Approach, John Wiley & Sons, Inc., Hoboken, NJ, USA, 2003. doi:10.1002/0471267295.
- [49] R. Steudel, Inorganic Polysulfides Sn²⁻ and Radical Anions Sn^{•-}, in: Top Curr Chem, 2003: pp. 127–152. doi:10.1007/b13183.
- [50] B. Milligan, B. Saville, J.M. Swan, 680. Trisulphides and tetrasulphides from Bunte salts, J. Chem. Soc. (1963) 3608–3614.

- [51] A. Hofmann, *Physical Chemistry Essentials*, Springer International Publishing, Cham, 2018. doi:10.1007/978-3-319-74167-3.
- [52] D.Y. Sorokin, J.G. Kuenen, Haloalkaliphilic sulfur-oxidizing bacteria in soda lakes, *FEMS Microbiol. Rev.* 29 (2005) 685–702. doi:10.1016/j.femsre.2004.10.005.
- [53] A.-C. Ahn, L. Overmars, D.Y. Sorokin, J.P. Meier-Kolthoff, G. Muyzer, M. Richter, T. Woyke, Genomic diversity within the haloalkaliphilic genus *Thioalkalivibrio*, *PLoS One*. 12 (2017) e0173517. doi:10.1371/journal.pone.0173517.
- [54] D.Y. Sorokin, H. Banciu, M. Van Loosdrecht, J.G. Kuenen, Growth physiology and competitive interaction of obligately chemolithoautotrophic, haloalkaliphilic, sulfur-oxidizing bacteria from soda lakes, *Extremophiles*. 7 (2003) 195–203. doi:10.1007/s00792-002-0313-4.
- [55] D.Y. Sorokin, J.G. Kuenen, G. Muyzer, The microbial sulfur cycle at extremely haloalkaline conditions of soda lakes, *Front. Microbiol.* 2 (2011). doi:10.3389/fmicb.2011.00044.
- [56] D.Y. Sorokin, M.S. Muntyan, A.N. Panteleeva, G. Muyzer, *Thioalkalivibrio sulfidiphilus* sp. nov., a haloalkaliphilic, sulfur-oxidizing gammaproteobacterium from alkaline habitats, *Int. J. Syst. Evol. Microbiol.* 62 (2012) 1884–1889. doi:10.1099/ij.s.0.034504-0.
- [57] D.Y. Sorokin, P.L.F. Van Den Bosch, B. Abbas, A.J.H. Janssen, G. Muyzer, Microbiological analysis of the population of extremely haloalkaliphilic sulfur-oxidizing bacteria dominating in lab-scale sulfide-removing bioreactors, *Appl. Microbiol. Biotechnol.* 80 (2008) 965–975. doi:10.1007/s00253-008-1598-8.
- [58] W. Wang, S.Q. Turn, V. Keffer, A. Douette, Study of process data in autothermal reforming of LPG using multivariate data analysis, *Chem. Eng. J.* 129 (2007) 11–19. doi:10.1016/j.cej.2006.10.027.
- [59] S.E. Hoeft, J.S. Blum, J.F. Stolz, F.R. Tabita, B. Witte, G.M. King, J.M. Santini, R.S. Oremland, *Alkalilimnicola ehrlichii* sp. nov., a novel, arsenite-oxidizing haloalkaliphilic gammaproteobacterium capable of chemoautotrophic or heterotrophic growth with nitrate or oxygen as the electron acceptor, *Int. J. Syst. Evol. Microbiol.* 57 (2007) 504–512. doi:10.1099/ij.s.0.64576-0.
- [60] M.T. García, A. Ventosa, E. Mellado, Catabolic versatility of aromatic compound-degrading halophilic bacteria, *FEMS Microbiol. Ecol.* 54 (2005) 97–109. doi:10.1016/j.femsec.2005.03.009.
- [61] D.Y. Sorokin, Oxidation of inorganic sulfur compounds by obligately organotrophic bacteria, *Microbiology*. 72 (2003) 641–653. doi:10.1023/B:MICL.0000008363.24128.e5.
- [62] L. Arellano-García, S. Le Borgne, S. Revah, Simultaneous treatment of dimethyl disulfide and hydrogen sulfide in an alkaline biotrickling filter, *Chemosphere*. 191 (2018) 809–816. doi:10.1016/j.chemosphere.2017.10.096.
- [63] X. Chen, Z. Liang, T. An, G. Li, Comparative elimination of dimethyl disulfide by maifanite and ceramic-packed biotrickling filters and their response to microbial community, *Bioresour. Technol.* 202 (2016) 76–83. doi:10.1016/j.biortech.2015.11.081.

- [64] X. Tu, M. Xu, J. Li, E. Li, R. Feng, G. Zhao, S. Huang, J. Guo, Enhancement of using combined packing materials on the removal of mixed sulfur compounds in a biotrickling filter and analysis of microbial communities, *BMC Biotechnol.* 19 (2019) 1–12. doi:10.1186/s12896-019-0540-8.
- [65] D.Y. Sorokin, A.M. Lysenko, L.L. Mityushina, T.P. Tourova, B.E. Jones, F.A. Rainey, L.A. Robertson, G.J. Kuenen, *Thioalkalimicrobium aerophilum* gen. nov., sp. nov. and *Thioalkalimicrobium sibericum* sp. nov., and *Thioalkalivibrio versutus* gen. nov., sp. nov., *Thioalkalivibrio nitratis* sp. nov. and *Thioalkalivibrio denitrificans* sp. nov., novel obligately a, *Int. J. Syst. Evol. Microbiol.* 51 (2001) 565–580.
- [66] M.S. Muntyan, D.A. Cherepanov, A.M. Malinen, D.A. Bloch, D.Y. Sorokin, I.I. Severina, T. V Ivashina, R. Lahti, G. Muyzer, V.P. Skulachev, Cytochrome cbb 3 of *Thioalkalivibrio* is a Na⁺ -pumping cytochrome oxidase, *Proc. Natl. Acad. Sci.* 112 (2015) 7695–7700. doi:10.1073/pnas.1417071112.
- [67] G. Muyzer, D.Y. Sorokin, K. Mavromatis, A. Lapidus, A. Clum, N. Ivanova, A. Pati, P. D’Haeseleer, T. Woyke, N.C. Kyrpides, Complete genome sequence of “*Thioalkalivibrio sulfidophilus*” HL-EbGr7, *Stand. Genomic Sci.* 4 (2011) 23–35. doi:10.4056/sigs.1483693.
- [68] D.Y. Sorokin, T.P. Tourova, O.L. Kovaleva, J.G. Kuenen, G. Muyzer, Aerobic carboxydutrophy under extremely haloalkaline conditions in *Alkalispirillum/Alkalilimnicola* strains isolated from soda lakes, *Microbiology.* 156 (2010) 819–827. doi:10.1099/mic.0.033712-0.
- [69] A. Quesada, M.I. Guijo, F. Merchan, B. Blazquez, M.I. Igeno, R. Blasco, Essential Role of Cytochrome bd-Related Oxidase in Cyanide Resistance of *Pseudomonas pseudoalcaligenes* CECT5344, *Appl. Environ. Microbiol.* 73 (2007) 5118–5124. doi:10.1128/aem.00503-07.
- [70] B.P. Lomans, C. Van der Drift, A. Pol, H.J.M. Op den Camp, Microbial cycling of volatile organic sulfur compounds, *Cell. Mol. Life Sci.* 59 (2002) 575–588.
- [71] R.P. Kiene, R.S. Oremland, A. Catena, L.G. Miller, D.G. Capone, Metabolism of reduced methylated sulfur compounds in anaerobic sediments and by a pure culture of an estuarine methanogen, *Appl. Environ. Microbiol.* 52 (1986) 1037–1045.
- [72] Z. Liang, T. An, G. Li, Z. Zhang, Aerobic biodegradation of odorous dimethyl disulfide in aqueous medium by isolated *Bacillus cereus* GIGAN2 and identification of transformation intermediates, *Bioresour. Technol.* 175 (2015) 563–568. doi:10.1016/j.biortech.2014.11.002.
- [73] N.A. Smith, D.P. Kelly, Mechanism of Oxidation of Dimethyl Disulphide by *Thiobacillus thioparus* Strain E6, *Microbiology.* 134 (2009) 3031–3039. doi:10.1099/00221287-134-11-3031.

Appendix A - Optimization of the GC-FPD method

The current method is prepared to analyze the DMDS concentration in samples containing colloidal sulfur particles. Therefore, we investigated the extraction time needed to obtain steady concentration of DMDS in the extract, in the absence and presence of colloidal biologically produced sulfur particles (5 g L^{-1}). Concentration of sulfur in these experiments corresponds to expected concentration in analyzed samples. At least 24 hours before starting the extraction in experiments with sulfur particles, DMDS was injected to sulfur-containing solution to obtain sulfur-DMDS saturated solution. From the results shown in Fig. A1 it follows that samples with and without sulfur particles require different extraction times. In absence of sulfur particles, extraction time required to obtain steady concentration of DMDS in the extract is 15 min (extraction efficiency $95 \pm 1\%$), while in the presence of sulfur particles, the extraction time is extended to 30 min (extraction efficiency $87 \pm 3\%$). Such high extraction efficiencies are result of high ratio between aqueous and organic layer, high partition coefficient of DMDS [15], and high salt content in samples. Increased extraction time for sulfur-containing samples is related to adsorption of DMDS on a surface of sulfur particles as observed earlier [7] and resulting equilibrium between liquid and solid phase. It can be noted that sulfur particles present in sample are dissolved in hexane and also can be quantified by the current method. Thus, in the presence of sulfur particles, the retention time of the method should be long enough to let sulfur elute from the analytical column.

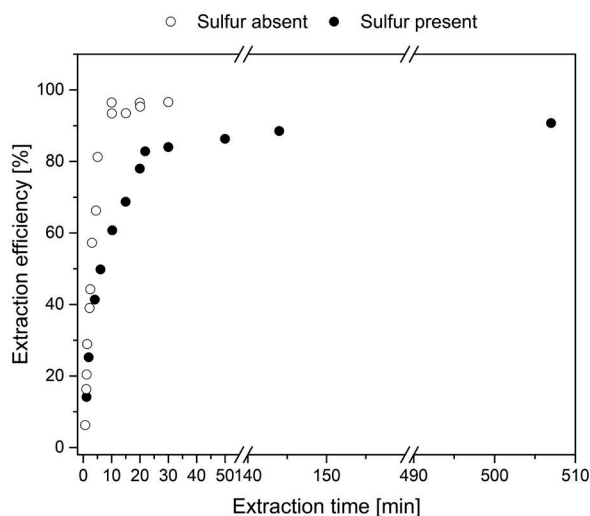


Fig. A1. Extraction efficiency at different extraction time. For extraction samples were kept on shaker at 600 rpm.

During method optimization, various injection volumes were tested using a standard solution of 120 mg L⁻¹ DMDS (equivalent to 82 mg S L⁻¹) and 388 mg L⁻¹ TAS in hexane. A volume of 0.8 µL was found to be optimal: recovery was 106% and relative standard deviation (RSD) was 1% over 5 replicate injections. It should be noted that TAS did show a significant deviation in accuracy, but from literature it is known that aromatic compounds have a quenching effect on the FPD response [53].

Higher diorgano polysulfanes (containing $4 \leq$ sulfur atoms) are unstable under high temperatures [10]. Therefore, to use described method to analyze samples containing such compounds, temperature of the liquid injection port should be lowered, and the method should be validated further. We investigated distribution of diorgano polysulfanes, formed in reaction between sulfur and methanethiol, at temperatures of the injection port ranging from 130 to 210 °C (Fig. A2). Obtained results at the injection port temperature of 150 °C, provide the highest average length of the sulfur chain of 4.9, which is close to the typical distribution of 5.28 in gas biodesulfurization systems [8].

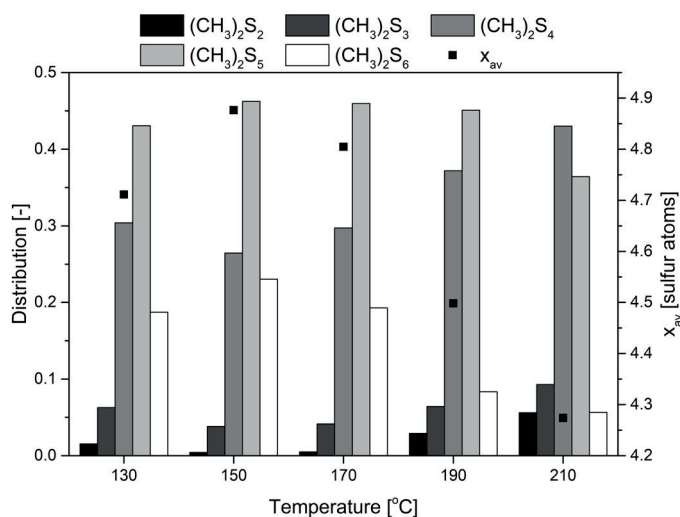


Fig. A2. Distribution of dimethyl polysulfanes and average length of the sulfur chain (x_{av}) at different temperatures of injection port of the GC-FPD system.

Appendix B - Factor for conversion of ppm mole H_2S to mM S

Since injection volumes differ when injecting gaseous (headspace/calibration) or liquid (extracts) samples, conversion factor had to be applied to properly close the mass balance in a gas-liquid system. When injecting gas samples to the GC-FPD system, a 250 μ L loop (thermostated at 50 °C) is filled and subsequently switched in line with the carrier gas flow, which means the actual injection volume is equal to the loop volume. The absolute number of moles H_2S (e.g. 200 ppm S) injected into the GC-FPD system is equal to:

$$n_{H_2S} = \frac{V_G}{V_M} \cdot C_{H_2S}^G = \frac{2.5 \cdot 10^{-4}}{26.5} \cdot \frac{200}{10^6} = 1.9 \cdot 10^{-9} \text{ mol S} \quad (\text{Eq. B1})$$

where: n_{H_2S} is number of H_2S moles [mol S]

V_G is injected gas volume [L]

V_M is gas molar volume at 50 °C [L mol⁻¹]

$C_{H_2S}^G$ is concentration of H_2S [ppm mol]

Concentration of H_2S in liquid samples ($C_{H_2S}^L$) can be calculated based on detected number of H_2S moles:

$$C_{H_2S}^L = \frac{n_{H_2S}}{V_{inj}} = \frac{1.9 \cdot 10^{-9}}{0.8 \cdot 10^{-6}} = 2.4 \cdot 10^{-3} \text{ M S} = 2.4 \text{ mM S} \quad (\text{Eq. B2})$$

where: V_{inj} is liquid injection volume [L]

Thus, factor (F) for conversion of ppm mol H_2S to mM S can be calculated as follows:

$$F = \frac{C_{H_2S}^L}{C_{H_2S}^G} = \frac{2.4}{200} = 0.0118 \quad (\text{Eq. B3})$$

Therefore, to recalculate from gas calibration units (ppm mol) to mM S in liquid, one simply multiplies the ppm mole with the factor F . Gaseous samples can also be converted to mM S (provided that the molecule has one sulfur atom) by dividing the ppm mole by a factor of 1000, e.g. 200 ppm mol equals to 0.2 mM S.

Appendix C – Respiration tests

Respiration tests have been performed to check effect of DMDS on biological sulfide oxidation rates. Thus, we compared biological sulfide epoxidation rates for SOB biomass used in the experiment with H_2S supply only, and with SOB biomass used in the experiments with DMDS addition.

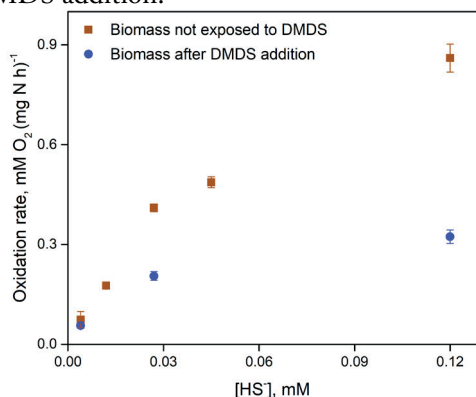


Fig. C1. Biological oxidation rates at different concentrations of HS^- in oxygen saturated buffer at pH 8.5, 1M Na^+ and 35 °C. Measured data points are average values of the experimentally measured duplicates.

Concentrations of sulfide and thiosulfate used in the experiment for reaction order (0.027 and 0.054 mM S).

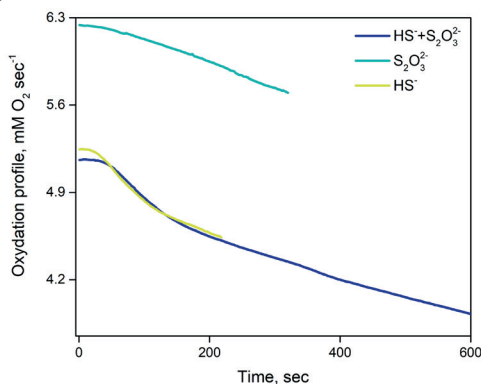


Fig. C2. An oxygen consumption profile in the presence of various substrates: sulfide, thiosulfate and sulfide together with thiosulfate, by the developed biomass in the biodesulfurization process with addition of DMDS.

Appendix D – The lab-scale gas biodesulfurization process performance at high biomass concentration and addition of DMDS.

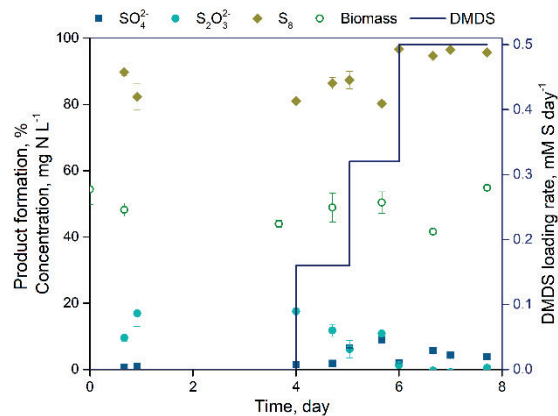


Fig. D1. Performance of the laboratory bioreactor at high biomass concentration during addition of H_2S + DMDS addition. The system was operated at ORP setpoint of -390 mV, pH setpoint of 8.5, T setpoint of 35 °C and the H_2S loading rate was 58.15 mM S day⁻¹.

Appendix F – Reaction between sulfide and dimethyl disulfide in the bioreactor medium

Reaction products between sulfide and DMDS were checked in the batch bottles experiments. To identify formed products, samples were analyzed using ion chromatography (Fig. F1) and high-performance liquid chromatography (Fig. F2).

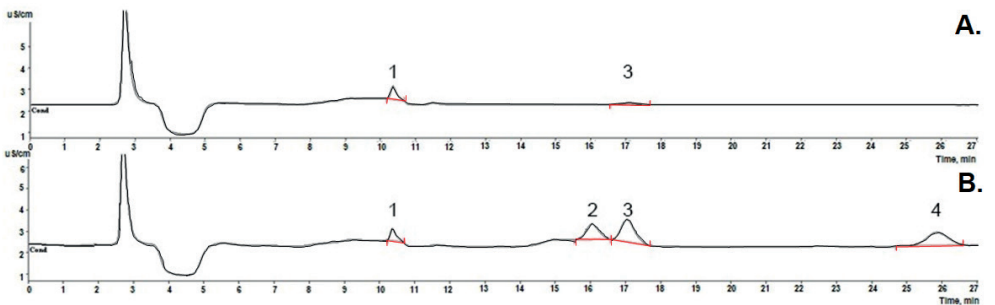


Fig. F1. Ion chromatography chromatograms from (A) HS^- 1.03 mM and (B) HS^- + DMDS of 1.03 mM and 0.35 mM respectively. Solutions were prepared in the process medium. Peaks identification: 1 - nitrate (NO_3^-), 2 - sulfite (SO_3^{2-}), 3 - sulfate (SO_4^{2-}), 4 - thiosulfate ($\text{S}_2\text{O}_3^{2-}$). Detected thiosulfate is a chemical product of sulfide oxidation.

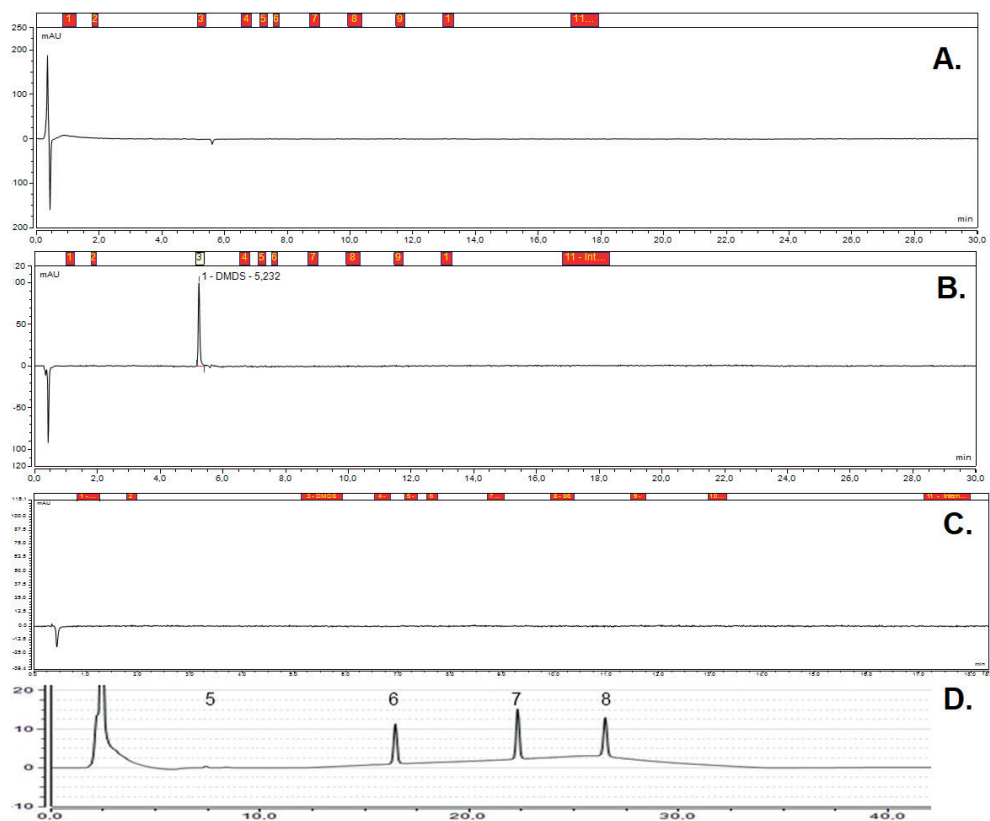


Fig. F2. High-performance liquid chromatography chromatograms from (A) HS^- 5 mM (B) DMDS 10 mM (C) process medium blank and (D) reaction between HS^- + DMDS of 1.03 mM and 0.35 mM respectively. Solutions were prepared in the process medium. Peaks identification: 5 - MT(CH_3SH), 6 – DMDS ($\text{CH}_3\text{S}_2\text{CH}_3$), 7 – DMTS ($\text{CH}_3\text{S}_3\text{CH}_3$), 8 – dimethyl tetrasulfide ($\text{CH}_3\text{S}_4\text{CH}_3$). Fig.F2 D varies from others as the older method for thiols was used on HPLC.

Appendix G – Finding IC_{50} value for *Thioalkalibacter halophilus* strain ALCO-1

To calculate IC_{50} value for *Thioalkaibacter halophilus* pure culture, we started from measuring oxidation reaction of 0.12 mM sulfide at eight concentration of DMDS (Fig. G1). Measured oxidation rates were fitted with exponential function where the equation of the fit was obtained. By using this equation, it is possible to derive IC_{50} value.

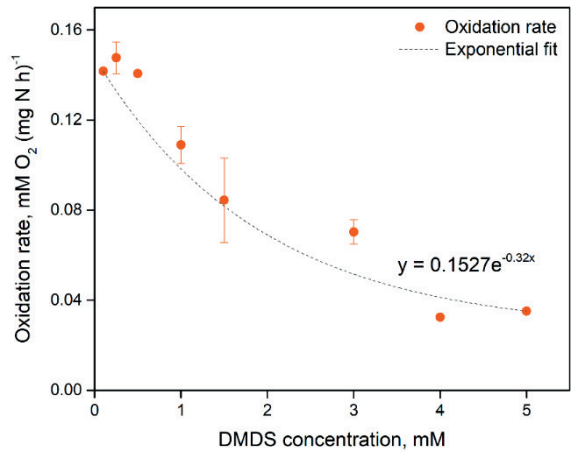


Fig. G1. Oxidation reaction rates of 0.12 mM sodium sulfide by a pure culture of *Thioalkaibacter halophilus* ALCO-1 in the presence of dimethyl disulfide (DMDS).

CHAPTER 5



Effect of methanethiol on the growth dynamics of sulfur-oxidizing bacteria and sulfur formation in the dual bioreactor gas biodesulfurization line-up

Abstract

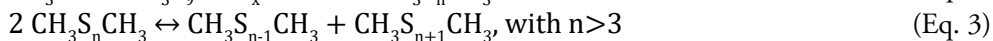
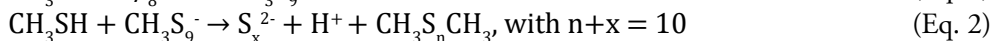
Removal of thiols and hydrogen sulfide from sour gas streams is required to reduce atmospheric pollution and to prevent negative health effects. Several physical-chemical processes are commercially available for simultaneous thiols and hydrogen sulfide removal. In addition, there are biotechnological processes available, amongst which the gas biodesulfurization - Thiopaq O&G. This technology uses naturally occurring sulfur-oxidizing bacteria (SOB) for sulfide oxidation to sulfur and sulfate. The objective of the process is to maximize sulfide oxidation and to solely form elemental sulfur. However, our previous research revealed that sulfur formation is highly susceptible to the presence of thiols, especially methanethiol. Thiols are toxic sulfur compounds that inhibit the microbial sulfur metabolism albeit that it is possible to grow a mixed population that can withstand moderate levels of thiols rendering sulfide oxidation feasible. In this paper we studied the effect of methanethiol on the SOB community dynamics and sulfur formation in the Thiopaq O&G Ultra setup. Moreover, we were interested in the SOB community dynamics in response to process perturbations. Results show an increased sulfur selectivity up to 90 mol% at 2 mM S day⁻¹ and 0.3 mM S of methanethiol, and highly decreased selectivity for sulfate formation, i.e. only 0.6 mol%, due to presence of dimethyl disulfide. This was accompanied with a shift in SOB community composition. The usually dominating *Thioalkalivibrio sulfidiphilus* was firstly outcompeted by *Alkalilimnicola ehrlichii*, and, when the methanethiol supply reached 2 mM S day⁻¹, *Thioalkalibacter halophilus* became the most abundant haloalkaliphilic SOB species.

A modified version of this chapter has been submitted for the publication as: Kiragosyan K., Picard M., Timmers P.H.A., Sorokin D.Y., Klok J.B.M., Roman P., Janssen A.J.H. Effect of methanethiol on the process performance differences, selectivity and dynamics of sulfur-oxidizing bacteria in the dual bioreactor gas biodesulfurization line-up.

5.1 Introduction

Amongst many reduced sulfur compounds, sour gas streams may contain thiols (RSH) and hydrogen sulfide (H_2S). Treatment of sour gas streams may be required in the processing of landfill gases and natural gases [1,2]. Thiols and H_2S need to be removed due to the obnoxious smell, low odor threshold, contribution to atmospheric pollution and corrosive nature. Various techniques are available for the simultaneous removal of thiols and H_2S , such as physicochemical acid/alkali scrubbing [3] and biological conversion [4]. Physicochemical methods for sour gas treatment are efficient but unsustainable, whereas biological conversion is environmentally friendly and cost-effective [5].

A gas biodesulfurization technology that has been recently developed by our team and commercialized as the “Thiopaq O&G” process is based on the adsorption of thiols and H_2S in a highly buffered alkaline solution, followed by an oxidation step where haloalkaliphilic sulfur-oxidizing bacteria (SOB) oxidize inorganic sulfur compounds to elemental sulfur and sulfate at oxygen-limiting conditions. The non-utilized fraction of sulfide can be chemically oxidized to thiosulfate through intermediate polysulfide formation. Elemental sulfur is the preferred end-product in comparison to the sulfate formation, because this will regenerate hydroxide ions and decrease air, energy and caustic consumption [6]. When thiols are also present in the feed-gas along with H_2S , a sequence of complex abiotic reactions will take place as these will react with produced bio-sulfur particles (S^0) to form diorgano polysulfanes (Eq. 1-2). Diorgano pentasulfide is the predominant productsuch as H_2S and SO_x [7], will lead to the unwanted formation of acid rain. In order to prevent this, biological processes can be employed to treat sulfur-containing gas streams. In this study, we describe a way to investigate the speciation of polysulfide anions in biodesulfurisation systems, which might enable further understanding and development of these processes. Abstract Environmental pollution caused by the combustion of fuel sources containing inorganic and organic sulfur compounds such as hydrogen sulfide (H_2S , which subsequently decompose to a mixture of organosulfur compounds (Eq. 3). Moreover, thiols will also be chemically oxidized in the presence of oxygen and by the formed biosulfur to form diorgano disulfides (Eq. 2 and 4).



Previous studies revealed that the formation of biological sulfur is highly susceptible to the presence of thiols [8,9] because they cause SOB inhibition. Thus, to improve the gas biodesulfurization process under development, Roman et al. tested the effects of various thiols and their oxidation products such as diorgano polysulfanes (DOPS)

on the SOB activity. They found that SOB activity was inhibited by short chain thiols (methane-, ethane- and propanethiol) at already very low concentrations, i.e. $0.6 \mu\text{M}$ [10]. To mitigate any negative effects of thiols and to make the biodesulfurization process more robust, thiol-resistant SOB were enriched to withstand the most prevalent and toxic thiol for microorganisms, namely methanethiol (MT). During two months of continuous process operation at gradually increasing MT supply rates, Roman et al. [11] found that the initial SOB microbial community drastically changed and a MT-resistant SOB became dominant. However, the measured sulfur selectivity was still low, i.e. $75 \text{ mol}\%$ at 2 mM S day^{-1} of MT whilst the process operation was unstable. To expand the operating window and to facilitate higher sulfur selectivity the process was modified by addition of an anaerobic bioreactor [12]. Therefore, the objective of this study is to investigate SOB composition dynamics in relation to process perturbations such as addition of MT, in order to identify the MT-resistant SOB population, which can ensure stable sulfide removal in the presence of high MT concentration.

5.2 Materials and Methods

5.2.1 Reactor operation

The laboratory experimental setup consisted of a falling film gas absorber followed by an anaerobic bioreactor and an aerobic bioreactor in series [13]. The purpose of the anaerobic reactor is to facilitate higher sulfur selectivities. The composition of the feed-gas was controlled by using mass flow controllers (type EL-FLOW, model F-201DV-AGD-33-K/E, Bronkhorst, the Netherlands). For each type of gas, a mass flow controller was selected with an appropriate orifice to precisely control the required dosing rate. For the supply of hydrogen sulfide a $0\text{--}17 \text{ NmL min}^{-1}$ mass flow controller was used. For nitrogen the flow range was $0\text{--}350 \text{ NmL min}^{-1}$, for oxygen $0\text{--}30 \text{ NmL min}^{-1}$ and carbon dioxide $0\text{--}40 \text{ NmL min}^{-1}$. Hydrogen sulfide and nitrogen gas were continuously supplied. Oxygen and carbon dioxide supply was controlled with a multiparameter transmitter (Liquiline CM442-1102/0, Endress+Hauser, Germany), which was paired with ORP sensor to control oxygen supply (Orbisint 12D-7PA41; Endress+Hauser, Germany) and with pH sensor to control carbon dioxide supply (Orbisint 11D-7AA41; Endress+Hauser, Germany). A digital gear pump was used to assure liquid recirculation between the aerobic bioreactor and the gas absorber (EW-75211-30, Cole-Palmer, USA) at a constant flow of 10 L h^{-1} . A gas compressor (N-820 FT.18, KNF Laboport, NJ, USA) was used to continuously recycle gas (20 L min^{-1}) over the aerobic bioreactor. The anaerobic bioreactor was equipped with a stirrer to ensure mixing. The gas absorber and the bioreactors' temperature were controlled at $35 \text{ }^{\circ}\text{C}$ by a thermostat bath (DC10, Thermo Haake, Germany).

Gas and liquid phase samples were collected for analyses. Liquid samples were taken from three different sampling points: one located at the bottom section of the absorber, second in the anaerobic bioreactor and third in the aerobic bioreactor. Gas-phase samples were taken from four different locations: gas inlet, both bioreactor headspaces, and absorber outlet. Sampling was done in triplicate for liquid samples while single samples were taken for gas analyses at regular time intervals. For microbial community analysis, a 50 ml aliquot from the aerobic bioreactor culture was centrifuged to obtain a cell pellet for further DNA extraction.

Two sets of experiments were conducted (Table 1). Firstly, we established a baseline by operating the system in the absence of MT and with H_2S as the sole S-compound in the feed-gas (Run 1). Subsequently, MT was stepwise supplied over a 77 days period at a constant H_2S load of $58.15 \text{ mM S day}^{-1}$ (Run 2). Due to the accumulation of biosulfur particles, the system became more difficult to operate due to poor separation of the liquid, gas and solid phases, resulting in entrainment of sulfur particles in the recirculation gas stream. Hence, a partial exchange of the medium was performed to lower the sulfur content. The aerobic bioreactor (2.5 L) was emptied and replenished with fresh medium and obtained biomass was returned to the bioreactor after removal of the sulfur particles.

The haloalkaline medium was buffered with $0.045 \text{ M Na}_2\text{CO}_3$ and 0.91 M NaHCO_3 . Detailed description of medium can be found in [13]. The pH of the medium was 8.5 ± 0.05 at 35°C .

5.2.2 Inoculum

A “super mix” inoculum was prepared by mixing biomass samples, originating from four different full-scale biodesulfurization installations, namely Oilfield - 1, Oilfield - 2, Landfill and Pilot plant [14,15]. The names of biomasses are on the application and feed gas compositions. “Oilfield – 1” is a full-scale installation treating associated gas from oil production wells containing low concentrations of thiols 50-200 ppm and 1-5 % of H_2S , whereas “Oilfield – 2” treats acid gas from an amine regeneration unit with 10 - 20 % of H_2S and thiols [14,15]. The Landfill installation treats landfill gas containing 0.3 % of H_2S , and the Pilot treats the synthetically prepared gas that represents amine acid gas with 4.45 % of H_2S [12]. Biomasses were mixed in the following volumetric proportion: 1:0.5:0.5:1, followed by a centrifugation step (15 min at 16,000g) to concentrate the suspended cells. The obtained cell pellet was used to inoculate a 5 L system (2.5 L per bioreactor).

The biomass mix served to inoculate the system for the first experimental run (Run 1, Table 1). After completing the first experiment the enveloped biomass was harvested and used as an inoculum for the second experiment (Run 2, Table 2).

Table 1. Overview of the process conditions of the experimental setup.

Parameter	Run 1 (H ₂ S supply)	Run 2 (H ₂ S + MT supply)
Active liquid volume, L	2.5	2.5
Total liquid volume, L	5	5
pH setpoint	8.50 ± 0.05	8.50 ± 0.05
Salinity, Na ⁺ M	1	1
Temperature setpoint, °C	35	35
H ₂ S loading, mM S day ⁻¹	58.15	58.15
CH ₃ SH loading, mM S day ⁻¹	0	0 – 2
ORP setpoint, mV	-390	-390

5.2.3 Microbial sludge sampling, sample preparation, and DNA extraction

During both experiments, SOB biomass samples were collected at equal time intervals. In operation with H₂S (Run 1), five samples were taken in triplicate over 15 days. In Run 2 15-time points were collected in triplicates over 77 days, yielding 45 samples. For this, the bioreactor samples were centrifuged (15 min at 16,000g) to separate the SOB biomass from the reactor suspension. Hereafter, the bacterial cells were washed two times with a 0.5 M Na⁺ bicarbonate buffer solution at pH 8.5. All 60 biomass samples were stored at -80 °C awaiting DNA extraction.

Genomic DNA was extracted using the DNeasy PowerLyzer PowerSoil Kit (Qiagen) following the manufacturer's instructions. Extracted DNA was quantified using the QuantiFluor dsDNA system on a Quantus™ fluorometer (Promega, the Netherlands). DNA integrity was evaluated with gel electrophoresis.

5.2.4 qPCR

qPCR was performed on all (60) samples, collected from Run 1 and Run 2. Samples were analyzed based on the absolute abundance of three SOB species of interest, including *Alkalilimnicola ehrlichii*, *Thioalkalivibrio sulfidiphilus* and *Thioalkalibacter halophilus* by using specifically developed species-specific primers [15]. For *Thioalkalivibrio sulfidiphilus*, primers were designed for a subcluster of this genus, as *Thioalkalivibrio sulfidiphilus* HL-EbGR7 is genetically related to another *Tv. sulfidiphilus* ALJ17 and to *Tv. denitrificans* [16,17]. However, our cloning results of the biodesulfurization process sludge and finding of Sorokin et al. indicate that only *Tv. sulfidiphilus* was found in the lab- and full-scale installations [15]. Hence, we concluded that the designed primer set quantified *Tv. sulfidiphilus* in the samples as it is the only *Thioalkalivibrio* species detected and dominantly present at low salt conditions in the gas biodesulfurization lab- and full-scale installations. In addition, we generated estimates of total bacterial 16S rRNA gene copy abundance using the universal bacterial primer set 338f/518r [18,19] to calculate relative target species abundances according to the quantification protocol described by [20].

5.2.5 Bacterial community analyses

Extracted DNA samples from each time point were amplified in triplicate using primers 515f (5'-GTGYCAGCMGCCGCGGTAA-3') and 926r (5'-CCGYCAATTYMTTTRAGTTT-3') with a barcoded forward primer. This primer set covers the 16S rRNA gene V4-V5 variable region, which was sequenced 2x300 bp [21]. Amplification was done using the HotStarTaq Plus Master Mix Kit (Qiagen, USA) under the following conditions: 94 °C for three minutes, followed by 30 cycles of 94 °C for 30 seconds, 53 °C for 40 seconds and 72 °C for 1 minute, with a final elongation step at 72 °C for five minutes. After amplification, PCR products of three separate reactions of each sample were pooled, and PCR products were checked on a 2 % agarose gel to determine the success of amplification products and their relative intensity of bands. Then, multiple samples were pooled together (e.g., 100 samples) in equimolar amounts based on their molecular weight and DNA concentrations. Pooled samples were purified using calibrated Ampure XP beads (Beckman Coulter, Indianapolis, IN, USA). Sequencing was performed at MR DNA (www.mrdnalab.com, Shallowater, TX, USA) on a MiSeq following the manufacturer's guidelines. Sequencing data were processed using the MR DNA analysis pipeline (MR DNA, Shallowater, TX, USA). In summary, barcodes were removed, and paired sequences were joined. Then, sequences <150bp and with ambiguous base calls were removed. Sequences were denoised, operational taxonomic units (OTUs) were generated, and chimeras were removed. OTUs were defined by clustering at 3 % divergence (97 % similarity), and final OTUs were taxonomically classified using BLASTn against a curated database derived from RDP II and NCBI (www.ncbi.nlm.nih.gov, <http://rdp.cme.msu.edu>). Demultiplexed sequences were submitted to the European Nucleotide Archive (ENA) EMBL-EBI with the project number PRJEB32001.

5.2.6 Statistical analysis

16S rRNA sequencing data were analyzed in R studio (version 1.2.1335) using the Microbiome R package [22]. Only OTUs with a minimum of 100 reads in all samples were kept, and total read abundance tables were used for statistical analysis. Ordination was done with multidimensional scaling (NMDS) to find mayor trends in the microbial community.

To evaluate whether absolute qPCR-based bacterial count estimates were dependent on process operations, we constructed a linear mixed-effects model to control for pseudo-replication of technical replicates. The linear mixed-effects model was constructed with bacterial species, process operation time, and their interaction as fixed effects and technical replicate as a random effect using the lme4 package [23] with R version 3.5.2. [24] in Rstudio software (Version 1.1.456). Denominator degrees of freedom were approximated using the Satterthwaite procedure in lmerTest package

[25] by overloading the anova and summary functions by providing p values for tests for fixed effects. We have implemented the Satterthwaite's method for approximating degrees of freedom for the t and F tests. We have also implemented the construction of Type I-II ANOVA tables. Furthermore, one may also obtain the summary as well as the anova table using the Kenward-Roger approximation for denominator degrees of freedom (based on the KRmodcomp function from the pbkrtest package and species-specific temporal slope estimates were inferred using the *phia* package [26]). To assess the relationships between bacterial abundance and process performance parameters (sulfate, thiosulfate, and MT concentrations), we used linear regression analysis. For this analysis of variance, we used the average values of technical triplicates because we had only a single measurement of the process performance parameters for each sample.

5.2.7 Analytical techniques

The biomass quantification was based on the amount of organically bound nitrogen that was oxidized to nitrate by digestion with peroxodisulphate (LCK238 and LCK338, Hach Lange, the Netherlands). Before the analysis, the cell pellet was washed from the residual urea and ammonia twice with the nitrogen-free medium with centrifugation at 20,238 x g for 5 min.

Sulfate and thiosulfate were quantified by ion chromatography (Metrohm Compact IC 761, Switzerland) with an anion column (Metrohm Metrosep A Supp 5, 150/4.0 mm, Switzerland) equipped with a pre-column (Metrohm Metrosep A Supp 4/5 Guard, Switzerland). The ion chromatography system included a chemical suppressor (Metrohm, Switzerland), CO₂ suppressor (853, Metrohm, Switzerland) and conductivity detector (Metrohm, Switzerland). In addition, suppressors for eluent conductivity and carbon dioxide were used (Metrohm, Switzerland). The mobile phase flow rate was 0.7 mL min⁻¹. Before the analyses, all solids were removed by filtration over a 0.45 µm membrane syringe filter (HPF Millex, Merck, the Netherlands). To prevent chemical sulfide oxidation the filtered sample was subsequently mixed with 0.2 M zinc acetate in a 1:1 ratio to form ZnS. Afterward, the sample was centrifuged to separate fractions of ZnS and supernatant.

The biological sulfur concentration was calculated from the sulfur mass balance based on the supplied amount of sulfide and the actual sulfate and thiosulfate concentrations, according to:

$$[S^0]_t = (\Delta t(H_2S \text{ supplied}) / V_{\text{liquid}}) - [SO_4^{2-}]_t - 2*[S_2O_3^{2-}]_t - (S_x^{2-})_t$$

where the initial sulfur concentration is assumed to be zero. This is a general method to calculate the concentration of accumulated sulfur [8,12,27,28]. Concentrations of dissolved sulfide and possible volatile organosulfur compounds were not taken into account, as their combined concentrations in comparison to the total concentration

of sulfur species is negligible [8]. We also assume a pseudo “steady-state” conditions of the system, which was confirmed by the consecutive liquid and gas samples [11,14,29].

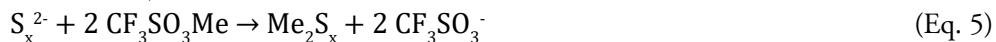
Sulfide was measured as total bisulfide (S^{2-}_{tot}) using a methylene blue method in a cuvette test (LCK653, Hach Lange, USA). Sulfide quantification was carried out immediately after sampling and samples were diluted in oxygen-free Milli-Q water (sparged with N_2 stream for 30 min) to exclude chemical oxidation. To see if sulfur balance is closed, we performed total S measurements on ICP-OES and compared concentration of measured sulfur with sum of sulfate and thiosulfate (data and full description can be found in Appendix A).

In addition to sulfur-containing anions, cations Na^+ and K^+ concentrations were measured with ion chromatography as described above for the anions. However, the mobile phase for a Metrohm Metrosep C4-150/4.0 mm column was 0.9 mL 3 mM HNO_3 min^{-1} .

In order to close the electron balance, the carbonate and bicarbonate ion concentrations need to be established using the Henderson-Hasselbalch equation [30] this article examines the evolution of the Henderson-Hasselbalch equation and presents a critical evaluation of its usefulness. The discussion centers on the titration of a weak acid with sodium hydroxide. Approximate pH values obtained from the Henderson-Hasselbalch equation are compared with exact hydrogen ion concentrations and the percentage errors are displayed as a function of the acid dissociation constant and buffer composition (titration mixture. Hence, liquid samples were analyzed on the total inorganic carbon using high-temperature catalytic oxidation at 680 °C with TOC-VCPH/CPN analyzer (Shimadzu, The Netherlands).

In total, two types of liquid samples were prepared, (1) filtrated and precipitated with zinc acetate for anions measurements and (2) unfiltered for biomass quantification and TOC analysis. All liquid samples were stored at 4 °C before being analyzed (about three days).

High-pressure liquid chromatography (HPLC) was used to determine dimethyl disulfide (DMDS), dimethyl trisulfide (DMTS) and polysulfides (dimethyl polysulfanes Me_2S_4 to Me_2S_8). For the quantification, polysulfide anions were derivatized to methyl polysulfanes with methyl trifluoromethanesulfonate (≥ 98 % pure, Sigma-Aldrich, the Netherlands) as follows:



HPLC was equipped with a UV detector (Dionex UltiMate 3000RS, USA) at a wavelength of 210 nm. An Agilent column (Zorbax Extend – C18 1.8 μm , 2.1 x 50 mm, the Netherlands) was used to separate the organic sulfur compounds at 20 °C. The mobile phase consisted of water and methanol. The flow rate was 0.371 mL min^{-1} , and the injection volume was 1.25 μL . The purity of the standards was above 98%

for DMS, DMDS, and DMTS (Sigma-Aldrich, the Netherlands). The detailed sample preparation and derivatization procedure are described in [7].

The gas-phase (H_2S , N_2 , CO_2 , and O_2) was analyzed with a gas chromatograph (Varian CP4900 Micro GC, Agilent, the Netherlands) equipped with two separate column modules, namely a 10-m-long Mol Sieve 5A PLOT (MS5) and a 10-m-long PoraPlot U (PPU). The required sample volume was 3 mL.

The gaseous MT and diorgano polysulfanes concentrations were measured with a gas chromatograph (Thermo scientificTM Trace GC Ultra with Trace GC Ultra valve oven, Interscience, Breda, the Netherlands) equipped with a Restek column (RT[®]-U-Bond, 30 m x 0.53 mm di x 20 μm df). The limits of quantification were 0.8 ppm(v) and 0.7 ppm(v), respectively. The analysis of sulfur compounds was performed using a flame photometric detector (150 °C) and thermal conductivity detector (160 °C). Inlet temperature was 190 °C. The oven temperature was gradually increased: first 2 min it was 70 °C, followed by an increase of 40 °C min^{-1} by reaching 190 °C, and subsequently finished with a temperature hold for 5 min. Helium was used as a carrier gas with a flow rate of 10 mL min^{-1} . Loop temperature was 50 °C, and the injection volume was 250 μL . To enable meticulous flushing total sample volume was 3 mL. All tubing was of the type Sulfiner[®], to prevent absorption and reaction of the sulfur compounds.

The concentration of MT and diorgano polysulfanes in the liquid phase were measured right after sample preparation with the same gas chromatography as gaseous samples, but the injection was done to the liquid port. Sample preparation followed with liquid-liquid extraction, where the sample was mixed with n-hexane (Sigma-Aldrich, the Netherlands) and internal standard (IST) stock solution in the ratio of 10:9:1 (sample: n-hexane: IST stock solution). Beforehand, the IST stock solution was prepared with 187.5 μL of thioanisole (TAS) (Sigma-Aldrich, the Netherlands) into 49.8 mL of hexane. TAS concentration in the stock solution was 1023 ppm S. To allow complete desorption of organosulfur compounds from the sulfur particles surface, the sample mixed with the IST in n-hexane was extracted on a rotary shaker (600 rpm) during 30 min, the upper liquid phase was sampled with a glass syringe, and 0.8 μL were injected using a sandwich method. A detailed description of this method can be found in [13].

5.3. Results and Discussion

5.3.1 Effect of methanethiol on process performance

To establish a stable baseline performance the feed during the first experimental run only consisted of H_2S , i.e., no MT was added to the system. This allowed us to assess the selectivity for sulfate, sulfur, and thiosulfate formation. After 15 days of stable

process operation, the selectivity of biologically produced sulfur was, on average, 91.5 ± 1.2 mol% with 6.7 ± 1.1 mol% of sulfate and 1.8 ± 0.3 mol% of thiosulfate [13], which is similar to the achieved sulfur selectivity in the traditional gas biodesulfurization setup, consisting of a gas absorber and aerobic reactor, i.e. no anaerobic reactor [14]. The term “selectivity” describes the mol fractions of products formed from a reactant or substrate. Hereafter, additional dosing of MT to the feed-gas was initiated. MT was supplied over 77 days of the process operation, whilst the loading rate was gradually increased from 0 to 2 mM S day⁻¹.

We experienced that operation of the setup in the fed-batch mode without a sulfur removal step has some serious limitations. For instance, the accumulation of sulfur particles results in poor gas, liquid and solid phase separation and hence oxygen buildup in the headspace of aerobic bioreactor. To enable stable process operation for a long-duration experiment, the process medium was exchanged four times to reduce the solids content. Thus, we calculated the average product selectivity for sulfate, thiosulfate, and sulfur per medium exchange in the experiment with MT addition (Fig. 1). The highest sulfur selectivity was 90 mol% that was achieved during the highest MT loading (day 29 to 44) while the lowest value 79 mol% was measured immediately after the startup of the process (day 1-11). The lower S production after start-up results from increased levels of thiosulfate and sulfate selectivity, 13 mol%, and 8 mol%, respectively. During days 45 to 77, the sulfur selectivity slightly dropped to 85 mol% with 6 mol% of sulfate and 9 mol% of thiosulfate formation. Thiosulfate selectivity decreased and stabilized at 9 mol% for the rest of the experiment. The observed thiosulfate selectivity in the presence of MT is almost five times higher than in the experiment with H₂S only, i.e. 9 mol % vs. 1.8 mol%. One of the reasons is the decreased biological rate of (poly)sulfide oxidation by SOB in the presence of MT (Appendix B, Fig. B1). The biological sulfide oxidation rate decreased by a factor of three, 0.9 ± 0.04 vs. 0.3 ± 0.01 mM O₂ (mg N h)⁻¹ at 0.12 mM of sulfide, after SOB biomass had been exposed to MT for 77 days. Because of the reduced biological oxidation capacity, there is more room for chemical sulfide oxidation, leading to the formation of thiosulfate, at elevated H₂S loading rates. Conversely, more thiosulfate will be formed at a constant H₂S loading upon increasing MT dosing rates. Moreover, any biological thiosulfate oxidation will be suppressed in the presence of DODS [10,13]. To overcome thiosulfate formation in the presence of MT, it is suggested to start process operation with a higher SOB biomass concentration.

In our biodesulfurization process, sulfate is formed from sulfide and thiosulfate oxidation by SOB (Eq. 2 and 5), albeit that the specific oxidation rates for each substrate are different. In our previous studies, we found that SOB oxidation rates of thiosulfate were three times lower than for sulfide oxidation, 0.09 ± 0.01 vs. 0.32 ± 0.02 mM O₂ (mg N h)⁻¹ [13]. Hence, we assume that the primary source for sulfate formation is biological (poly)sulfide oxidation. The addition of MT contributed to a decrease in

sulfate selectivity. At MT loading rates below $1.4 \text{ mM S day}^{-1}$, the selectivity for sulfate formation was about 8 mol% and started to decrease at higher MT loading rates (Fig. 1) and reached 0.6 mol% at the highest MT supplied. This indicates the effect of the MT loading rate on the sulfate formation. In previous studies, it was found that sulfate formation was inhibited in the presence of VOSCs [31]. Less than 0.5 mol% sulfate selectivity was observed 15 mol% of thiosulfate, and 85 mol% of sulfur. In subsequent studies Roman et al. found that the sulfate selectivity was $\sim 5 \text{ mol\%}$ with $\sim 20 \text{ mol\%}$ of thiosulfate and 75 mol% of sulfur [11]. Furthermore, from our previous study, it can be concluded that the product of MT oxidation – DMDS – selectively inhibits sulfate formation. For instance, at a higher MT loading rate more DMDS was produced (Appendix C, Fig. C1).

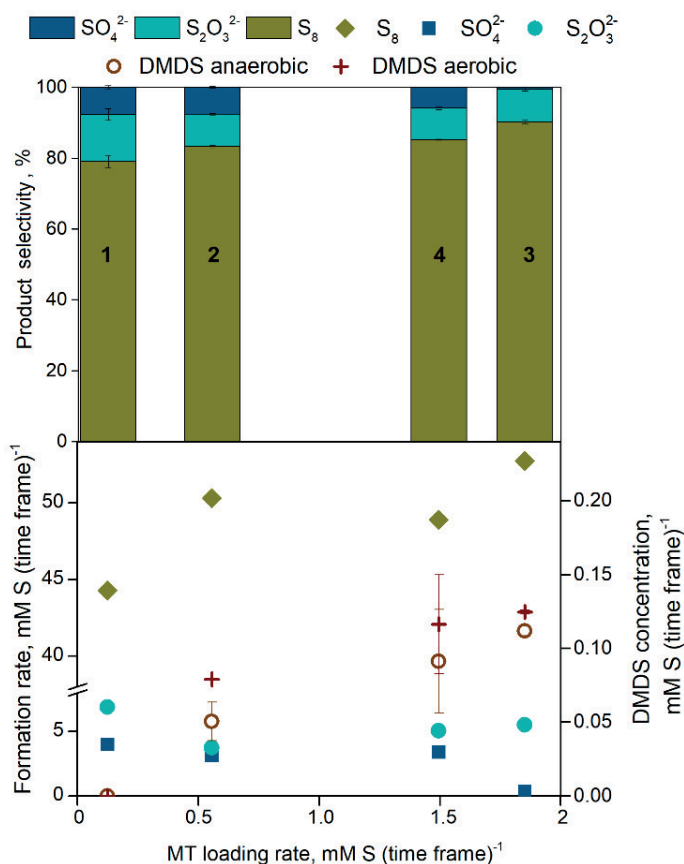


Fig. 1. An average product selectivity and the formation rates of sulfate, thiosulfate, and dimethyl disulfide (DMDS) during the lab-scale biodesulfurization process operation with the addition of methanethiol (MT). Numbers in the bars indicate the time frame: 1 – day 1 to 11, 2 – day 12 to 29, 3 – day 29 to 44, and 4 – day 44 to 47.

We found that the formed DMDS selectively inhibited sulfate formation as follows from a decrease in selectivity from 8 mol% to 0.6 mol% at 29 to 44 days and triggered a slight increase in the thiosulfate formation rate (Fig. 1). This result is in line with our previous findings [13], where it was confirmed that sulfate formation is susceptible to the presence of DMDS. In addition to the detected DMDS, we also measured MT and other (diorgano)polysulfides (tri- and tetrasulfides). From the results of liquid GC-FPD analysis, it followed that the second most abundant diorgano polysulfane was dimethyl trisulfide (DMTS). Dimethyl tetrasulfide was detected only in the last days of process operation, while any MT was not detected (Appendix C, Fig. C1). In addition, the headspaces of both bioreactors and the outlet of the absorber were analyzed to detect any sulfur-containing gases. The concentration of DMDS in the headspace of the aerobic bioreactor and the gas outlet increased along with an increase of the MT loading rate (Appendix C, Fig. C2). This dependency confirms that the liquid and gas phases were in pseudo-equilibrium. The same correlation was observed in the traditional gas biodesulfurization system by Roman et al. [27]. However, the concentration of DMDS in the headspace of the anaerobic bioreactor remained constant, regardless of the increase of the MT loading rate (Appendix C, Fig. C2). This result indicates that the liquid and gaseous phases in the laboratory setup are in equilibrium.

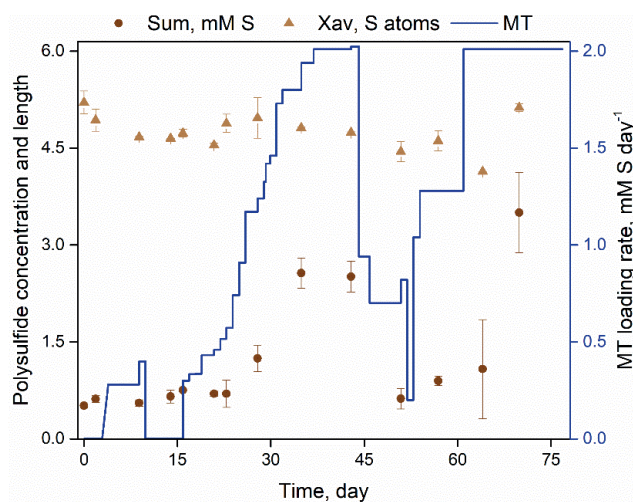


Fig. 2. Average Sum of polysulfides and their length in the process liquid to the supplied methanethiol (MT) loading rate to the lab-scale biodesulfurization setup.

In addition to diorgano polysulfanes, also inorganic polysulfides were detected in the bioreactor suspension (Eq. 4 and 7). The average chain length of the polysulfides x_{av} was found to be 4.8 ± 0.2 S atoms (Fig. 2). This is in good agreement with the values reported by Roman et al. [7]. The sum of polysulfides was constant for about 25 days

(0.6 ± 0.1 mM S) until the MT loading was increased to 2 mM S day⁻¹. The increase in MT loading rate possibly triggered an increase in the sum of polysulfide species (Eq. 7) on days 29 to 44 and day 60 to 75; this was also observed by Roman et al [9]. As mentioned before, polysulfides are formed from the reaction between produced bio-sulfur and sulfide (Eq. 4). Hence, the sulfide concentration in liquid and the sum of polysulfide species were similar. This indicates that all supplied sulfide immediately reacted with sulfur to form polysulfides. From this observation, we conclude that the electron donor in our lab-scale biodesulfurization setup was polysulfide.

5.3.2 Effect of methanethiol on sulfur-oxidizing bacterial community dynamics

The biomass grown in the experiment fed with sulfide alone was subsequently used as the inoculum for the experiment with sulfide and MT as feed gases. Thus, a relative abundance of SOB community and absolute 16S rRNA copy number of *Alkalilimnicola ehrlichii*, *Thioalkalivibrio sulfidophilus*, and *Thioalkalibacter halophilus* were of the similar value at the end of the experiment with sulfide and at the beginning of the experiment with sulfide+MT (Fig. 3A and B). From the results of 16S amplicon sequencing and qPCR, it appears that the presence of MT provided a competitive advantage to *Thioalkalibacter* genus with a significant change in its 16S rRNA log copies number ($p=3.814 \times 10^{-16}$). The only described species in this genus is the obligate chemolithoautotrophic facultative alkaliphile *Thb. halophilus* [32]. The presence of DMDS, and not the MT itself, proved to be a direct factor for the proliferation of *Thb. halophilus* [13], as assumed before. The second in abundance was a haloalkaliphilic SOB *Alkalilimnicola ehrlichii*, which became dominant in Run 1 and was dominant in the experiments with MT. However, on the 44th day of the process operation, when the highest MT loading rate was reached (2 mM S day⁻¹), the relative abundance of *Alkalilimnicola* drastically declined (Fig. 3B). The intoxication of the bacteria with MT/DMDS and competition with a more thio-adapted *Thioalkalibacter* could be the cause of this outcome.

Moreover, the bacterial community composition entirely shifted when the MT loading reached 2 mM S day⁻¹ at day 29 (Appendix D, Fig. D1). These included gammaproteobacterial genera, including *Thioalkalimicrobium*, *Halomonas*, and *Thioalkalivibrio*, were also detected in the inocula in both experimental runs. *Halomonas* species are aerobic or facultative anaerobic chemoorganotrophic haloalkaliphilic SOB that can utilize a wide range of organic substrates (such as fatty acids and sugars, but also hydrocarbons) and oxidize inorganic sulfur compounds incompletely to tetrathionate [33,34]. From the beginning of the experiment with sulfide, the relative abundance of *Halomonas* declined and continued to decrease with introduction of MT. A possible reason is the low concentration of available organics in the feed gas and the inability of *Halomonas* to withstand methanethiol toxicity [31].

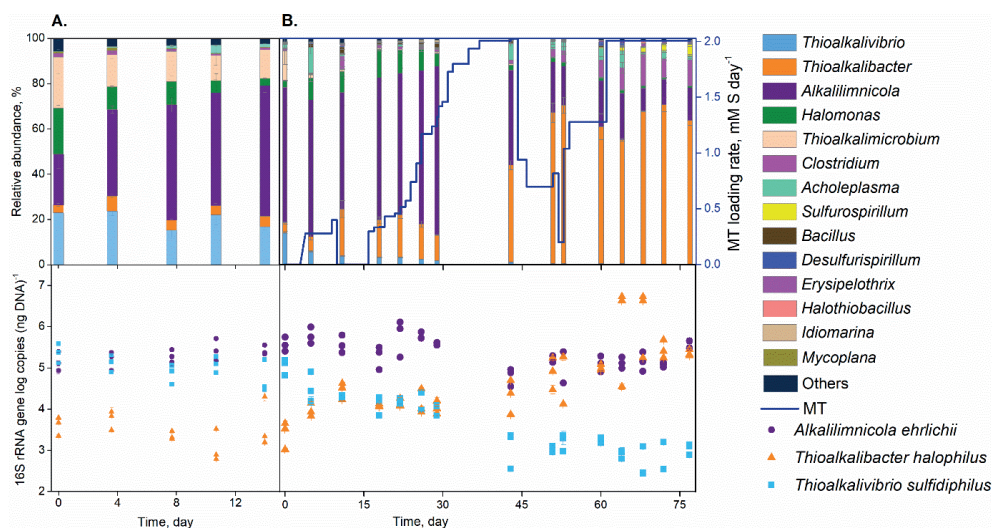


Fig. 3. The relative abundance of the microbial composition (top) and quantified 16S rRNA gene copies (bottom) of *Thioalkalivibrio sulfidiphilus*, *Thioalkalibacter halophilus*, and *Alkalilimnicola ehrlichii* during (A) H₂S and (B) H₂S + methanethiol (MT) supply. Only bacteria with a relative abundance higher than 0.5 % are listed (remaining species are clustered into “Others”). Relative abundance results represent the average value, and the error bar represents the standard deviation of the three biological replicates. 16S rRNA gene log copies are an average value of the measured technical duplicates, whereas each data point is a biological replicate at each time point. Error bars indicate the standard deviation between technical duplicates. The lab-scale gas biodesulfurization bioreactor system was operated at a low oxidation-reduction potential of -390 mV, pH 8.5, and H₂S loading rate was 58.12 mM S day⁻¹.

In comparison to *Halomonas*, the genera: *Thioalkalivibrio* and *Thioalkalimicrobium* are obligate chemolithoautotrophic haloalkaliphilic SOB that dominate in natural soda lakes [35]. The relative abundance of *Thioalkalimicrobium* and *Thioalkalivibrio* was constant during the sulfide supply only, whereas in the experiment with addition MT supply, the relative abundance of *Thioalkalimicrobium* drastically decreased within first 10 days of MT supply. In addition, the relative abundance of *Thioalkalivibrio* slightly decreased from 14 to 1.8 % during 29 days of the process operation and reached a minimum on the 44th day at the highest MT supply. The most probable explanation for the apparent low tolerance of *Tv. sulfidiphilus* to thiols is the fact that its only cytochrome oxidase is of the *cbb*₃ type, which is highly sensitive to inhibition by organic sulfur compounds [9,10,13,27,31]. Thus, a decline in the relative abundance of *Tv. sulfidiphilus* is associated with the presence of organosulfur compounds. More to that, the drop in the relative abundance of *Tv. sulfidiphilus* provided an advantage for the growth of *Thb. halophilus* and *Alk. ehrlichii*. However, with the results from 16S amplicon sequencing, we cannot answer questions on species interaction and dynamics. Thus, qPCR was performed to monitor growth dynamics and establish absolute 16S rRNA counts of the three SOB key-players: *Thb. halophilus*, *Tv. sulfidiphilus* and *Alk. ehrlichii*.

qPCR results showed that throughout process operation, the absolute abundance of *Thb. halophilus* rRNA increased with 2 log copies (ng DNA)⁻¹, and *Thioalkalivibrio sulfidiphilus* decreased with 2.3 log copies (ng DNA)⁻¹ by the end of the process operation with MT (Fig. 3B). These estimates of absolute abundance corroborate the observed pattern of relative abundances of the genera *Thioalkalibacter* and *Thioalkalivibrio*. However, while the absolute abundance of *Alk. ehrlichii* only marginally decreased by about 0.6 log copies (ng DNA)⁻¹, its relative abundance decreased drastically by 46 % when the highest MT loading rate was reached (2 mM S day⁻¹) (Fig. 3B). The absolute quantity of total bacterial 16S rRNA log copies (ng DNA)⁻¹ remained almost constant over 29 days of process operation, with only a slight decline at a high MT concentration. These seemingly discrepant estimates of *Alk. ehrlichii* between qPCR and amplicon sequencing might be caused by different *Alk. ehrlichii*-specific amplification efficiencies of the universal 335F/518R primer set (amplicon sequencing) and the highly species-specific primer set (qPCR) [36].

Moreover, this discrepancy may further be enhanced by primer binding competition, and PCR bias as 16S rRNA amplicon sequence counts depend on the abundance of other detected species in the sample [37]. This problem is thus particularly pertinent for relatively low abundant species. In contrast to 16S amplicon sequencing, the qPCR outcome does not depend on the abundance of other detected species and is conventionally used as a proxy for the absolute bacterial count [38] though well-known, still insufficiently addressed and can potentially lead to a completely different interpretation of experimental results. This review provides a critical assessment of next generation sequencing (NGS).

We further analyzed a possible correlation between the SOB key species and process performance parameters, including sulfate and thiosulfate concentrations, as well as MT loading rate, to evaluate whether these SOBs were responsible for sulfate and thiosulfate formation. After we have corrected for pseudo-replication and the accumulation of thiosulfate and sulfate, only methanethiol loading rate was having a significant effect on the species absolute counts (Appendix E, Fig. E1 and E2). MT concentration predicted species growth and lapse: MT positively affected *Thb. halophilus* growth (lmer Bonferroni adjustment, $p=2\times 10^{-16}$), whereas MT negatively affected the growth of *Tv. sulfidiphilus* (lmer Bonferroni adjustment, $p=2\times 10^{-16}$) and *Alk. ehrlichii* (lmer Bonferroni adjustment, $p=0.04$) (Fig. E1). These results are in concordance with our previous study, where *Thb. halophilus* abundance rapidly increased within five days of DMDS addition, and where growth dynamics of *Tv. sulfidiphilus* and *Alk. ehrlichii* did not change from the inoculum stage (Kiragosyan et al., unpublished data). The difference in the growth dynamics of SOB key species between the additions of MT and DMDS likely depends on the differential toxicity of these compounds and their effects

on bacterial activity. MT is known as a competitive inhibitor for the bacterial sulfide oxidation, while DMDS is non-competitive (Appendix C, Fig.C1) [10].

Nevertheless, in both cases, *Thb. halophilus* growth was enhanced, and one of the main reasons is the presence of the highly inhibitor-resistant quinol oxidase *bd* in addition to cytochrome c oxidase *cbb₃* (according to the genomic data) of *Thb. halophilus* [39]. As a comparison, inhibitor-sensitive cytochrome oxidase *cbb₃* (heme-Cu family) is the only oxidase present in the genome of *Tv. sulfidophilus* and other dominant SOB species in the gas biodesulfurization systems [27,40]. These results provide valuable information on the application and use of *Thioalkalibacter halophilus* species in the gas biodesulfurization system to achieve high sulfur selectivity and stable process operation in the presence of thiols.

5.4 Conclusions

Modification of the traditional gas biodesulfurization line-up with the addition of an anaerobic bioreactor resulted in the enhancement of sulfur selectivity up to 90 mol% during 29 to 44 days of process operation. This selectivity was achieved when MT loading was still being increased, whereas at a constant MT loading of 2 mM S day⁻¹ only 85 mol% of sulfur selectivity was reached (day 44 to 77) and the sulfate selectivity increased from 0.6 mol% to 6 mol%. Low achieved sulfate selectivity of 0.6 mol% is the result of selective suppression of sulfate formation by chemically formed DMDS from MT oxidation.

The high selectivity for the sulfur formation and stable gas biodesulfurization process operations depends on the composition of the SOB community. In a single reactor system with the only H₂S in the feed gas *Thioalkalivibrio sulfidophilus* is the dominant SOB. In the dual reactor line-up, we found that *Alkalilimnicola ehrlichii* became the dominant organism. However, after the addition of MT *Thioalkalibacter halophilus* became the most abundant haloalkaliphilic SOB species. These shifts in SOB community composition indicate a resilience of the mixed microbial communities to withstand process perturbations and, therefore, broadening the operational window of the gas biodesulfurization system. The overall outcome of this work provides a deeper understanding of the microbial sulfide oxidation and community composition dynamics in a gas biodesulfurization process for H₂S and methanethiol.

Acknowledgments

This work has been performed within the cooperation framework of Wetsus, European Centre of Excellence for Sustainable Water Technology (wetsus.nl), Wageningen University and Research (wur.nl) and Paqell B.V. (paqell.com). Wetsus is co-funded by the Netherlands' Ministry of Economic Affairs and Ministry of Infrastructure and Environment, the European Union's Regional Development Fund, the Province of Fryslan and the Northern Netherlands Provinces. Wetsus is also a coordinator of the WaterSEED project that received funding from European Union's Horizon 2020 research and innovation program under Marie Skłodowska-Curie grant agreement No. 665874. The research of Peer H.A. Timmers was supported by the Soehngen Institute of Anaerobic Microbiology (SIAM) Gravitation grant (024.002.002) of the Netherlands Ministry of Education, Culture, and Science and the Netherlands Organization for Scientific Research (NWO). We would like to thank Pieter van Veelen for the guidance and help with statistical analyses.

References

- [1] X. Wang, M. Economides, Natural gas processing, in: X. Wang, M. Economides (Eds.), *Adv. Nat. Gas Eng.*, Elsevier, 2009: pp. 115–169. doi:10.1016/C2013-0-15532-8.
- [2] M. Chen, X.Z. Yao, R.C. Ma, Q.C. Song, Y. Long, R. He, Methanethiol generation potential from anaerobic degradation of municipal solid waste in landfills, *Environ. Sci. Pollut. Res.* 24 (2017) 23992–24001. doi:10.1007/s11356-017-0035-x.
- [3] E. Smet, P. Lens, H. Van Langenhove, Treatment of waste gases contaminated with odorous sulfur compounds, *Crit. Rev. Environ. Sci. Technol.* 28 (1998) 89–117. doi:10.1080/10643389891254179.
- [4] M. Syed, G. Soreanu, P. Falletta, M. Béland, Removal of hydrogen sulfide from gas streams using biological processes - A review, *Can. Biosyst. Eng.* 48 (2006) 1–14.
- [5] C. Cline, A. Hoksberg, R. Abry, A. Janssen, Biological Process for H₂S Removal From Gas Streams: the Shell-Paques / ThiopaTM Gas Desulfurization Process, *Proc. Laurance Reid Gas Cond. Conf.* (2003) 1–18.
- [6] P.L.F. Van Den Bosch, O.C.C. Van Beusekom, C.J.N. Buisman, A.J.H. Janssen, Sulfide Oxidation at Halo-Alkaline Conditions in a Fed-Batch Bioreactor, *Biotechnol. Bioeng.* 97 (2007) 1053–1063. doi:10.1002/bit.
- [7] P. Roman, M.F.M. Bijmans, A.J.H. Janssen, Quantification of individual polysulfides in lab-scale and full-scale desulfurisation bioreactors, *Environ. Chem.* 11 (2014) 702–708. doi:10.1071/EN14128.
- [8] P.L.F. Van Den Bosch, M. Fortuny-Picornell, A.J.H. Janssen, Effects of Methanethiol on the Biological Oxidation of Sulfide at Natron-Alkaline Conditions, *Environ. Sci. Technol.* 43 (2009) 453–459. doi:10.1021/es801894p.
- [9] P. Roman, M.F.M. Bijmans, A.J.H. Janssen, Influence of methanethiol on biological sulphide oxidation in gas treatment system, *Environ. Technol.* 3330 (2016) 1–11. doi:10.1080/09593330.2015.1128001.
- [10] P. Roman, J. Lipińska, M.F.M. Bijmans, D.Y. Sorokin, K.J. Keesman, A.J.H. Janssen, Inhibition of a biological sulfide oxidation under haloalkaline conditions by thiols and diorganopolysulfanes, *Water Res.* 101 (2016) 448–456. doi:10.1016/j.watres.2016.06.003.
- [11] P. Roman, J.B.M. Klok, J.A.B. Sousa, E. Broman, M. Dopson, E. Van Zessen, M.F.M. Bijmans, D.Y. Sorokin, A.J.H. Janssen, Selection and Application of Sulfide Oxidizing Microorganisms Able to Withstand Thiols in Gas Biodesulfurization Systems, *Environ. Sci. Technol.* (2016) acs.est.6b04222. doi:10.1021/acs.est.6b04222.
- [12] R. De Rink, J.B.M. Klok, D.Y. Sorokin, G.J. Van Heeringen, A. Ter Heijne, R. Zeijlmaker, Y.M. Mos, V. De Wilde, K.J. Keesman, C.J.N. Buisman, Increasing the selectivity for sulfur formation in biological gas desulfurization, *Environ. Sci. Technol.* 53 (2019) 4519–4527. doi:10.1021/acs.est.8b06749.

- [13] K. Kiragosyan, M. Picard, D.Y. Sorokin, J. Dijkstra, J.B.M. Klok, P. Roman, A.J.H. Janssen, Effect of dimethyl disulfide on the sulfur formation and microbial community composition during the biological H₂S removal from sour gas streams, *J. Hazard. Mater.* 386 (2020). doi:10.1016/j.jhazmat.2019.121916.
- [14] K. Kiragosyan, J.B.M. Klok, K.J. Keesman, P. Roman, A.J.H. Janssen, Development and validation of a physiologically based kinetic model for starting up and operation of the biological gas desulfurization process under haloalkaline conditions, *Water Res.* X. 4 (2019) 100035. doi:10.1016/j.wroa.2019.100035.
- [15] K. Kiragosyan, P. van Veelen, S. Gupta, A. Tomaszewska-Porada, P. Roman, P.H.A. Timmers, Development of quantitative PCR for the detection of *Alkalilimnicola ehrlichii*, *Thioalkalivibrio sulfidiphilus* and *Thioalkalibacter halophilus* in gas biodesulfurization processes, *AMB Express.* 9 (2019) 99. doi:10.1186/s13568-019-0826-1.
- [16] D.Y. Sorokin, M.S. Muntyan, A.N. Panteleeva, G. Muyzer, *Thioalkalivibrio sulfidiphilus* sp. nov., a haloalkaliphilic, sulfur-oxidizing gammaproteobacterium from alkaline habitats, *Int. J. Syst. Evol. Microbiol.* 62 (2012) 1884–1889. doi:10.1099/ij.s.0.034504-0.
- [17] A.-C. Ahn, L. Overmars, D.Y. Sorokin, J.P. Meier-Kolthoff, G. Muyzer, M. Richter, T. Woyke, Genomic diversity within the haloalkaliphilic genus *Thioalkalivibrio*, *PLoS One.* 12 (2017) e0173517. doi:10.1371/journal.pone.0173517.
- [18] D.J. Lane, 16S/23S rRNA sequencing, in: E. Stackebrandt, M. Goodfellow (Eds.), *Nucleic Acid Tech. Bact. Syst.*, John Wiley & Sons, Inc., New York, 1991; pp. 115–175.
- [19] G. Muyzer, E.C.D.E. Waal, A.G. Uitertlinden, Profiling of Complex Microbial Populations by Denaturing Gradient Gel Electrophoresis Analysis of Polymerase Chain Reaction-Amplified Genes Coding for 16S rRNA, *Appl. Environ. Microbiol.* 59 (1993) 695–700.
- [20] R. Pallares-Vega, H. Blaak, R. van der Plaats, A.M. de Roda Husman, L.H. Leal, M.C.M. van Loosdrecht, D.G. Weissbrodt, H. Schmitt, Determinants of presence and removal of antibiotic resistance genes during WWTP treatment: A cross-sectional study, *Water Res.* (2019). doi:10.1016/j.watres.2019.05.100.
- [21] A.E. Parada, D.M. Needham, J.A. Fuhrman, Every base matters: Assessing small subunit rRNA primers for marine microbiomes with mock communities, time series and global field samples, *Environ. Microbiol.* 18 (2016) 1403–1414. doi:10.1111/1462-2920.13023.
- [22] L. Lahti, S. Shetty, V. Obenchain, J. Salojärvi, R. Gilmore, T. Blake, N. Turaga, H. Pagès, M. Ramos, A. Salosensaari, Tools for microbiome analysis in R, (2017). <http://microbiome.github.com/microbiome>.
- [23] D. Bates, M. Mächler, B. Bolker, S. Walker, Fitting Linear Mixed-Effects Models using lme4, (2014). doi:10.18637/jss.v067.i01.
- [24] R Core Team, R: A language and environment for statistical computing., R Found. Stat. Comput. Vienna, Austria. (2018).
- [25] A. Kuznetsova, P.B. Brockhoff, R.H.B. Christensen, lmerTest Package: Tests in Linear Mixed Effects Models, *J. Stat. Softw.* 82 (2017). doi:10.18637/jss.v082.i13.

- [26] H. de Rosario-Martinez, phia: Post-Hoc Interaction Analysis. R package version 0.2-1., (2015). <https://cran.r-project.org/package=phia>.
- [27] P. Roman, R. Veltman, M.F.M. Bijmans, K.J. Keesman, A.J.H. Janssen, Effect of Methanethiol Concentration on Sulfur Production in Biological Desulfurization Systems under Haloalkaline Conditions, *Environ. Sci. Technol.* 49 (2015) 9212–9221. doi:10.1021/acs.est.5b01758.
- [28] J.B.M. Klok, P.L.F. Van Den Bosch, C.J.N. Buisman, A.J.M. Stams, K.J. Keesman, A.J.H. Janssen, Pathways of sulfide oxidation by haloalkaliphilic bacteria in limited-oxygen gas lift bioreactors, *Environ. Sci. Technol.* 46 (2012) 7581–7586. doi:10.1021/es301480z.
- [29] P.L.F. Van Den Bosch, D.Y. Sorokin, C.J.N. Buisman, A.J.H. Janssen, The effect of pH on thiosulfate formation in a biotechnological process for the removal of hydrogen sulfide from gas streams, *Environ. Sci. Technol.* 42 (2008) 2637–2642. doi:10.1021/es7024438.
- [30] H.N. Po, N.M. Senozan, The Henderson-Hasselbalch Equation: Its History and Limitations, *J. Chem. Educ.* 78 (2001) 1499–1503. doi:10.1021/ed080p146.
- [31] P.L.F. Van Den Bosch, M. De Graaff, M. Fortuny-Picornell, R.C. Van Leerdam, A.J.H. Janssen, Inhibition of microbiological sulfide oxidation by methanethiol and dimethyl polysulfides at natron-alkaline conditions, *Appl. Microbiol. Biotechnol.* 83 (2009) 579–587. doi:10.1007/s00253-009-1951-6.
- [32] H.L. Banciu, D.Y.Y. Sorokin, T.P. Tourova, E.A. Galinski, M.S. Muntyan, J.G. Kuenen, G. Muyzer, Influence of salts and pH on growth and activity of a novel facultatively alkaliphilic, extremely salt-tolerant, obligately chemolithoautotrophic sulfur-oxidizing Gammaproteobacterium *Thioalkalibacter halophilus* gen. nov., sp. nov. from South-Western Siber, *Extremophiles*. 12 (2008) 391–404. doi:10.1007/s00792-008-0142-1.
- [33] M.T. García, A. Ventosa, E. Mellado, Catabolic versatility of aromatic compound-degrading halophilic bacteria, *FEMS Microbiol. Ecol.* 54 (2005) 97–109. doi:10.1016/j.femsec.2005.03.009.
- [34] D.Y. Sorokin, Oxidation of inorganic sulfur compounds by obligately organotrophic bacteria, *Microbiology*. 72 (2003) 641–653. doi:10.1023/B:MICI.0000008363.24128.e5.
- [35] C.D. Vavourakis, A.-S. Andrei, M. Mehrshad, R. Ghai, D.Y. Sorokin, G. Muyzer, A metagenomics roadmap to the uncultured genome diversity in hypersaline soda lake sediments, *Microbiome*. 6 (2018) 168. doi:10.1186/s40168-018-0548-7.
- [36] M. Leray, J.Y. Yang, C.P. Meyer, S.C. Mills, N. Agudelo, V. Ranwez, J.T. Boehm, R.J. Machida, A new versatile primer set targeting a short fragment of the mitochondrial COI region for metabarcoding metazoan diversity: Application for characterizing coral reef fish gut contents, *Front. Zool.* 10 (2013) 1–14. doi:10.1186/1742-9994-10-34.
- [37] L.A.S. Snyder, N. Loman, M.J. Pallen, C.W. Penn, Next-generation sequencing - The promise and perils of charting the great microbial unknown, *Microb. Ecol.* 57 (2009) 1–3. doi:10.1007/s00248-008-9465-9.

- [38] F. Bonk, D. Popp, H. Harms, F. Centler, PCR-based quantification of taxa-specific abundances in microbial communities: Quantifying and avoiding common pitfalls, *J. Microbiol. Methods*. 153 (2018) 139–147. doi:10.1016/j.mimet.2018.09.015.
- [39] D.Y. Sorokin, A.Y. Merkel, G. Muyzer, Genus *Thioalkalibacter*, in: *Bergey's Man. Syst. Archaea Bact.*, John Wiley & Sons, Inc., 2020. doi:10.1002/9781118960608.gbm01692.
- [40] G. Muyzer, D.Y. Sorokin, K. Mavromatis, A. Lapidus, A. Clum, N. Ivanova, A. Pati, P. D'Haeseleer, T. Woyke, N.C. Kyrpides, Complete genome sequence of “*Thioalkalivibrio sulfidophilus*” HL-EbGr7, *Stand. Genomic Sci.* 4 (2011) 23–35. doi:10.4056/sigs.1483693.

Appendix A – Closing sulfur balance

During the measurements of sulfate and thiosulfate on ion-chromatography and analysis of the same samples on total sulfur with ICP-OES, we found that there was a gap between sum of sulfate and thiosulfate and total measured sulfur. Moreover, when we restarted lab-scale setup with a refreshed medium in aerobic reactor we observed reoccurring trend of sulfide concentration decrease (Fig. A1). We tried to understand the underlying mechanism and found out that a decrease in sulfide concentration was strongly correlated with a gap in the sulfur balance (Fig. A1). To trace if the gap increased with a similar rate every time setup was restarted, we calculated rates of the sulfur gap increase and found that the highest rate was observed during the first 11 days of operation $14.6 \text{ mM S day}^{-1}$. Afterward, a gap rate decreased to $9.2 \text{ mM S day}^{-1}$ (12 - 29 days) with a followed further decrease to $8.6 \text{ mM S day}^{-1}$ (day 29 - 44). During 44 to 77 days gap rate increased to $11.5 \text{ mM S day}^{-1}$. To identify the cause of the increasing gap, we initially investigated whether the gap is coming from the ICP analysis itself. Results showed no detection of extra sulfur through any possible contamination from nitric acid and the equipment itself. Furthermore, as the ion balance was closed, we can assume that the compound that is contributing to the gap is neutrally charged. However, to have full certainty in identifying the missing compound, more research is required.

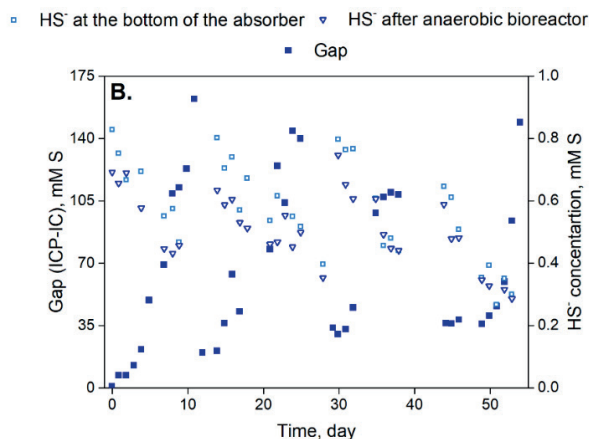


Fig. A1. Measured sulfide concentration and a sulfur gap in the liquid of the lab-scale biodesulfurization setup.

Appendix B – Respiration tests

Respiration rates of SOB biomass were measured after process operation with H_2S and after run with $\text{H}_2\text{S}+\text{MT}$. A detailed description of the performed test can be found in [13].

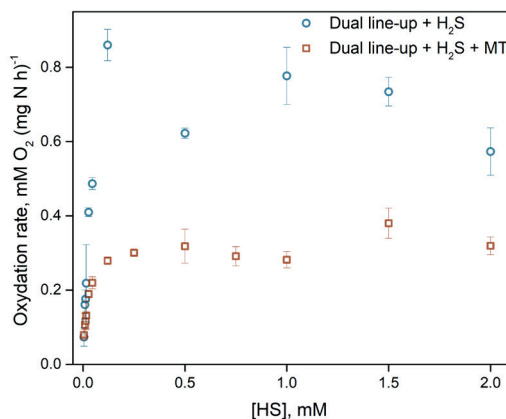


Fig. B1. Biological oxidation rates at different concentrations of HS^- in oxygen saturated buffer at pH 8.5, 1 M Na^+ and 35 °C. Measured data points are the average values of the experimentally measured duplicates.

Appendix C – GC-FPD analysis of liquid and gas samples from the biodesulfurization lab-scale setup

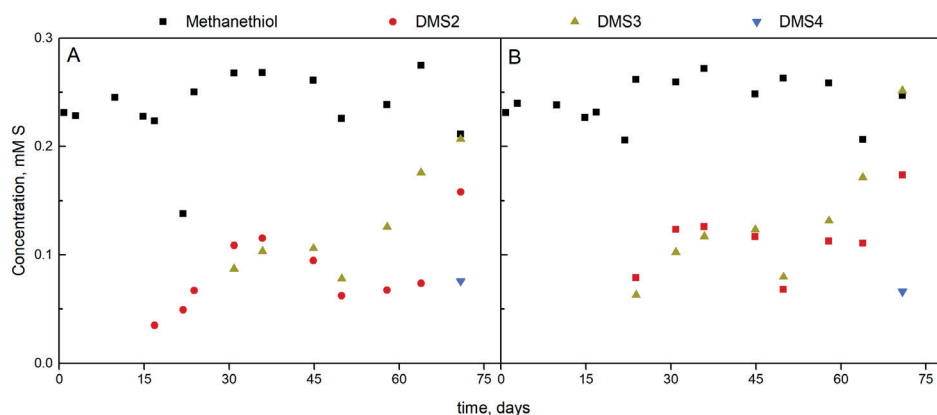


Fig. C1. Measured concentrations of methanethiol, dimethyl di- (DMS2), -tri- (DMS3) and -tetrasulfide (DMS4) in the process liquid from (A) the anaerobic and (B) the aerobic bioreactors during 77 days of biodesulfurization process operation with a gradual increase of methanethiol supply. The system was operated at ORP of -390 mV, pH = 8.5, T = 35 °C and the H_2S loading rate was $58.15 \text{ mM S day}^{-1}$.

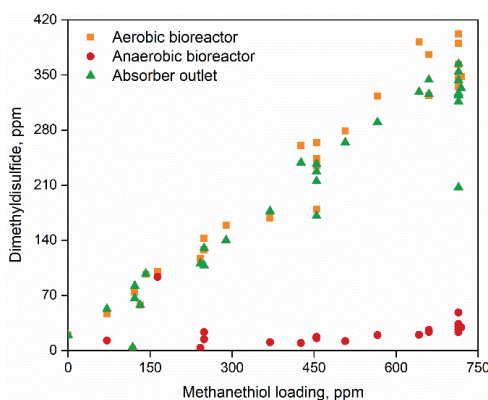


Fig. C2. The detected gas concentrations of dimethyl disulfide (DMDS) in the headspace or the anaerobic, the aerobic bioreactors, and the gas outlet during biodesulfurization process operation with a gradual increase of methanethiol supply. The system was operated at ORP of -390 mV, pH = 8.5, T = 35 °C and the H_2S loading rate was $58.15 \text{ mM S day}^{-1}$.

Appendix D – Non-metric multidimensional scaling of 16S amplicon sequences

To understand how the bacterial community composition changes, a *non-metric multidimensional scaling* (NMDS) on the 16S rRNA amplicon sequencing results was performed (Fig. D1). Clear differentiation between 45 samples taken in the experiment with methanethiol (MT) can be noticed, where three clusters can be distinguished. The first cluster has a similar community structure (samples MT1 to MT21) as MT loading rate was relatively low (0 to 30 days). The second cluster includes only one data point (MT22 – MT24), which samples were taken at day 44 after several days of the process operation at a high MT loading rate of 2 mM S day⁻¹. The third cluster includes the rest of the samples that were taken after the previous high MT loading rate (MT25 – MT45).

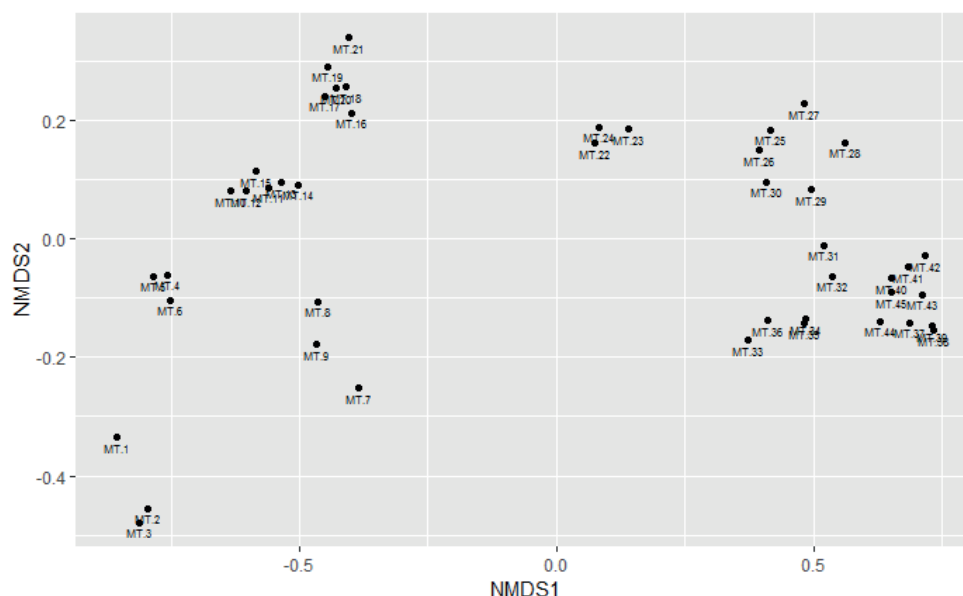


Fig. D1. Non-metric multidimensional scaling (axes NMDS1 vs. NMDS2) of the bacterial community at the lab-scale biodesulfurization setup loaded with sulfide and methanethiol. Dots denote samples, including time point triplicates, which were taken at 15 different time points. The system was operated at ORP of -390 mV, pH = 8.5, T = 35 °C and the H₂S loading rate was 58.15 mM S day⁻¹.

Appendix E – Statistical analysis of the qPCR results

We have used generalized linear mixed models (GLMM) approach with lmer function to analyze qPCR data and to find dependencies between variables of interest (thiosulfate and sulfate formation, methanethiol loading rate represented as time). We have expressed methanethiol loading over time, as both variables are highly dependent. After we have corrected for pseudoreplication (technical replicates) and accumulation of thiosulfate and sulfate, only methanethiol loading rate was having a significant effect on the species absolute counts.

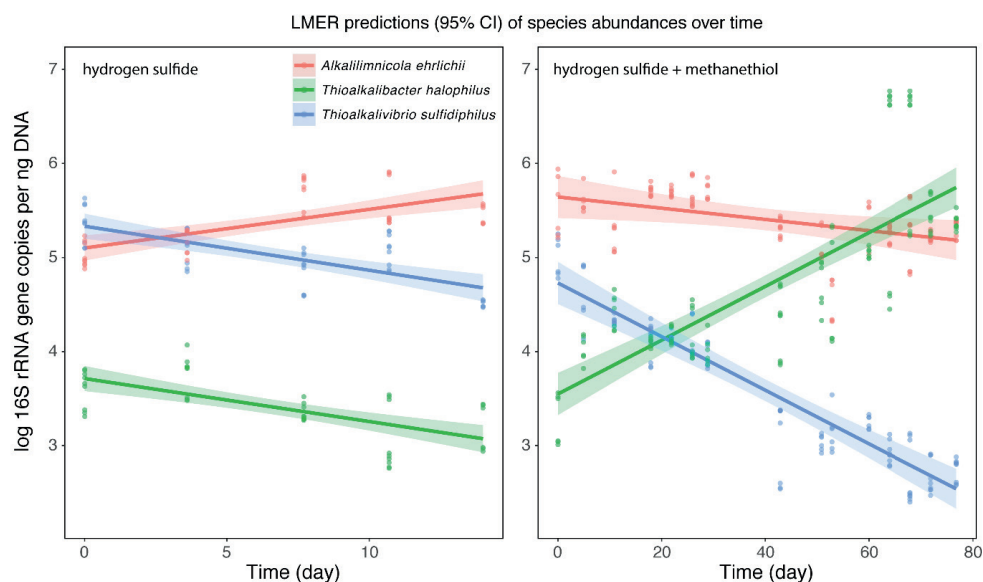


Fig. E1. Generalized linear mixed effect model (LMER) predictions for the absolute species abundance counts over time. Lines indicate significant model predictions and 95 % confidence interval (CI). The system was operated at ORP of -390 mV, pH = 8.5, T = 35 °C and the H₂S loading rate was 58.15 mM S day⁻¹.

In addition, we checked the relation between three key-species from the experiment with MT (Fig. E2). Furthermore, all three interactions were highly significant ($< 2.2 \times 10^{-16}$). Taking into account the observed dynamics of all three species, it can be concluded that *Thb. halophilus* proliferation affected decrease of *Alk.ehrlichii* abundance. In addition, intoxication by MT most likely played a role in the decrease of *Alk.ehrlichii*. Together, *Alk. ehrlichii* and *Thb. halophilus* outcompete *Thioalkalivibrio sulfidiphilus*.

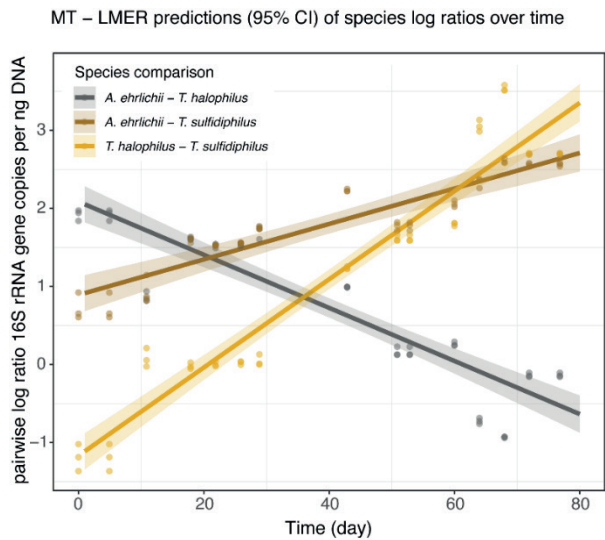


Fig. E2. Relations between three SOB key-species. Lines indicate significant model predictions and a 95 % confidence interval. The system was operated at ORP of -390 mV, pH = 8.5, T = 35 °C and the H₂S loading rate was 58.15 mM S day⁻¹.

CHAPTER 6



A feedforward control strategy for oxygen supply in a gas biodesulfurization process

Abstract

In this work, a feedforward control strategy is proposed for the oxygen supply to a gas biodesulfurization process for the treatment of biogas, landfill and high-pressure natural gas. Traditionally, PI or PID feedback control is used when the feed gas contains H_2S only. The oxidation-reduction potential (ORP) is largely dominated by the dissolved sulfide concentration. Therefore, the feedback controller maintains a constant sulfide concentration in the bioreactor by maintaining an ORP setpoint by controlling the oxygen supply. However, when the feed gas also contains volatile organic sulfur compounds, i.e. thiols, this process control becomes unfeasible, as absorbed thiols disturb the ORP measurement. Hence, an alternative control strategy is proposed, which controls the $\text{O}_2/\text{H}_2\text{S}$ supply ratio. The alternative feedforward control strategy was validated by a variable supply of H_2S (26.5 to 126.5 mM S day⁻¹) and in the presence of ethanethiol (0.8 to 1.16 mM S day⁻¹). We achieved sulfur selectivity above 95 mol% at an $\text{O}_2/\text{H}_2\text{S}$ supply ratio of about 0.63 mol mol⁻¹. This work shows that fluctuations in the H_2S loading rate in full-scale systems can be controlled by applying the alternative control strategy. For this strategy, the online measurement of the H_2S concentration in the feed gas is required.

This chapter has been submitted for the publication as: Kiragosyan K., Roman P., Keesman K.J., Janssen A.J.H., Klok J.B.M. A feedforward control strategy for oxygen supply in a gas biodesulfurization process.

6.1 Introduction

In general, the objective of all industrial production processes is to ensure safe and stable process performance while maximizing product yield and minimizing energy and chemical consumptions. This objective is usually achieved by the implementation and optimization of process control strategies, based on sensor technology [1]. The control of bioprocesses can be challenging due to the complex nature of biological processes, as these, in general, do not reach steady-states due to changes in the biological matrix. Hence, various monitoring and control strategies are available to measure and control process variables of interest. The most commonly used sensors in bioprocesses are temperature, pH, redox (also known as oxidation-reduction potential or ORP) and dissolved oxygen (DO). Amongst these parameters, dissolved oxygen is known to be a challenging parameter, as sometimes the optimal operation window for DO is tight. In addition, DO sensors are subjected to delayed responses and/or oxygen transfer is coupled to other physical processes such as separation of gas, liquid and solid phases. For example, in fermentation processes, it is crucial to accurately control the DO values in the process solution to avoid under and over oxidation of the desired products [2]. Similarly, to obtain high product yields of polyhydroxyalkanoate (PHA), the DO needs to be controlled at microaerophilic conditions [3]. The latter is challenging because often the concentrations are below the sensor's detection limits [4]. As an alternative, an oxygen supply strategy can be based on ORP measurements. It is known that ORP measurements can be sensitive to more dominating and reducing dissolved compounds present in the process solution, or in wastewater treatment systems [5–7].

The ORP sensor was also implemented for the biodesulfurization process by Janssen and co-workers, to control biological sulfide oxidation in a micro-aerated bioreactor [8,9]. The gas biodesulfurization is a biotechnological process, which removes H_2S from sour gas streams and subsequently converts it into predominantly elemental sulfur by haloalkaliphilic sulfur-oxidizing bacteria (SOB) [10,11]. When DO levels exceed thresholds (100 nmol L^{-1}) [12], sulfide is oxidized to sulfate, which requires caustic addition to maintain pH levels of the process solution. Hence, the end product of biological sulfide oxidation is strongly determined by the amount of oxygen (O_2) that is supplied and consumed by the SOB [8], as shown in the following equations:



To enable a high selectivity for the formation of elemental sulfur, the supply of oxygen/air must be carefully controlled. As DO levels for optimal sulfur formation rates are below the DO detection limits, current state-of-the-art full-scale systems are equipped with ORP sensors [9]. This sensor is connected to a proportional-integral-derivative (PID) feedback, closed-loop, controller to steer the oxygen/air supply to the system [13].

In full-scale installation, the ORP feedback control strategy shows, in general, a good operational stability and reliability. However, several process parameters affect the stability of the control strategy. For instance, variations in the inflow of the feed gas and concentration of H_2S in the feed gas will cause oscillations in the ORP signal, which in turn triggers instability in process and product formation. A second parameter that affects the ORP is the presence of thiols and diorgano polysulfanes in the process. Roman and co-workers found that when thiols (RSH) and di-organo polysulfanes (R_2S_x ; DOPS) are present in the gas feed, efficiency and stability of the process dropped significantly [14]. This was caused by the negative impact of thiols on the signal from the ORP probe, i.e. DOPS were formed from thiols autoxidation that affected the ORP measurements. Hence, triggering the oxygen supply to maintain the desired ORP levels [17]. A third parameter affecting the ORP values was recently found, i.e. the SOB themselves [15]. SOB were found to have a charge shuttling capacity, where they pick up sulfide under anaerobic conditions and then produce an electrical current in the presence of an anode that is acting as an electron acceptor [15]. Giving these aspects, using only ORP measurements are not sufficient to control the biodesulfurization process when also thiols are present. Hence, an alternative control strategy is required to overcome variations in the gas feed and process matrix.

In recent work, a process adjustment was suggested to optimize the process of the biological desulfurization process. An extra anaerobic bioreactor was added to the existing Thiopaq O&G process line-up, called Thiopaq O&G Ultra [16]. This reactor was placed between the absorber column and the aerobic bioreactor to suppress the biological formation of sulfate and to increase the efficiency in sulfide-to-sulfur bioconversion [16]. An extra benefit of this anaerobic reactor is the damping of large fluctuations in the H_2S feed to the system, resulting in more stable process performance and hence, improved product selectivity [17]. Nonetheless, some form of feedforward control is required to ensure high sulfur formation rates.

In this paper, we present a feedforward control strategy that manipulates the oxygen supply that is based on maintaining a constant $\text{O}_2/\text{H}_2\text{S}$ dosing ratio. This controller requires a continuous monitoring of the H_2S concentration in the sour gas. From previous studies, it followed that at an $\text{O}_2/\text{H}_2\text{S}$ dosing ratio of 0.6 mol mol⁻¹ the sulfur selectivity was between 90–100 mol% [18–20]. Hence, a setpoint value of 0.6 ± 0.05 mol mol⁻¹ was taken to compute the oxygen supply rate at various sulfide load patterns. In addition, we tested the feedforward control strategy under the addition of ethanethiol.

6.2 Materials and Methods

6.2.1 Reactor operation

The laboratory setup consisted of a falling film gas absorber connected to two bioreactors in series, i.e., an anaerobic reactor for process stabilization followed by an aerobic reactor for sulfide oxidation (Fig. 1). The composition of the feed-gas was controlled using mass flow controllers (type EL-FLOW, model F-201DV-AGD-33-K/E, Bronkhorst, the Netherlands). For the supply of hydrogen sulfide, a 0–17 mL min⁻¹ mass flow controller was used, for nitrogen 0–350 mL min⁻¹, for oxygen 0–30 mL min⁻¹, carbon dioxide 0–40 mL min⁻¹ and for ethanethiol 0–60 mL min⁻¹. Hydrogen sulfide and nitrogen gas were continuously supplied, whereas the supply rate of oxygen and carbon dioxide was pulse-wise controlled with a multiparameter transmitter (Liquiline CM442-1102/0, Endress+Hauser, Germany). When using the conventional feedback control strategy, oxygen supply was controlled based on the signal from an ORP sensor, equipped with an internal Ag/AgCl reference electrode (Orbisint 12D-7PA41; Endress+Hauser, Germany). The carbon dioxide supply was controlled by the signals sent from a pH sensor (Orbisint 11D-7AA41; Endress+Hauser, Germany). A fiber-optic oxygen probe PSt 3 was used to monitor the oxygen concentration in the headspace of the aerobic bioreactor (PreSens Precision Sensing GmbH, Regensburg, Germany). More details on the used equipment can be found in [17].

During process operation the system was sampled in both gas and liquid phases. Liquid samples were taken from two sampling points located at the bottom section of the absorber and in the aerobic bioreactor. Gas-phase samples were taken from three locations: gas inlet, bioreactor headspace, and absorber outlet at regular time intervals. Sampling was done in triplicate for liquid samples and single measurements for gaseous samples.

Table 1 Overview of the process conditions of the experimental setup.

Parameter	Run 1 Feedback control	Run 2 Feedforward control	Run 3 Feedforward control
Active liquid volume, L	2.5	2.5	2.5
pH setpoint	8.50 ± 0.05	8.50 ± 0.05	8.50 ± 0.05
Ethanethiol, mM S day ⁻¹	0	0	0.8 – 1.16
Salinity, Na ⁺ M	1	1	1
Temperature, °C	35	35	35
ORP setpoint, mV	-390	Not applicable	Not applicable
O ₂ /H ₂ S supply ratio, mol mol ⁻¹	Not applicable	0.63	0.63

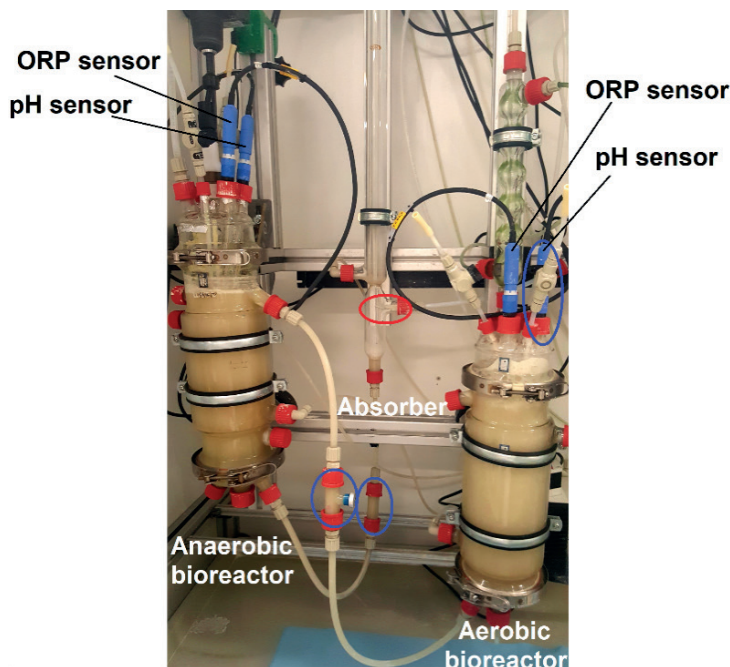


Fig. 1. Laboratory scale fed-batch experimental setup used for the experiments. Blue circles indicate liquid sampling points, and a red circle indicates gas inlet. Block diagram of the setup can be found [17].

We conducted three sets of experiments (Table 1). First, we operated the process with ORP as a control variable and oxygen supply as a manipulated variable at different H_2S supply patterns: constant, pulse wave, triangle wave, and a randomly varying signal (Fig. 2). To tune the PID controller of our fed-batch lab-scale gas biodesulfurization setup, we used the Ziegler-Nichols' closed-loop tuning method [21,22]. In the constant supply mode, H_2S flow rate was constant at 2.5 NmL min^{-1} (N stands for normal conditions). The pulse wave supply alternates between 2.5 and 5 NmL min^{-1} every 50 h , this supply mode mimics process start-up and emergency shut off the unit. The triangle wave supply mode comprises a stepwise increase of the H_2S supply rate from 1.5 to 9.5 NmL min^{-1} with 20 min for each step. This supply mode mimics slow process start-up. In the last tested mode H_2S supply rate randomly varied between 1.5 to 9.5 NmL min^{-1} with 5 min for each step. Subsequently, we tested the alternative feedforward strategy for oxygen supply, where the same H_2S supply patterns were evaluated. In addition, we validated the feedforward control strategy after the addition of ethanethiol (ET) (Table 1). For this last experiment, we chose the randomly varying H_2S supply pattern, as this is a very challenging feed pattern for stable process operation. Randomly varying supply pattern is unlikely to occur in the natural gas sites. However, it can occur in the anaerobic water treatment, where produced biogas is collected in a gas buffer that is irregularly emptied.

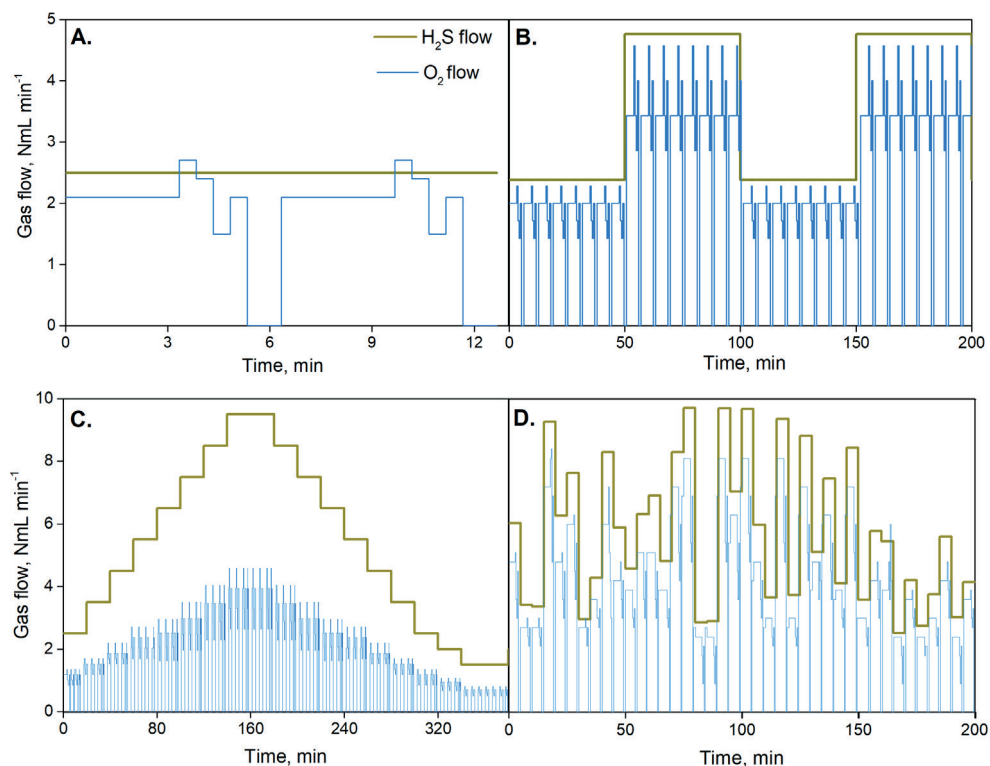


Fig. 2. Oxygen supply as derived from the basic feedforward pattern (A) with respect to the supplied H₂S pattern: (A) constant, (B) pulse wave, (C) triangle wave, and (D) randomly varying signal. The supply of H₂S and O₂ is presented in NmL min⁻¹.

In the ORP-based feedback control, the O₂/H₂S ratio was constantly monitored. Two O₂/H₂S ratios can be determined: supplied and actual ratios. The supplied ratio is equal to the amount of oxygen passed through the mass flow controller per supplied sulfide, whereas actual or consumed O₂/H₂S ratio is calculated based on the formed products and how much oxygen is required for their formation. In experiments with the O₂/H₂S-based feedforward control strategy (Run 2 and 3), ORP was not controlled. However, ORP measurements were used to enable a comparison between the various runs 1-3.

In what follows, ORP-based feedback control will be referred to as feedback control and O₂/H₂S-ratio based feedforward control as feedforward control.

6.2.2 ORP-based feedback control

A proportional-integral-derivative (PID) feedback controller was implemented. This controller automatically steers the oxygen supply (output) in the biodesulfurization process on the basis of continuous ORP measurements (input). Selection and tuning of respectively the P, I, and D actions is a challenge in bioprocess control applications as it

does not account for changes in microbial activity such as natural adaptation [23–26], resulting from complex and often unknown underlying biochemical processes. However, it is possible to re-tune PID controller once the steady state is reached. Nonetheless, we frequently use PID controllers in bioprocesses, especially in the lab-scale installations. To eliminate the sensitivity of the D-action with respect to high frequent process noise, different filters can be applied to damp the effect of noise. The built-in PID controller in the Endress and Hauser multichannel transmitter also contains an anti-windup scheme for limiting the integrator [27].

6.2.3 Alternative feedforward control

From previous studies, it is known that the amount of oxygen supplied should be proportional to the amount of sulfide gas supplied, and when SOB biomass activity is high an ORP value can be maintained that is close to the setpoint value [9,28]. Therefore, we decided to base the alternative oxygen supply on maintaining a constant average O_2/H_2S ratio of $0.63 \text{ mol mol}^{-1}$ (Fig. 2A). Moreover, from previous studies and chemical reactions on sulfide oxidation (Eq. 1 – 2) we know that sulfur selectivity is higher at lower O_2/H_2S ratio and at O_2/H_2S ratio of about $0.60 \pm 0.05 \text{ mol mol}^{-1}$ sulfur selectivity is between 90 to 100 mol% [18,29] operating at natronophilic conditions, formation of thiosulfate ($S_2O_3^{2-}$). Giving this, we calculated the oxygen supply in the feedforward strategy from an O_2/H_2S ratio at around $0.63 \text{ mol mol}^{-1}$, which is a little bit higher than the theoretical ratio of 0.5 mol mol^{-1} (Eq. 1), but such that high sulfur selectivity can be achieved.

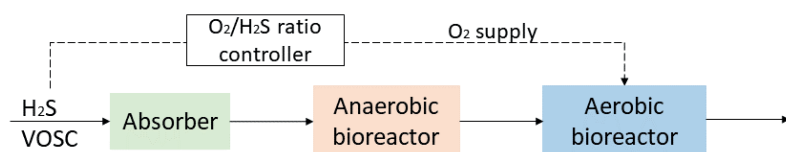


Fig. 3. Block scheme of the feedforward control strategy with VOSC the volatile organic sulfur compounds.

To enable feedforward control, we wrote an algorithm in FlowPlot software V3.35 to calculate the oxygen supply under varying H_2S supply rates (Bronkhorst, the Netherlands), where oxygen supply was calculated based on the supply of H_2S . For example, 2.5 NmL min^{-1} of H_2S will result in $\sim 1.6 \text{ NmL min}^{-1}$ of oxygen. However, it can be noticed in Fig. 2 that the implemented oxygen supply is not constant but comprised of a repetitive pattern. This pattern was created due to the system's slow response and traveling time of the supplied sulfide from the absorber to the aerobic bioreactor (retention time $\sim 15 \text{ min}$). Hence this occurred delay due to the liquid retention time allows to maintain

stable oxygen concentration and continuous sulfide inflow. At the beginning of the pattern, we slightly overdosed the system with oxygen to be able to distribute oxygen in the bioreactor before sulfide enters, and afterward decreased it. The pattern consists of six steps, which on average gives an O_2/H_2S supply ratio of $0.63 \text{ mol mol}^{-1}$. The pattern was achieved by trial and error adjustments of the oxygen supply. Whenever the oxygen supply changed, we calculated the resulting O_2/H_2S supply ratio to see if it fits into the desired ratio and if ORP oscillating within a range of $\pm 10 \text{ mV}$. When both conditions were fulfilled, we let the calculated oxygen supply pattern run for several cycles for about four hours to see if the pattern suffices for longer-term experiments. After some modifications we just fixed the oxygen supply pattern. The average O_2/H_2S ratio of $0.63 \text{ mol mol}^{-1}$ and corresponding heuristic control pattern (Fig. 2A) were maintained over the process operation at various H_2S supply patterns.

6.2.4 Medium composition

The haloalkaline medium was buffered with $0.045 \text{ M Na}_2\text{CO}_3$ and 0.91 M NaHCO_3 . The medium contained $1.0 \text{ g K}_2\text{HPO}_4$, $0.20 \text{ g MgCl}_2 \times 6\text{H}_2\text{O}$, and 0.60 g urea , each per 1 L of ultrapure water (Millipore, ISO 3696) and trace elements solution as described in [30]. The pH of the medium was 8.5 ± 0.05 at 35°C .

6.2.5 Inoculum

Biomass mix was prepared by mixing four different biomasses, originating from three biodesulfurization installations: Oilfield - 1, Oilfield - 2, and Pilot plant [17]. Names of biomasses are denoted as the industry that a biodesulfurization installation treats gas from. The Oilfield - 1 full-scale installation treats associated gas containing low concentrations of thiols $50\text{--}200 \text{ ppm}$ and $1\text{--}5 \%$ of H_2S , whereas Oilfield - 2 treats acid gas with $10\text{--}20 \%$ of H_2S and thiols [31,32]. Biomasses were mixed in a proportion $2:1:2$, consequently the cells were concentrated by centrifugation (15 min at $16,000g$), and the cell pellet was used to inoculate the 5 L bioreactor.

The prepared biomass mix was used to inoculate the lab-scale biodesulfurization system for the first experimental run (Run 1, Table 1). Afterwards, developed biomass was used as an inoculum for the second and third experiment (Run 2 and Run 3, Table 1).

6.2.6 Analytical techniques

The biomass quantification was based on the amount of organically bound nitrogen that was oxidized to nitrate by digestion with peroxodisulfate (LCK238 and LCK338, Hach Lange, the Netherlands). Prior to the analysis, we washed the cell pellet twice at $20,238 \text{ g}$ for 5 min with the nitrogen-free medium. Washing was performed to exclude the quantification of the nitrogen present in the medium in the form of urea.

We determined the concentrations of sulfate and thiosulfate by ion chromatography (Metrohm Compact IC 761, Switzerland) with an anion column (Metrohm Metrosep A Supp 5, 150/4.0 mm, Switzerland) equipped with a pre-column (Metrohm Metrosep A Supp 4/5 Guard, Switzerland). Before the analyses, all solids were removed by filtration over a 0.45 μm membrane syringe filter (HPF Millex, Merck, the Netherlands). Subsequently, the filtered sample was mixed with 0.2 M zinc acetate in a 1:1 ratio to form ZnS and to prevent chemical sulfide oxidation.

Produced biological sulfur concentration was calculated from the sulfur mass balance based on the supplied sulfide and the actual sulfate and thiosulfate concentrations, and is given by:

$$[\text{S}^0]_t = \Delta t(\text{H}_2\text{S supplied} / V_{\text{liquid}}) - [\text{SO}_4^{2-}]_t - 2*[\text{S}_2\text{O}_3^{2-}]_t - (\text{S}_x^{2-})_t$$

where the initial sulfur concentration is assumed to be zero. This is a general method to establish the sulfur mass balance to calculate sulfur selectivities [16,20,33,34]. Concentrations of dissolved sulfide, polysulfides, and possible volatile organosulfur compounds were not taken into account, as their combined contribution to the total concentration of sulfur species is negligible [34]. We also assume 'pseudo' steady-state conditions of the system, which was confirmed by the consecutive liquid and gas samples [14,29,32].

Sulfide was measured as a total sulfide using a methylene blue method with a cuvette test (LCK653, Hach Lange, USA). Sulfide quantification was carried out immediately after sampling, and samples were diluted in oxygen-free Milli-Q water (sparged with N_2 stream for 30 min) to exclude chemical oxidation.

In addition to sulfur-containing anions, cations Na^+ and K^+ concentration were also measured with ion chromatography as described earlier for the anions (Roman et al. 2015). However, the mobile phase for a Metrohm Metrosep C4-150/4.0 mm column was 0.9 mL 3 mM HNO_3 min^{-1} .

In order to close the electron balance, carbonate and bicarbonate ions concentration were calculated using the Henderson-Hasselbalch equation [35]. Hence, liquid samples were analyzed on the total inorganic carbon using high-temperature catalytic oxidation at 680 $^\circ\text{C}$ with TOC-VCPH/CPN analyzer (Shimadzu, The Netherlands).

In total, two types of liquid samples were prepared, filtrated, and precipitated with zinc acetate for anions measurements and non-filtrate for biomass quantification and TOC analysis. All liquid samples were stored at 4 $^\circ\text{C}$ before being analyzed (about three days).

The gas-phase (H_2S , N_2 , CO_2 , and O_2) was analyzed with a gas chromatograph (Varian CP4900 Micro GC, Agilent, the Netherlands). The gaseous ethanethiol (ET) and diorganopolysulfanes concentrations were measured with a gas chromatograph (Thermo scientificTM Trace GC Ultra with Trace GC Ultra valve oven, Interscience, Breda, the Netherlands) equipped with a Restek column (RT[®]-U-Bond, 30 m x 0.53

mm di x 20 μ m df). To enable meticulous flushing total sample volume was 3 mL. All tubing was of the type Sulfinert®, to prevent absorption and reaction of the sulfur compounds.

The liquid ET and diorganopolysulfanes concentrations were measured with the same gas chromatography as gaseous samples, but injection was done to the liquid port. Samples preparation followed with liquid-liquid extraction, where the sample was mixed with n-hexane (Sigma-Aldrich, the Netherlands) and international standard (IST) stock solution in the ratio of 10:9:1 (sample: n-hexane: IST stock solution). Beforehand, the IST stock solution was prepared with 187.5 μ L of thioanisole (TAS) (Sigma-Aldrich, the Netherlands) into 49.8 mL of hexane. TAS concentration in the stock solution was 1023 ppm S. To allow complete desorption of organosulfur compounds from the sulfur particles surface, the preparation with the sample, IST in n-hexane was extracted on a rotary shaker (600 rpm) during 30 min afterward, upper liquid phase was sampled with a glass syringe, and 0.8 μ L were injected using a sandwich method. A detailed description of the method and other used analytical techniques are described in [17].

6.3. Results and Discussion

6.3.1. Importance of oxygen concentration

In the biological oxidation process of sulfide and in the absence of thiols, a feedback control allowed us to accurately manipulate the oxygen supply in order to maintain the desired ORP setpoint at -395 ± 5 mV at randomly varying H_2S supply (Fig. 4A). Except, when applying perturbations in the sulfide loading, an increase in oxygen concentration was triggered. In the headspace of the aerobic bioreactor, oxygen increased from 1.7 % to 12 %, while maintaining a stable ORP setpoint (Fig. 4A). At this latter high oxygen concentrations, product formation shifted towards sulfate selectivity, which resulted in a decrease of sulfur selectivity. From these results, it follows that maintaining the ORP setpoint with feedback control cannot optimize sulfur selectivity when H_2S concentration in the feed gas fluctuates strongly (Fig. 4A).

Klok and co-workers formulated a model, which describes the relationship between dissolved oxygen concentration, dissolved sulfide, and ORP-value under halo-alkaline conditions (Appendix A, Fig. A1), which in turn can predict biological end-product formation (Appendix A, Fig. A2) [12]. From these predictions it follows that sulfur selectivity is more sensitive to DO concentration when ORP sensor is sensitive to reduced sulfur compounds, i.e. sulfide. Moreover, ORP-based control cannot guarantee a high sulfur selectivity, as it cannot control oxygen concentration at fluctuating gas feeds. Given these outcomes, the use of feedback control is insufficient to secure high sulfur selectivity at fluctuating sulfide gas feeds, as shown in Fig. 4A.

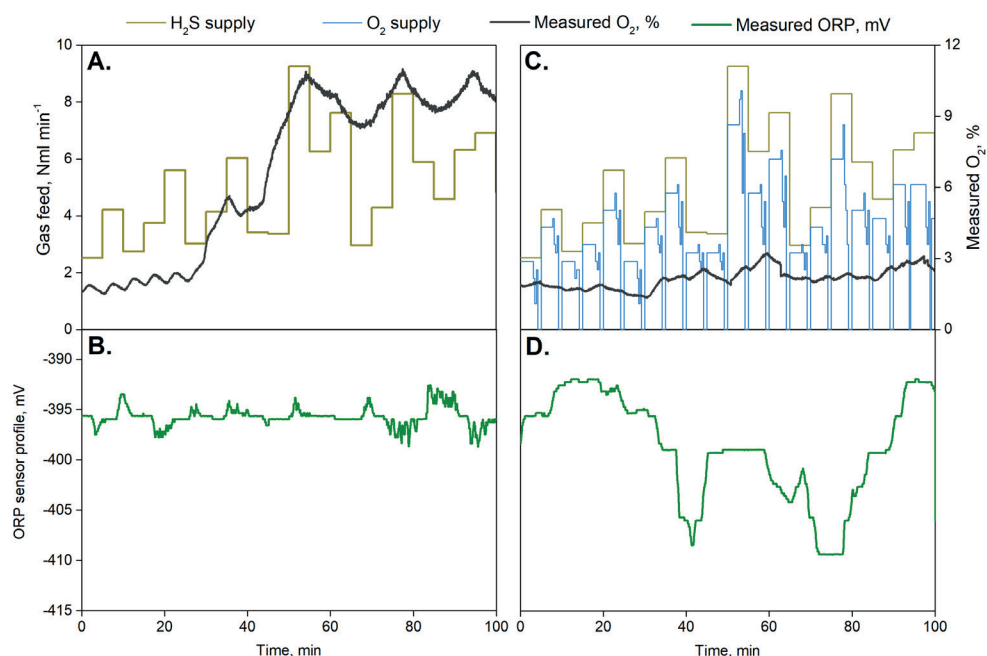


Fig. 4. A fragment of the measured oxygen concentration in the headspace of aerobic bioreactor and corresponding readings from oxidation-reduction potential (ORP) sensor in the experiments with (A-B) ORP-based feedback control and (C-D) O₂/H₂S ratio-based feedforward control during a randomly varying supply of sulfide.

In comparison with feedback control, the proposed feedforward controller showed stable oxygen concentrations (2 ± 0.5 %) in the headspace of the aerobic bioreactor (Fig. 4C). Moreover, measured ORP values show more substantial variations, with an average of -410 ± 10 mV after a week of process operation, than with the use of feedback control. Moreover, it can be noticed that ORP values varied between -390 mV and -410 mV. Previous studies showed a logarithmic relationship between ORP values and sulfide concentration [9]. This relationship results in insensitivity of ORP sensor at high sulfide concentrations, or at low ORP values. Therefore, process operation at low ORP values, i.e. below -400 mV, becomes challenging, i.e., as dissolved sulfide accumulates in the process solution [18,36]. As a result, SOB respiration rates decrease and drop below supply rates. Moreover, due to gas-liquid equilibrium, substantial concentration of sulfide will also be present in the gas-phase, which subsequently will lead to increased levels of sulfide in the treated gas.

However, during experiments with feedforward control, no dissolved sulfide was detected in the process solution, even at an ORP value of -420 mV. Hence, use of the feedforward control allows to operate gas biodesulfurization process at low ORP values. This finding indicates that ORP values are more sensitive to sulfide levels,

whereas biological product formation is susceptible to oxygen concentration. Therefore, in the gas biodesulfurization process with large fluctuations in H_2S feed, ORP might be still used as a controlled variable in, for instance a model-based (predictive) control strategy.

6.3.2. Process performance

A comparison in terms of process performance was also made between the conventional ORP-based feedback control versus the newly proposed $\text{O}_2/\text{H}_2\text{S}$ ratio feedforward control. In both cases, similar H_2S dosing patterns were applied. It can be seen that with the conventional controller, the sulfur selectivity showed more variations (Fig 5A) at fluctuating H_2S supply than was found for the feedforward controller (Fig 5B). At constant H_2S supply, sulfur selectivity was similar between control strategies (Table 2; see also Appendix B, Fig. B1). Initially, sulfur selectivity was about 90 mol% and then decreased to about 60 mol% (Fig. 5A). The observed decrease in sulfur selectivity corresponds with the increase of $\text{O}_2/\text{H}_2\text{S}$ supply ratio, which ranged from 0.8 to 1.4 mol mol⁻¹. Increased $\text{O}_2/\text{H}_2\text{S}$ supply ratio resulted in the higher selectivity for sulfate as more oxygen was available. Subsequently, sulfate selectivity increased with increasing SOB biomass activity. Thus, chemical oxidation of sulfide to thiosulfate was absent or low, resulting in 0 mol% thiosulfate selectivity. However, it is also possible that thiosulfate was formed and was further oxidized to sulfate. Furthermore, the reason why selectivity for thiosulfate was still 0 mol% is that rates for thiosulfate formation and its oxidation were similar [19,32]. Same low thiosulfate selectivity 0 mol% was observed by Van den Bosch and co-workers when fed-batch lab-scale biodesulfurization setup was operated at high oxygen concentrations and a 2 mol mol⁻¹ $\text{O}_2/\text{H}_2\text{S}$ ratio resulted in 100 mol% of sulfate selectivity [29].

Table 2. Average product selectivity in the experiments with ORP-based feedback and $\text{O}_2/\text{H}_2\text{S}$ ratio-based feedforward control at various sulfide supply patterns and ethanethiol[†] (ET) addition (0.8 to 1.16 mM S day⁻¹).

H_2S supply pattern	Feedback control			Feedforward control			Feedforward control + ET [†]		
	SO_4^{2-}	$\text{S}_2\text{O}_3^{2-}$	S_8	SO_4^{2-}	$\text{S}_2\text{O}_3^{2-}$	S_8	SO_4^{2-}	$\text{S}_2\text{O}_3^{2-}$	S_8
Constant	*7 ± 1	2 ± 0	92 ± 1	8 ± 0	0 ± 2	92 ± 2	Not tested		
Pulse wave	34 ± 1	0 ± 0	66 ± 1	2 ± 0	0 ± 3	98 ± 3			
Triangle wave	28 ± 4	0 ± 1	72 ± 4	4 ± 0	0 ± 7	96 ± 7			
Randomly varying signal	44 ± 1	0 ± 0	56 ± 1	3 ± 0	0 ± 1	97 ± 1	4 ± 2	0 ± 0	96 ± 2

* Process operation data of the ORP-based control with constant H_2S flow is presented in Appendix B, Fig. B1.

After the experiment using the ORP-based control strategy, we initiated experiments with the feedforward strategy. From the results in Fig. 5B and C, it can be noticed that the product formation was stable. On average the selectivity for sulfur selectivity is about 97 ± 2 mol%. During startup of the experiments with feedforward control we started with constant H_2S feed and altering the oxygen pattern (Fig. 2A).

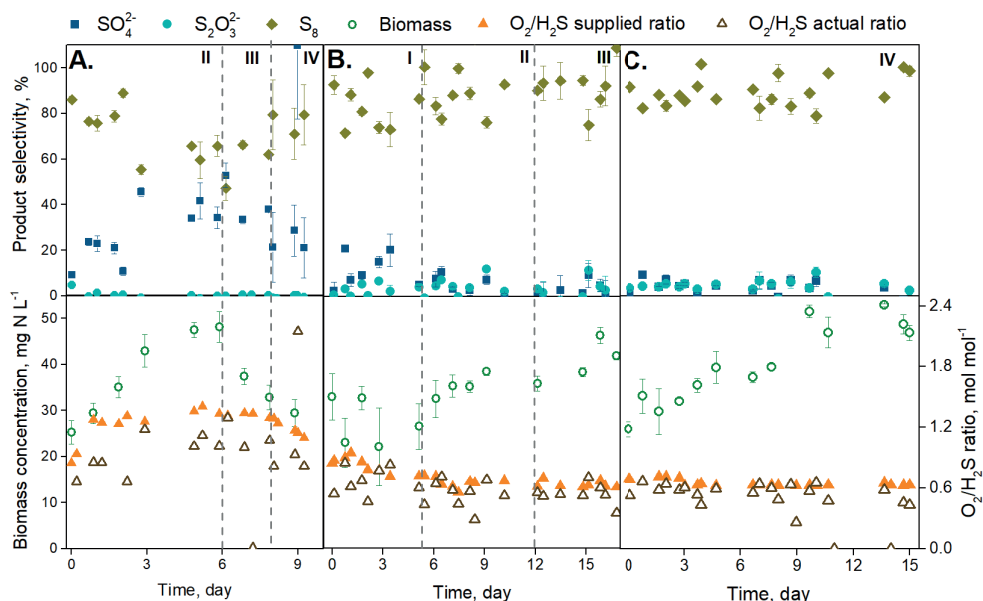


Fig. 5. Process performance using (A) ORP-based feedback control and (B-C) O_2/H_2S ratio-based feedforward control for oxygen supply in the double bioreactor gas biodesulfurization line-up. Presented data points are averages of the analyzed triplicates. The system was operated at pH = 8.5, $T = 35^\circ\text{C}$. Vertical dashed lines indicate a change in H_2S supply pattern: I – constant (H_2S loading $58.2\text{ mM S day}^{-1}$), II – pulse wave ($116.3\text{ mM S day}^{-1}$), III – triangle wave ($126.5\text{ mM S day}^{-1}$), IV – randomly varying signal ($26.5\text{ mM S day}^{-1}$). S_8 is elemental sulfur that is shaped into a crystal form from S^0 .

We started from 0.84 mol mol^{-1} O_2/H_2S ratio and slowly decreased it to 0.70 mol mol^{-1} by reducing the oxygen supply. By the end of day five, we managed to come up with an oxygen supply pattern that fits the 0.63 mol mol^{-1} ratio. At this ratio with corresponding H_2S supply pattern (Fig. 2A) the change from constant to any of the other three patterns also resulted in lower sulfur selectivity $92 \pm 2\text{ mol}\%$ and higher sulfate selectivity $8 \pm 0\text{ mol}\%$ (Table 2). Sulfur selectivity during the constant, triangle wave, and randomly varying H_2S supply were all around $96\text{ mol}\%$ with about $4\text{ mol}\%$ of sulfate. Based on these results we concluded that the feedforward control strategy in the gas biodesulfurization process results in a more stable process operation with higher selectivity for sulfur formation as compared with the ORP-based feedback control strategy (Table 2).

To test the robustness of the novel feedforward control strategy, we continued experiments at randomly varying H_2S feed pattern and with the addition of ethanethiol (ET) to the gas biodesulfurization setup (Fig. 6). For randomly varying oxygen supply we used an O_2/H_2S ratio of 0.63 mol mol^{-1} . After 10 days of stable process operation, the sulfur selectivity in the presence of ET was, on average, $96 \pm 2\text{ mol}\%$, with $4 \pm 2\text{ mol}\%$ of sulfate (Table 2). Moreover, the process operation was steady, with a daily

sulfur selectivity always above 90 mol%. Whereas, in our previous study the process operation was less stable, as the oxygen supply was affected by drifting of the ORP sensor due to the presence of diorgano polysulfanes [14,17,33]. It is important to notice that biomass concentration in the presence and absence of ethanethiol (Fig. 5 and 6) is more or less similar. This shows that possibly SOB biomass adapted to ethanethiol. Hence, the biomass activity did not decrease, because supplied ethanethiol concentration (with loading rate of 1.16 mM day^{-1}) is less than IC_{50} reported before [17,37].

We found ethanethiol and its autoxidative products diethyl disulfide and diethyl trisulfide in the headspace of both bioreactors and gas outlet (Appendix C). However, no organic sulfur compounds were determined in the liquid, possibly due to the high volatility and low concentration of ethanethiol. Nonetheless, the presence of ethanethiol and di-organo polysulfanes did not affect process performance when the feedforward control strategy was used. This observation indicates the robustness of the feedforward control in the presence of thiols or other volatile organic compounds that can affect the ORP of the medium. However, the $\text{O}_2/\text{H}_2\text{S}$ ratio-based control strategy requires measurements of the concentration of sulfide feed to the gas biodesulfurization installation. Hence, sensors for H_2S measurement are required to be installed in the feed gas line, so that oxygen supply can be calculated based on the incoming sulfide. Existing sensors for sulfide measurements in liquid, such as amperometric microsensors, might be applied. However, presence of biosulfur and other inorganic and organic sulfur compounds might interfere.

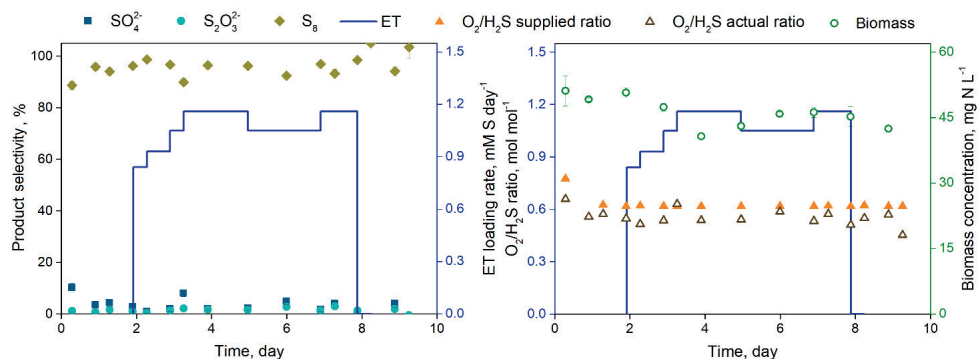


Fig. 6. Performance of the laboratory bioreactor with feedforward control for oxygen supply in the presence of ethanethiol (ET). Presented data points are averages of the analyzed triplicates. The system was operated at $\text{pH} = 8.5$, $T = 35^\circ\text{C}$ and randomly varying signal pattern for H_2S supply. S_8 is elemental sulfur that is shaped into a crystal form from S^0 .

6.4 Conclusions

Our findings show that, in principle, the O_2/H_2S ratio-based feedforward control for oxygen supply could be a promising alternative to the traditionally used ORP-based feedback control, especially when sulfide loadings strongly vary or when other reducing compounds such as thiols and diorgano polysulfanes are present in the feed gas. With the application of a feedforward control strategy, the overall selectivity for sulfur formation is enhanced, mainly because it is less prone to variations during upset process conditions, i.e. fluctuating sulfide loading rates. In addition, it is important to maintain the oxygen concentration in the aerobic bioreactor at low levels and at low ORP to achieve high sulfur selectivity > 90 mol%. By achieving high sulfur selectivities, the selectivities for sulfate and thiosulfate formation remain low. This results in a reduction of the caustic consumption and in the decreased formation of waste streams. Furthermore, O_2/H_2S ratio-based control shows good results in the presence of thiols. However, more research is required to identify limits of the feedforward control at higher loading rates of various thiols. For the implementation in full-scale installations, robust and reliable (hardware/software) sensors are required for H_2S detection in the gas or liquid streams, with a connection to an oxygen/air mass flow controller to regulate oxygen supply based on the incoming H_2S flow/concentration.

Acknowledgments

This work has been performed within the cooperation framework of Wetsus, European Centre of Excellence for Sustainable Water Technology (wetsus.nl), Wageningen University and Research (wur.nl) and Paqell B.V. (paqell.com). Wetsus is co-funded by the Netherlands' Ministry of Economic Affairs and Ministry of Infrastructure and Environment, the European Union's Regional Development Fund, the Province of Fryslan and the Northern Netherlands Provinces. Wetsus is also a coordinator of the WaterSEED project that received funding from European Union's Horizon 2020 research and innovation program under Marie Skłodowska-Curie grant agreement No. 665874.

References

- [1] C.F. Mandenius, N.J. Titchener-Hooker, *Measurement, Monitoring, Modelling and Control of Bioprocesses*, Springer Berlin Heidelberg, Berlin, Heidelberg, 2013. doi:10.1007/978-3-642-36838-7.
- [2] R. Oliveira, R. Simutis, S. Feyo De Azevedo, Design of a stable adaptive controller for driving aerobic fermentation processes near maximum oxygen transfer capacity, *J. Process Control*. 14 (2004) 617–626. doi:10.1016/j.jprocont.2004.01.003.
- [3] S. Pratt, A. Werker, F. Morgan-Sagastume, P. Lant, Microaerophilic conditions support elevated mixed culture polyhydroxyalkanoate (PHA) yields, but result in decreased PHA production rates, *Water Sci. Technol.* 65 (2012) 243–246. doi:10.2166/wst.2012.086.
- [4] C.-G. Liu, J.-C. Qin, Y.-H. Lin, Fermentation and Redox Potential, in: *Ferment. Process.*, InTech, 2017: p. 13. doi:10.5772/64640.
- [5] K.C. Chen, C.Y. Chen, J.W. Peng, J.Y. Houn, Real-time control of an immobilized-cell reactor for wastewater treatment using ORP, *Water Res.* 36 (2002) 230–238. doi:10.1016/S0043-1354(01)00201-9.
- [6] B. Li, P. Bishop, Oxidation-reduction potential (ORP) regulation of nutrient removal in activated sludge wastewater treatment plants, *Water Sci. Technol.* 46 (2002) 35–38.
- [7] L. Kjaergaard, The redox potential: Its use and control in biotechnology, in: *Adv. Biochem. Eng.* Vol. 7, Springer-Verlag, Berlin/Heidelberg, 2006: pp. 131–150. doi:10.1007/BFb0048444.
- [8] A.J.H. Janssen, R. Sleyster, C. Van der Kaa, A. Jochemsen, J. Bontsema, G. Lettinga, Biological sulphide oxidation in a fed-batch reactor, *Biotechnol. Bioeng.* 47 (1995) 327–333. doi:10.1002/bit.260470307.
- [9] A.J.H. Janssen, S. Meijer, J. Bontsema, G. Lettinga, Application of the Redox Potential for Controlling a Sulfideoxidizing Bioreactor, *Biotechnol. Bioeng.* 60 (1998) 147–155. doi:10.1002/(SICI)1097-0290(19981020)60:2<147::AID-BIT2>3.0.CO;2-N.
- [10] A.J.H. Janssen, P.N.L. Lens, A.J.M. Stams, C.M. Plugge, D.Y. Sorokin, G. Muyzer, H. Dijkman, E. Van Zessen, P. Luimes, C.J.N.N. Buisman, Application of bacteria involved in the biological sulfur cycle for paper mill effluent purification, *Sci. Total Environ.* 407 (2009) 1333–1343. doi:10.1016/j.scitotenv.2008.09.054.
- [11] D.Y. Sorokin, A.J.H. Janssen, G. Muyzer, Biodegradation Potential of Halo(alkali)philic Prokaryotes, *Crit. Rev. Environ. Sci. Technol.* 42 (2011) 811–856. doi:10.1080/10643389.2010.534037.
- [12] J.B.M. Klok, M. de Graaff, P.L.F. van den Bosch, N.C. Boelee, K.J. Keesman, A.J.H. Janssen, A physiologically based kinetic model for bacterial sulfide oxidation, *Water Res.* 47 (2013) 483–492. doi:10.1016/j.watres.2012.09.021.
- [13] A.J.H. Janssen, B.J. Arena, S. Kijlstra, New developments of the Thiopaq process for the removal of H₂S from gaseous streams, (2000) 11.

- [14] P. Roman, J.B.M. Klok, J.A.B. Sousa, E. Broman, M. Dopson, E. Van Zessen, M.F.M. Bijmans, D.Y. Sorokin, A.J.H. Janssen, Selection and Application of Sulfide Oxidizing Microorganisms Able to Withstand Thiols in Gas Biodesulfurization Systems, *Environ. Sci. Technol.* (2016) acs.est.6b04222. doi:10.1021/acs.est.6b04222.
- [15] A. Ter Heijne, R. De Rink, D. Liu, J.B.M. Klok, C.J.N. Buisman, Bacteria as an Electron Shuttle for Sulfide Oxidation, *Environ. Sci. Technol. Lett.* 5 (2018) 495–499. doi:10.1021/acs.estlett.8b00319.
- [16] R. De Rink, J.B.M. Klok, D.Y. Sorokin, G.J. Van Heeringen, A. Ter Heijne, R. Zeijlmaker, Y.M. Mos, V. De Wilde, K.J. Keesman, C.J.N. Buisman, Increasing the selectivity for sulfur formation in biological gas desulfurization, *Environ. Sci. Technol.* 53 (2019) 4519–4527. doi:10.1021/acs.est.8b06749.
- [17] K. Kiragosyan, M. Picard, D.Y. Sorokin, J. Dijkstra, J.B.M. Klok, P. Roman, A.J.H. Janssen, Effect of dimethyl disulfide on the sulfur formation and microbial community composition during the biological H₂S removal from sour gas streams, *J. Hazard. Mater.* 386 (2020). doi:10.1016/j.jhazmat.2019.121916.
- [18] P. Roman, M.F.M. Bijmans, A.J.H. Janssen, Influence of methanethiol on biological sulphide oxidation in gas treatment system, *Environ. Technol.* 3330 (2016) 1–11. doi:10.1080/09593330.2015.1128001.
- [19] P.L.F. Van Den Bosch, O.C. Van Beusekom, C.J.N. Buisman, A.J.H. Janssen, Sulfide oxidation at halo-alkaline conditions in a fed-batch bioreactor, *Biotechnol. Bioeng.* 97 (2007) 1053–1063. doi:10.1002/bit.21326.
- [20] J.B.M. Klok, P.L.F. Van Den Bosch, C.J.N. Buisman, A.J.M. Stams, K.J. Keesman, A.J.H. Janssen, Pathways of sulfide oxidation by haloalkaliphilic bacteria in limited-oxygen gas lift bioreactors, *Environ. Sci. Technol.* 46 (2012) 7581–7586. doi:10.1021/es301480z.
- [21] J.G. Ziegler, N.B. Nichols, Optimum settings for automatic controllers, *ASME.* 64 (1942) 759–768.
- [22] F. Haugen, Ziegler-Nichols' Closed-Loop Method, (2010) 1–7. http://techteach.no/publications/articles/zn_closed_loop_method/zn_closed_loop_method.pdf.
- [23] J. Cassidy, H.J. Lubberding, G. Esposito, K.J. Keesman, P.N.L. Lens, Automated biological sulphate reduction: A review on mathematical models, monitoring and bioprocess control, *FEMS Microbiol. Rev.* 39 (2015) 823–853. doi:10.1093/femsre/fuv033.
- [24] I.J. Dunn, E. Heinzle, J. Ingham, P.J.E., Automatic Bioprocess Control Fundamentals, in: *Biol. React. Eng.*, Wiley-VCH Verlag GmbH & Co. KGaA, Weinheim, FRG, 2005: pp. 161–179. doi:10.1002/3527603050.ch7.
- [25] J.A. Chandra, R. S. Samuel, Modeling, Simulation and Control of Bioreactors Process Parameters - Remote Experimentation Approach, *Int. J. Comput. Appl.* 1 (2010) 103–110. doi:10.5120/216-365.
- [26] L. Mailleret, O. Bernard, J.P. Steyer, Nonlinear adaptive control for bioreactors with unknown kinetics, *Automatica.* 40 (2004) 1379–1385. doi:10.1016/j.automatica.2004.01.030.

- [27] Endress+Hauser, Operating Instructions Liquiline CM442 / CM444 / CM448 Universal four-wire multichannel controller, 2019.
- [28] P. Roman, M.F.M. Bijmans, A.J.H. Janssen, Quantification of individual polysulfides in lab-scale and full-scale desulfurisation bioreactors, *Environ. Chem.* 11 (2014) 702–708. doi:10.1071/EN14128.
- [29] P.L.F. Van Den Bosch, D.Y. Sorokin, C.J.N. Buisman, A.J.H. Janssen, The effect of pH on thiosulfate formation in a biotechnological process for the removal of hydrogen sulfide from gas streams, *Environ. Sci. Technol.* 42 (2008) 2637–2642. doi:10.1021/es7024438.
- [30] N. Pfennig, K.D. Lippert, Über das Vitamin B₁₂-Bedürfnis phototropher Schwefelbakterien, *Arch. Mikrobiol.* 55 (1966) 245–256. doi:10.1007/BF00410246.
- [31] K. Kiragosyan, P. van Veelen, S. Gupta, A. Tomaszewska-Porada, P. Roman, P.H.A. Timmers, Development of quantitative PCR for the detection of *Alkalilimnicola ehrlichii*, *Thioalkalivibrio sulfidiphilus* and *Thioalkalibacter halophilus* in gas biodesulfurization processes, *AMB Express.* 9 (2019) 99. doi:10.1186/s13568-019-0826-1.
- [32] K. Kiragosyan, J.B.M. Klok, K.J. Keesman, P. Roman, A.J.H. Janssen, Development and validation of a physiologically based kinetic model for starting up and operation of the biological gas desulfurization process under haloalkaline conditions, *Water Res.* X. 4 (2019) 100035. doi:10.1016/j.wroa.2019.100035.
- [33] P. Roman, R. Veltman, M.F.M. Bijmans, K.J. Keesman, A.J.H. Janssen, Effect of Methanethiol Concentration on Sulfur Production in Biological Desulfurization Systems under Haloalkaline Conditions, *Environ. Sci. Technol.* 49 (2015) 9212–9221. doi:10.1021/acs.est.5b01758.
- [34] P.L.F. Van Den Bosch, M. Fortuny-Picornell, A.J.H. Janssen, Effects of Methanethiol on the Biological Oxidation of Sulfide at Natron-Alkaline Conditions, *Environ. Sci. Technol.* 43 (2009) 453–459. doi:10.1021/es801894p.
- [35] H.N. Po, N.M. Senozan, The Henderson-Hasselbalch Equation: Its History and Limitations, *J. Chem. Educ.* 78 (2001) 1499–1503. doi:10.1021/ed080p146.
- [36] P.L.F. Van den Bosch, Biological sulfide oxidation by natron-alkaliphilic bacteria Application in gas desulfurization, Wageningen University, 2008.
- [37] P. Roman, J. Lipińska, M.F.M. Bijmans, D.Y. Sorokin, K.J. Keesman, A.J.H. Janssen, Inhibition of a biological sulfide oxidation under haloalkaline conditions by thiols and diorgano polysulfanes, *Water Res.* 101 (2016) 448–456. doi:10.1016/j.watres.2016.06.003.

Appendix A – A dependency of ORP on sulfide concentration and oxygen concentration

Figure A1 illustrates how ORP of the process medium will change in response to the oxygen and sulfide concentration. To predict ORP values at various concentrations of oxygen and sulphide, we propose the following equation for ORP, based on the Nernst equation:

$$\text{ORP} = \xi_1 + \xi_2 \log(\gamma \text{O}_2) + \xi_3 \log(\gamma \text{HS}^-) \quad (\text{Eq. A1})$$

Where ξ_i is an empirical ORP coefficient and γ describes the activity coefficient of the dissolved compound.

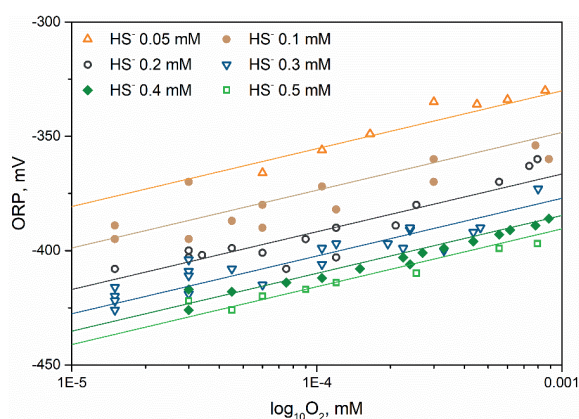


Fig. A1. ORP dependency for oxygen and sulfide concentration (semi-logarithmic scale) (adapted from Chapter 6 of Klok's PhD thesis [41]). The symbols indicate measured data points and solid lines indicate the model fit based on the equation Eq. A1.

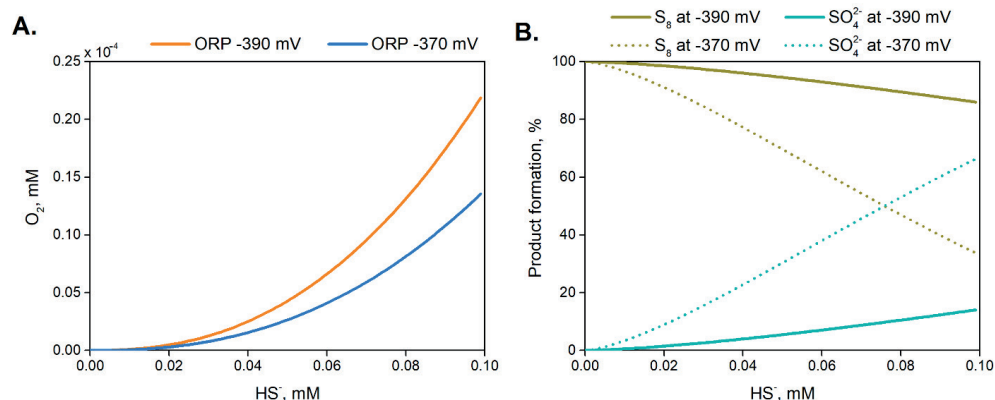


Fig. A2. The dependency between oxygen concentration and formation of sulfur and sulfate at two oxidation-reduction potential (ORP) setpoints. S_8 is an elemental sulfur that is shaped into a crystal form from S^0 .

Appendix B – Gas biodesulfurization process performance with use of ORP-based feedback control for oxygen supply

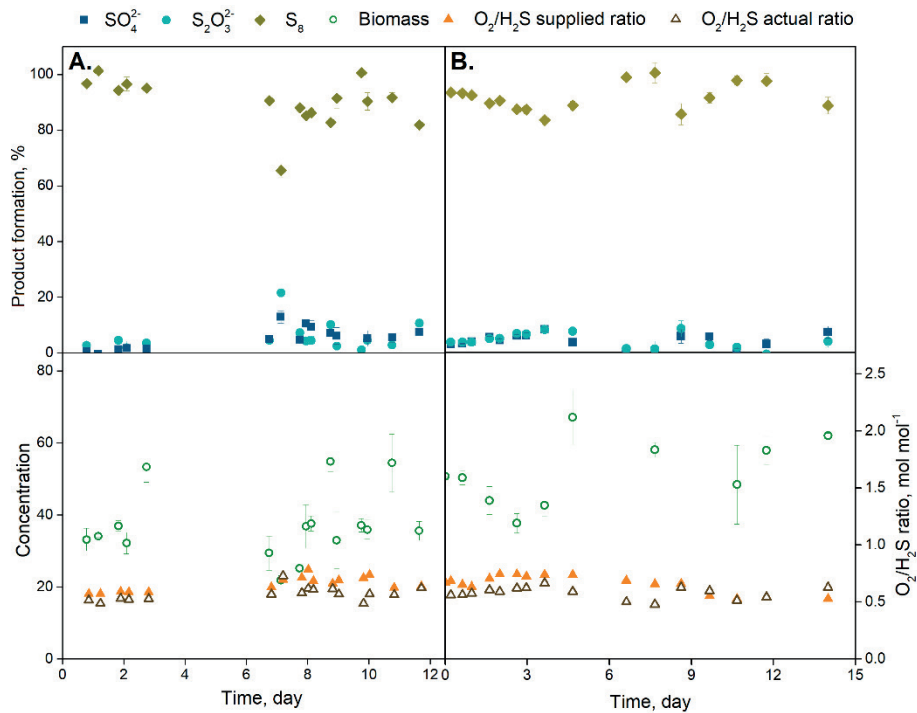


Fig. B1. Product formation during H₂S oxidation in (A) the traditional and (B) the double bioreactor gas biodesulfurization line-ups. The system was operated at ORP of -390 mV, pH = 8.5, T = 35 °C and the H₂S loading rate was constant at 58.15 mM S day⁻¹.

Appendix C – Concentrations of inorganic and organic sulphur compounds in the liquid and gas samples from the lab-scale gas biodesulfurization setup operation with ethanethiol addition.

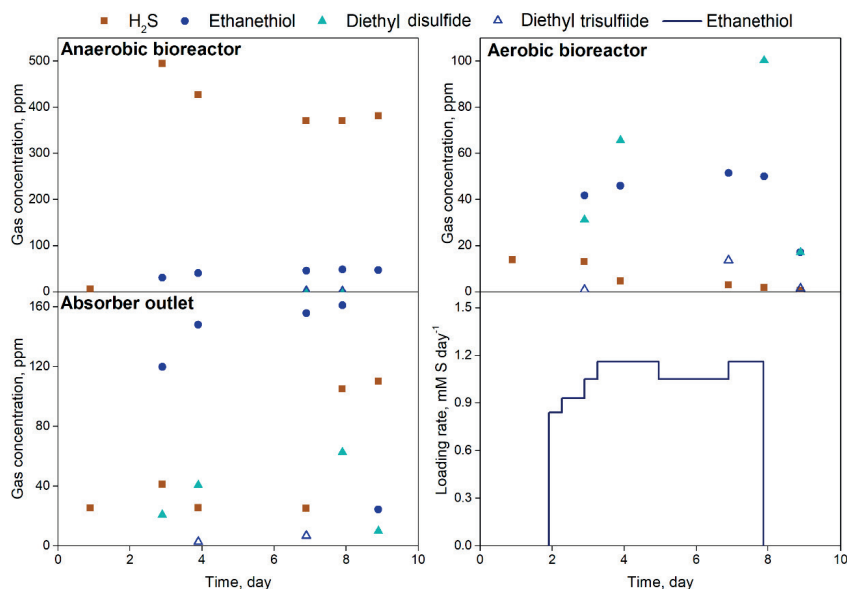


Fig. C1. The detected gas concentrations in the headspace or the anaerobic, the aerobic bioreactors and the gas outlet during biodesulfurization process operation with a gradual increase of ethanethiol supply. The system was operated at pH = 8.5, T = 35 °C and the randomly varying supply of H_2S (26.5 mM S day⁻¹).

7

CHAPTER 7

Summary and general discussion

7.1. Introduction

The growth of the global population and its associated increased demands for energy, food, and water has resulted in the intensification of industry and land use and hence loss of biodiversity and climate change. The overuse of natural resources, anthropogenic gas emissions and wastewater discharges into open waters cause environmental pollution, which, as a chain reaction, trigger changes in the natural habitats of flora and fauna [1–3]. Moreover, accumulation of CO_2 , N_2O , CH_4 and SO_2 gases in the atmosphere cause health problems for millions of people and accelerate climate change [4].

To sustain a global population of 7.7 billion people and manage their environmental footprint sustainably, the industry should transition towards a circular economy by using renewable resources and implementation of sustainable technologies. One such technology is the gas biodesulfurization process developed by our group in the Department of Environmental Technology at Wageningen University in cooperation with Delft University of Technology, University of Amsterdam, and industrial partners: Paqell B.V, Paques B.V and Shell. This technology emerged in the early 1990s when physicochemical desulfurization processes were dominating the market. Our biodesulfurization technology distinguishes itself because of its reduced operational and capital expenditures, and smaller environmental footprint. Since then, gas biodesulfurization has been intensively studied in order to facilitate higher sulfur recovery rates (>90 mol%) and stable process operations while treating a variety of gas feed streams. A high selectivity for sulfur is preferred because this will regenerate hydroxide ions, which are consumed when H_2S is removed from gas streams. In addition, the consumption of air, energy, and caustic at sulfur-producing conditions are lower relative to the formation of sulfuric acid [5]. Furthermore, the recovered sulfur slurry can be used as fertilizer and as fungicide [6]. To maintain a stable sulfur selectivity, the biodesulfurization process operation should remain stable as well, especially when gas feed composition and sulfide concentration fluctuate. The composition of the feed gas depends on the industry that generates the sour gas. For example, biogas formed from the anaerobic digestion of wastewater in paper mill facilities has a relatively low amount of H_2S (0.7 vol.%), whereas sour gas streams in the oil and gas industry are composed of up to 95 vol.% of H_2S , a fraction of CO_2 , hydrocarbons, and thiols. The H_2S concentration can vary greatly, not only between industries but also during the operation of a single installation. The daily H_2S loading rate between Thiopaq installations may range from 10 kg day^{-1} up to 150 ton day^{-1} . Therefore, the aim of this research was to achieve more sulfur formation and stable process operation in the presence of thiols; see **Chapter 1** for main research questions. In the following section we will discuss which measures can be applied to increase process stability and sulfur formation under variations in gas feeds.

7.2. Achieving optimal process performance

In the studies described in this thesis, we made use of a variety of scientific disciplines ranging from molecular biology, toxicology, process technology to process modeling and process control in order to better understand the four key elements required for achieving optimal process requirements. These elements are described below:

1. **Development of a methodology for selecting SOB biomass to start up a full-scale gas biodesulfurization installation.** SOB have two enzymatic routes for sulfide oxidation that have been known so far. The majority of SOB were found to use flavocytochrome *c* oxidase to transfer electrons to cytochrome *c*. This route is called FCC that converts HS^- to S_8 . The second route that is used by some SOB species, i.e. *Alkalilimnicola*, is sulfide-quinone reductase (SQR) that uses quinones as electron carriers. It was found that SQR pathway is more energetically favorable and less sensitive to toxic compounds such as thiols [7]. Furthermore, Klok and colleagues found that SQR route prevails when sulfide oxidation takes place under oxygen limiting conditions and stimulates elemental sulfur formation [8]. Therefore, finding ratio between expression rates of sulfide oxidation enzyme routes FCC and SQR will enable to understand capacity of the chosen SOB form sulfur and sulfate. This FCC/SQR ratio is derived from the respiration rate data and introduced as an α value. In our study, we found that at $\alpha < 0.8$, sulfur formation prevailed in the process, whereas product formation shifted towards sulfate formation at $\alpha > 0.8$ (Chapter 2). This dependency between α , sulfate and sulfur formation can be used as an assessment tool for a process engineer/installation operation to assess product formation rates and develop debottlenecking strategies for full-scale installations. In addition, it can be used to evaluate a chosen inoculum on its potential for sulfur and sulfate formation before starting the process.
2. **Evaluation of the dual biodesulfurization line-up in the presence and absence of thiols by investigating underlying biochemical reactions of H_2S oxidation and SOB community dynamics.** In our study, we achieved a sulfur selectivity of ~92 mol% in both the double-bioreactor setup and the traditional line-up during short-term experiments of about 2 weeks of operation (Chapters 2 and 4). However, we noticed that the addition of a second, anaerobic, bioreactor to the line-up resulted in the increase of the process operability as both formation rates and ORP values were more stable in that setup. It appeared that the added anaerobic bioreactor in the double-bioreactor line-up was damping fluctuations of the sulfide-rich solution flow into the aerobic bioreactor. The ORP sensor readings showed that the values measured in anaerobic bioreactor were consistently more negative than in the aerobic bioreactor (~-430 mV vs. ~-390 mV), meaning that no oxygen was present in the anaerobic bioreactor and that conditions in the anaerobic bioreactor were

more reduced. This difference in the ORP values and oxygen availability affects the state of bacterial cells, more importantly state of the enzymatic routes for biological sulfide oxidation [9]. Moreover, the addition of an anaerobic bioreactor increased the biomass retention time and the interaction of SOB with organic and inorganic sulfur compounds. These improvements prompted us to study the effect of thiols on the process operation of the double bioreactor setup (**Chapter 5**). In this work, we identified that almost all sulfide supplied to the system in the feed gas was in the form of polysulfide. This indicates that, in our experimental setup, the dominating electron donor for SOB was polysulfide. Moreover, we found that when the double bioreactor was added to the process line-up, we were able to increase the selectivity for sulfur formation up to 90 mol% when methanethiol (MT) was supplied at a loading rate of 2 mM S day⁻¹, whereas in the traditional line-up, the maximum for sulfur formation was 75% [10].

In addition to the above, we observed that the anaerobic bioreactor provided selective pressure on the SOB microbial community. To assess SOB dynamics, we initially performed 16S rRNA gene amplicon analyses on samples collected at equal time intervals during experiments with and without MT addition (**Chapters 4 and 5**). The output of amplicon sequencing provides the relative abundance of microbial species present in the community at the moment of sampling. These abundances are relative as they depend on an abundance of other species within the SOB community. Therefore, in addition, a quantitative assay was performed to answer more profound questions on species interactions, dependency of the process performance and growth dynamics. We cloned our sludge and identified the three most dominant SOB species: *Thioalkalivibrio sulfidiphilus*, *Alkalilimnicola ehrlichii*, and *Thioalkalibacter halophilus*. For these species, we developed species-specific primers and qPCR assay (**Chapter 3**). The qPCR results show that proliferation of *Thioalkalibacter halophilus* and decrease of *Thioalkalivibrio sulfidiphilus* was strongly correlated to the presence of MT and/or its oxidation product dimethyl disulfide (DMDS). IC₅₀ values of *Thioalkalibacter halophilus* confirmed its high tolerance to dimethyl disulfide (IC₅₀ value at 2.37 mM of DMDS) (**Chapter 4**).

3. Selective inhibition of sulfate formation by DMDS addition. The idea for this experiment originated from the findings of Roman et al. (2016b), describing the inhibition modes of organic sulfur compounds. In this study, we found that DMDS inhibits the oxidation of internal poly sulfur compounds into sulfate. The first experimental run showed a strong reduction of sulfate formation. The quantified sulfate selectivity of about ~ 1 mol% was reduced with ~7 mol% compared with sulfate formation in the absence of DMDS (**Chapter 4**). However, no differences were found for sulfur formation in the absence or presence of DMDS, i.e. both runs showed selectivity for sulfur formation of ~90 mol%. The remaining sulfide was chemically converted to thiosulfate at ~9 mol%. Chemical oxidation rates of

dissolved sulfide increased when biological sulfide oxidation rates were suppressed. To prove that thiosulfate formation can be reduced by increasing biological activity, we performed a test with a doubled biomass concentration. We achieved 0 mol% thiosulfate formation with ~96 mol% sulfur formation. In **Chapter 4**, we also presented a new method developed in-house for the quantification of organic sulfur compounds in liquid samples. With this method, we could identify diorgano polysulfanes which formed in the process medium. The identification of formed diorgano polysulfanes resulted in the proposition of the novel reaction between sulfide and dimethyl disulfide, which leads to the formation of longer-chain diorgano polysulfanes, i.e., dimethyl trisulfide and dimethyl tetrasulfide.

4. **Development of an alternative oxygen supply control strategy to enable stable process operation with high sulfur selectivity (>95 mol%) in the presence of thiols.** Most of the industrial processes use automated control to steer product formation and operational parameters such as pH, dissolved oxygen, alkalinity, and ORP. In the current gas biodesulfurization process, an integrated PID feedback-based controller is used, which regulates the air supply based on input signals from the ORP sensor. To increase the sulfur formation rate and to overcome fluctuations of H_2S and thiols concentration in the feed gas, we developed an alternative, feedforward control strategy for oxygen supply (**Chapter 6**). This strategy is based on a fixed $\text{O}_2/\text{H}_2\text{S}$ supply ratio to the aerated bioreactor. In the past, this ratio was used by our research group to assess the system's performance. In our study, we used this parameter as a control variable. Based on the available set of previous studies, we knew that the highest selectivity for sulfur formation was achieved at an $\text{O}_2/\text{H}_2\text{S}$ supply ratio of ~0.60 mol mol⁻¹ [5,12,13]. Therefore, we selected a control value for the feedforward control of ~0.60 mol mol⁻¹. The results of our experiments with feedforward control show stable process performance and high sulfur selectivity of ~96 mol% at the randomly varying H_2S supply. Preliminary results also show that the high sulfur formation rate of ~95 mol% is not affected by the presence of ethanethiol (1.16 mM S day⁻¹).

By the completion of all experimental runs. We found out that process operation in terms of sulfur selectivity was higher than 90 mol%, when lab-scale set-up was inoculated with SOB biomass from the full-scale facilities that operate well. **Chapter 2** shows differences in process operation with four SOB biomasses taken from four different full-scale installations. Sulfur selectivity was higher when the SOB biomass was taken from a full-scale installation that was operating well. By “operating well”, we mean stable process operation for a prolonged period of time with a sulfur selectivity of ~90 mol%. Moreover, SOB composition was also found to determine process performance. Therefore, to be able to optimize process performance, the SOB community should be able to withstand feed gas composition. For instance, in the

experiments with addition of DMDS (**Chapter 4**) and MT (**Chapter 5**) the inoculum consisted of a mix of SOB from various installations: 40% was from the Oilfield - 1 installation, which treats associated gas with low concentrations of thiols 50-200 ppm and 1-5 % of H_2S . Another 40% was SOB biomass from a pilot plant, which treats the synthetically prepared gas that represents amine acid gas with 4.45 % of H_2S where a high abundance of *Alkalilimnicola ehrlichii* was found [14]. 10% was from Oilfield – 2 installations located in South-East Asia where the feed gas contains next to H_2S also a high concentration of thiols. The final 10% was from an installation treating landfill gas, with a SOB biomass showed high sulfur selectivity in the presence of sulfide (**Chapter 2**). By preparing a mixture of the inocula, we increased the chances of developing a SOB community that would be able to oxidize sulfide in the presence of MT and DMDS. After enrichment, we identified two important species that are vital to enable stable process performance in the presence of MT: *Thioalkalibacter halophilus* and *Alkalilimnicola ehrlichii*. By contrast, in the absence of MT, *Thioalkalivibrio sulfidiphilus* species are essential to enable stable process operation.

7.3. Identified knowledge gaps

Throughout 30 years of research by our group, numerous studies have been performed to understand and optimize the biological desulfurization process. Many analytical tools and microbiological identification methods have been developed to analyze biological systems that are now commercially available. Therefore, new questions can be addressed and studied in more depth, such as the ecophysiology of the species within the SOB community and which enzyme system is used by the SOB for sulfide oxidation in the presence and absence of VOSCs. Furthermore, it might be possible to find SOB species that are not only able to withstand thiols but also perform conversion of thiols.


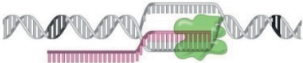
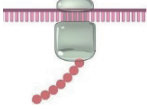
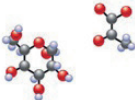
Another issue that requires more investigations is the robustness and up-scaling of the developed feedforward control. In the described research, we observed significant differences between feedback and feedforward control with fluctuating H_2S load. Feedforward control could be beneficial in gas biodesulfurization systems to achieve better operational stability and potentially higher sulfur selectivity in the presence of thiols. Therefore, further studies should aim at investigating the robustness of feedforward control at the elevated thiol loading rates. In addition, a feedforward control strategy should be implemented in a pilot installation and perform fully automated control by quantification of H_2S in the gas feed. As a first step, H_2S sensors need to be screened and tested for high robustness and reliability.

7.3.1 Ecophysiology of the species within SOB community

In bioprocesses, the emphasis is often centered on product formation and on maximizing yields or recovery factors of the compounds of interest. However, major changes occur within, especially, mixed bacterial communities. Furthermore, it is essential to link microbial activity and engineering performance, as well as to gain knowledge on the physiology of the species makeup of the SOB community as it enables optimal use of the community in bioprocesses [15]. Nowadays, bioprocess engineers usually perform 16S rRNA amplicon sequencing to determine community structure and to associate process performance with the generally most abundant species. However, the dominant organisms may not necessarily play the critical role in the community structure as well as in product formation [16]. Therefore, only performing 16S sRNA analysis is not enough to answer more profound questions such as why certain products were formed, and why one bacterial species proliferates at certain conditions.

In the era of genomics, various assays have been already developed (Table 1) that can help us understand the dynamics and structure of SOB communities under certain process conditions [17]. Moreover, these -omics assays can provide crucial information on the sulfur metabolism of each species in the SOB community, as we may not even know what these species can do more of. Currently, the S-metabolism of only a few SOB species is known, and more importantly what their capacities are and what those species actually do in the gas biodesulfurization process. Therefore, the S-metabolism of other SOB species in the gas biodesulfurization process needs to be unraveled as well, to gain a better understanding of which bacteria are responsible for which activity. This will enable us to tailor the inoculum to fit the gas feed composition and facilitate higher process efficiencies. For instance, in our research, we found two bacterial species highly abundant in the presence of MT and DMDS: *Thioalkalibacter halophilus* and *Alkalilimnicola ehrlichii*. However, little is known about their role in gas biodesulfurization, their S-metabolism, oxidation capacity and why they are able to thrive in the presence of MT. What makes the number of other species decrease drastically in the presence of MT? That is why more insight is required into the genomes of SOB species and their -omics.

Table 1 Various -omics technologies to assess functionality of the bacterial community.

Metagenomics	Metatranscriptomics	Metaproteomics	Metabolomics
			
DNA	RNA	Protein	Metabolites
assesses the density of microbial communities and their genetic and functional diversity ¹ .	concentrates on expressed genes in the entire microbial community and provides a view of the active functions of the community of microorganisms ² .	assesses the “expressed” metabolism and physiology of microbial community members, the functioning of ecosystem ³ .	provides information on the metabolites (composition), which helps to understand the functional dynamics influencing community and host interactions ¹ .

¹ – [19], ² – [20], ³ – [21].

7.3.2 Development of molecular tools to monitor expression of FCC and SQR enzymes

Apart from using -omics assays, which are time-consuming and comparatively costly, real-time PCR (RT-PCR) allows fast analyses of environmental samples on singular or multiple gene expression [18]. The genes of interest are the ones that encode the flavocytochrome c oxidase (FCC) and sulfide-quinone oxidoreductase (SQR) pathways that are used by SOB for sulfide oxidation (Fig. 1). It is of high importance to understand which enzymatic route SOB species are using in the presence of thiols. This may also provide information on the mechanism of detoxification.

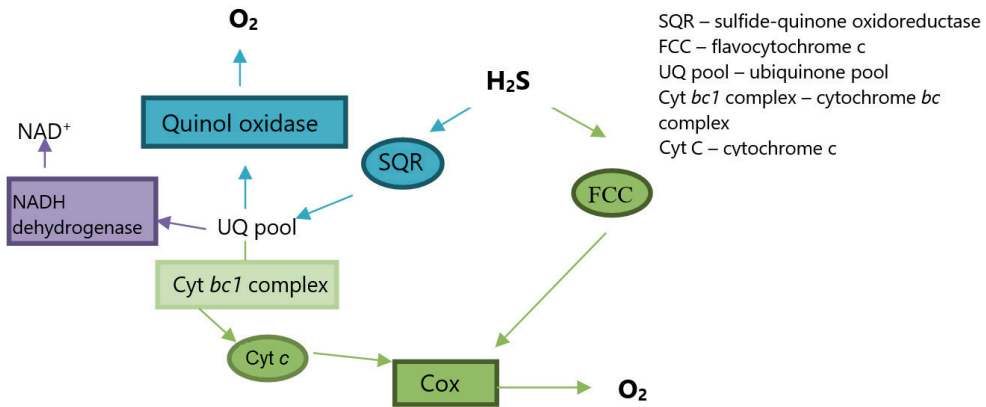


Fig. 1. Schematic representation of the chemolithotrophic electron transport chain from sulfide during bacterial respiration (adapted from [22])flavocytochrome c and sulfide-quinone reductase (SQR).

7.3.3 Robustness of the feedforward control at *thigh thiol loadings*

The presented feedforward control shows promising results for the gas biodesulfurization process control resulting in an increase in sulfur formation of to 96 mol%. However, before implementing feedforward control in full-scale installations, it needs to be implemented and tested in a larger pilot installation. In addition, the robustness of the feedforward control needs to be tested with addition of thiols, BTEX and other compounds that are present in the gas feed in full-scale installations.

In addition, it might be possible to combine feedforward control into model predictive control (MPC). The idea is to pair sulfide readings from the gas feed, with a computer, and have a software perform in-line calculations of the required oxygen supply based on the set O_2/H_2S ratio limits. The oxygen/air valve could then be controlled this way, and oxygen supplied to the aerobic bioreactor as needed. In addition to setting O_2/H_2S ratio limits, it might be possible to integrate MPC with control objective prioritization, symptom-aided diagnosis [23,24].

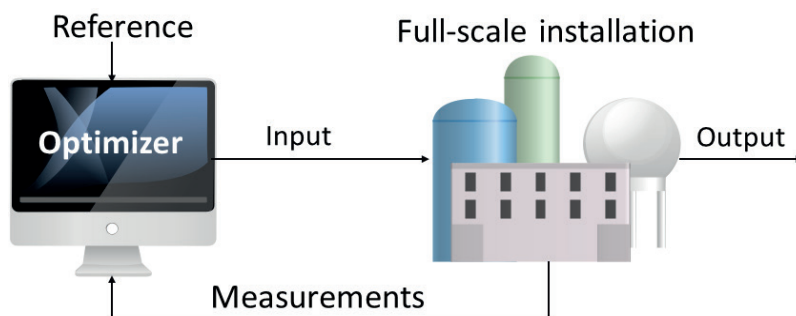


Fig. 2. Schematic representation of the basic structure of model predictive control.

References

- [1] T. Elmqvist, E. Maltby, T. Barker, A.M. Mortimer, C. Perrings, J. Aronson, R. Groot, A. Fitter, J. Norberg, I. Sousa Pinto, I. Ring, J.-M. Salles, Biodiversity , ecosystems and ecosystem services, in: *Econ. Ecosyst. Biodivers. Ecol. Econ. Found.*, 2010: p. 97.
- [2] T.K. Parmar, D. Rawtani, Y.K. Agrawal, Bioindicators: the natural indicator of environmental pollution, *Front. Life Sci.* 9 (2016) 110–118. doi:10.1080/21553769.2016.1162753.
- [3] World health organization and Secretariat of the Convention on Biological Diversity, *Connecting Global Priorities: Biodiversity and Human Health. A state of Knowledge Review*, (2015) 14.
- [4] R.K. Pachauri, Climate change 2014 synthesis report summary chapter for policymakers, 2014. doi:10.1017/CBO9781107415324.
- [5] P.L.F. Van Den Bosch, O.C. Van Beusekom, C.J.H. Buisman, A.J.H. Janssen, Sulfide Oxidation at Halo-Alkaline Conditions in a Fed-Batch Bioreactor, *Biotechnol. Bioeng.* 97 (2007) 1053–1063. doi:10.1002/bit.
- [6] J. Lim, J. Pyun, K. Char, Recent approaches for the direct use of elemental sulfur in the synthesis and processing of advanced materials, *Angew. Chemie - Int. Ed.* 54 (2015) 3249–3258. doi:10.1002/anie.201409468.
- [7] D.C. Brune, Sulfur oxidation by phototrophic bacteria, *Biochem. Biophys. Acta.* 975 (1989) 189–221.
- [8] J.B.M. Klok, M. de Graaff, P.L.F. van den Bosch, N.C. Boelee, K.J. Keesman, A.J.H. Janssen, A physiologically based kinetic model for bacterial sulfide oxidation, *Water Res.* 47 (2013) 483–492. doi:10.1016/j.watres.2012.09.021.
- [9] A. Ter Heijne, R. De Rink, D. Liu, J.B.M. Klok, C.J.N. Buisman, Bacteria as an Electron Shuttle for Sulfide Oxidation, *Environ. Sci. Technol. Lett.* 5 (2018) 495–499. doi:10.1021/acs.estlett.8b00319.
- [10] P. Roman, J.B.M. Klok, J.A.B. Sousa, E. Broman, M. Dopson, E. Van Zessen, M.F.M. Bijmans, D.Y. Sorokin, A.J.H. Janssen, Selection and Application of Sulfide Oxidizing Microorganisms Able to Withstand Thiols in Gas Biodesulfurization Systems, *Environ. Sci. Technol.* (2016) acs.est.6b04222. doi:10.1021/acs.est.6b04222.
- [11] P. Roman, J. Lipińska, M.F.M. Bijmans, D.Y. Sorokin, K.J. Keesman, A.J.H. Janssen, Inhibition of a biological sulfide oxidation under haloalkaline conditions by thiols and diorgano polysulfanes, *Water Res.* 101 (2016) 448–456. doi:10.1016/j.watres.2016.06.003.
- [12] P. Roman, M.F.M. Bijmans, A.J.H. Janssen, Influence of methanethiol on biological sulphide oxidation in gas treatment system, *Environ. Technol.* 3330 (2016) 1–11. doi:10.1080/09593330.2015.1128001.
- [13] K. Kiragosyan, J.B.M. Klok, K.J. Keesman, P. Roman, A.J.H. Janssen, Development and validation of a physiologically based kinetic model for starting up and operation of the biological gas desulfurization process under haloalkaline conditions, *Water Res. X.* 4 (2019) 100035. doi:10.1016/j.wroa.2019.100035.

- [14] R. De Rink, J.B.M. Klok, D.Y. Sorokin, G.J. Van Heeringen, A. Ter Heijne, R. Zeijlmaker, Y.M. Mos, V. De Wilde, K.J. Keesman, C.J.N. Buisman, Increasing the selectivity for sulfur formation in biological gas desulfurization, *Environ. Sci. Technol.* 53 (2019) 4519–4527. doi:10.1021/acs.est.8b06749.
- [15] J. Hassa, I. Maus, S. Off, A. Pühler, P. Scherer, M. Klocke, A. Schlüter, Metagenome, metatranscriptome, and metaproteome approaches unraveled compositions and functional relationships of microbial communities residing in biogas plants, *Appl. Microbiol. Biotechnol.* 102 (2018) 5045–5063. doi:10.1007/s00253-018-8976-7.
- [16] E.A. Dinsdale, R.A. Edwards, D. Hall, F. Angly, M. Breitbart, J.M. Brulc, M. Furlan, C. Desnues, M. Haynes, L. Li, L. McDaniel, M.A. Moran, K.E. Nelson, C. Nilsson, R. Olson, J. Paul, B.R. Brito, Y. Ruan, B.K. Swan, R. Stevens, D.L. Valentine, R.V. Thurber, L. Wegley, B.A. White, F. Rohwer, Functional metagenomic profiling of nine biomes, *Nature*. 452 (2008) 629–632. doi:10.1038/nature06810.
- [17] N. Srivastava, B. Gupta, S. Gupta, M.K. Danquah, I.P. Sarethy, Analyzing Functional Microbial Diversity: An Overview of Techniques, in: *Microb. Divers. Genomic Era*, Elsevier Inc., 2019: pp. 79–102. doi:10.1016/B978-0-12-814849-5.00006-X.
- [18] T. Wang, M.J. Brown, mRNA quantification by real time TaqMan polymerase chain reaction: Validation and comparison with RNase protection, *Anal. Biochem.* 269 (1999) 198–201. doi:10.1006/abio.1999.4022.
- [19] T. Bouchez, A.L. Blieux, S. Dequiedt, I. Domaizon, A. Dufresne, S. Ferreira, J.J. Godon, J. Hellal, C. Joulain, A. Quaiser, F. Martin-Laurent, A. Mauffret, J.M. Monier, P. Peyret, P. Schmitt-Koplin, O. Sibourg, E. D'oiron, A. Bispo, I. Deportes, C. Grand, P. Cuny, P.A. Maron, L. Ranjard, Molecular microbiology methods for environmental diagnosis, *Environ. Chem. Lett.* 14 (2016) 423–441. doi:10.1007/s10311-016-0581-3.
- [20] R.K. Dubey, V. Tripathi, R. Prabha, R. Chaurasia, D.P. Singh, C.S. Rao, A. El-Keblawy, P.C. Abhilash, Metatranscriptomics and Metaproteomics for Microbial Communities Profiling, in: *Unravelling Soil Microbiome*, 2020: pp. 51–60. doi:10.1007/978-3-030-15516-2.
- [21] M. Kleiner, Metaproteomics: Much More than Measuring Gene Expression in Microbial Communities, *MSystems*. 4 (2019) 1–6. doi:10.1128/msystems.00115-19.
- [22] C. Griesbeck, G. Hauska, M. Schütz, Biological sulfide oxidation: sulfide-quinone reductase (SQR), the primary reaction, in: S.G. Pandalai (Ed.), *Recent Res. Dev. Microbiol.*, Research Signpost, Trivandrum, India, 2000: pp. 179–203.
- [23] M. Morari, J. H. Lee, Model predictive control: past, present and future, *Comput. Chem. Eng.* 23 (1999) 667–682. doi:10.1016/S0098-1354(98)00301-9.
- [24] A. Bemporad, M. Morari, Robust model predictive control: A survey, *Robustness Identif. Control.* (2007) 207–226. doi:10.1007/bfb0109870.

Epilogue

Author's publications and patents

K. Kiragosyan, M. Picard, D.Y. Sorokin, J. Dijkstra, J.B.M. Klok, P. Roman, A.J.H. Janssen, Effect of dimethyl disulfide on the sulfur formation and microbial community composition during the biological H₂S removal from sour gas streams, J. Hazard. Mater. 386 (2020). doi:10.1016/j.jhazmat.2019.121916.

K. Kiragosyan, J.B.M. Klok, K.J. Keesman, P. Roman, A.J.H. Janssen, Development and validation of a physiologically based kinetic model for starting up and operation of the biological gas desulfurization process under haloalkaline conditions, Water Res. X. 4 (2019) 100035. doi:10.1016/j.wroa.2019.100035.

K. Kiragosyan, P. van Veelen, S. Gupta, A. Tomaszewska-Porada, P. Roman, P.H.A. Timmers, Development of quantitative PCR for the detection of *Alkalilimnicola ehrlichii*, *Thioalkalivibrio sulfidophilus* and *Thioalkalibacter halophilus* in gas biodesulfurization processes, AMB Express. 9 (2019) 99. doi:10.1186/s13568-019-0826-1.

J.B.M. Klok, R. De Rink, K. Kiragosyan, P. Roman, A.J.H. Janssen, K. Keesman. A feedforward control strategy for oxygen supply was submitted for a patent with an application number N2024456. Filled December 13th, 2019.

Acknowledgments

Four last years were a roller coaster, but we made it. Coming to the finish line would not be possible without the support of many people in one way or another.

I want to thank my supervisors, Pawel and Jan, for giving me such an opportunity. **Pawel**, I would not make it without you. You had a lot of patience when I was learning when I was stubborn and did things how I thought better. Nevertheless, every time I wanted to brainstorm, or I was not sure how to proceed with experiments or in conversations, you supported me and helped me to sort things out. I truly appreciate you coming with me to the lab and giving me a push to start. **Jan**, we had some time when we did not know how to approach one another, but after getting to know each other we made it work! Thank you for being enthusiastic and seeing a bright side on my obtained data and my research. I know that I was not a calm student and I gave you both some hard times. I cannot be grateful enough that even in those times you stand by me.

I would like to thank **Albert**, my promotor, for giving me this chance to get into the world of biodesulfurization. Thank you for your suggestions and visions in the paper and presentations, and your practical insights. Also, thank you for the discussions on my future perspectives and learning curve.

There are many other people that contributed to this project and shared the burden of making lab smell. **Dimitrii**, thank you for your support and guidance in the sulfur-oxidizing bacteria world. **Annemerel**, you are the person who can understand me without much saying how it feels to work with H_2S and it was great that I can share that with you. **Margo**, you are a courageous person because you joined the sulfur team to work on thiols degradation, I wish you all the luck. And finally, **Rieks**, thank you for sharing your insights in process operation. There is no doubt that you guys will do great!

My work would have never been accomplished without help and support of the **analytical** and **technical team** at Wetsus. **Mieke**, **Marianne**, **Jan-Willem**, and **Lisette** thank you for fast analysis of sulfate and thiosulfate samples as well as performing other analyses. Additional thank you to Marianne and Mieke, which helped me with HPLC analysis. **Jelmer**, I haven't forgotten about you 😊. Thank you a lot of helping me out with gas analysis and co-development of the GC-FPD method for thiols analysis. **Agnieszka**, thank you a lot for your support and guidance in micro-lab. **Pieter**, it was a great time to work together and you are an amazing addition to micro-lab team at Wetsus. My dear technical team: **Jan T.**, **Ernst**, **Harm**, **John** and **JJ**, thank you very much for putting my setup together and coping with my bossiness. A big thanks to **Jan T.** for shifting bioreactors while they in operation, changing gas tubing and many more adjustments of the system. But more importantly for a conversation about my personal struggles and your support. And of course, I want to thank **Janneke** for letting me spend

Saturdays and sometimes Sundays at Wetsus. Thank you to everyone and each one of you.

Thank you, **Wetsus secretaries**, for taking care of paperwork and help with the students. Thank you **Liesbeth**, for helping with paperwork in Wageningen too. **Gerben**, thank you for a great vibe in the canteen and knowing each and every one of us, it was great to organize a PV trip with you.

To all my **Wetsusians**, thank you for a great time and memories of a lifetime. Especial thanks to my office mates: **Jaap, Ricardo, Rik, and Maurits**. You guys willingly wanted to share your office with me. You never knew what a surprise I was until I came into the office. **Maarten**, you coped with me every single time even with my crazy idea to attend “insanity” workouts. **Paulina**, thank you for bringing a southern warmth and Mexican colors to the office and sharing my love for coriander. Thank you, **Stan**, for our trips to Wageningen. The newbies: **Nimmy, Steffen, Chris, Mariana, and Kevin** thank you for bringing your enthusiasm into the office and a broader variety of the meals during the office dinner.

I would also like to thank **Victor T, Tania Mubita, Aga, Marianne** and **Natasha** for joining Strong Viking run. It was a great experience that we shared together. **Terica** (the Queen) thank you for making funny times at Wetsus and our cinema outs in pajamas. Thank you, **Wokke, Rita, Suyash, Sebastian, Raquel, Slavek, Angel, Yuchen, Mark, Mariana, Andrew, Fabian, Casper, Sam, Jan Willem, Joao, Jordi, Ettore, Carlo, Gosia**, for being there for a good talk, laugh, dance, BBQs, or for helping me out at some point.

Special thank you to my students: **Magali, Beatriz, Franka, Teresa, and Larissa**, who wanted to join me and with whom I learned a lot.

Rebechka, thank you so much for not only being a great colleague but more importantly a great friend. It is hard to count how many times we cried and laughed together on the couch at home. How many conversations we had about lots of random stuff together with **Anja**. And of course, our house parties were epic. **Thomasito**, thank you for your regular enthusiasm and crazy game ideas. And of course, the trip to Alsace was amazing, we met your parents and got the flavor of authentic France. **Hector** (Hombre), we have done so many things together. Our salsa parties, King days's festivals, Amsterdam dance event and you even went with me for two weeks to plattenland Drenthe to learn Nederlands. You were my partner in crime for all the possible ideas I had. **Goncalito**, thank you for your analyzer capabilities and for listening to all my complaints. I am really thankful to you guys for our countless movie nights and dinners that made my PhD life brighter.

I would like to thank my family for their support, my **Mom** and **Dad** for their sacrifices, patience and believe in me. Дорогие мама и папа, спасибо вам за все. Мам, без твоей поддержки этого всего бы небыло. My sister Gayane, the

person who knows and understands me without any words, thank you for being there for me and letting me go to the Netherlands. My friends from Bremen: **Fabichka, Anja, Anna, Sveta, Frank,** and **Anika** thanks for your support and for coming to visit me in the Netherlands.

To **Laurens**, I love you. Thank you for coping with me through my PhD, I can be a real nightmare especially when experiments were not working out. Thank you for believing in me, even when I could not see it.

About the author



Karine Kiragosyan was born on December 22nd in Krasnodar, Russia at 21.45 leading the way for her twin sister. Love to biology started from high school at Natural Science class. In 2007 she started a study in Bio-Ecology at the Kuban State University (KubSU). During studies she travelled to USA to work every summer. This experience left a big footprint on her, she was dreaming big and had a drive to succeed. Therefore, gaining BSc. in Bio-Ecology was not enough, she was determined and dreaming to develop her skills in biotechnology. However, no biotechnology masters were accepting with an Ecology degree. Thus, she decided to get a study where she can choose external classes in biotechnology. And successfully in 2013 she started her MSc. in Ecology at Bremen University, Germany. For her research internship she joined a team at Aquatic Biotechnology department at Rijksuniversiteit Groningen. Continued to develop lab-skills and be a part of a big international project she joined Plant-Fish project and went to conduct measurements of threespine stickleback at Stockholm University, Sweden. In 2016 Karine obtained her MSc. in Ecology by completing a thesis on environmental studies: *Chubby and chic, or lean and mean: Morphological diversification of threespine stickleback along the coastline of the western Baltic Sea*.

From February 2016, Karine moved to Leeuwarden and started her new adventure – a PhD life. She joined Sulfur theme at Wetsus European Center of Excellence for Sustainable Water Technology. Her project was a cooperation between Environmental technology department at Wageningen University and Research, Paqell B.V. and Wetsus. The results and achievements obtained during her PhD are presented in this dissertation.



*Netherlands Research School for the
Socio-Economic and Natural Sciences of the Environment*

DIPLOMA

for specialised PhD training

The Netherlands research school for the
Socio-Economic and Natural Sciences of the Environment
(SENSE) declares that

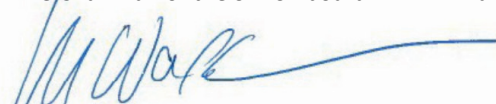
Karine Kiragosyan

born on 22 December 1989 in Krasnodar, USSR

has successfully fulfilled all requirements of the
educational PhD programme of SENSE.

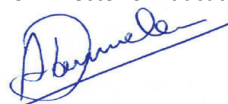
Wageningen, 8 April 2020

The Chairman of the SENSE board



Prof. dr. Martin Wassen

the SENSE Director of Education



Dr. Ad van Dommelen



The SENSE Research School has been accredited by the Royal Netherlands Academy of Arts and Sciences (KNAW)

KONINKLIJKE NEDERLANDSE
AKADEMIE VAN WETENSCHAPPEN



The SENSE Research School declares that **Karine Kiragosyan** has successfully fulfilled all requirements of the educational PhD programme of SENSE with a workload of 37.9 EC, including the following activities:

SENSE PhD Courses

- o Environmental research in context (2016)
- o Research in context activity: 'Co-organizing the International Conference on Biogas Microbiology – 3 (Wageningen, 1-3 May 2017)'
- o Scientific writing (2019)

Other PhD and Advanced MSc Courses

- o Advanced course in Environmental biotechnology, TU Delft (2016)
- o How to supervise BSc/MSc students, Wetsus (2017)
- o Advanced Scientific Writing for researchers, VU Amsterdam (2019)
- o Advanced course in Downstream processing, TU Delft (2019)

Site specific training

- o Nogepa H₂S training, Wageningen University (2016)

Management and Didactic Skills Training

- o Supervising three MSc students with thesis (2018-2019) o
- Supervising three BSc student with thesis (2017-2019)

Oral Presentations

- o *Biotechnological removal of H₂S under haloalkaline conditions*. Wetsus congress, 30 November 2017, Leeuwarden, The Netherlands
- o *Biotechnological removal of H₂S under haloalkaline conditions*. IWA resource recovery, 8-12 September 2019, Venice, Italy

Poster Presentations

- o *Biological removal of H₂S in the presence of thiols from sour gas streams*. 3rd International conference on biogas microbiology (ICBM – 3), 1-3 May 2017,
- o *Effect of methanethiol on biodesulfurization process under haloalkaline conditions*. 5th International Symposium on Microbial Sulfur Metabolism (ISMSM – 5), 16-18 April 2018, Vienna, Austria

SENSE coordinator PhD education

Dr. ir. Peter Vermeulen

This work has been performed within the cooperation framework of Wetsus, European Centre of Excellence for Sustainable Water Technology (wetsus.nl), Wageningen University and Research (wur.nl) and Paqell B.V (paqell.com). Wetsus is co-funded by the Netherlands' Ministry of Economic Affairs and Ministry of Infrastructure and Environment, the European Union's Regional Development Fund, the Province of Fryslan and the Northern Netherlands Provinces. Wetsus is also a coordinator of the WaterSEED project that received funding from European Union's Horizon 2020 research and innovation program under Marie Skłodowska-Curie grant agreement No. 665874.

Financial support from both Wageningen University and Wetsus for printing this thesis is gratefully acknowledged.

Cover design by Elena Resko, www.elenaresko.com

Thesis design by ProefschriftMaken, proefschriftmaken.nl

Printed by ProefschriftMaken/Digiforce on FSC-certified paper

